https://ntrs.nasa.gov/search.jsp?R=19680007413 2020-03-12T09:20:23+00:00Z

REVIEW AND EVALUATION OF PAST SOLAR CELL DEVELOPMENT EFFORTS

by

P. A. Crossley *(Project Scientist)*
G. T. Noel
M. Wolf *(Project Supervisor)*

N 68-16882
(ACCESSION NUMBER) (THRU)
225
(PAGES) (CODE)
CR-92679 03
(NASA CR OR TMX OR AD NUMBER) (CATEGORY)
FACILITY FORM 602

GPO PRICE $
CFSTI PRICE(S) $
Hard copy (HC) 3.00
Microfiche (MF) .65
ff 653 July 65

DECEMBER 1967

Distribution of this report is provided in the interest of information exchange. Responsibility for the contents resides in the author or organization that prepared it.

PREPARED UNDER CONTRACT NASW-1427

BY

ASTRO-ELECTRONICS DIVISION
DEFENSE ELECTRONIC PRODUCTS
RADIO CORPORATION OF AMERICA
PRINCETON, NEW JERSEY 08540

NATIONAL AERONAUTICS AND SPACE ADMINISTRATION

PRECEDING PAGE BLANK NOT FILMED.

ABSTRACT

This report contains a description of work done during the reporting period, a bibliography of further literature examined during the period, and a historical account of research on the photovoltaic effect and devices in which this effect is used for power generation covering the period 1940 to the present time.

TABLE OF CONTENTS

		Page
SUMMARY		1
I	CONTRACT WORK DURING THE REPORTING PERIOD	2
	A. Literature Search and Related Activities	2
	B. Organization of Written Material	3
	C. Remarks to the Present Report, Plans for Future Work	3
II	BIBLIOGRAPHY	4
	A. Published Papers	4
	B. Government Contract Reports	15
III	THE DEVELOPMENT OF PRACTICAL ENERGY CONVERSION DEVICES (1940 - 1955)	25
	A. Introduction	25
	B. Materials Technology	26
	1. Introduction	26
	2. Material Purification, Crystal Growth, and Semiconductor Properties	26
	3. Junction Formation	30
	C. Experimental Solar Cell Development	31
	1. Selenium and Germanium Photovoltaic Cells	31
	2. Silicon Cells	36
	3. Compound Semiconductor Photovoltaic Cells	41
	D. Development of the Theory	46
	1. Progress in Supporting Fields	46
	2. Continuation of Work on Rectification Theory	49
	3. Theory of Photovoltaic Cells	62
	E. The Electron-Voltaic Effect and Radiation Damage	74
	1. Semiconductor Damage and Annealing Studies	74
	2. The Electron-Voltaic Effect	74
IV	CONTEMPORARY DEVELOPMENTS (1955 - PRESENT)	78
	A. Theory	78
	1. Junction Characteristics	78
	2. Ultimate Conversion Efficiencies	88
	3. Power Loss Processes	104
	4. Heterojunctions	115

TABLE OF CONTENTS (Continued)

Page

B. Silicon Solar Cells 123
  1. Introduction 123
  2. Development of the Present Cell Types 124
  3. A Brief History of Various Unsuccessful or Incomplete Attempts at Cell Improvement 144
C. Compound Semiconductor Cells 150
  1. Gallium Arsenide 151
  2. GaP and GaP-GaAs Cells 160
  3. Other III-V Compounds 165
  4. Cadmium Sulfide 170
  5. Cadmium Telluride 176
  6. Other II-VI Semiconductors 179
  7. Summary 181
D. High-Voltage Photovoltaic Effect 181
E. Photoeffects in Organic Materials 188
  1. Electrical Conduction in Organic Solids 188
  2. Sensitization 192
  3. Photovoltaic Effects 194

REFERENCES 197

LIST OF ILLUSTRATIONS

Figure		Page
8.	"Photopeak" characteristic	33
9.	Photodiode structure, after Benzer	34
10.	Current-voltage characteristic of photodiode	35
11.	Representation of melt, showing photovoltaic barrier and photocell, after Ohl	36
12(a).	Spectral response (equal energy) of silicon photocell, after Ohl	37
12(b).	Illumination dependence of photocell current and voltage, after Ohl	37
13.	Blue shifted and "normal" ion-bombarded photocell responses, after Kingsbury and Ohl	39
14(a).	Cross section of Bell solar battery, after Chapin et al	40
14(b).	Intensity variation of Bell solar battery characteristics	40
15.	Photoresponse of an InAs photovoltaic cell at 77 °K, after Talley and Enright	42
16.	Current-voltage characteristic of GaAs photocell for different intensities, after Welker	43
17(a).	Variation of open-circuit voltage with intensity for GaAs photocell, after Gremmelmaier	44
17(b).	Variation of short-circuit current with intensity for GaAs photocell, after Gremmelmaier	44
18.	Spectral response of a CdS crystal with silver and indium electrodes, after Reynolds	45
19(a).	Band structure for intrinsic semiconductor	47
19(b).	Band structure for n-type semiconductor	47
19(c).	Band structure for p-type semiconductor	47
20.	Log(I) vs. V for usual experimental diode	52
21(a).	Energy levels at semiconductor surface	54
21(b).	Formation of band-bending at semiconductor surface, after Bardeen	54
22.	Band structures of semiconductor of various conductivity types	55

LIST OF ILLUSTRATIONS (Continued)

Figure		Page
23.	Energy levels in n-type semiconductor in thermal equilibrium, and with injected carriers	57
24.	Band structure and energy levels in a p-n junction at equilibrium and under forward bias, after Shockley	59
25.	Junction structure in PbS, after Sosnowski et al	63
26.	Simplified equivalent circuit of a photovoltaic cell	68
27.	Photovoltaic junction geometry, after Cummerow	70
28.	Schematic of electron-voltaic cell	75
29.	Energy band scheme for a semiconductor with trapping levels, after Sah et al	79
30.	Band structures in the three regions of a p-n junction with trapping levels, after Sah et al	82
31.	Band structure of a p-n junction under small forward bias	86
32.	Energy conversion system, after Müser	93
33.	Energy flow chart for a p-n junction photovoltaic cell	105
34.	Band diagram showing the effect of low carrier concentration in reducing V_{oc}	107
35(a).	Equivalent circuit for a solar cell	111
35(b).	Cross section of a solar cell, showing dimensions as used by Prince for R_s calculation	112
36.	Cell geometry used by Wolf for R_s calculation	113
37.	Current paths in a cell, as used by Handy for R_s calculation	115
38(a).	Band structure in a photovoltaic junction, barrier height = E_g	116
38(b).	The same, barrier height $< E_g$	116
39(a).	Band structure of a surface-barrier cell, equilibrium condition	117
39(b).	The same, under illumination	117
40.	Band structure of a heterojunction cell	119
41.	Band structures in a graded-bandgap semiconductor	120

LIST OF ILLUSTRATIONS (Continued)

Figure		Page
42.	Band structure of a graded bandgap p-n junction cell, (a) in equilibrium, (b) under illumination	121
43.	I-V characteristic of a graded-bandgap p-n junction cell	122
44.	Silicon solar cell circa 1958, after Prince and Wolf	132
45.	Popular cell types circa 1960	136
46.	Characteristics of typical gridded and nongridded silicon cells of equal efficiency, after Evans and Menetrey	137
47.	Comparison of the performance of n/p and Li-doped silicon sells under irradiation	143
48.	Band structure of a GaP-GaAs heterojunction solar cell	161
49.	Transitions occurring in a GaP cell to cause extrinsic spectral response, after Grimmeis	162
50.	Band diagram of a 'Mott Barrier'	179
51(a).	Disposition of crystallites in a CdTe film showing the high-voltage photoeffect, after Pensak	182
51(b).	Band structure of a CdTe film showing the high-voltage photoeffect, after Pensak	182
52.	Band structure leading to the high-voltage photoeffect, after Tauc	184
53.	Band structure leading to the high-voltage photoeffect, after Neumark	186
54.	Representation of the π orbital for a benzene ring	190
55.	The structure of TEA salt of TCNQ	190
56.	The structure of DPPH	191
57.	Cells for the investigation of conductivity in organic films	195

LIST OF SYMBOLS

The usage of the major symbols is consistent throughout this report, and this usage is indicated on the following list. However, because of the large number of variables needed, subscripts have been widely used. Where the subscripted symbols have unique meanings, these have been included on the list, but subscripts frequently have a local meaning, and where this has occurred a suitable indication and definition has been given in the test.

A empirical constant in diode equation, or a constant as designated

b ratio of electron to hole mobility

D carrier diffusion constant

E energy

E_F Fermi energy

ΔE energy difference

E_{fn} quasi-Fermi level for electrons

E_{fp} quasi-Fermi level for holes

g generation rate density

h Planck's constant

I current

I_d current through diode

I_m maximum-power current

I_o reverse saturation current in diode equation

I_{sc} short-circuit current

J current density or illumination intensity

J_o reverse saturation current density

k Boltzmann's constant

L diffusion length

m^* effective mass of carriers

N donor or acceptor level density

N_d donor density

N_a acceptor density

n_i density of holes and electrons in intrinsic semiconductor

n electron density

P probability of occupancy of an energy level

p hole density

P_{max} maximum power

q charge on electron

Q quantum efficiency

R_L load resistance

R_o resistance of diode at zero point

R_s series resistance

R_{sh} shunt resistance

T absolute temperature

U rate of loss of carriers

V potential difference

V_m maximum-power voltage

V_o barrier height

V_{oc} open-circuit voltage

W space charge region width

x spatial coordinate

α optical absorption constant or constant in diode equation

η efficiency

κ dielectric constant

μ carrier mobility

ψ electrostatic potential energy

τ lifetime

SUMMARY

The end product of this contract will be a review of the past research effort in the field of photovoltaic solar energy converter cells, and recommendations for further research and development efforts which would have a good chance of significant future advancements in this field. To arrive at these recommendations, all of the available information on relevant research and development efforts will be assembled. An evaluation and analysis of this material will provide the foundation on which recommendations for future research efforts can be based.

This report covers work performed in the period June 1, 1967 through November 30, 1967. During this period, the literature search and abstraction described in previous reports* have been continued, to cover Government contractor reports, fill gaps in the literature previously obtained, and keep up with new publications. The coverage of this search is now all but complete, and such gaps as are known to exist are detailed, and the efforts made to cover these are described. A bibliography lists those papers and reports which have been read and abstracted during the reporting period.

The main body of this report is a historical review of the scientific work performed on photovoltaic effects, and the development done on energy conversion devices using this effect, covering the period from 1940 to the present time. This historical account is complementary to the account published in Semiannual Report #2*, covering the period 1839-1940.

*Semiannual Reports #1 and 2, NASW-1427.

I. CONTRACT WORK DURING THE REPORTING PERIOD

A. Literature Search and Related Activities

During the past six months, the reading and abstracting activity described in the previous report has been continued, using the same indexing system. The papers and reports read during this period are listed below, and this bibliography, taken in conjunction with those published in the two previous reports, provides a complete tabulation of all papers, reports, and books on index at November 30th, 1967. It will be seen that a major effort has been made to obtain complete coverage of Government Contract Reports during the past six months, but full satisfaction has not yet been achieved in this direction. The reasons for this are twofold:

(i) The only classified and comprehensive index listing reports on photovoltaic energy conversion contracts sponsored by NASA and the Armed Services which has been discovered is the Power Information Center Index, whose coverage does not extend to work before 1960, and whose coverage appears to have not become complete until quite recently. Whereas it has been possible to obtain details of some contracts not listed in the PIC index because of the participation of personnel at RCA in this work, there remains the probability that some projects have not been accounted for.

(ii) The system for obtaining reports from both the Scientific and Technical Information Facility, and the Defense Documentation Center, has been difficult unless the Accession Number assigned to the report by these agencies was known. Since the PIC index does not give these accession numbers, and often does not give any identification for reports on a particular contract, it has been frequently difficult and sometimes impossible to obtain needed reports. This situation has been remedied for accessions by these agencies during the last two years by the provision of indices classifying reports by contract number, but for reports on work done before this time, the situation remains as described above. It appears that a solution would be for the PIC briefs to give report accession numbers as assigned by DDC or STIF, but the delay in assigning these numbers complicates the application of this solution.

In an effort to obtain reports, and also conference papers and other publications, contract monitors and a number of prominent workers in the photovoltaics field have been contacted directly during the past six months. In general, the response to these requests has been most helpful, and those working on this contract take this opportunity to express their gratitude to the following:

Mr. W. R. Cherry, Dr. D. A. Cusano, Prof. H. Y. Fan, Dr. P. Fang, Dr. A. Golubovic, Dr. W. King, Dr. E. Kittl, Prof. J. J. Loferski, Dr. M. B. Prince, Prof. Dr. H. J. Queisser, Mr. E. L. Ralph, Mr. P. Rappaport, Dr. D. C. Reynolds, Mr. M. Rodot, Mr. R. S. Schlotterbeck, Mr. F. A. Shirland, and Mr. R. I. Walker.

Translations of certain Russian papers not already available in English have been needed during the reporting period. The authors of this report are grateful to Prof. J. J. Loferski, himself an eminent contributor to the field, for performing such translations for the purposes of this report.

B. Organization of Written Material

It is planned that the historical accounts contained in Section II of Semiannual Report #2 and in Section III of this report, will be reprinted in the Final Report to provide a coherent history. To minimize duplication of production effort, and to minimize confusion, the numbering schemes for sections, figures, tables, and references in the historical section of this report have been made to follow on from those of the earlier historical account in Semiannual Report #2. In addition, the bibliography section of the present report is supplementary to the bibliographies of the previous reports.

C. Remarks to the Present Report, Plans for Future Work

This report is the last Semiannual Report, to be followed by the Final Report at the end of the contracting period.

Although Section IV of the historical review, covering the period from 1955 to the present, was not scheduled to appear until the Final Report, it has been included in this Semiannual Report in a preliminary form.

Section IV needs still to be brought to the technical and editorial level of the earlier chapters, and this preliminary version contains gaps, including the entire area of thin-film cell development, and possibly mis-statements. However, since many of the readers of this report have been contributors to the field of photovoltaic solar energy conversion during the period covered in this section, or have otherwise been intimately connected with this field, and since this semiannual report presents the last chance to stimulate feedback of comments from and discussion with these readers before the end of the contract, the authors of this report have thought it to be beneficial to include this preliminary version in the present report.

They therefore not only invite, but even urge the readers to please contact them, with comments, suggestions, or additional material, so that their contributions may be incorporated into the final version.

The Final Report is then planned to include the complete historical review, a summary account of the technical evaluation, and recommendations towards future potentially fruitful areas of research and development.

II. BIBLIOGRAPHY

A. Published Papers

Adirovich, E. I.
"Relaxation of Anomalously Large Photovoltages in Cadmium Telluride Films"
Sov. Phys. Doklady 12, 226 (1967).

Armstrong, L. D.
"P-N Junctions by Impurity Introduction through an Intermediate Layer"
Proc. IRE 40, 1341 (1952).

Bardsley, A.
"Some Recent Improvements in the Economics of Solar Energy Conversion by Silicon Photovoltaic Cells"
(Publication information on this paper is not available.)

Becker, M.
"Photovoltaic Effect of P-N Junctions in Germanium"
Phys. Rev. 78, 301 (1950).

Beckman, W. A.
"An Experimental High Flux Solar Power System"
Proc. 20th Annual Power Sources Conf., p. 190 (1966).

Benzer, S.
"High Voltage and Photosensitive Characteristics in Germanium"
Phys. Rev. 69, 683 (1946).

Benzer, S.
"High Inverse Voltage Germanium Rectifiers"
J. Appl. Phys. 20, 804 (1949)

Berman, P.
"Improved Solar Cells for use in Concentrated Sunlight"
Proc. 18th Annual Power Sources Conf. (1964).

Bernard, J.
"Sur le Mécanisme de L'Effet Photovoltaique dans les Photopiles au Tellurure de Cadmium"
Revue de Physique Appliquée 1, 211 (1966).

Brattain, W. H.
"Changes in Conductivity of Germanium Induced by Alpha-Particle Bombardment"
Phys. Rev. 80, 846 (1950).

Bugai, A. A.
"Large Area Germanium Photocells with Diffused p-n Junctions"
Proc. Conf. Kiev (1957).

Bujatti, M.
"Photovoltaic Effect in a Metal-Semiconductor Junction"
Proc. IEEE 55, 1634 (1967).

Burton, J. A.
"The Distribution of Solute in Crystals Grown from the Melt. Part I. Theoretical"
J. Chem. Phys. 21, 1987 (1953).

Burton, J. A.
"Distribution of Solute in Crystals Grown from the Melt. Part II Experimental"
J. Chem. Phys. 21, 1991 (1953).

Burton, J. A.
"Effect of Nickel and Copper Impurities on the Recombination of Holes and Electrons in Germanium"
J. Phys. Chem. 57, 853 (1953).

Burton, J. A.
"Impurity Centers in Ge and Si"
Physica 20, 845 (1954).

Butcher, O. C.
"Development Status of Solar Generators Based on Silicon Photovoltaic Cells"
(Publication information on this paper is not available.)

Cherry, W. R. (Chairman)
"Radiation-Resistant Solar Cells" - A Panel Discussion
Proc. 16th Annual Power Sources Conf. (1962).

Cherry, W. R.
"Solar Energy Systems for Space Application"
Proc. 17th Annual Power Sources Conf. (1963).

Cherry, W. R.
"Large Area Solar Cells"
Proc. 13th Annual Power Sources Conf., p. 62 (1959).

Cleland, J. W.
"The Effect of Fast Neutron Bombardment on the Electrical Properties of Germanium"
Phys. Rev. 83, 312 (1951).

Crawford, J. H.
"Energy Levels in Ge Produced by Nucleon Bombardment"
Phys. Rev. 86, 641 (1952).

Cusano, D. A.
"CdTe Hole Lifetime from the Photovoltaic Effect"
Solid State Comm. 2, 125 (1964).

Cusano, D. A.
"Photovoltaic Effects"
Physics and Chemistry of II-VI Compounds, (John Wiley and Sons, Inc., New York, 1967) pp. 753-760.

Dale, B.
"High Efficiency Silicon Solar Cells"
Proc. 14th Annual Power Sources Conf., p. 22 (1960).

David, J. P.
"Etude de la Preparation et des Propriétés Electriques de Couches Minces Semiconductrices d'Antimonide d'Aluminum"
Revue de Physique Appliquée 1, 172 (1966).

Davis, R. E.
"Neutron-Bombarded Germanium Semiconductors"
Phys. Rev. 74, 1255 (1948).

Desvigues, F.
"Aspects Economiques de la Fabrication et de l'Utilisation des Cellules Solaires"
Acta Electronica 5, 379 (1961).

Ehrenreich, H.
"Theoretical Considerations in Solar Cell Design"
General Electric Lab. Report No. 59-RL-2220, May 1959.

Elliott, J. F.
"Large Area Film Type Solar Cells"
Proc. 15th Annual Power Sources Conf., p. 109 (1961).

Esposito, R.
"Concerning the Possibility of Observing Life Time-Gradient and Dember Photovoltages in Semiconductors"
J. Appl. Phys. 38, 825 (1967).

Georgobiani, A. N.
"Electrical and Photoelectric Properties of P-N Junctions in Zinc Sulfide"
Sov. Phys. Semiconductors 1, 270 (1967).

Gosar, P.
"Sur l'Effet Photovoltaique Lateral dans les Jonctions P-N"
Comptes Rendus 247, 1975 (1958).

Gosar, P.
"Forces Photo-Magnetomécaniques sur les Jonctions p-n soumise à un Eclairement non uniforme"
Compt. Rend. 248,(1959).

Gosar, P.
"Sur la Mesure de Duree de Vie des Porteurs Minoritaires par l'Effet Photovoltaique à la Surface"
Compt. Rend. 249, (1959).

Hall, R. N.
"Segregation of Impurities During the Growth of Germanium and Silicon Crystals"
J. Phys. Chem 57, 836 (1953).

Hall, R. N.
"Recrystallization Purification of Germanium"
Phys. Rev. 78, 645 (1950).

Handy, R. J.
"Theoretical Analysis of the Series Resistance of a Solar Cell"
Solid State Electronics 10, 765 (1967).

Heeger, A. J.
"The Solar Cell-Conditions for Optimum Performance"
Solar Energy 3, 12 (1959).

Herchakowski, A.
"Design Considerations for Photovoltaic Conversion System using Concentrators"
Proc. 15th Annual Power Sources Conf. (1961).

Hietanen, J. R.
"The Status of the Clevite CdS Thin Film Solar Cell"
Record, Sixth Photovoltaic Specialists' Conf. (1967).

Hunrath, G.
"Solar Power Supplies for Ground Use"
Proc. 17th Annual Power Sources Conf. (1963).

Hunter, G. S.
"Requirements for Solar Arrays Spurring New Techniques"
Aviation Week and Space Tech., Aug. 14, 1967.

Hunter, G. S.
"Cell Studies Spur Solar Power Advances"
Aviation Week and Space Tech., Aug. 28, 1967.

Ignatyuk, V. A.
"High-Voltage Photo-Emf in Epitaxial Films of Zinc Telluride"
Sov. Phys. Solid State 8, 2929 (1967).

Ikushima, H.
"Structure and Electrical Properties of Thin Oxide Film Diode with Sputtered Titanium Base"
Japanese J. Appl. Phys. 6, 906 (1967).

Kajiyama, K.
"Electrical and Optical Properties of SnO_2-Si Heterojunctions"
Japanese J. Appl. Phys. 6, 905 (1967).

Keck, P. H.
"Crystallization of Silicon from a Floating Liquid Zone"
Phys. Rev. 89, 1297 (1953).

Klontz, E. E.
"Displacements Produced by Electron Bombardment of Germanium"
Phys. Rev. 86, 643 (1952).

Klontz, E. E. et al
"Electron Bombardment of Ge"
Phys. Rev. 82, 763 (1951).

Komashcenko, V. N.
"Nature of the Photo-Barrier Effect in Cadmium Selenide"
Sov. Phys. - Semiconductors 1, 411 (1967).

Lamond, P.
"Recent Advances in N on P Cells"
Proc. 15th Annual Power Sources Conf., p. 106 (1961).

Lamorte, M. F.
"New Solar Cell Developments, Part I"
Proc. 16th Annual Power Sources Conf. (1962).

Lark-Horovitz, K.
"Deuteron Bombarded Semiconductors"
Phys. Rev. 73, 1256 (1948).

Loferski, J.
"Recent Solar Converter Research"
Proc. 13th Annual Power Sources Conf., p. 59 (1959).

Loferski, J. J.
Notes on Radiation Damage Effects on Solar Cells
(Course of lectures, Brown Univ., Providence, R. I. 1967).

Loferski, J. J.
"Recent Research on Photovoltaic Solar Energy Converters"
Proc. IRE 51, 672 (1963).

Magee, V.
"Radiation Resistant High Efficiency Silicon Solar Cells for Space Vehicle Power Supplies"
Paper presented at IEE Conf. on Components and Materials used in Electronic Engineering London May 17-20 (1965).

Mandelkorn, J.
"Comparison of p-n and n-p Silicon Solar Cells"
Proc. 14th Annual Power Sources Conf. (1960).

Mandelkorn, J.
"Fabrication and Characteristics of Phosphorus-Diffused Silicon Solar Cells"
J. Electrochem. Soc. 109, 313 (1962).

Mandelkorn, J.
"Behaviour of Modified Radiation-Resistant Solar Cells"
Proc. 15th Annual Power Sources Conf., p. 102 (1961).

Mandelkorn, J.
"New Silicon Solar Cell for Space Use"
Proc. 20th Annual Power Sources Conf., p. 194 (1966).

Mandelkorn, J.
"Improved Solar Cell"
Proc. 19th Annual Power Sources Conf. (1965).

Mann, A. E.
"Spectrally Selective Optical Coatings"
Proc. 14th Annual Power Sources Conf. (1960).

Martin, J. H.
"Some Effects of Electron Irradiation and Temperature on Solar Cell Performance"
Proc. 17th Annual Power Sources Conf. (1963).

Martin, J. H.
"Radiation Damage to Thin Silicon Cells"
Photovoltaic Workshop, Intersoc, Energy Conversion Engineering Conf. (1967).

Matlow, S. L.
"A Low-Resistance Ohmic Contact for Silicon Semiconductor Devices"
Solid-State Electronics 2, 202 (1961).

Matlow, S. L.
"Ohmic Aluminum n-Type Silicon Contact"
J. Appl. Phys. 30, 541 (1959).

NASA-Goddard Space Flight Center Report #X-710-67-412
"ATS-1 Solar Cell Radiation Damage Experiment, first 120 days" (Aug. 1967).

Nasledov, D. N.
"Gallium Arsenide Photocells"
Proc. of Conf. in Kiev (1957).

Naumov, G. P.
"The Efficiency of Transformation of Direct Solar Radiation Energy into Electric Energy using a CdTe Photocell"
Sov. Phys. Solid State 3, 2714 (1962).

Okimura, H.
"Photovoltaic Properties of CdS-P-Si Heterojunction Cells"
Japanese J. Appl. Phys. 6, 908 (1967).

Pearson, G. L.
"Silicon P-N Junction Alloy Diodes"
Proc. IRE 40, 1348 (1952).

Pfann, W. G.
"Principles of Zone-Melting"
J. Metals 4, 747 (1952).

Prince, M. B.
"New Developments in Silicon Photovoltaic Devices"
J. Brit. IRE 18, 583 (1958).

Prince, M. B.
"Latest Developments in the Field of Photovoltaic Conversion of Solar Energy"
U. N. Conf. on New Sources of Energy (1961).

Prince, M. B.
"Large Area Silicon Solar Cells"
Proc. 14th Annual Power Sources Conf., p. 26 (1960).

Prystaloski, D. F.
"Measurement Techniques for Silicon Solar Cells"
Proc. 20th Annual Power Sources Conf. (1966).

Queisser, H. J.
"Stacking Faults in Epitaxial Silicon"
J. Appl. Phys. 33, 1536 (1962).

Queisser, H. J.
"Some Theoretical Aspects of the Physics of Solar Cells"
Energy Conversion for Space Power (Academic Press, Inc., New York, 1961) pp. 317-323.

Queisser, H. J.
"Creation and Motion of Dislocations in Silicon Surface Layers"
Disc. Faraday Soc. 38, 305 (1964).

Queisser, H. J.
"Diffused Three-Layer Structures along Small Angle Grain Boundaries in Silicon"
IRE Solid-State Devices Conf. (1961).

Raisbeck, G.
"The Solar Battery"
Scientific American, Dec. 1965.

Ralph, E. L.
"Pre-Flight Calibration and Matching of Solar Cells for a Band-Pass Filter Experiment"
(Publication information on this paper is not available.)

Ralph, E. L.
"Some Considerations Regarding the Production of Improved Solar Cells"
Proc. 5th Photovoltaic Specialists' Conf. (1965).

Ralph, E. L.
"The Infrared Transmissivity of Silicon Crystals and Silicon Solar Cells in the Wavelength Range of 0.5 μ to 10 μ"
Final Report - Internal Project - Hoffman, August 1960.

Ralph, E. L.
"Use of Concentrated Sunlight with Solar Cells for Terrestrial Applications"
Solar Energy Soc. Ann. Meeting, Phoenix (1965).

Ralph, E. L.
"Radiation Effects on Polycrystalline Solar Cells"
Proc. 18th Annual Power Sources Conf. (1963).

Rappaport, P.
"The Photovoltaic Effect and its Utilization"
Proc. Adv. Energy Sources Conf. (1958).

Rappaport, P.
"Photoelectric Processes"
Advanced Energy Conversion 1, 3 (1961).

Rappaport, P.
"The Revolution in Electrical Energy Sources"
RCA Engineer 11, 42, (1962).

Rappaport, P.
"Minority Carrier Lifetime in Semiconductors as a Sensitive Indicator of Radiation Damage"
Phys. Rev. 94, 1409 (1954).

Rappaport, P.
"Photovoltaics for Space Applications"
Proc. AIChE - I Chem E Joint Meeting London 1965 "Materials Associated with Direct Energy Conversion".

Rappaport, P.
"Photovoltaic Power"
J. Spacecraft and Rockets 4, 838 (1967).

Reynolds, D. C.
"Photovoltaic Solar Converters"
First Suppl. to Encyclopedia of Chemical Technology, (Interscience. Publ., New York 1957).

Riel, R. K.
"Large Area Solar Cells Prepared on Silicon Sheet"
Proc. 17th Annual Power Sources Conf. (1963).

Rodot, M.
"Conversion d'Energie Solaire en Energie Electrique et Mécanique: les Photopiles Solaires"
J. des Recherches du CNRS 65, 621 (1964).

Scaff, J. H.
"Development of Silicon Crystal Rectifiers for Microwave Radar Receivers"
Bell Syst. Tech. J. 26, (1947).

Scaff, J. H.
"P-Type and N-Type Silicon and the Formation of the Photovoltaic Barrier in Silicon Ingots"
Trans. AIME 185, 383 (1949).

Schoffer, P.
"High Power Density Solar Photovoltaic Conversion"
Proc. 18th Annual Power Sources Conf. (1964).

Shirland, F. A. and Augustine, F.
"Thin Film Plastic Substrate CdS Solar Cells"
Paper presented at Fifth Photovoltaic Specialists' Conf. (1965).

Shirland, F. A. and Hietanen, J. R.
"Thin Film CdS Solar Cell"
Paper presented at Fifth Photovoltaic Specialists' Conf. (1965).

Shirland, F. A.
"The History, Design, Fabrication and Performance of CdS Thin Film Solar Cells"
Adv. Energy Conv. 6, 201 (1966).

Shirland, F. A.
"Low Cost Thin Film CdS Solar Cells"
Paper presented at Ann. Meeting Solar Energy Soc., Phoenix, March 1965.

Taylor, W. E.
"Comparison of Thermally Induced Lattice Defects in Germanium and Silicon with Defects Produced by Nucleon Bombardment"
Phys. Rev. 86, 642 (1952).

Teal, G. K.
"Growth of Germanium Single Crystals"
Phys. Rev. 78, 647 (1950).

Valdman, H.
"Photopiles et Thermopiles de haut Rendement"
Comm. du Colloque International Sur Les Dispositifs à Semiconducteurs (1961).

Valdman, H.
"Preparation et Etude des Piles solaires au Silicium de haut Rendement"
Compt. Rend. 252, 246 (1961).

Velde, T. S.
"Mono-grain Layer Solar Cells"
Paper given at 29th Meeting of Propulsion and Energetics Panel, AGARD, Liège
Belgium, June 1967.

Waldner, N.
"Characteristics of Silicon p-n Junctions formed by Sodium and Cesium Ion Bombardment"
Solid State Elec. 7, 925 (1964).

Welker, H.
"Semiconducting Intermetallic Compounds"
Physica 20, 893 (1954).

Welker, H.
"Neuere Untersuchungen der Halbleitereigenschaften von III-V Verbindungen"
Scientia Electrica 1, 152 (1954).

Welker, H.
"Über Neue Halbleitende Verbindungen II"
Z. Naturforsch. 8a, 248 (1953).

Wise, J. F.
"Progress in Thin Film Photovoltaic Cell Development"
Proc. 18th Annual Power Sources Conf. (1964).

Wolf, M.
"Recent Investigations Towards Silicon Solar Cell Improvement"
Proc. AIChE - I ChemE Joint Meeting, London, 1965; "Materials Associated with Direct
Energy Conversion".

Wolf, M.
"Effect of Thickness on Short-Circuit Current"
Proc. 4th Photovoltaic Specialists' Conf. (1964).

B. Government Contract Reports

Celvite Corp.
NAS3-8502, "Study of Thin-Film Large Area Photovoltaic Solar Energy Converter"
Final Report, NASA CR 72159, December 1966.

Celvite Corp.
NAS3-6461, "Development of Cadmium Sulfide Thin-Film Photovoltaic Cells"
NASA CR-54806 (1966).

Clevite Corp.
NAS3-2795, "Study of Thin Film Large Area Photovoltaic Solar Energy Converter"
Second Quarterly Report, Jan. 1, 1964 to March 31, 1964.

Clevite Corp.
NAS3-2795, "Study of Thin Film Large Area Photovoltaic Solar Energy Converter"
Third Quarterly Report, Apr. 1, 1964 to June 30, 1964.

Clevite Corp.
NAS3-2795, "Study of Thin Film Large Area Photovoltaic Solar Energy Converter"
Final Report, Oct. 1, 1963 to Sept. 30, 1964.

Electro-Optical Systems, Inc.
AF33(616)-7482, "Research on Materials Exhibiting Photovoltaic Phenomena"
Final Report ASD-TDR-62-841, Jan. 1963.

Electro-Optical Systems, Inc.
AF33(616)-6791, "Energy conversion systems reference handbook. Vol. 5 direct solar conversion"
Final Report, Sept. 1960.

General Atomic
NAS7-91, "Radiation Effects on Silicon Solar Cells"
GA-4797, Dec. 1963.

General Electric Co.
AF33(615)-2695, "Thin Film Photovoltaic Cell Array Investigation"
Quarterly Report No. 1, June 1965 to Aug. 1965.

General Electric Co.
AF33(616)-8308, "CdTe Research for Solar Energy Conversion Application"
Final Report, May 15, 1961 to May 15, 1962.

General Electric Co.
AF33(657)-10601, "Research on Thin Film Polycrystalline Solar Cells"
Interim Report No. 1, Sept. 1962-Dec. 1962.

General Electric Co.
AF33(657)-10601, "Research on Thin Film Polycrystalline Solar Cells"
Quarterly Report No. 5, Oct. 1963 through Dec. 1963.

General Electric Co.
AF33(657)-10601, "Research on Thin Film Polycrystalline Solar Cells"
Final Report, Sept. 1, 1962 to Dec. 31, 1964.

Harshaw Chemical Co.
AF33(615)-1248, "Investigation of CdS Thin-Film Solar Cells"
Annual Report, Nov. 1963 to Dec. 1964.

Harshaw Chemical Co.
AF33(616)-3466, "Photovoltaic Cadmium Sulfide"
Final Report, March 1958 to May 1960.

Harshaw Chemical Co.
AF33(657)-7916, "Research on Photovoltaic Cells"
Seventh Quarterly Report, Feb. 1964.

Harshaw Chemical Company
AF33(657)-7916, "Research on Photovoltaic Cells"
Interim Report, May 1, 1963 to April 30, 1964.

Harshaw Chemical Company
AF33(657)-7916, "Research on Photovoltaic Cells"
Final Report, May 1, 1962 to April 30, 1965.

Harshaw Chemical Co.
AF33(657)-9975, "Investigation of Thin Film Cadmium Sulfide Solar Cells"
Final Report, Sept. 1962 to Nov. 1963.

Harshaw Chemical Co.
NAS3-4177, "Research and Development in CdS Photovoltaic Film Cells"
First Quarterly Report, May 19, 1964 to Aug. 19, 1964.

Harshaw Chemical Co.
NAS3-4177 "Research and Development in CdS Photovoltaic Cells"
Second Quarterly Report, Aug. 19, 1964 to Nov. 19, 1964.

Harshaw Chemical Co.
NAS3-4177, "Research and Development in CdS Photovoltaic Film Cells"
Final Report May 19, 1964 to May 19, 1965.

Harshaw Chemical Co.
NAS3-2493, "The Manufacture of Cadmium Sulfide Thin Film Solar Cells at the Rates of 1 Kilowatt per Month and 5 Kilowatts per Month"
May 29, 1964.

Harshaw Chemical Co.
NAS3-2493, "Research and Development in CdS Photovoltaic Film Cells"
Final Report, May 29, 1962 to June 19, 1964.

Harshaw Chemical Co.
NAS3-7631 "Research and Development in CdS Photovoltaic Film Cells"
NASA CR-54856, First Quarterly Report, June 28, 1965 to Sept. 28, 1965.

Harshaw Chemical Co.
NAS3-7631, "Research and Development in CdS Photovoltaic Film Cells"
Second Quarterly Report, Sept. 28, 1965 to Dec. 29, 1965.

Harshaw Chemical Co.
NAS3-6464, "Development of Optical Coatings for CdS Thin-Film Solar Cells"
NASA CR-54336, First Quarterly Report, Dec. 2, 1964 to March 1, 1965.

Harshaw Chemical Co.
NAS3-6464, "Development of Optical Coating for CdS Thin-Film Solar Cells"
Second Quarterly Report, March, 1, 1965 to June 1, 1965.

Harshaw Chemical Co.
NAS3-6464, "Development of Optical Coatings for CdS Thin-Film Solar Cells"
Third Quarterly Report, June 1, 1965 to August 1, 1965.

Harshaw Chemical Co.
NAS3-6464, "Development of Optical Coatings for CdS Thin-Film Solar Cells"
Final Report, December 1965.

Heliotek
DA-36-039-SC-90777, "High Efficiency Silicon Solar Cells"
Second Quarterly Report, Sept. 1962 to Dec. 1962.

Heliotek
DA-36-039-SC-90777, "High Efficiency Silicon Solar Cells"
3rd Quarterly Report, Dec. 1962 to March 1963.

Heliotek
AD-36-039-SC-90777, "High Efficiency Silicon Solar Cells"
Final Report, June 15, 1962 to July 15, 1964

Hoffman Electronics Corp.
"Methods for Improving Efficiency of Silicon Solar Cells"
Proposal from Hoffman Science Center, Santa Barbara, Calif.

Hoffman Electronics Corp.
AF33(600)-40497, "Pilot Line Production of High Efficiency Solar Cells"
Interim Report #2, 1 April 1960 to 30 June 1960.

Hoffman Electronics Corp.
AF33(616)-7946, "Solar Energy Measurement Techniques"
Final Report, May 1961 to Aug. 1962.

Ion Physics Corp.
AF33(615)-2292, "Ion Implantation Junction Techniques"
Quarterly Report No. 2, Feb. 1, 1965 to April 15, 1965.

Ion Physics Corp.
AF33(615)-2292, "Ion Implantation Junction Techniques"
Third Quarterly Report, May 1965 to August 1965.

Ion Physics Corp.
NAS5-10236 "Solar Cell Cover Glass Development"
2nd Quarterly Report, Sept. 1, 1966 to Nov. 30, 1966.

Monsanto Research Corp.
NAS3-2776 "Development of Improved Single Crystal GaP Solar Cells"
Final Report, June 12, 1963 to Aug. 12, 1964.

NASA-LEWIS
NASA TN D-3849, "Mechanism of CdS Film Cell"

NASA-LEWIS
"Conventional and Thin Film Solar Cells"
NASA Special Publication SP-131, pp. 55-72, August 1966.

NASA-LEWIS
NAS TN D-2508 "Calibration of Solar Cells Using High-Altitude Aircraft"

NASA-LEWIS
NASA-TN-D-2562, "Filter Wheel Solar Simulator"

NASA-LEWIS
NASA TN D-2711, "Effects of Impurities on Radiation Damage of Silicon Solar Cells"

NASA-LEWIS
NASA TN D-3556, "Thermal Cycling of Thin-Film Cadmium Sulfide Solar Cells"

NASA-LEWIS
NASA TN D-3663 "Effect of Moisture on Cadmium Sulfide Solar Cells"

NASA-LEWIS RESEARCH CENTER
NASA TN D-3788, "Comparison of Solar Direct-Energy Conversion Systems Operating between 1.0 and 0.1 Astronomical Units"

NASA-GSFC
X-710-67-412, "ATS-1 Solar Cell Radiation Damage Experiment, First 120 Days"
NASA Report, Aug, 1967.

NASA-GSFC
NASA TMX-55049, "The Electrical Characteristics of Irradiated Silicon Solar Cells as a Function of Temperature"
March 30, 1964.

NASA-GSFC
NASA TM X-55098, "Post Irradiation Room Temperature Electrical Characteristics of N/P Silicon Solar Cells"

RCA Astro-Electronics Division
AF33(616)-7415 "Solar Cell Array Optimization"
Interim Technical Report, July 1960 to March 1961.

RCA Astro-Electronics Division
AF33(657)-8490 "Applied Research Program on High Temperature Radiation Resistant Solar Array"
First Quarterly Report, May to July 1962.

RCA Astro-Electronics Division
AF33(657)-8490 "Applied Research Program on High Temperature Radiation Resistant Solar Cell Array Vol. 1"
First Year Report, April 1962 to April 1963.

RCA Astro-Electronics Division
AF33(657)-8490, "Applied Research Program on High Temperature Radiation Resistant Solar Cell Array, Vol. II"
Final Report, April 1963 to October 1963.

RCA Laboratories
DA-36-039-SC-64643 "Investigation of Materials for Photovoltaic Solar Energy Converters
First Interim Report, April 15 to July 15, 1955.

RCA Laboratories
DA-36-039-SC-64643, "Investigation of Materials for Photovoltaic Solar Energy Converters"
Second Interim Report, July 16, 1955 to Jan. 31, 1956.

RCA Laboratories
DA-36-039-SC-64643, "Investigation of Materials for Photovoltaic Solar Energy Converters"
Third Interim Report, Feb. 1, 1956 to June 30, 1956.

RCA Laboratories
DA-36-039-SC-64643, "Investigation of Materials for Photovoltaic Solar Energy Converters"
Fourth Interim Report, July 1, 1956 to Oct. 31, 1956.

RCA Laboratories
DA-36-039-SC-64643 "Investigation of Materials for Photovoltaic Solar Energy Converters"
Fifth Interim Report, Nov. 1, 1956 to Feb. 28, 1957.

RCA Laboratories
DA-36-039-SC-64643 "Investigation of Materials for Photovoltaic Solar Energy Converters"
Final Report, April 15, 1955 to Aug. 31, 1957.

RCA Laboratories
DA36-039-SC-78184 "Investigation of High Temperature, Improved Efficiency Photovoltaic Solar Energy Converter"
Fourth Triannual Progress Report, July 15, 1959 to Nov. 15, 1959.

RCA Laboratories
DA36-039-SC-78184, "High Temperature, Improved Efficiency, Photovoltaic Solar Energy Converter"
Final Report, July 15, 1958 to Oct. 31, 1960.

RCA Laboratories
DA36-039-SC-87414, "Semiconductor Photovoltaic Conversion"
First Triannual Report, Nov. 1, 1960 to Feb 28, 1961.

RCA Laboratories
DA36-039-SC-87414 "Semiconductor Photovoltaic Conversion"
Second Triannual Report, March 1, 1961 to June 30, 1961.

RCA Laboratories
DA36-039-SC-87417, "Semiconductor Photovoltaic Conversion"
Final Triannual Report, Nov. 1961.

RCA Laboratories
AF33(615)-2259, "Improved Thin-Film Solar Cells"
Quarterly Report No. 1, Nov. 1964 to Feb. 1965.

RCA Laboratories
AF33(615)-2259, "Improved Thin-Film Solar Cells"
Quarterly Report No. 2, Feb. 1965 to May 1965.

RCA Laboratories
AF33(615)-2259, "Improved Thin-Film Solar Cells"
Quarterly Report No. 3, May 1965 to August 1965.

RCA Laboratories
AF33(615)-2259, "Improved Thin-Film Solar Cells"
Final Report, Nov. 1964 to Nov. 1965.

RCA Laboratories
AF33(615)-3486, "Advanced Thin-Film Solar Cells"
First Quarterly Report, Nov. 1965 to Feb. 1966.

RCA Laboratories
AF33(615)-3486, "Advanced Thin-Film Solar Cells"
Second Quarterly Report, March 1966 to May 1966.

RCA Laboratories
AF33(615)-3486, "Advanced Thin-Film Solar Cells"
Third Quarterly Report, June 1966 to Augusut 1966.

RCA Laboratories
AF33(615)-3486, "Advanced Thin-Film Solar Cells"
Final Report, Nov. 1965 to Nov. 1966.

RCA Laboratories
NAS7-202, "Thin Film Large Area Photovoltaic Solar Cells"
First Quarterly Report, 1 Oct. 1962 to 31 Dec. 1962.

RCA Laboratories
NAS7-202, "Thin Film Large Area Photovoltaic Solar Cells"
Second Quarterly Report, Jan 1, 1963 to March 31, 1963.

RCA Laboratories
NAS7-202, "Thin Film Large Area Photovoltaic Solar Cells"
Third Quarterly Report, April 1, 1963 to June 30, 1963.

RCA Laboratories
NAS7-202, "Thin Film Large Area Photovoltaic Solar Cells"
Fourth Quarterly Report, July 1, 1963 to Sept. 30, 1963.

RCA Laboratories
NAS3-2796, "Materials and Methods for Large Area Solar Cells"
Midpoint Report, Oct 1, 1963 to March 31, 1964.

RCA Laboratories
NAS7-202 and NAS3-2796, "Materials and Methods for Large Area Solar Cells"
Final Report, Oct. 1, 1962 to Sept. 30, 1964.

RCA Laboratories
NAS3-6466, "Thin Film Photovoltaic Solar Energy Converters"
Midpoint Report, Dec. 17, 1964 to June 16, 1965.

RCA Laboratories
NAS3-6466, "Thin Film Photovoltaic Solar Energy Converters"
Final Report, Dec. 17, 1964 to Dec. 16, 1965.

RCA Laboratories
NAS3-8510, "Thin Film GaAs Photovoltaic Solar Energy Cells"
Midpoint Report, Nov. 17, 1966.

RCA Laboratories
NAS3-8510, "Thin Film GaAs Photovoltaic Solar Energy Cells"
Final Report, Aug. 28, 1967.

RCA Mountaintop
NAS5-3686, "Research and Development Study on Improved Radiation Resistance and Conversion Efficiency of Silicon Solar Cells"
First Quarterly Report, Feb. 20, 1964 to May 31, 1964.

RCA Mountaintop
NAS5-3686, "Research and Development Study on Improved Radiation Resistance and Conversion Efficiency of Silicon Solar Cells"
Third Quarterly Report, Aug. 31, 1964 to Nov. 30, 1964.

RCA Mountaintop
NAS5-3812, "Research and Development Study on Improvement of Advanced Radiation-Resistant Modularization Techniques"
Final Report, May 15, 1964 to Nov. 30, 1964.

RCA Mountaintop
NAS5-9576, "Materials Development for Solar Cell Applications"
First Quarterly Report, June 1, 1965 to Aug. 31, 1965.

RCA Somerville
AF33(616)-6615 "Gallium Arsenide Solar Cell"
Scientific Report No. 6, Sept. 1960 to Dec. 1960.

RCA Somerville
AF33(616)-6615 "Gallium Arsenide Solar Cell"
Scientific Report No. 7, Dec. 1960 to Feb. 1961.

RCA Somerville
AF33(616)-6615, "Gallium Arsenide Solar Cell"
Scientific Report No. 9, June 1961 to Aug. 1961.

RCA Somerville
AF33(616)-6615, "Gallium Arsenide Solar Cell"
Scientific Report No. 11, undated.

RCA Somerville
AF33(616)-6615, "Development of Improved Solar Energy Converters from Gallium Arsenide"
Final Report, April 1959 to May 1962.

RCA Somerville
AF33(657)-8921, "Applications Report on Manufacturing Methods Program for Gallium Arsenide Solar Cells"
Applications Technical Documentary Report, 15 June (?) to 28 Feb. 1964.

RCA Somerville
AF33(657)-8921, "Manufacturing Methods Program for Gallium Arsenide Solar Cells"
Final Report, 15 June (?) to 28 Feb. 1964.

Shockley Transistor
AF33(616)-6707, "Research Study of Photovoltaic Solar Cell Parameters"
ASD-TDR-61-423.

Shockley Transistor
AF33(616)-7785, "A Study of Photovoltaic Solar Cell Parameters"
ASD-TDR-62-776, Final Report, Dec. 15, 1960 to Dec. 15, 1961.

Texas Instruments, Inc.
NAS5-9609, "Advancement in the State-of-the-Art in the Production of Drift Field Solar Cells"
Fourth Monthly Report, Oct. 1965.

Texas Instruments, Inc.
NAS5-10319, "Solar Cell Integral Cover-Glass Development"
First Quarterly Progress Report, Feb. 1967 to May 1967.

U. S. Navy-Marine Engineering Laboratory
Technical Memorandum 3/67, Assignment No. 91 195 "A Compilation of Selected Data on Solar Radiation at Sea Level"

Westinghouse Electric Corporation
AF33(657)-7649, "Research on Improved Solar Generator"
Final Report, Oct. 1961 to Oct. 1962.

Westinghouse Electric Corp.
AF33(657)-11274, "Manufacturing Methods for Silicon Dendrite Solar Cells"
Final Report, May 1963 to July 1965.

III. THE DEVELOPMENT OF PRACTICAL ENERGY CONVERSION DEVICES (1940-1955)

A. Introduction

As described in Section II*, the progress made before 1940 concerned devices made mainly with copper oxide or selenium, and these were intended for detection purposes rather than energy conversion. However, the experimental work had provided enough background that the fundamentals of semiconductor theory and photovoltaic effect analysis could also be established. During the late 1930's and early 1940's, the need for microwave mixer and detector diodes for radar equipment provided a great stimulus for experimental work on silicon, and also created an active interest in the development of a theory to permit analysis of semiconductor point-contact diodes made of this material. The resulting cooperative effort between industrial laboratories and academic institutions, coordinated by the M.I.T. Radiation Laboratory, produced great progress in the materials technology of silicon, and advances in the theory of semiconductor and rectifier properties.

Building on the earlier theoretical work, and from the experimental measurements made on germanium and silicon devices, Shockley developed the diffusion theory of p-n junction rectification and transistor theory, which has been most widely used for device analysis. The technology advances made during the early 1940's were extended to allow development of the transistor as a practical device, which in turn prompted an intensified program of semiconductor research. This ultimately provided the materials technology for growing large single crystals of silicon, and the solid-state diffusion process, which were combined to produce the first practical solar cell in 1954.

During the 1950's, compound semiconductors began to receive attention again, after the earlier work of the 1930's had been overshadowed by the results with silicon and germanium. Thus, almost simultaneously with the announcement of the silicon solar cell, Reynolds obtained good energy conversion efficiency with the CdS solar cell, and early reports of photovoltaic measurements on III-V semiconductor compounds also began to appear.

During the years 1940-1955, therefore, a very large research and development effort on semiconductors resulted, among others, in the development of practical energy conversion devices. This section is devoted to an account of the advances made during this period.

*Semiannual Report #2, NASW1427.

B. Materials Technology

1. Introduction

The development of today's highly sophisticated semiconductor device industry can be traced directly to the tremendous advances in materials technology which occurred, for the most part, in the decade or two following the late 1930's. It was during this period that the materials purification and crystal growth techniques were developed which made possible the transistor and the myriad of related devices. The development of these techniques was coincident with an intensive study of the properties of semiconducting materials and of the effects of various impurities on these properties. The major effort was concentrated on germanium and silicon. These studies, combined with the development of impurity diffusion processes in semiconductors, provided the necessary background for the controlled formation of the p-n junction, the essential part of the majority of semiconductor devices, including the present day solar cells. The experimental investigations were often paralled by, and also in many instances stimulated, a strong theoretical interest in semiconductor phenomena which led to an increased understanding of the physics of semiconductors and provided a feedback for further experimental work. A brief discussion of this early development is necessary to any historical survey on the development of photovoltaic cells; indeed, it was during these early investigations of crystal growth and materials properties that the p-n junction photovoltaic effect in silicon was inadvertently discovered (87-89).

2. Material Purification, Crystal Growth, and Semiconductor Properties

a. Elemental Semiconductors: One of the more positive effects of World War II was to provide a jolting stimulus to the field of semiconductor physics. The impetus was supplied in the form of contracts under the sponsorship of the National Defense Research Committee (NDRC) to a number of universities and commercial laboratories in the United States (90). The motive for this interest was the development of crystal rectifiers and crystal mixers for radar applications. Prior to the war the field of single crystal-semiconductor technology was relatively dormant. Available materials were not highly refined, many of the properties of the materials were not generally understood, and applications for semiconducting materials were few. The major application for germanium appears to have been as a thin-film resistor (evaporated on glass) in electric circuits, although the rectifying properties of germanium-metal point-contacts were well known. Silicon was used in the fabrication of point-contact rectifiers for microwave detectors in laboratory studies. The war-time needs, both in the United States and England and in Germany, caused a dramatic change.

The first requirement for producing semiconducting devices with predictable and controllable properties is a source of relatively pure material. During the early work at Bell Laboratories around 1940 (Reference 90, p. 311), the normal impurity segregation which takes place with crystal growth by the Bridgman technique was used to purify the then available silicon. This silicon was commercial electromet material with a purity

of 99.8%. The growth procedure resulted in ingots approximately 4 1/2 in. long and 1 5/8 in. in diameter of which the bottom 2 in. were discarded.

During the period 1940-1944 the DuPont Company developed a technique which produced, consistently and uniformly, silicon of purity better than 99.9%.

The essential part of the technique was a reaction chamber process utilizing the zinc reduction of silicon tetrachloride by zinc vapor. The reaction was carried out at a temperature such that the zinc, zinc chloride, and excess silicon tetrachloride were carried off in the form of vapor, while the pure silicon remained in the reaction chamber in the form of crystals. After removal from the chamber the silicon was leached in hydrochloric acid and rinsed in distilled water.

A similar method was used by DuPont to produce high-purity germanium. A second method used for the purification of germanium by H.Q. North of General Electric was the reduction of germanium oxide by hydrogen. Ingots grown with these materials were sufficient for the fabrication of rectifiers, and while tolerating wide production distributions and low yields, it was often not necessary to discard portions of the ingots because of impurities. The precise measurement of physical properties, and the development of sophisticated devices as well as of economical production processes, however, required materials of greater purity (better than 1 part in 10^8 or less) than these processes could provide.

It was not until the early 1950's, which saw the introduction of the zone refining process (91) and later the floating zone technique for silicon of Keck and Golay (92), that germanium and silicon of this purity became available. These zone purification techniques consist of melting a narrow region or "zone" of the crystal and then moving this region along the length of the crystal, carrying along with it the impurities which are rejected in the re-freezing process and which are deposited at the end of the crystal, which portion can then be discarded. The reason for the segregation of the impurities is their lower solubility in the solid phase of the semiconductor than in the liquid. Some of the moving zone techniques were later adapted for growing single-crystal ingots both of germanium and silicon.

Methods for the growth of large single crystals of many organic and inorganic materials have been known since the middle of the nineteenth century. Most of the early work was concerned with growth from a solution, but melt-growth techniques, such as those of Bridgman (93) and Czochralski (94), had been developed for the growth of metals, approximately two decades before World War II. These techniques, with modifications, were finally settled on for the growth of silicon and germanium ingots. During the early work at Bell Laboratories, performed under NDRC contract, silicon ingots were grown by simply heating a large mass of silicon to a temperature well above its melting point and then allowing it to cool slowly (88, 89). Due to the impurity segregation process in freezing, a gradient in purity existed from the outer surface to the core of the ingot. Ingots grown in this fashion were generally cracked because of the anomalous negative

expansion coefficient of the material upon freezing, which causes the central portion of the ingot, which is the last to solidify, to break its confinement. The cracking was highly undesirable, so that other techniques were sought. A process which successfully eliminated the cracking was to heat the material in the normal manner but, instead of allowing the material to cool by slowly reducing the power supplied to the furnace, the material was slowly withdrawn from the furnace which was maintained at a constant temperature. This was an adaptation of the Bridgman method. The ingots produced were relatively crack-free, with an impurity gradient from top to bottom. In the early silicon ingots produced at Bell Laboratories the upper half of the ingot exhibited p-type conductivity, while the lower half was n-type. It was during experiments with rods and plates cut from sections of such ingots that the p-n junction photovoltaic effect in silicon was discovered in 1941 (88, 89).

The techniques used to grow germanium ingots during the early and mid 1940's were essentially the same as those used to prepare silicon crystals. They normally consisted of variants of the Bridgman method insofar as either the tube containing the melt was slowly removed from the furnace or the furnace itself was physically raised to expose the tube. The material produced was satisfactory for point-contact rectifier uses, although a large amount of waste was incurred and the material was probably highly polycrystalline since the technique of "necking" the tube so that only one crystal will act as a seed to the melt appears to have not yet been used. Crystals of germanium grown in this manner occasionally contained regions of n-type and p-type conductivity, similar to those found in silicon and it was discovered, around 1944, that the boundaries of such regions exhibited photovoltaic sensitivity (95, 96). The electrical properties of the germanium could be altered by the addition of small amounts of impurities, such as antimony and arsenic, to the melt.

The properties of the silicon ingots could be controlled to some extent by the same process. However, because of its highly reactive nature, silicon tended to become contaminated by whatever material was used as a crucible, making its properties more difficult to control than those of germanium. In the late 1940's and early 1950's after the introduction of the Czochralski or "crystal pulling" techniques for the production of silicon and germanium ingots, the method of adding impurities to the melt during crystal growth was used to prepare p-n junctions (97). In general, the Czochralski method has been found to produce crystals with a lower defect density than other known techniques, and to provide sufficient control of impurity concentrations, so that this technique has become the one generally used for the production of crystals for solar cell fabrication.

The necessity for controlling the electrical characteristics of the semiconductors led to an extensive study of the properties of the materials and the effects of impurities on these properties. Particularly, the effects of boron and phosphorus on the conductivity type and resistivity of silicon were explored in the 1940's by Scaff et al (88, 98). They determined that boron and other group III elements caused the material to exhibit p-type conductivity, while the addition of phosphorus, arsenic, and other group V elements resulted in n-type conductivity. Compensation effects were also noted. Extensive

measurements of resistivity and Hall effect as a function of temperature on silicon samples containing from 0.0005 to 1.0 percent boron or phosphorus were reported by Pearson and Bardeen (99). Similar studies were performed on germanium by Lark-Horowitz and Johnson. Most of this early work was performed during World War II under the NDRC and was described rather thoroughly by Torrey and Whitmer (90).

In the early 1950's the results of numerous detailed studies of impurity effects on the properties of silicon and germanium began to appear in the published literature. Experimental studies of solubilities, impurity distributions, diffusion coefficients, ionization coefficients, ionization energies, and capture cross sections covering a wide range of elements were published. J.A. Burton's paper (100) provides a good review and bibliography of this work, much of which occurred at the Bell Laboratories. The theoretical work of Burton (101), Pfann (91), and others laid the basis for understanding and predicting the behavior of impurities during crystal growth and zone purification. All of this work provided the foundation for the production of crystals with highly controlled and well-known impurity concentrations whose electrical and optical properties could be studied with confidence. Investigators such as Prince (102, 103) and Burton (104) of Bell Laboratories studied the effects of impurity concentration on mobility and lifetime, while others such as Dash and Newman (105) of General Electric studied optical absorption. As a result of these and many other investigations the general understanding of semiconductor properties was increased dramatically during the early 1950's, at least as far as elemental semiconductors were concerned.

b. Compound Semiconductors: There was no burst of interest in the compound semiconductors during the 1940's corresponding to that which occurred for silicon and germanium. These elemental semiconductors possessed sufficient known properties to make them by far the most interesting materials for wartime and, post-war, for commercial uses. As a consequence, almost all of the scientific investigations were centered on these materials. The compounds are more difficult to prepare, and consequently, it was not possible at that time to investigate their physical and electrical properties systematically. Because of differences in the bonding scheme of the atoms, the models developed for the covalently bonded materials (Si and Ge) could, in general, not be extended to other materials. However, it was known that some semiconducting compounds form wurtzite and zinc-blende lattice structures and, hence, that the binding mode of these materials is similar to that of germanium and silicon. Materials known to crystallize in the above forms include II-VI compounds such as zinc sulfide, I-VII compounds such as AgI, and III-V compounds such as AlN. In the early 1950's several investigators began to explore the properties of some of these materials. H. Welker was the first to make a thorough and systematic study of the III-V compounds (106-108). His investigations showed that these compounds were indeed semiconductors and that they had some very interesting properties, some of them very similar to those of silicon and germanium. The properties of some of the materials, such as indium antimonide had obvious technical possibilities, and interest in the III-V compounds was greatly increased as a result of this work. The publication of Welker's work was followed by a host of studies on the electrical and optical properties of III-V compounds. A good bibliography for this

work can be found in Madelung's book (109). Also around this period, interest in the semiconducting properties of the II-VI compounds (110, 111, 112) as well as of compounds from other elements began to rise. Smith (111), investigating conductivity, found that cadmium sulfide exhibited only n-type conductivity. Reynolds et al (112), while investigating conductivity and rectification in cadmium sulfide, observed photovoltaic effects. The interest in the properties of these materials resulted in rapid advances in the technologies for their preparation, and by the middle 1950's the possibilities of devices fabricated from these materials began to be explored in earnest.

3. Junction Formation

a. Early Techniques: The earliest rectifiers were of the point-contact or cat-whisker type (90, p.6). This type of device was adequate, albeit at times frustrating, for detector use in early radio and later microwave and radar work. Major disadvantages of this contact type included instability, unreliability, and limited power-handling capability. The introduction of alloyed junction techniques (113), whereby donor or acceptor type metal electrodes are fused to a homogeneous silicon or germanium crystal by heating (114, 115), resulted in diodes with a high degree of reproducibility, very low reverse currents, good temperature stability, improved high-frequency performance, and good power-handling capabilities (116). These techniques were readily applicable to devices of relatively small area and were good for fabricating general-purpose diodes and zener diodes. However, the alloying techniques proved difficult to apply to large areas, and were therefore not practical for the early development of necessarily large-area devices such as high-power rectifiers and solar cells.

The first broad-area p-n junctions to be made under controlled conditions were produced by the grown-junction technique of Teal, Sparks, and Buehler (117). Using the Czochralski crystal-pulling process, they introduced the necessary impurities during the growth of a germanium crystal to change the conductivity type. This produced a crystal with one portion having n-type conductivity and the other portion having p-type conductivity, with a p-n junction at the interface. These junctions were found to approach very closely the ideal conditions and were used in experiments to verify the quantitative features of Shockley's diode theory (118). However, silicon junctions produced by the same technique were not so well behaved, exhibiting anomalous reverse saturation current behavior (119). It was suggested that the large values of saturation current were caused by the generation of carriers in the space charge region (114). The alloyed- and grown-junction techniques were developed at about the same time.

b. Diffused Junctions The "power-formed" or "welded" variety of point contacts used in early general-purpose diodes (1N34) were actually diffused junctions formed at relatively low temperatures and short diffusion times and were recognized as such by the researchers who made use of this technique. Alloyed junctions, which are actually solution-grown junctions based on the regrowth heat cycle after alloying, were used in some of the early attempts to study the diffusion of impurities in semiconductors (120, 121), a phenomenon which began to be investigated in the early 1950's. The object of these studies was to

measure and calculate the extent of the thin diffused region under the alloy. The more practical system (from a device and production point of view) of high-temperature vapor diffusion was not introduced until 1954. In 1954 Fuller and Ditzenberger (122, 123) reported the successful fabrication of p-n and n-p junctions by heating single-crystal silicon of n-type or p-type conductivity in the presence of boron trichloride or phosphorus vapor, respectively. The temperatures used ranged from 1050°C to 1250°C, with diffusion times between 16 and 112 hours. The process was immediately applied to the fabrication of power rectifiers (123) and of a p-n junction photovoltaic energy conversion device(124). Similar work on high-temperature diffusion was reported by Dunlap et al. (125) at approximately the same time. The introduction of this process caused not only more intensive studies of the diffusion process itself, but also a veritable epidemic of work on diffused junction transistors and other devices. A bibliography of this work can be found in the paper by F.M. Smits (126).

In summary, the materials preparation work of the 1940's and the development of the diffusion technique for the introduction of impurities and junction formation provided the foundation for today's semiconductor device technology. During this period, the purity of the materials produced was raised by at least three to four orders of magnitude (from a prewar best of about 10 ppm), and techniques for growing single crystals of semiconductors with dislocation densities of the order of 10^2 cm^{-2} or less (germanium) were developed. The refinement of these techniques to extend their capabilities and to permit precise control as well as the possibility of introducing predetermined impurity profiles over large areas were the final steps necessary for large-scale device production. In the course of these early developments on elemental semiconductors a new understanding of the properties was built up and previously unknown effects were discovered, among them the p-n junction photovoltaic effect.

C. Experimental Solar Cell Development

In the years between 1940 and 1950, photovoltaically sensitive p-n junctions were discovered in a number of materials including silicon, germanium, and lead sulfide. Although the phenomenon was first discovered in silicon, most of the experimental investigations of the effect during this period as well as the early 1950's were performed on germanium samples. This was primarily due to the much more rapid advance of the germanium technology, which was caused by the greater chemical inertness of this material. The effect was not seriously considered for energy conversion purposes until the introduction of junction formation by diffusion in silicon which took place in the mid-1950's. It was also at this time that other materials, the compound semiconductors, came into consideration.

1. Selenium and Germanium Photovoltaic Cells

As was mentioned in Section II* selenium photovoltaic cells appeared to be of little scientific interest after about 1930, although they continued to be used in photoelectric

*Semiannual Report #2, NASW 1427.

detectors. It is of historical interest, however, to make a brief mention of some work published in the late 1940's. This work was concerned with the energy conversion efficiency of the selenium barrier layer photocell and appears to be the first instance in which a solid-state photovoltaic cell was considered as an energy conversion device.

In 1948, R.A. Houstoun, disturbed by claims of 50% conversion efficiency from light energy to electrical energy contained in a leaflet accompanying a commercial photocell, undertook a series of experiments which were intended to determine the actual efficiency of the cells (127). Houstoun found a maximum efficiency of 6.2×10^{-5} for white light illumination, while the efficiency for monochromatic light was 6.4×10^{-8} (at 636 μm). These experiments lacked in several aspects. These include the facts that the light level was extremely low for the monochromatic measurements and that the load resistance was far from optimum. Although other factors influencing these measurements, including the quality of the cells and the characteristics of the filter used, cannot be determined any more, however, it is safe to assume that the results were too low. However, this work is of interest because it constitutes the first (although admittedly crude) attempt to evaluate the energy conversion capabilities of a photovoltaic device and because it stimulated more careful study by some other investigators. Billig and Plessner (128), disturbed in their turn by the results of Houstoun, published, in the following year, their own studies on the efficiency of selenium barrier layer photocells. First, using the theoretical expressions of Lehove (129) and manufacturers' data, they showed that an efficiency of 1 to 4% for monochromatic light near 550 μm should be expected. A typical photocell I-V characteristic (fourth quadrant) was shown in the referenced paper, with maximum power point indicated. The cells were apparently badly limited by series resistance as indicated by the quoted typical fill factor value of 0.36. Measurements were made on actual cells. Care was taken in optimizing the load resistance and isolating the wavelength of the radiation. An efficiency of 1.41% was measured for the mercury green line with an incident intensity of 0.73 $mW \cdot cm^{-2}$ while a sunlight measurement (January on a cloudy day, with no collimation) gave a maximum efficiency of 0.95%. These values agreed fairly well with the predicted values, and the authors concluded that Houstoun's results were in error. While these experiments were stimulated by academic rather than practical considerations, they were the first published experiments in which photovoltaic energy conversion was seriously investigated. Further consideration was not given to this subject until the introduction of the Bell solar battery.

Photovoltaic effects in germanium were first observed by P.R. Bell at the Radiation Laboratory of the Massachusetts Institute of Technology around 1944 (Reference 90, p. 393). These observations led to a detailed study by S. Benzer, whose results appeared in NDRC reports in November 1944 and October 1945 (ibid.), but were not published in the general literature at the time. The first published mention of photovoltaic effects in germanium appeared in 1946 in the form of abstracts of two talks given at American Physical Society meetings in April and June of that year (130, 131); in these abstracts the photosensitive properties of certain germanium crystals when contacted by metal points, were described. The crystals contained naturally occurring n- and p-type regions. Two types of behavior were observed and were labeled photodiode and photo-peak behavior, respectively. The photodiode behavior was that which one would expect when

operating a photocell at reverse bias. The photocurrent was found to vary linearly with intensity at a rate of several milliamperes per lumen for white light and to be independent of voltage. The threshold wavelength for stimulating photovoltaic response was observed to be approximately 1.5 μm with peak response occurring at about 1.3 μm. The photo-peak behavior is somewhat more unusual, and the abstract does not provide sufficient information to deduce the nature of the effect. The devices which exhibited this effect had I-V characteristics similar to that shown in Figure 8. The voltage peak, which occurred before the negative resistance region in the I-V characteristic was reached, was reduced by illuminating the devices, and at high illumination levels the peak (and hence the negative resistance region) was eliminated. Heating was observed to have a similar effect on the peak. The effect could possibly be explained as being due to two opposed diodes, one of which undergoes zener breakdown. This structure agrees with that indicated by Benzer in later publications.

In 1947, Benzer responded to remarks by L. Sosnowski who speculated that p-n junction photosensitivity, similar to that which he had observed in lead sulfide (132), might also be observed in silicon and germanium. Benzer stated (133) that such effects had indeed been observed and investigated in germanium. He described, briefly, some of the results of the earlier work under the NDRC. The structure that was investigated in this work is shown in Figure 9. The inhomogeneity of the crystal (n- and p-type regions)

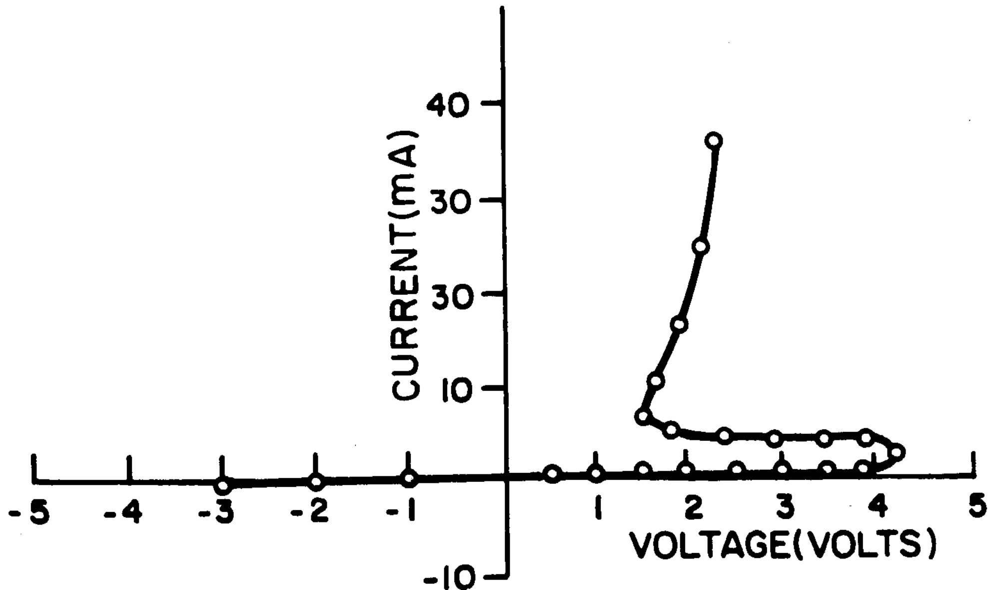

Figure 8. "Photopeak" characteristic

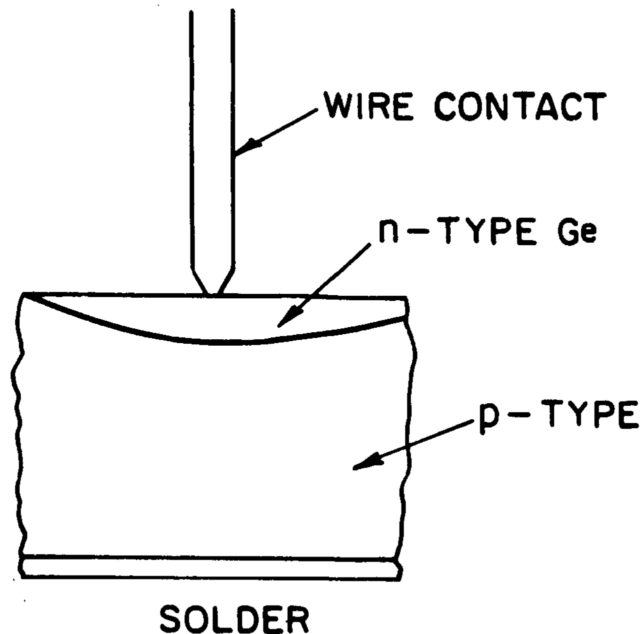

Figure 9. Photodiode structure, after S. Benzer

was apparently not intentionally produced. The device had a peculiar I-V characteristic (Figure 10) which was apparently due to the presence of two barriers, one at the metal-semiconductor contact and the other at the p-n junction. Both photovoltaic and "photoconductive" effects were noted as well as negative resistance and "self-oscillations". The "photoconductive" effects appear, in actuality, to have been photodiode type behavior (i.e., the I-V characteristics shift but do not rotate). Magnitudes of the photovoltages observed are not given.

Three years after Benzer's letter was published, Becker and Fan (134) published data from experiments on germanium p-n junctions in which it was verified that the photovoltage varies linearly with light intensity for low intensities and more slowly for high intensities as predicted by Fan in a previous publication (135). Data on the temperature dependence of the spectral response of the photovoltage and the variation of photovoltage with load resistance were also given in this paper. Other investigations were reported by F.S. Goucher et al. (118) and by W.J. Pietenpol (136) both of whom used p-n junctions prepared by the grown-junction technique described in Section III-B-3-a above. Most of the device-oriented interest in the p-n junction photoeffect during this period was centered on its possible use in low-intensity radiation detection, as illustrated by the papers of Rothlein (137, 138) and Shive (139). These studies were concerned primarily with the sensitivity of the photocurrent or photovoltage to changes in light intensity rather than energy conversion as such although Rothlein estimated the ratio of the energy developed by the cell to the incident energy to be of the order of 0.01 (for

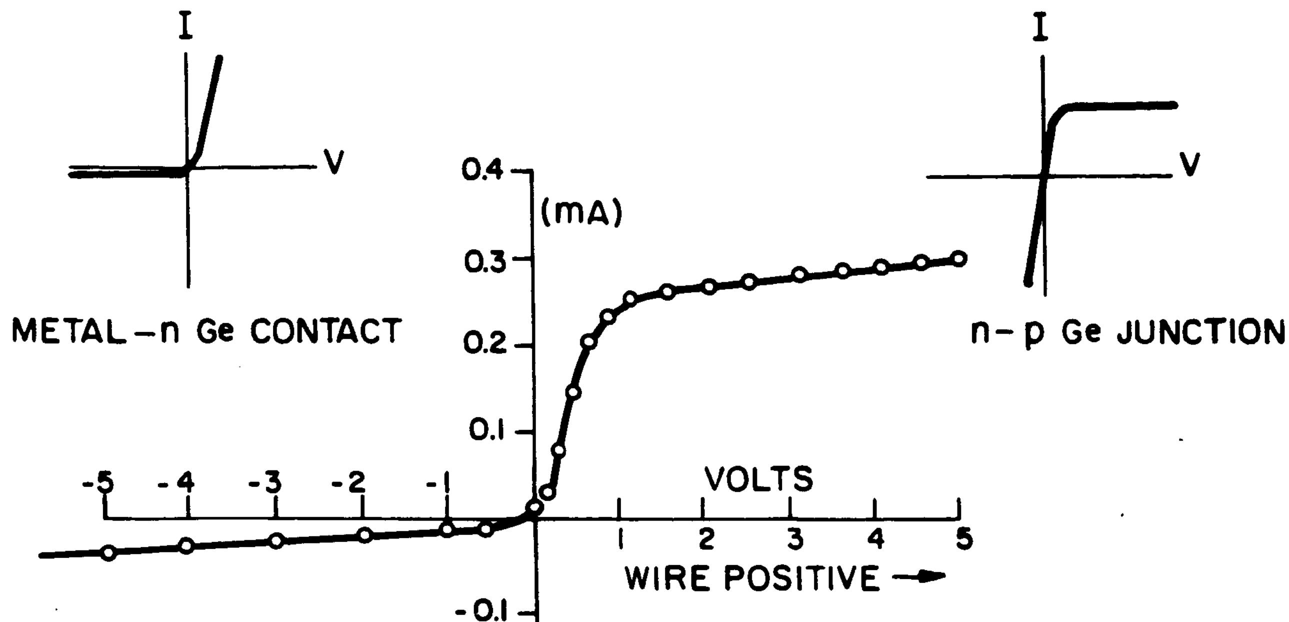

Figure 10. Current-voltage characteristic of photodiode

radiation corresponding to peak response). A brief interest in the energy conversion capabilities of germanium p-n junctions was roused when the results of Chapin et al. (124) on silicon were made public in 1954. Ruth and Moyer (140) published a letter in that year describing an experimental investigation of the variation of conversion efficiency with light intensity. Efficiencies up to about 0.5% were measured for intensities approaching that of sunlight (using a 3200°K photoflood lamp as a light source). The elimination of reflection losses and other improvements were expected to raise the efficiency to approximately 2%. Another investigation was published by Pfann and van Roosbroeck at about the same time (141). They considered the possibility of using p-n junctions as both radioactive (electron-voltaic) and photovoltaic power sources, and presented theoretical and experimental results both for silicon and germanium. From theoretical considerations the authors predicted an ideal efficiency of 18% for silicon solar cells under sunlight illumination. However, their experimental work dealt only with the electron-voltaic effect. As a result of this and other work (152) it became apparent that germanium was not ideally suited for solar energy conversion use. Consequently, the interest shifted to other materials which held more promise for this purpose, and very little further work was done with germanium photovoltaic cells.

2. Silicon Cells

Early in 1941, R.S. Ohl, a metallurgist at the Bell Laboratories, discovered, in a melt of commercial "high-purity" silicon, a "well-defined barrier having a high degree of photovoltaic response" (87, 88). This observation marks the discovery of the p-n junction photovoltaic effect. The reasons for the occurrence of this junction were outlined in Section III-B-3 of this report, dealing with materials technology. Figure 11 is a drawing of the silicon melt showing the position of the naturally occurring photovoltaic barrier and a "surface type" photocell made from the barrier. In addition to the "surface type" cells, many of the cells were cut in the form of long rods or bars with the junction in the center normal to the surface. Figure 12(a) shows such a cell with a typical spectral response curve as shown by Kingsbury and Ohl (89). Figure 12(b) illustrates the variation of open-circuit voltage and short-circuit current with intensity for the "bar type" of cell. The "surface type" cells showed more response in the visible than the "bar type". The illumination source for the intensity dependence measurements was a 2848°K tungsten lamp. The cells were noted to be extremely stable under drastic temperature changes. Heating to red heat and immediately quenching in water apparently had no effect on the cell characteristics. Some of the cells were used in test circuits for ten years without any serious change in their properties. Ohl took the precaution of immediately patenting the device, but, it appears, did not publish his findings in the general literature or in an NDRC report until 11 years later. J.H. Scaff, who had worked with Ohl and also held a patent on the device, mentioned some of the findings in a paper published in 1949 (88). It is apparent, however, that Ohl's findings were not generally known, since Torrey and Whitmer attributed the discovery of photovoltaic effects in silicon to Miller and Greenblatt (Ref. 90, pages 392 and 393) around 1944 to 1945. Miller and Greenblatt's observations were made on point-contact rectifiers, and it is not clear if p-n junctions were present. Currents of 0.15 μA were obtained under illumination intensities of 12 mW$\cdot$cm^{-2} of monochromatic light (wavelength 1.5 μm-maximum of the spectral distribution curve). The magnitude of the photovoltage was not given. There was very little interest in the photovoltaic properties of silicon during the

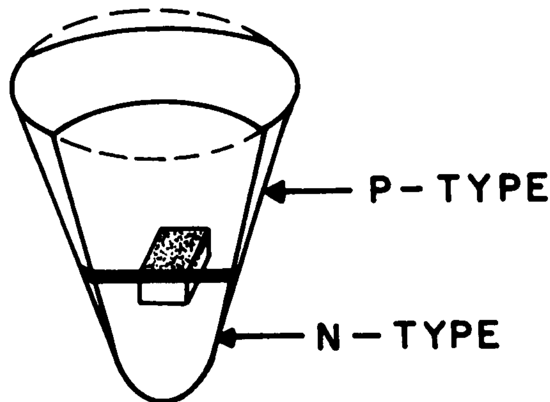

Figure 11. Representation of melt, showing photovoltaic barrier and photocell, after Ohl

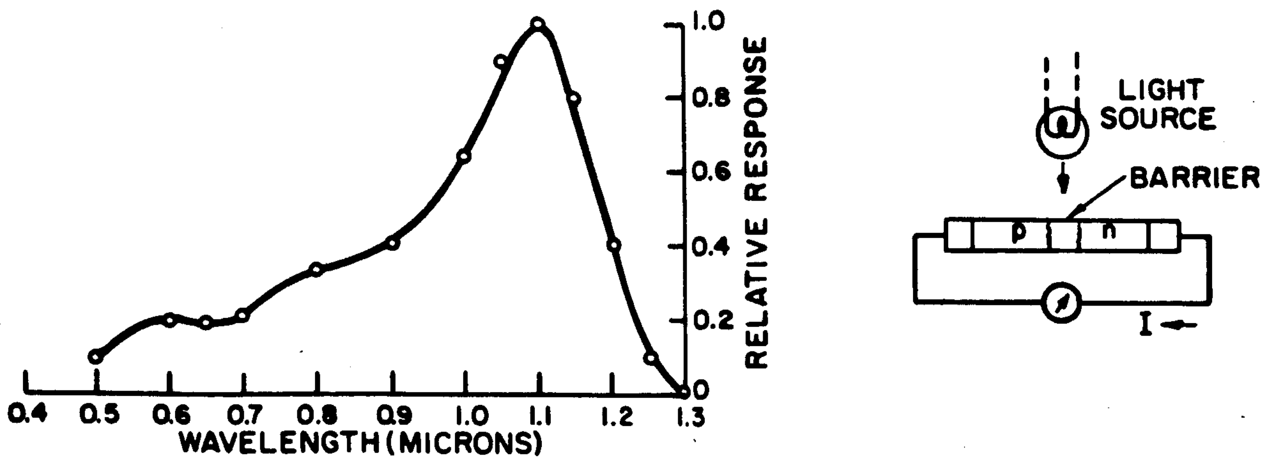

Figure 12(a). Spectral response (equal energy) of silicon photocell, after Ohl

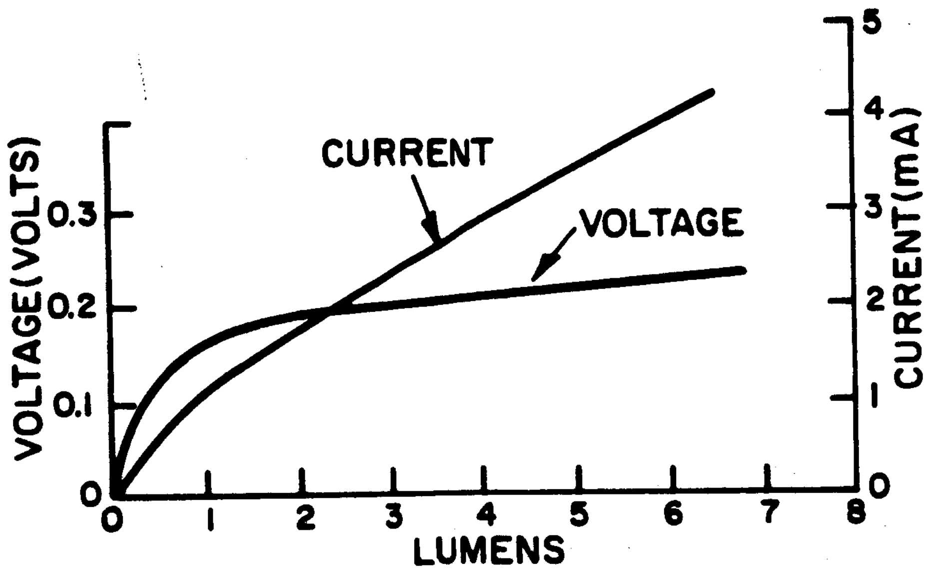

Figure 12(b). Illumination dependence of photocell current and voltage, after Ohl

period between the early 1940's and the early 1950's. Some observations on contact potential changes under the influence of light were published by Brattain (142) but these were concerned with surface state studies.

The next publication of interest was that of Kingsbury and Ohl (89) in 1952. After a brief account of Ohl's earlier work the authors discussed some experiments on the formation of photovoltaically sensitive barriers by ionic bombardment of silicon. This work was motivated by a search for techniques whereby large areas of silicon surfaces might be uniformly activated (i.e., a barrier formed). Such a technique was expected to produce photocells competitive with those available at the time. "Hyper-purity" silicon was used in this work to avoid the formation of natural barriers by impurity segregation. The activation process consisted of exposing the polished face of a silicon wafer to a uniform beam of helium ions with energies ranging from 100 eV to 30 keV. The pressure during bombardment was 10^{-3} to 10^{-4} mm Hg, and the silicon surface was maintained at a temperature of 395°C. Three cell sizes were constructed, with areas of 0.005 cm^2, 0.40 cm^2, and 8.0 cm^2. Most of the measurements were made on the intermediate area cells. The wafer thickness was 0.025 in. Attempts were made to evaluate the relation between ion velocity and junction depth by measuring spectral response as a function of accelerating voltage. Cells subjected to extremely low energy bombardment (100 to 226 eV) showed a definite blue shift (sensitive at shorter wavelengths), but bombardment at intervals in the higher energy range (570 eV to 30 KeV) yielded cells which, while more red sensitive than the low energy cells, were essentially identical among themselves. Figure 13 shows the spectral response curves of a blue shifted and a "normal" cell. In addition, cells made with relatively impure silicon were found to be blue-shifted compared with those made with pure silicon. To obtain highly photosensitive cells it was necessary to maintain the silicon at an elevated temperature during bombardment. The optimum temperature was found to be around 395°C. Cells made at temperatures above this had soft reverse characteristics while those made at lower temperatures had poor photosensitivity. The ion-bombarded cells were extremely stable and had photosensitivities of the order of 3000 μA per lumen for tungsten light and for daylight. Although Kingsbury and Ohl were interested in developing competitive photodetectors rather than an energy conversion device, this work was the precursor of the more recent investigations of ion-bombardment techniques for solar cell fabrication.

The development of high-temperature vapor diffusion techniques by C.S. Fuller around 1953 to 1954 solved the problem of "uniformly activating" large-area semiconductor surfaces. This made it possible for Bell Laboratories to demonstrate their solar battery in April 1954 at the annual meeting of the National Academy of Sciences in Washington (143). The device was developed by G.L. Pearson, C.S. Fuller, and D.M. Chapin, (Physicist, Chemist, and Electrical Engineer, respectively). At about the same time the developers published data on the characteristics of the device (124). The cells had an open-circuit voltage of approximately 0.5 V and a conversion efficiency of 6% under sunlight illumination. The diffused layer thickness was 0.0001 in. A theoretical computation indicated an efficiency limit near 22% for the device. The actual device was limited by several practical factors which were thought to include reflection losses

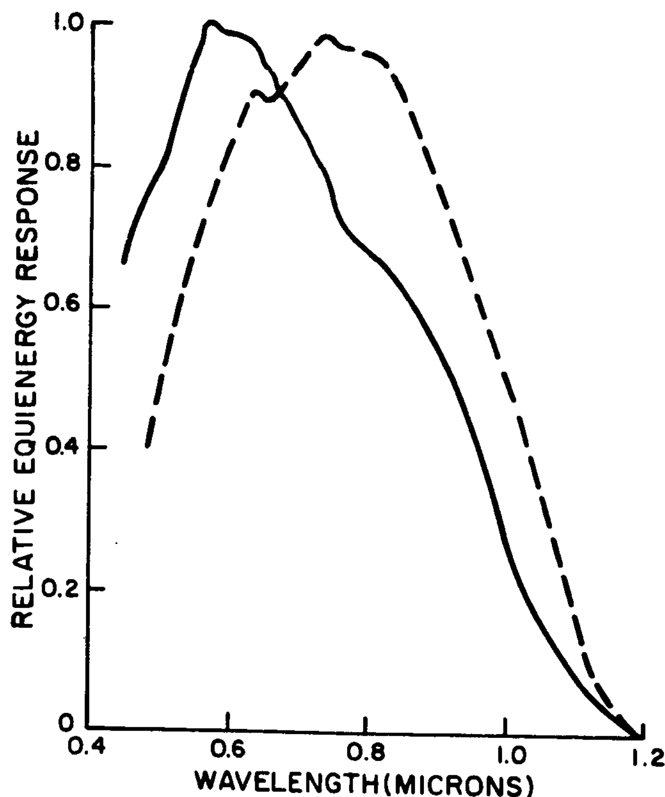

Figure 13. Blue shifted and "normal" ion-bombarded photocell responses, after Kingsbury and Ohl

approaching 50% and large series resistance losses, primarily in the thin p-type diffused region. Improved surface treatments were expected to improve the reflection problem while special contact geometries were planned to deal with the resistance of the diffused layer.

A number of publications followed the initial work, including a second one by Chapin, Fuller, and Pearson, providing more detailed information, presented in a popularized fashion (144). Figures 14(a) and 14(b) contain a cutaway view of the "Bell Solar Battery" and a plot of the intensity dependence of the device characteristics respectively. The open-circuit voltage for sunlight illumination is seen to have been approximately 0.52 V and the short-circuit current density was 25 $mA \cdot cm^{-2}$. The cell was considered for use as a power source for telephone amplifiers in remote areas, and results on battery-charging studies under varying weather conditions were presented. This publication appeared one year after the initial disclosure, and mentioned that at this time the average efficiency had been raised to 8%, with some units reaching 11%. In the same year (1955), Prince published a paper (145) which compared theoretical predictions with experimental results on silicon cells. The results of this study indicated that the most serious problem limiting the efficiency of the early devices had been series resistance in the contacts. The theory showed that total series resistance could and should be reduced to less than 1 ohm, partially through adoption of suitable cell geometry. Prince also investigated the use of antireflection coatings to reduce reflection losses. An experiment which attempted to use a piece of soft glass cemented to the cell surface did not improve the short-circuit

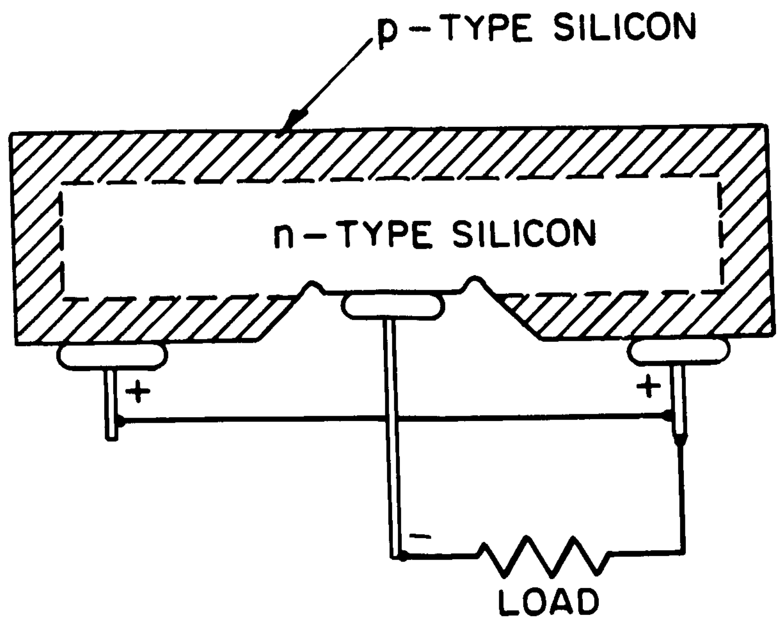

Figure 14(a). Cross section of Bell solar battery, after Chapin et al.

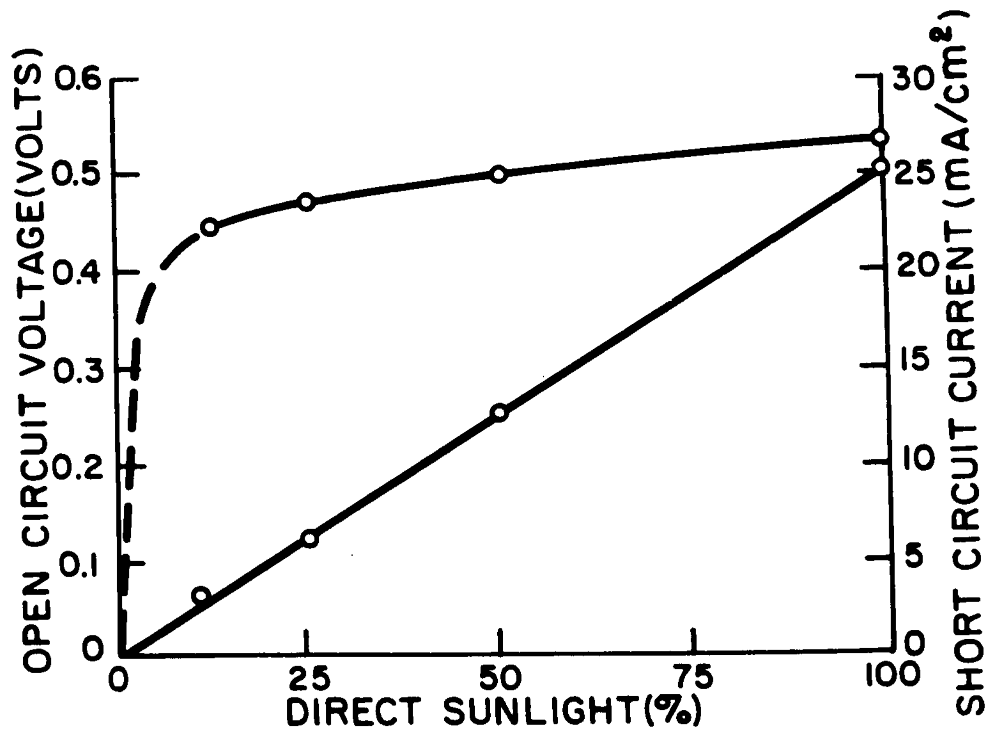

Figure 14(b). Intensity variation of Bell solar battery characteristics

current. The results of the experiment were explained as possibly due to a silicon dioxide layer on the cells, which would provide antireflection properties.

From this beginning silicon has continued to dominate the field of photovoltaic energy conversion to this day. The success of silicon, however, did stimulate interest and work on other materials. These developments are discussed in the following section.

3. Compound Semiconductor Photovoltaic Cells

Although most of the important developments in compound semiconductor solar cells occurred after the introduction of the Bell solar battery, the first reported observation of an identifiable p-n junction photovoltaic effect in a compound material was that of Sosnowski, Starkiewicz, and Simpson in lead sulfide in 1947 (132, 146). Photovoltaic effects had been observed in many compound materials, notably silver sulfide, several decades prior to the discoveries of Sosnowski, et al.; however, most of these observations were associated with contact phenomena and were not identifiable as p-n junction effects. In a paper authored by Starkiewicz, Sosnowski, and Simpson (147) in 1946, photovoltaic effects in lead sulfide films under infrared illumination (1 μm to 3.5 μm) were reported. The effect observed was actually a "high-voltage photovoltaic effect", since the measured photovoltage (2V) was greater than the bandgap. Sosnowski et al. (146) postulated a multi-p-n junction mechanism to explain the effect and constructed such junctions experimentally by bringing together two pieces of lead sulfide, one containing excess lead and the other containing excess oxygen. The junctions were extremely thin and their operation was thought to be governed by "diode theory" rather than diffusion theory. Sosnowski reported that he observed photovoltaic effects across such junctions and developed a theory to explain his observations. Unfortunately, he gave no indication as to the magnitude of the photoeffects observed. Because of its narrow bandgap (0.3eV), lead sulfide is not of interest for photovoltaic solar energy conversion applications, although it is an important material in infrared radiation detection. A number of other compounds with energy bandgaps above 1 eV, are of interest, at least from a theoretical point of view. The most important of these fall into the groups of II-VI and III-V compounds. The developments on these are discussed in the remainder of this section.

After the establishment of the semiconducting nature of the III-V compounds by Welker (106), these materials attracted considerable attention among investigators interested in new photoconductors. Many of the experiments led to the discovery of photovoltaic effects in these materials. Talley and Enright (148) reported having observed photovoltaic effects in indium arsenide. The photovoltages were detected across p-n junctions which occurred naturally in grown ingots of the material, and which were located by thermoelectric measurements. Figure 15 is a graph of the photoresponse of a typical indium arsenide photovoltaic cell as measured by Talley and Enright. The measurements were made at liquid-nitrogen temperature. Photovoltaic effects were observed at room temperature but increased by three orders of magnitude at the lower temperature. The response of the cell was primarily in the infrared with a bandgap of approximately 0.27 eV, making it of little interest in solar energy conversion.

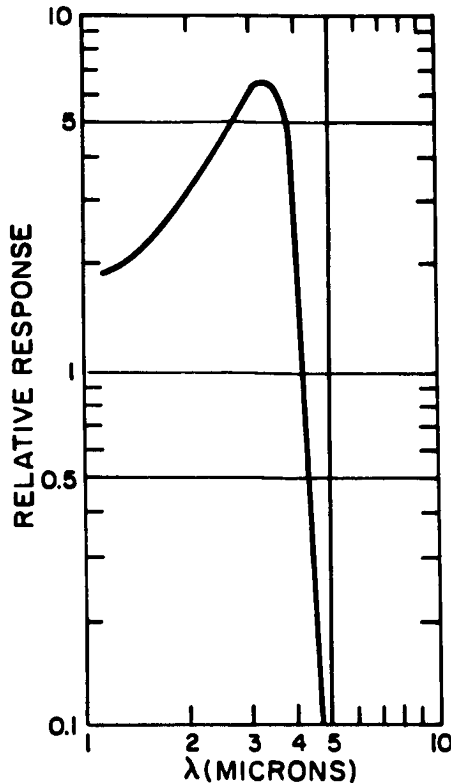

Figure 15. Photoresponse of an InAs photovoltaic cell at 77°K, after Talley and Enright

There were two reported observations of photovoltaic effects in indium antimonide in 1954. The first was that of D.G. Avery et al. (149) who were studying photoconductive effects. The second was by G.R. Mitchell et al. (150) who had intentionally produced photovoltaic cells by the grown-junction technique. The observations of Avery et al. were made on a point-contact device consisting of a piece of pure single-crystal indium antimonide contacted by a tungsten probe. Spectral sensitivity measurements were made at about room temperature. The data showed the sensitivity beginning to rise at a wavelength of about 8 μm reaching about 80% of peak at 7 μm (0.176eV). For wavelengths shorter than 6 μm the photodiode exhibited an approximately constant energy sensitivity (i.e., response per unit energy input). The measurements of Mitchell et al. were made at 77°K and indicated a band edge corresponding to 5.7 μm (0.22eV) at this temperature. Most of the discussions in this paper were concerned with the signal-to-noise ratio of the photocell. Again the material is not of interest for solar energy conversion.

Welker himself seems to be the first to report photovoltaic effects in gallium arsenide. In a survey paper on "Semiconducting Intermetallic Compounds" published in 1954, he showed the I-V characteristics of a GaAs photocell under several intensities but gave no discussion (107). Figure 16 shows these characteristics. In the following year Gremmelmaier reported his findings (151) on a photocell with an area of 23 mm^2 which was cut from polycrystalline material. The n-type crystal had a layer of p-type

material about 10^{-2}mm thick grown onto its surface. Under sunlight illumination (sea level) the cell had an open-circuit voltage of 0.66 V, a short-circuit current density of 2.6 mA·cm^{-2} and an efficiency of about 1%. Under focused sunlight an open-circuit voltage of 0.87 V and a current density of 70 mA·cm^{-2} were obtained. Figures 17(a) and 17(b) show the intensity variation of the photocurrent and photovoltage. The photovoltage was surprisingly linear with intensity at intensities approaching that of sunlight. The details of the measurements were not given. A second photocell was made and had an efficiency of approximately 4% under a sunlight intensity of 60 mW·cm^{-2}. This cell had an open-circuit voltage of 0.73 V and a current density of 4.8 mA·cm^{-2}. Gremmelmaier anticipated considerably higher efficiencies from single-crystal cells.

In 1955, working under an Army Signal Corps contract, Loferski, Rappaport, and Linder of RCA developed a theoretical analysis which indicated that a number of the III-V compounds (InP, GaAs, and AlSb) as well as at least one of the II-VI compounds (CdTe) should yield photovoltaic cells with efficiencies higher than silicon (152). Later that year Jenny, Loferski, and Rappaport (153) reported measurements on cells made by diffusing cadmium into n-type gallium arsenide wafers in which efficiencies as high as 6.5% were achieved. The analysis of Loferski et al. (152) indicated that gallium arsenide was the most promising of the III-V compounds from a combined theoretical and technological point of view, and as a result, a large percentage of the effort to develop alternative solar cell materials has been expended on gallium arsenide.

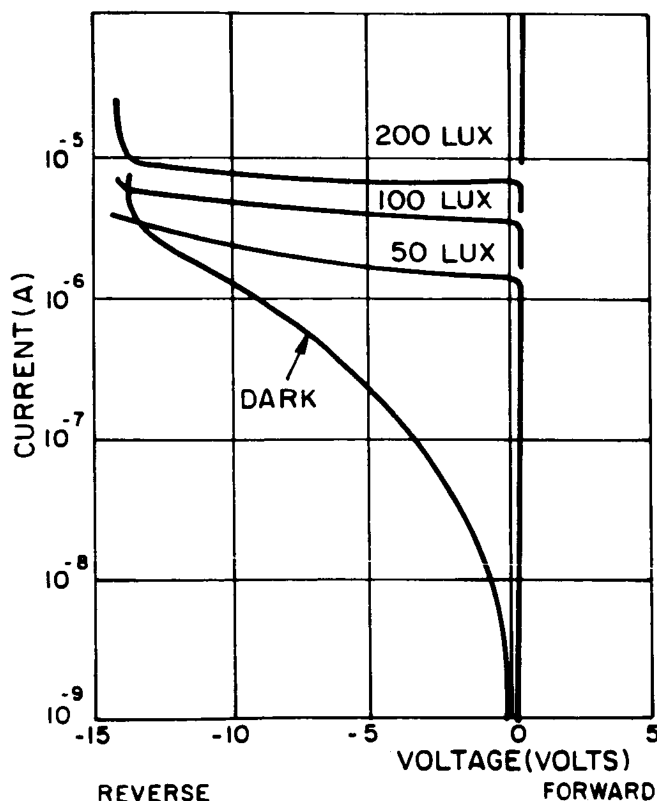

Figure 16. Current-voltage characteristic of GaAs photocell for different intensities, after Welker

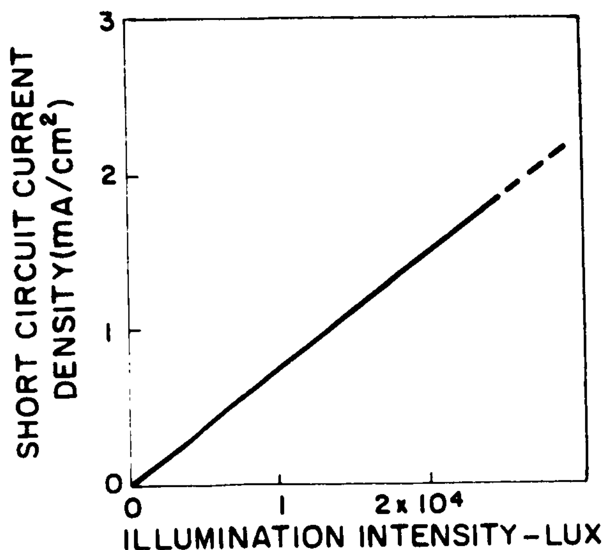

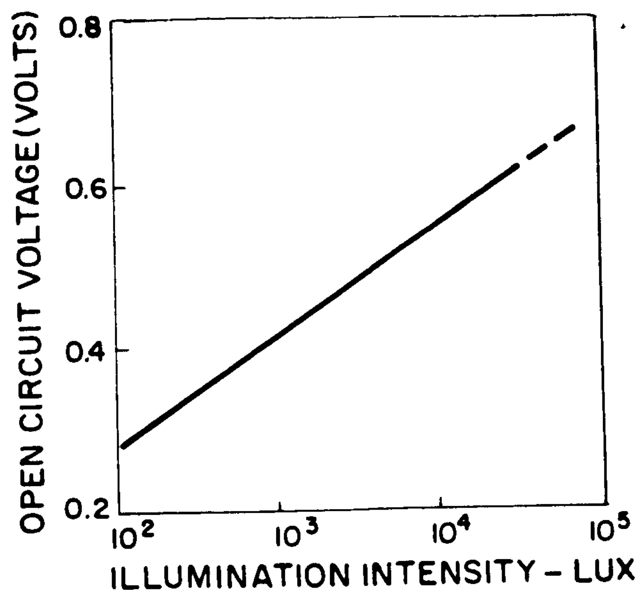

Figure 17(a). Variation of open-circuit voltage with intensity for GaAs photocell, after Gremmelmaier

Figure 17(b). Variation of short-circuit current with intensity for GaAs photocell, after Gremmelmaier

Of the II-VI compounds which aroused the interest of investigators during the early and middle 1950's, cadmium sulfide and cadmium telluride were the most outstanding and the only two on which any significant amount of work toward photovoltaic solar energy conversion was done. Cadmium telluride derived interest from the fact that its bandgap is near the optimum for solar energy conversion as indicated by the analysis of Loferski et al. (152). The investigations of cadmium sulfide, which started earlier and became more extensive, however, arose from a completely different set of circumstances. Cadmium sulfide's bandgap (2.4eV) is so large, that, at normal temperatures, it should be relatively inefficient for photovoltaic solar energy conversion since a considerable portion of the sun's photons are not energetic enough to excite carriers in the intrinsic material. D.C. Reynolds and G.M. Leies, in the course of investigating photoconduction and rectification in cadmium sulfide, discovered pronounced photovoltaic effects (154).

The first observations of the photovoltaic effect in cadmium sulfide occurred while testing cadmium sulfide rectifiers. The rectifiers were constructed by attaching an indium base electrode and a top electrode of silver, copper, gold, or platinum.to crystals approximately 3 mm thick. The electrodes were apparently opaque but when the rectifiers were illuminated from the side, some of them were found to be photovoltaically sensitive. Open-circuit voltages of 0.4 V, and short-circuit current densities as high as 15 $mA \cdot cm^{-2}$ were observed under sunlight illumination. The spectral response of these photovoltaic effects did not conform to that predicted on the

basis of the bandgap of cadmium sulfide (155), but showed a considerable peak in the red, which in some crystals was higher than that of the intrinsic (green) peak (Figure 18). It was also observed that the short-circuit current at a given wavelength was dependent on the wavelength of light used in prior illumination of the crystal. These effects were attributed to the presence of an impurity band in the forbidden zone into which a portion of the excited electrons could pass. If these electrons were long lived and could move freely in the impurity band, then it would act like a conduction band, assuming the proper electrode conditions. This was felt by Reynolds to be the most plausible mechanism to explain both the photoconductive and photovoltaic effects observed (156).

Photovoltaic effects were also observed in compressed cadmium sulfide powders, although the photocurrents were relatively low. The discovery of the unusual photovoltaic properties of cadmium sulfide when treated with certain metals initiated a series of investigations into the energy conversion possibilities of this material, especially in thin-film form, which is still in progress. Many of the peculiar properties discovered in the earliest cadmium sulfide photovoltaic cells are still eluding a satisfactory explanation by today's investigators.

The photovoltaic properties of cadmium telluride received very little experimental attention until after 1955. The fact that photovoltaic effects had been observed in cadmium telluride was mentioned in one of the early Signal Corps reports written by RCA Laboratories investigators (153), but no details were given. As mentioned, theoretical analysis showed that cadmium telluride should have an efficiency exceeding that of silicon on the basis of the width of its bandgap. As a result, cadmium telluride was subjected to intensive developmental work during the years following 1955.

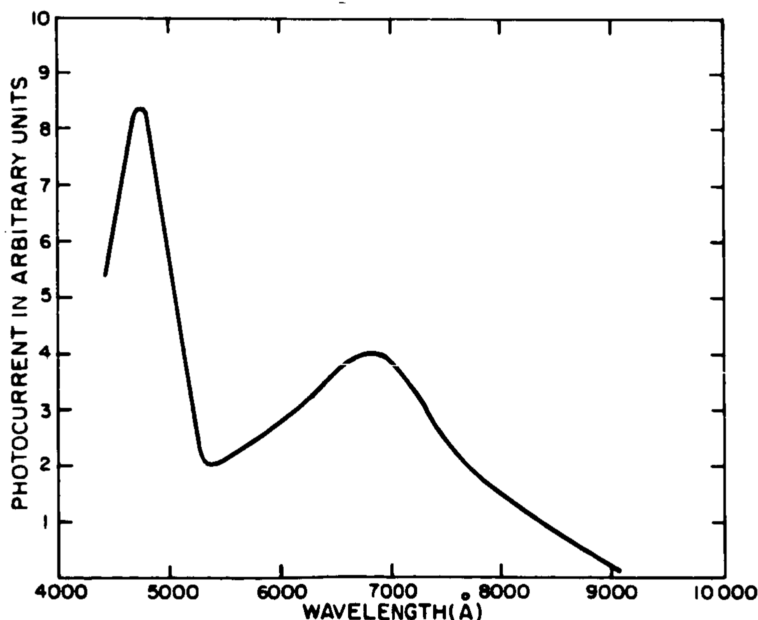

Figure 18. Spectral response of a CdS crystal with silver and indium electrodes, after Reynolds

1. Progress in Supporting Fields

The development of a satisfactory theoretical account of semiconductor rectification by Mott and Schottky during the late 1930's was based in part on supporting work in solid-state theory during the same period. It would be inappropriate to trace this in detail here, but some mention of the main points is in order.

The most important development was the band theory of energy levels in solids. This was derived from the quantum theory, originally by M. J. O. Strutt in 1928, with mathematical investigation of the concept by L. Brillouin, P. M. Morse, R. Peierls, and R. L. Kronig and W. G. Penney in 1930 and 1931. Seitz's book (157) on solid-state theory, originally published in 1940, reviews the development of the subject, and gives a full account of the state of the theory up to the late 1930's. The explanation given by this theory of the differences in electrical behavior of metals, semiconductors, and insulators is, of course, that used at the present time. For pure semiconductors, the electrical properties were shown to be determined by that part of the electronic band structure which consists of a lower-energy band (valence band) whose states would be completely filled by electrons at zero absolute temperature, separated by an energy gap, from a higher-energy band of allowed states (conduction band) which would be unoccupied at 0°K. The situation is as illustrated in Figure 19(a). The energy gap between the two bands represents a range of energies which the electrons cannot possess ('forbidden bandgap'), because of the restrictions described by the quantum theory. This remains true in a chemically pure single crystal of a semiconductor even when the temperature is raised above absolute zero. However, as the temperature is raised, there exists a finite increasing probability that a few electrons may acquire sufficient thermal energy to transfer from the lower (valence) band into the upper (conduction) band.

Since electrical conductivity requires that motion in a preferred direction be imparted to electrons by an electric field, some electrons in a solid through which a current is passing must have higher energies than electrons in a solid not carrying a current. In a semiconductor at absolute zero, the electrical conductivity must therefore be zero since there are no allowed higher energy states available to electrons, all energy levels in the valence band being occupied, unless they can cross the forbidden band. Normal electrical fields cannot supply sufficient energy to an electron to permit it to make the transition across the bandgap. However, if the temperature is raised above absolute zero, thermal excitation can provide sufficient energy to permit some electrons to occupy states in the higher energy band. Now each band consists of allowed energy levels separated by extremely small energy increments. Hence, application of an electrical field at a temperature other than absolute zero causes electrons in both bands to move by transferring to allowed states of very slightly higher energy. These are available both in the higher-energy band (because its states are normally unfilled), and in the lower-energy band,

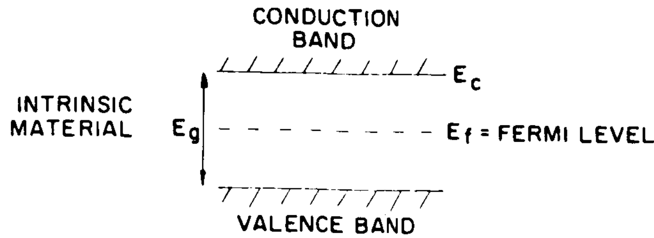

Figure 19(a). Band structure for intrinsic semiconductor.

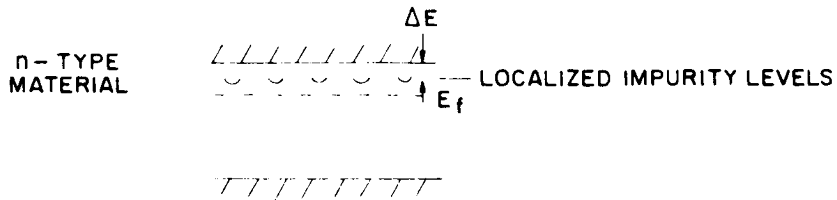

Figure 19(b). Band structure for n-type semiconductor.

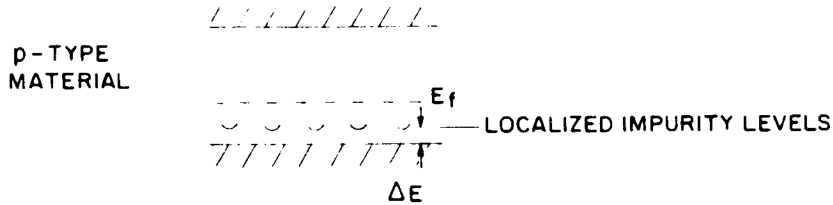

THE DIAGRAMS ARE GRAPHS WITH SCALES: ELECTRON ENERGY, SPATIAL COORDINATE

Figure 19(c). Band structure for p-type semiconductor.

because electrons can transfer into states left vacant by electrons thermally excited into the higher band. It was realized that the latter process could be regarded as the motion of a charge of equal magnitude and opposite sign to that of an electron, and this concept of 'hole' conduction was used immediately by Mott and others.

Now the experimental work of Schottky had shown that small amounts of chemical impurities or departures from stoichiometry could cause the conduction process to be greatly enhanced, and to be dominated by either motion of electrons in the conduction band or by motion of holes in the valence band.

The theory showed that these effects could be explained by the creation of allowed energy states within the forbidden bandgap, these states lying close to one of the semiconductor band edges, and being spatially associated with the impurity atom giving rise to the energy level. If the species causing the state also provided an electron to fill the state at absolute zero, then at a higher temperature the electron could transfer to the conduction band. Species having such properties are called donors. The probability of transfers to the conduction band occurring is much enhanced for electrons occupying energy states close to the conduction band. Based on such a large transition probability, only a small concentration of donors would be necessary to dominate the conduction process at relatively low temperatures, where the thermal transfer of electrons directly from the valence to the conduction band is unlikely. The converse process, leading to the formation of holes in the valence band, occurs through the presence of a species providing an energy level close to the valence band, but no electron to fill it. Such species is called an acceptor.

It was found convenient to consider an energy level at which there would be a 50% probability for the occupancy of a state at that energy. This level is called the Fermi level (E_f), and for most cases of a semiconductor it lies inside the forbidden band. Then the probability P(E) of occupancy of an energy level E by an electron is described by

$$P(E) = \frac{1}{1 + \exp\left(\frac{E-E_f}{kT}\right)} \tag{14}$$

Equation (14) is the Fermi-Dirac distribution function, often called "Fermi function", and is used frequently as a factor to a distribution of allowed energy states, thus describing their actual occupancy. In the general case, E_F does not have to represent an energy level half-filled with electrons, since E_F may be in the forbidden bandgap; then the Fermi level is a conceptual level only. The Fermi function, Eq. (14), characterizes a distribution such that there is an equal number of higher energy levels above E_F occupied, as there are unoccupied levels of energy less than E_F.* The band-structure for three types of semiconductor can now be visualized, as shown in Figure 19.

In the early 1930's, both A. H. Wilson and R. H. Fowler provided methods for calculating the density of conduction electrons or holes. The results showed that

$$n = \frac{\nu}{2} \exp\left(\frac{-\Delta E}{kT}\right) \left[\left(1 + \frac{4N}{\mu} \exp\frac{\Delta E}{kT}\right)^{1/2} -1\right] \tag{15}$$

---

*It should be noted that at energies sufficiently removed from E_f (that is, $\frac{E-E_f}{kT} >> 1$, Eq. (14) describes the distribution obtained earlier by the methods of Maxwell and Boltzmann.

where

$$\nu = 2\left(\frac{2\mu\, m^* kT}{h^2}\right)^{3/2} \tag{16}$$

n = density of electrons or holes
m^* = effective mass of electrons or holes in the lattice
k = Boltzmann's constant
T = absolute temperature
h = Planck's constant
ΔE = energy difference between impurity level and adjacent band edge, as illustrated in Figure (19) for electrons or holes
N = density of donors or acceptors

Thus, the electrical conductivity will increase exponentially with temperature until all the carrier-contributing species are ionized. Then the density of free carriers will remain constant with increase of temperature until sufficiently high temperatures are reached to allow thermal excitation across the bandgap to contribute a significant number of carriers. At still higher temperatures, the carrier concentration will then again increase exponentially with temperature, as in a pure semiconductor without impurity level.

This band theory was used by Mott and Schottky in their theoretical models accounting for semiconductor-metal junction I-V characteristics in 1939.

2. Continuation of Work on Rectification Theory

a. Metal-Semiconductor Contacts (1940-46): Mott's theory (76), published in 1939*, described a device having no space charge in the barrier layer. This approximation is not wholly valid, and Schottky provided an analysis dealing with two cases nearer the experimental facts:

(i) A device in which all carrier-generating species in the space-charge region are ionized ("exhaustion layer"), and

(ii) a device in which the ionization is incomplete.

In common with Mott, Schottky assumed a barrier region 10^{-4} to 10^{-5} cm thick, in which a current carrier would experience multiple scattering events as it passed through the junction. Both theories were based on a free-carrier diffusion process, and in the case of an "exhaustion" layer, essentially the same results were obtained in both theories, with an exponential dependence of current on applied voltage.

---

*In the Final Report of this contract, this account of Schottky's further work will appear in Section II-C-2.

Thus, the work of Mott and Schottky laid the foundations for the presently accepted theories of p-n junctions. Both theories accounted satisfactorily for the junction width, the I-V characteristic, and its behavior under temperature changes. The I-V characteristic is of the form:

$$J = J_0 (\exp \alpha V - 1) \tag{17}$$

and was called the 'rectifier equation' in the terminology of the period, but is now known as the 'diode equation'. The differences between these theories and later ones are concerned with details of the band structure and charge distribution in the barrier layer. These differences give rise to differing values of J_0, and discussion of this highly interesting parameter is postponed to later sections of this report.

The great deal of experimental work done on mixer and detector diodes for radar microwave systems during the second World War*, was accompanied by theoretical work by various groups. Notable among these were Bethe at the Radiation Laboratory of MIT, Seitz and others at the University of Pennsylvania, and Sachs and others at Purdue University.

The principal objective of this work lay in explaining the electrical behavior of point-contact metal-to-semiconductor rectifiers. The semiconductors used were silicon and germanium. In general, the I-V characteristics followed the expected exponential law, and the main consideration was to provide a theoretical explanation of the I_0 values in the diode equation, by analyzing device models with various band structures. Because of the nature of the devices (a metal point pressed against the surface of a crystal of semiconductor), this amounted to finding the band structure at the free surface of a semiconductor. Bethe (158) analyzed this by integrating Poisson's equation with suitable boundary conditions, and concluded that at the metal-semiconductor contact a barrier region of 10^{-6} cm thickness would be formed. This analysis was done for silicon, and it was pointed out that a much thinner region would result if the semiconductor dielectric constant were to be considerably less than the value 13.0 of silicon. Bethe also noted that tunnelling and image forces which were considered in some earlier rectifier theories, do not contribute significant effects in this type of device, chiefly due to the large value of the dielectric constant possessed by silicon, and also germanium.

---

*A note on the literature of this period: Work during World War II was classified at the time and, hence, did not immediately appear in the open literature. The results were recorded in a series of contract reports, which were not declassified until 1960. A group of papers by some of those who had been involved in the work were presented at the Meeting of the American Physical Society at Cambridge, Mass., April 25-27th 1946. Abstracts for these papers are to be found in Phys. Rev. 69, 628 (1946). An account of the work was published in Vol. 15 of the Radiation Lab. Series (Reference 90) in 1948, from which most of the information in this section has been obtained, this being the most coherent source readily available.

Now this barrier thickness is much less than the 10^{-5} to 10^{-4} values measured in the copper-copper oxide rectifiers to which Mott's and Schottky's analyses applied. In fact, the barrier thickness in the silicon devices was now of the same order of magnitude as the mean free path of the carriers, and hence a diffusion analysis of the electrical characteristics was not applicable. Bethe discussed an alternative "diode analysis" which is applicable when scattering processes in the transit of carriers across the barrier can be neglected. This analysis is the same as that for the thermionic diode (hence the appellation), and is based on an electron distribution given by the Maxwell-Boltzmann approximation. Hence, the I-V equation is again of the same form as Eq. (17), but with a different J_o value:

$$J_o = nq \sqrt{\frac{2kT}{\pi m^*}} \exp\left(\frac{-q V_o}{kT}\right) \qquad (18)$$

$$I_o = (\text{device area}) \times J_o \qquad (19)$$

where V_o = barrier height, as shown in Figure 7(a). When the barrier width is of the same order of magnitude as the mean free path, it is not immediately apparent that scattering processes can be neglected. However, Bethe pointed out that the mean free path should not be compared with the total boundary region thickness, but rather with the distance over which the potential changes by an amount kT.

In summation, Bethe analyzed the point-contact rectifier, showing that the electrical behavior could be reasonably well explained by the (thermionic) diode theory, with a boundary layer about 10^{-6} cm thick arising from the bulk properties of the semiconductor alone without the necessity for introduction of an electrically active species at the semiconductor surface to explain the barrier layer properties.

The results of this theory were critically examined by comparison with actual devices, mainly by the Purdue University group. This appears to have been the first occasion on which Log (I) versus V plots were used for analysis, and the work was probably the first systematic demonstration of the departures in the behavior of experimental diodes from accepted theories including the present ones. The form of typical results is shown in Figure 20. One sees two linear regions in the curve, with different slopes and corresponding different values of J_o. These results showed that:

(i) The theoretical value of α in Eq. (17) was too large by an amount varying from close to 1 to 4 or even more.

(ii) Values of I_o consistent with the forward characteristic were incompatible with the reverse characteristic.

The inconsistency between forward and reverse characteristics appears to have been due to barrier leakage, but the anomalies in α are still observed today, and will be further

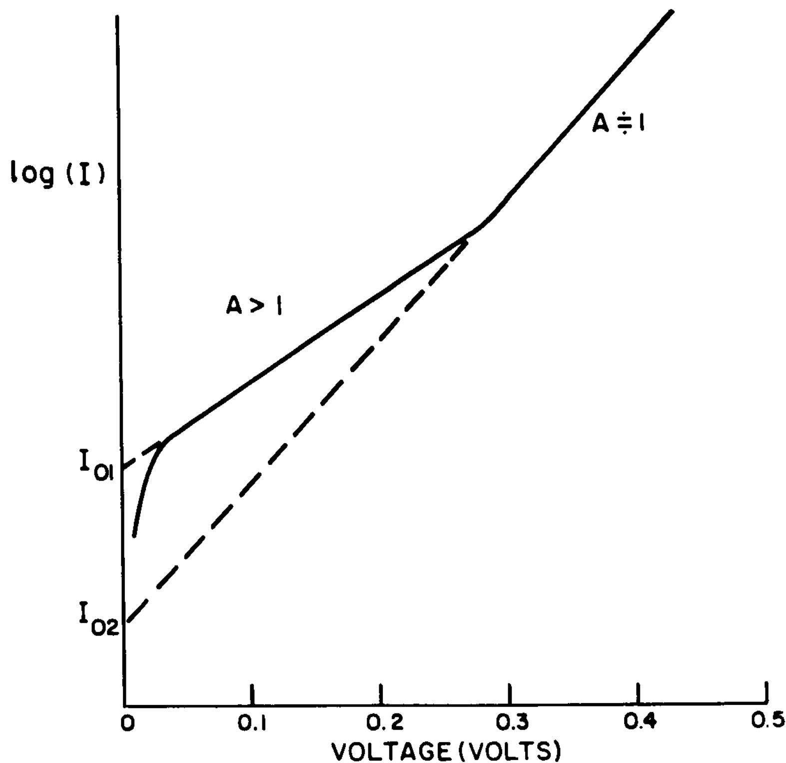

Figure 20. Log (I) vs. V for usual experimental diode

considered in later sections. Since this analysis concerns a device that is clearly not applicable to power generation, discussion has been limited to those aspects of the work which contributed to the progress of semiconductor junction theory.

b. Progress—1946 to 1955: During the war years, a great deal of experimental work was done at Bell Laboratories on the preparation of silicon and on fabrication of crystal diodes. After the war, this interest in crystal diodes was continued and led eventually to development of the transistor and the solar cell. The experimental work was the basis for significant advances in the theory which also came from Bell Laboratories, notably by Brattain, Barden, Shockley, and others.

Meyerhoff (159) conclusively established that for metallic contacts to n- and p-type silicon, the experimental facts did not fit the theory of the junction electrical properties. The disparity arose over the question of the relation between barrier height [V_0 in Eq. (18)] and the work function differences between the metal and the semiconductor. Whereas Brattain, as quoted by Bardeen (160), had found a correlation between work function difference and rectification for metal contacts evaporated onto cuprous oxide, Meyerhoff found no correlation between work function difference and barrier height, but rather, the same metal could make a rectifying contact to both n- and p-type silicon, only the direction of easy current flow being reversed by the semiconductor type change.

Bardeen (160) accounted for this behavior by considering surface states lying inside the forbidden band. Surface states are energy levels associated with the properties of a semiconductor surface, and are physically located there. They may or may not be associated with impurity atoms. Bardeen assumed the surface states to be both acceptor and donor type levels distributed over a range of energies in the forbidden band, but no assumption about the form of the distribution was made. Most of the donor levels lying above the Fermi level E_f will be vacant, and the remaining ions will provide a positive charge at the surface. Similarly, most of the acceptor levels lying below the Fermi level will be occupied by electrons, and will provide a negative charge at the surface. Acceptor levels above the Fermi level and donor levels below the Fermi level, will be largely un-ionized and thus electrically neutral. Hence, an energy E_o may be defined for which, according to the Fermi function, the number of ionized surface donor levels above E_o equals the number of ionized surface acceptor levels below E_o, when the Fermi level would be at E_o [see Figure 21(a)]. The magnitude of E_o will therefore be determined by the distribution of the surface states. In thermal equilibrium, the Fermi energy must be constant throughout the material. To obtain this condition and simultaneously maintain overall charge neutrality in the semiconductor, bending of the valence and conduction bands in general occurs, as shown in Figure 21(b) for n-type material. This means that at equilibrium, the net surface charge (caused by $E_f \neq E_o$) is balanced by a charge near the surface due to ionized donors which are not compensated by free electrons. Thus a space charge region is created below the surface. For p-type material, the converse occurs. Now it is clear that if the density of surface states is high, the difference between E_F and E_o need be very small regardless of the doping density and type of the semiconductor bulk. Hence, the band-bending, and particularly the barrier height V_o, will be rather independent of the semiconductor properties, provided the surface state density is high, and the Fermi level in the semiconductor bulk is not near the center of the gap, which means that the semiconductor properties have to be strongly influenced by the donors or acceptors. By the same mechanism, when a metal-semiconductor junction is formed, creating a large density of surface states with rather uniform distribution, the Fermi level at the semiconductor surface need move by only a small amount to provide a surface dipole layer of sufficient magnitude to compensate for the difference in work functions of the metal and semiconductor. Thus, V_o will again be only little affected by the work function of the metal, in correspondence with the experimental results of Meyerhoff.

It is interesting to note that Bardeen's paper appears to contain the first mention in a theoretical context of a junction between p- and n-type regions of the same material. This reflects the progress made in the preparation of semiconductors, since it was now possible for the first time to prepare a material with both conductivity types, and, hence, it became worthwhile to consider theoretically a p-n junction rather than a metal-semiconductor junction.

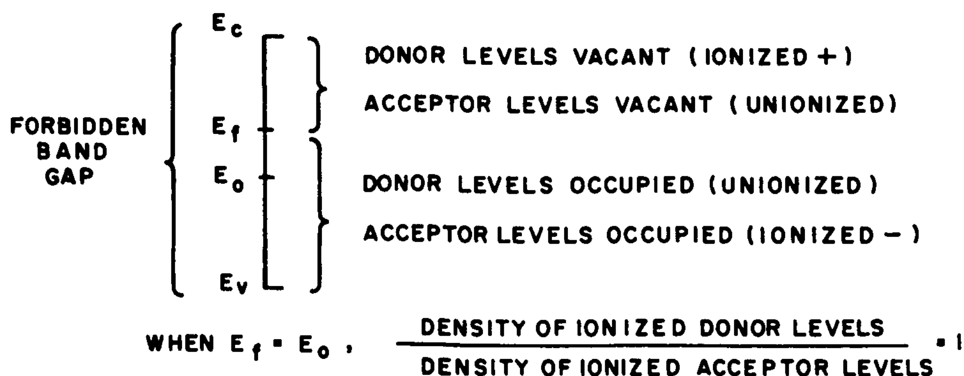

Figure 21(a). Energy levels at semiconductor surface

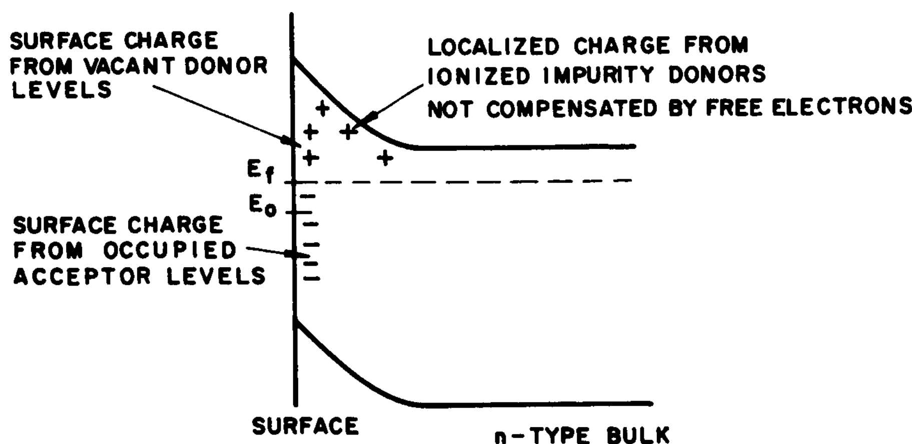

Figure 21(b). Formation of band-bending at semiconductor surface, after Bardeen

Sosnowski (132) appears to have been the first to publish results of an analysis of p-n junction behavior. However, Sosnowski considered the case of a very narrow junction region, with a transition region width less than the scattering length for carrier-lattice interactions. (Sosnowski's analysis is therefore to be contrasted with the results of Shockley, whose analysis concerned a junction sufficiently wide so that diffusion effects occurred in the junction region.) In the result of Sosnowski's theory the hole and electron currents followed the familiar exponential dependence on applied bias, leading to the rectifier characteristic. This analysis was performed to describe experimental effects seen in lead sulfide. The specimens were thin layers, with localized "excess" and "defect" characteristics, the p- and n-regions arising from oxygen impurity and excess lead, respectively. These specimens were photosensitive, and further mention of this work will be found in Section IV-D below.

The results of the most important theoretical work on p-n junction characteristics were published by Shockley in 1949 (161). As these results are the basis for much of the present understanding and viewpoints on p-n junction behavior, they will be considered in some detail.

The band structure of the semiconductor under consideration is shown in Figure 22,* for various situations.

It is convenient to define an electrostatic potential ψ, midway between the valence and conduction bands. At thermal equilibrium, the hole and electron densities in the valence and conduction bands, respectively, are determined by the Fermi energy, and the electrostatic potential according to the expressions:

$$p = n_i \exp \frac{q(\psi - E_f)}{kT} \tag{20}$$

$$n = n_i \exp \frac{q(E_f - \psi)}{kT} \tag{21}$$

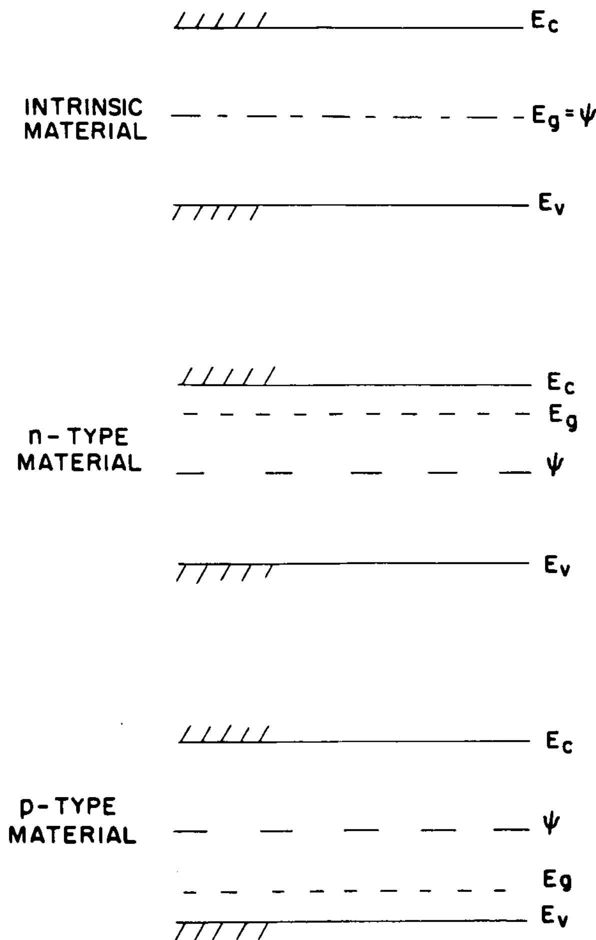

Figure 22. Band structures of semiconductor of various conductivity types

*To maintain consistency in this report, electron energy is plotted as increasing in the positive direction on the ordinate. Shockley's original diagram was plotted in the inverted sense.

where

n_i = free electron density in intrinsic material
n = free electron density in extrinsic material
p = free hole density in extrinsic material.

One observes that Eqs. (20) and (21) apply for the "nondegenerate" case, where the Fermi function can be described by the Maxwell-Boltzmann distribution (see Section D-1 above). This provides commonality with Schottky's and Mott's work, and as before, the exponential I-V curve arises from this basic relationship. In the nonequilibrium case, existing, for instance, when excess holes are present in n-type material, the distribution of electrons and holes in the conduction and valence bands cannot strictly be described by a Fermi level.

However, in analogy to Eqs. (20) and (21), two separate quasi-Fermi levels can be used to describe the nonequilibrium densities of holes and electrons, as exemplified in Figure 23.

$$p = n_i \exp \frac{q\left(\psi - E_{fp}\right)}{kT} \tag{22}$$

$$n = n_i \exp \frac{q\left(E_{fn} - \psi\right)}{kT} \tag{23}$$

Currents in the semiconductor may arise either from nonuniform carrier distribution (diffusion effects) or from electrostatic potential gradients (drift effects). Hence, the hole and electron currents are described by

$$I_p = q\,(D_p \nabla p - \mu_p p\, \nabla\psi) \tag{24}$$

$$I_n = bq\,(D_p \nabla n + \mu_p n \nabla\psi) \tag{25}$$

where

μ_p = hole mobility
D_p = diffusion constant for holes
b = ratio of electron to hole mobility

Noting that

$$\mu_p = \frac{qD_p}{kT} \quad \text{(Einstein relation),} \tag{26}$$

Eqs. (24) and (25) can be rewritten using Eqs. (22) and (23):

$$I_p = q\mu_p p \nabla E_{fp} \tag{27}$$

$$I_n = qb\mu_p n \nabla E_{fn} \tag{28}$$

If it is assumed that all acceptors and donors are ionized, then the net charge density at a point in the semiconductor is

$$\rho = q\,(p - n + N_d - N_a) \tag{29}$$

where

$$N_d = \text{local donor density}$$
$$N_a = \text{local acceptor density} \tag{30}$$

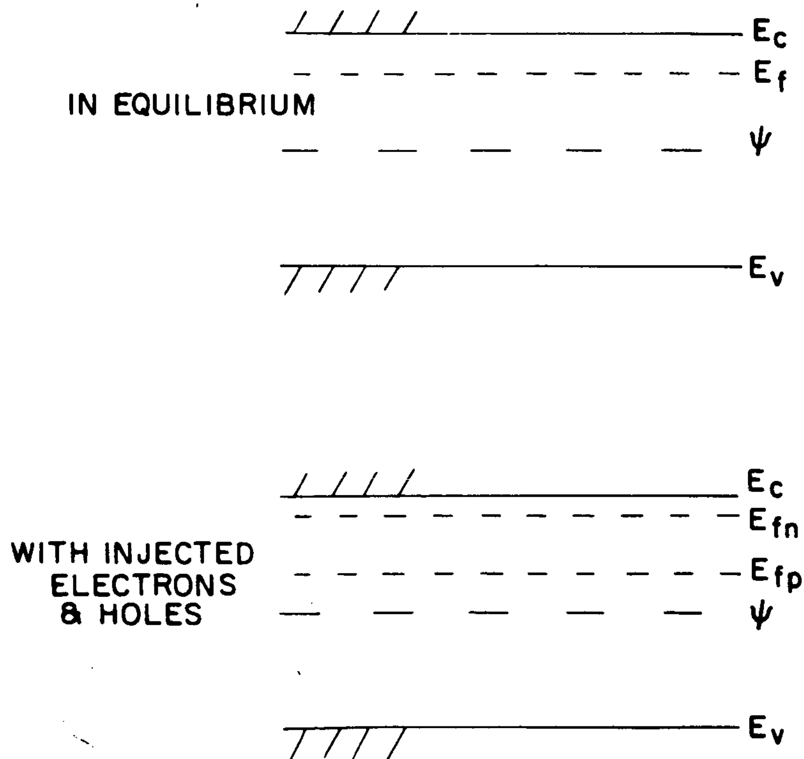

Figure 23. Energy levels in n-type semiconductor in thermal equilibrium, and with injected carriers

Considering a semiconductor in which the values of N_a and N_d are spatially varying, so that a junction between p- and n-type regions exists, Shockley showed that two cases can be obtained:

(i) If N_a and N_d change sufficiently slowly in moving spatially through the material, the changes caused by ionization of the acceptors and donors are neutralized by the presence of balancing charges from the free carriers.

(ii) If N_a and N_d change rapidly, then this charge balancing does not occur, and localized net space charge densities exist in the junction region.

It is convenient to set E_f - 0 under equilibrium conditions. Now Poisson's equation relates the charge density to the electric field:

$$\nabla^2 \psi = \frac{4 \pi \rho}{\kappa} \tag{31}$$

where

κ = dielectric constant

Substituting for ρ from Eq. (29), Eq. (31) can be integrated twice to yield the potential distribution in the junction region. Two boundary conditions are needed: one is applied by putting $\psi = 0$ at $x = 0$ (i.e., $x = 0$ is placed at the center of the junction, where $\psi = 0$ coincides with $E_f = 0$; see Figure 24). The second is applied by putting $(d\psi/dx) = 0$ at $x = x_m$, x_m being the edge of the space-charge layer, where ψ assumes the bulk equilibrium value. Hence, the width of the space-charge layer and the potential distribution in the layer are obtained in their dependence on the distribution of the fixed charges $N_d - N_a$. In deriving the junction I-V characteristic, Shockley assumed that the diffusion length for minority carriers is long compared with the transition region width. This is an important assumption which is not always fulfilled in actual devices, but which facilitates the following derivation by making the hole and electron currents remain uniform across the transition region, which extends between x_{Tn} and x_{Tp}, as shown in Figure 24, and serves to illustrate the case under consideration. He also assumed that the currents are sufficiently small so as not to alter significantly the minority-carrier lifetimes and diffusion constants outside the transition region. Shockley's derivation was done in such a way as to obtain both the dc and ac behavior (particularly the impedance) of the junction. For solar cell purposes, this is an unnecessary complication, so that attention shall be confined to the dc component.

The hole density at the point x_{Tn} under an applied bias $\delta\varphi = (q/kT)\delta E_f$ is given by

$$p(x_{Tn}) = n_i \exp\left[\frac{q(\psi_a - E_{fa} - \delta E_f)}{kT}\right] \tag{32}$$

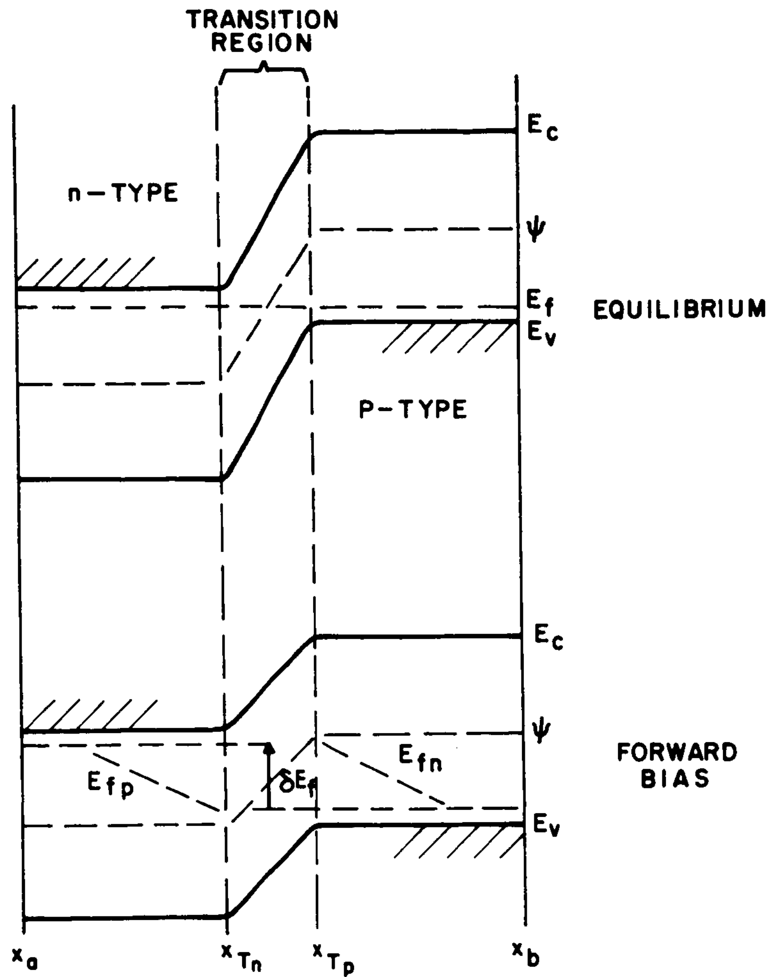

Figure 24. Band structure and energy levels in a p-n junction at equilibrium and under forward bias, after Shockley.

$$p(x_{Tn}) = p_n \exp\left(\frac{-q\,\delta E_f}{kT}\right) \tag{33}$$

where

x_{Tn} = edge of transition region

p_n = equilibrium hole concentration in the n region

E_{fa} = E_{fn} at $x = x_a$

$\delta E_f = E_{fn} - E_{fp}$ in transition region and the subscript a denotes a value sufficiently far from the junction that the equilibrium values are obtained; see Figure 24. The hole current is carried by that part of $p(x_{Tn})$ which is in excess of the equilibrium value; i.e., the hole density carrying the hole current is

$$p_o(x_{Tn}) = p_n \left[\exp\left(\frac{-q\,\delta E_f}{kT}\right) -1 \right] \tag{34}$$

Now the current carried by the holes is given by

$$I_p(x_{Tn}) = qD_p \cdot \frac{dp}{dx} \tag{35}$$

(dp/dx) is governed by the rate at which the excess holes (p_o) are removed by recombination according to the relation: $p = p_o \exp(-x/L_p)$ so that

$$\frac{dp}{dx} = \frac{-p_o}{L_p}$$

where L_p = diffusion length for holes in the n-region. Hence,

$$I_p(x_{Tn}) = \frac{qD}{L_p} \cdot p_o(x_{Tn}) \tag{36}$$

Placing ($x = x_{Tn}$) to obtain p_o at this point, and by similar considerations for the electron current, the total junction current is obtained:

$$I = I_p(x_{Tn}) + I_n(x_{Tn}) = qD_p \left(\frac{p_n}{L_p} + \frac{b\,n_p}{L_n}\right) \left[\exp\left(\frac{-q\,\delta E_f}{kT}\right) -1 \right] \tag{37}$$

The junction equation can now be re-written in the familiar form

$$I = I_o \left[\exp\left(\frac{qV}{kT}\right) -1 \right] \tag{38}$$

where

$$V = -\delta E_f \cdot q$$

$$I_o = I_{po} + I_{no} = qD \left(\frac{P_n}{L_p} + \frac{b\,n_p}{L_n}\right) \tag{39}$$

By writing, according to Eqs. (20) and (21):

$$n_i^2 = p_n \times n_n = p_p \times n_p$$

$$I_o = qD_p n_i^2 \left(\frac{1}{L_p n_n} + \frac{1}{L_n P_p} \right) \tag{40}$$

Thus, I_o is seen to depend on the intrinsic carrier density n_i, and on the majority-carrier densities on the two sides of the junction. I_o thus is expected to decrease with increasing E_g (since this reduces n_i exponentially), and to decrease with increasing impurity density (n_n and p_p).

Shockley then showed that, if there exists a localized region of high recombination rate in the transition region, an ohmic component of conductance is added in parallel with the rectifying characteristic of the junction. This will be particularly noticeable in the reverse characteristic.

Assuming that (i) the ohmic contact to the p-region injects only holes, (ii) the ohmic contact to the n region injects only electrons, (iii) there is no recombination, and (iv) that the charges introduced into the specimen by changing the applied reverse-bias voltage, change only the charge distribution at the space charge region of the p-n junction, so that the direct current flow does not change across the latter, then the device behaves as a variable capacitor. Shockley derived expressions for the value of the capacitance for two cases: (i) the linearly graded junction, for which it was shown that $1/C^3$ is a linear function of applied voltage, and (ii) the abrupt junction (in which N_d and N_a are step functions at $x = 0$), for which $1/C^2$ is a linear function of applied voltage. The capacitance is the only junction parameter in Shockley's theory which is dependent on the detail of the junction structure, and, hence, provides an invaluable diagnostic approach to analysis of p-n junction geometries. It should be noted, however, that the assumptions used in the derivation limit the results to the case of reverse bias, and neglect the reverse saturation current.

Thus, Shockley provided an equation for the current which would be expected to flow in a device containing a p-n junction [Eq. (37)]. This showed that, provided:

(i) the change in impurity concentration is sufficiently sharp, that local space charges occur;

(ii) diffusion governs the motion of excess carriers in the material outside of the space-charge region [Eqs. (24) and (25)];

(iii) the recombination of carriers in the transition region can be neglected (diffusion length is long compared with the transition region width); and

(iv) the densities of injected charge carriers are small compared with the equilibrium values;

(then the I-V characteristic of the device depends only on the values of the bulk material parameters included in Eq. (37), and does not depend on the detailed way in which the donors and acceptors are distributed in forming the junction.

It is interesting to consider why Shockley's analysis should have proved so valuable in later work. Naturally, the reasons lie largely in the analytical talents and experience brought to bear on the problem. Shockley had been working on solid-state theory from 1935 and is cited by Seitz as having made contributions to the latter's work. It also seems that the experimental work done during the war period at B.T.L., provided a good working knowledge of the likely values for the various materials parameters. This compilation of data on ionization energies of impurities, carrier densities, lifetimes, diffusion lengths, mobilities, and junction widths enabled appropriate approximations and simplifications to be made in the analysis. Thus, a balance could be struck between a rigorous treatment dealing with every conceivable process (which, even had it been possible, would have led to intractable solutions), and a solution so simplified as to be of little value.

Shockley's main contribution appears to have been the application of the solid-state band theories and the carrier transport equations to a particular physical situation, which approximates the generally occurring one satisfactorily. Shockley also provided a unification of existing ideas, giving a synoptic analysis which could be used as a starting point for later work in a wide variety of fields.

3. Theory of Photovoltaic Cells

a. Photoeffects at p-n Junctions: During the 1930's, a primary interest in semiconductor research lay in the photoeffects which were seen in copper-copper oxide photocells. During this period, Schottky and others provided the basic theory of the photovoltaic effect, as discussed previously. In the period which followed, the major fields of interest for semiconductor research lay in the use of point-contact metal-semiconductor diodes for microwave applications, and later in transistor action. Thus, the major theoretical work was done on diode characteristics, with notable advances being made in p-n junction theory, an account of which has been given in the preceding section. Although it was well established that p-n junctions were photosensitive, very little work was done in this area until experimental work on single-crystal silicon solar cells indicated that the photovoltaic effect could have application to power generation. Work on the photovoltaic effect and the theory and analysis of devices using the effect then proliferated. It should be realized, however, that all of these analyses were based on the concepts developed during the early work on copper oxide cells, even though many

of those involved appear to have been unaware of this. The account which follows describes the progress of the theory of the photovoltaic effect, and the next section of this report describes the progress of device analysis.

As described in Section III-C-2 of this report, Ohl and others at Bell Telephone Laboratories had observed photosensitivity at p-n junctions in silicon about 1940. However, this observation appears to have not been reported at the time, nor was it followed up during the wartime work. Hence, it appears that Sosnowski, Starkiewicz, and Simpson, working at the Admiralty Research Laboratory in England, were the first to report a photoeffect which was positively identified as occurring at a p-n junction (162-164). The specimen was lead sulfide, rendered p-type by oxygen impurity and n-type by excess lead, and the junctions occurred at the grain boundaries in thin layers used as infrared-sensitive photoconductors. The phenomena were explained by an energy band diagram for the p-n junction as shown in Figure 25, which is close to presently accepted ideas. The mechanism proposed for the photovoltaic effect was that electrons are transferred from the ground state to the conduction band, diffuse across the barrier, lose energy by collision with the lattice and are thus prevented from returning across the barrier.

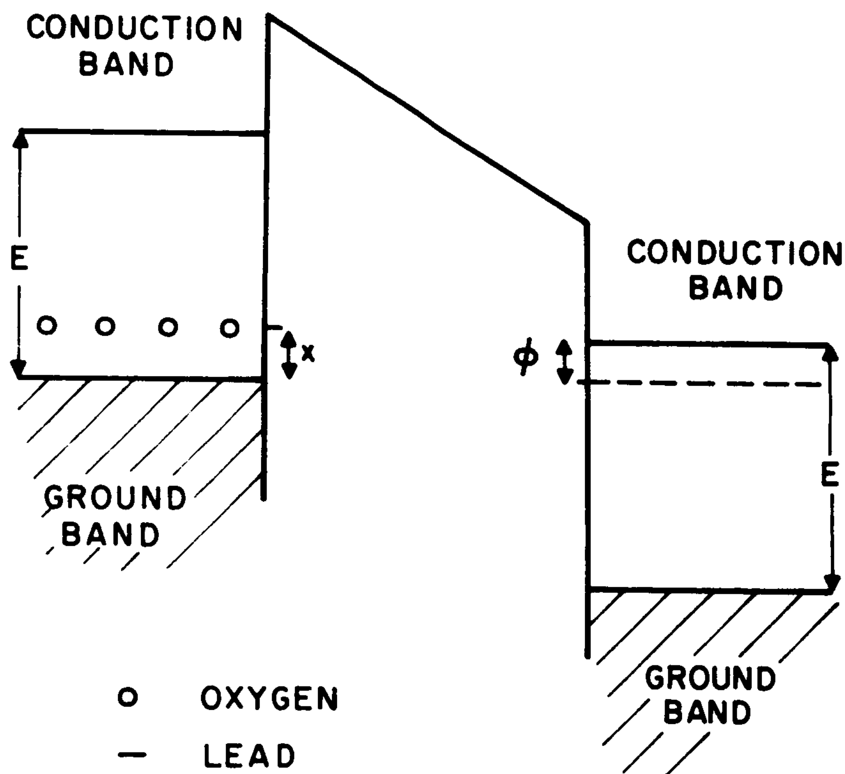

Figure 25. Junction structure in PbS, after Sosnowski et al.

This hypothesis was checked against experiment for direction of the photovoltage, and found to be correct. No quantitative analysis was reported, though an analysis of the I-V characteristic of the junction was provided, as described above. The important point of this work was the p-n junction band structure, which followed from earlier work, and probably had been used previously, but which had not appeared in the literature before.

In 1948, Lehovec published the results of theoretical work aimed at giving a comprehensive description of the photovoltaic effect in metal-semiconductor junction cells (1-29), building on the results of Schottky and Mott. The assumptions underlying the analysis were:

(i) An "effective barrier layer width" can be defined in a metal-semiconductor junction cell, and only carriers released in this region contribute to external current. This region may be approximately equal to the barrier region width determined by capacitance measurements.

(ii) Both drift and diffusion contribute to carrier motion.

(iii) Recombination in the active region may be neglected because free carrier densities are low in this region.

(iv) Absorption of a photon creates both free electrons and free holes, and these behave in exactly the same way as thermally generated free carriers.

Equating the density of carrier generation (using the exponential fall-off of light intensity with distance-Lambert's law) with the rate of change of current density with distance [right-hand side of Eq. (41)]:

$$\frac{J}{h\nu} \cdot \alpha \cdot \beta \exp(-\alpha x) = -\frac{1}{q}\frac{d}{dx}\left(-nq\mu_n \frac{dV}{dx} + qD_n \frac{dn}{dx}\right) \qquad (41)$$

where

J = illumination intensity
$h\nu$ = energy per photon
α = optical absorption constant
β = number of electrons released per photon absorbed
x = distance coordinate
μ_n = electron mobility
D_n = electron diffusion constant

This equation was solved to give a general "equation of state":

$$\left(\frac{Jq}{h\nu}\right) \cdot \beta A + I = n_o q \mu F \; [\exp(qV/kT) - 1] \tag{42}$$

with

$$A = \frac{1}{\left(1 + \frac{\alpha kT}{qF}\right)} - \exp(\alpha d)$$

and

F = absolute value of field intensity at $x = 0$

$$V = V_o + \frac{kT}{q} \ln\left(\frac{n_d}{n_o}\right)$$

V_o = barrier height
n_o = electron density at $x = 0$
n_d = electron density at $x = d$
d = "effective thickness" of barrier layer
I = current

Equation (42) has the general form of the presently used equation for the description of the solar cell characteristics. The first term of the left-hand side of Eq. (42) represents the light-generated current, the right-hand side the diode current. Lehovec pointed out that A effectively governs the quantum yield of the device. $A = 1$ is obtained if all incident quanta are absorbed in the active region, and all electrons generated are collected.

Working from Eq. (42), Lehovec showed that:

(i) The predicted photovoltage and photocurrent directions agreed with experiment for both p- and n-type semiconductors.

(ii) For $J = 0$, the dark dc characteristic of the device was given.

(iii) The short-circuit current (I_{SC}) was directly proportional to the light intensity.

(iv) The open-circuit voltage (V_{OC}) was proportional to J for $V \ll kT/q$, and proportional to log (J) for $V > kT/q$.

Although these results had been obtained before by separate analyses, Lehovec's major contribution was to derive all of these major device characteristics from a unified starting point.

Lehovec also pointed out that it is useful to consider a maximum power point on the characteristic curve, and that an approximation to the maximum available power (P_{max}) is the $V_{oc} \times I_{sc}$ product, though this will be higher than the actual value. It was also pointed out that P_{max} increases as (J^2) at very low light intensities ($V_{oc} << kT/q$), and as J x log (J) at high light intensities ($V_{oc} > kT/q$).

The most important points made by Lehovec were:

(i) The photons must create free carriers of both types if an external current is to be obtained.

(ii) Consideration of a maximum power point is useful.

Because of the changing technology, interest then moved to p-n junctions, and germanium devices were studied almost exclusively during the 1949-54 period. In 1949 and 1950, Fan (165) and Becker (134) reported work on germanium p-n junction devices, in which the open-circuit voltage V_{oc} was described by

$$V_{oc} = \frac{kT}{q} \ln \left(1 + \frac{\Delta n_p}{n_{po}} \right) \tag{43}$$

where

n_{po} = unilluminated (equilibrium) free electron density
Δn_p = excess electron density generated by light

This predicted open-circuit voltage was compared with experiment. Since the device was illuminated at the edge of the junction only (the junction was normal to the exposed face), various extraneous effects were introduced (shunting by the unactivated junction, leading to high temperature sensitivity, and surface recombination effects).

A more advanced germanium p-n junction device was investigated by Ruth and Moyer (140) and reported in 1954. Here a grown junction was parallel to and about 0.1 mm below the exposed surface. Experiments which measured the power conversion efficiency of the device confirmed in general the theoretical analysis of Lehovec, showing that the efficiency increased proportionally to the light intensity under low illumination, and as the logarithm of the illumination at higher illumination levels. A theoretical analysis of the current-voltage characteristic and of the photovoltaic performance of this device was performed and published early in the same year by Cummerow. A review of this work is presented in the Section III-D-3-b.

Rothlein and Fowler (138) also presented a theoretical analysis of a germanium photovoltaic cell with a junction formed by alloying. The analysis was based on established concepts, and applied to a device type which is no longer of general interest for power conversion.

The publication of the results from the Bell Laboratories work on diffused silicon cells included a number of similar analyses occurring about the same period, and present-day discussions on the photovoltaic effect also often include a similar analysis. Both the equivalent circuit and the derived expressions for I-V characteristics are fundamentally similar to the work done by Schottky during the early 1930's. An analysis of both the electron-voltaic and the photovoltaic effects was given by Pfann and van Roosbroeck (141) in 1954.

The equivalent circuit used is shown in Figure 26. (In the following the symbols and some of the current directions have been altered to make them consistent with the rest of this report.) Then

$$I = I_D - I_L \tag{44}$$

$$I_D = \left(\frac{kT}{qR_o}\right)\left[\exp\left(\frac{qV}{kT}\right) - 1\right] \tag{45}$$

where

$$R_o = \frac{kT}{qI_o} = \left(\frac{dV}{dI_D}\right)_{V=0}$$

R_o is the zero-point resistance of the diode, directly related to the saturation current.

$$V = -IR_L \tag{46a}$$

and the power output

$$P = IV = I^2R_L \tag{46b}$$

To find the load resistance giving maximum power (R_L'):

$$\frac{dP}{dR_L} = 0 \quad \text{(at optimum load)}$$

and hence,

$$I_L = \left(\frac{kT}{qR_L}\right) \ln\left(\frac{R_o}{R_L}\right) + \left(\frac{kT}{q}\right)\left(\frac{1}{R_L} - \frac{1}{R_o}\right) \tag{47}$$

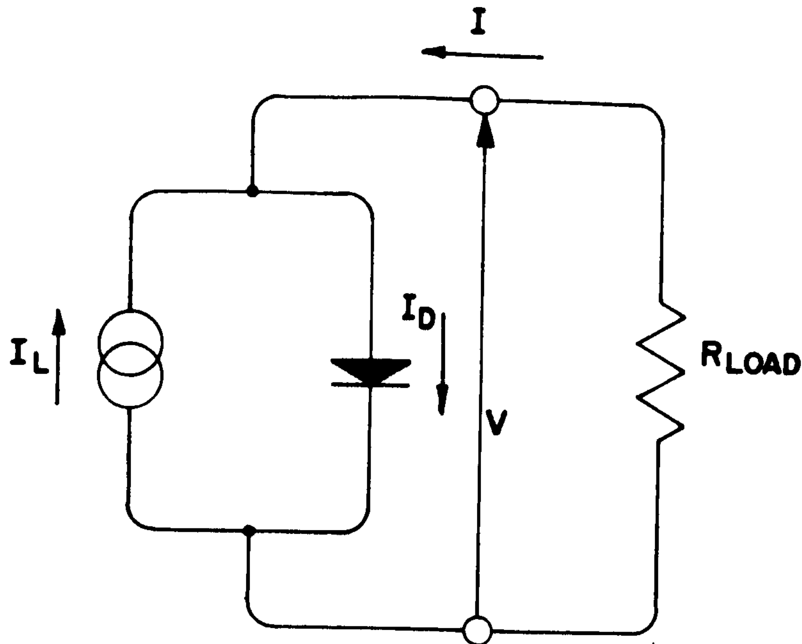

Figure 26. Simplified equivalent circuit of a photovoltaic cell

Equation (48) is based on the cell equivalent circuit which neglects R_s and R_{sh} (as shown in Figure 26), and it is assumed that the diode characteristic obeys Shockley's diffusion theory. Equation (47) must be solved numerically to obtain R_L'.

Pfann and van Roosbroeck then provided a series of manipulations to simplify the resulting relationships. Thus, they obtained an expression for the maximum power available, in terms of the optimum load resistance:

$$P_m = \frac{1}{R_L'}\left(\frac{kT}{q}\ln\frac{R_o}{R_L'}\right)^2 \tag{48}$$

Pfann and van Roosbroeck also provided an analysis of the effect of recombination in reducing the light-generated current, by introducing a factor Q, for quantum efficiency of the cell, defined as the ratio:

$$Q = \frac{\text{number of hole-electron pairs separated by the p-n junction}}{\text{number of photons absorbed in the semiconductor}}$$

An expression for Q in terms of the junction depth, the surface recombination velocity, the optical absorption constant for the semiconductor, and the diffusion lengths in the p- and n-regions, was then given, without derivation, for the case of an infinite base thickness, with collection based on diffusion only. This appears to be the first detailed analysis of the quantum efficiency or collection efficiency, as it was called later by some authors, based on semiconductor material properties.

The significance is the realization by these authors, without their stating it, that the light-generated current density, or the collection efficiency, can be analyzed separately from the current-voltage characteristic of the device, based on the linear superposition of the current. These authors had to solve the same continuity equation which Cummerow used slightly earlier, but the analysis of light generated current only, provided simpler boundary conditions and easier manipulation of the solutions. Thus this analysis set the model for later theories, which included refinements to approximate the actual devices more closely.

Pfann and van Roosbroeck also noted that germanium junctions generally follow the theoretical diode equation with $A = 1$:

$$I_D = I_o \left(\exp \frac{qV}{AkT} - 1 \right) \tag{49}$$

However, they noted that silicon junctions frequently show values of $A > 1$.

Thus, by the end of 1954, the fundamental analyses of both the junction characteristic and the photovoltaic effect in a p-n junction device were well established. Work from 1955 to the present time has refined these basic results and shown how various imperfections in the cells contribute to losses in conversion efficiency.

b. *Ultimate Conversion Efficiency:* The photovoltaic germanium p-n junction device of Ruth and Moyer, which showed a sunlight conversion efficiency approaching 1%, stimulated Cummerow (who was working in the same laboratory of the General Electric Company), to analyze theoretically the maximum power conversion efficiency achievable with a germanium device (166). The geometry of the device considered is shown in Figure 27. The illumination generates hole-electron pairs in the semiconductor, but it was assumed that the rate of generation is not sufficient to substantially alter the majority-carrier density on either side of the junction. It was also assumed that the width of the transition (space-charge) region of the junction is much less than the diffusion length of minority carriers, and also much less than $(1/\alpha)$, the characteristic optical absorption length in the material.

The Shockley-Read theory of recombination (a brief account is given in Section IV-A-1) was then applied to determine the net rate of generation of carriers, accounting for thermal generation, photon-absorption generation, and recombination through trapping levels. This net generation was then equated to the spatial rate of change of current,

which was assumed to occur only by diffusion. This resulted in the general continuity equation:

$$g_p + g(x) - \left(\frac{p}{\tau_p}\right) + D_p \frac{d^2 p}{dx^2} = 0 \tag{50}$$

for holes in the n-type region, where

g_p = rate of thermal generation of holes in the n-type region
$g(x)$ = rate of hole generation by light absorption in the n-type region
p = nonequilibrium hole concentration in the n-type region
x = spatial coordinate
D_p = diffusion constant for holes in the n-type region.

Now light absorption in the semiconductor will be spatially dependent; hence,

$$g(x) = g_o \exp(\alpha x) \tag{51}$$

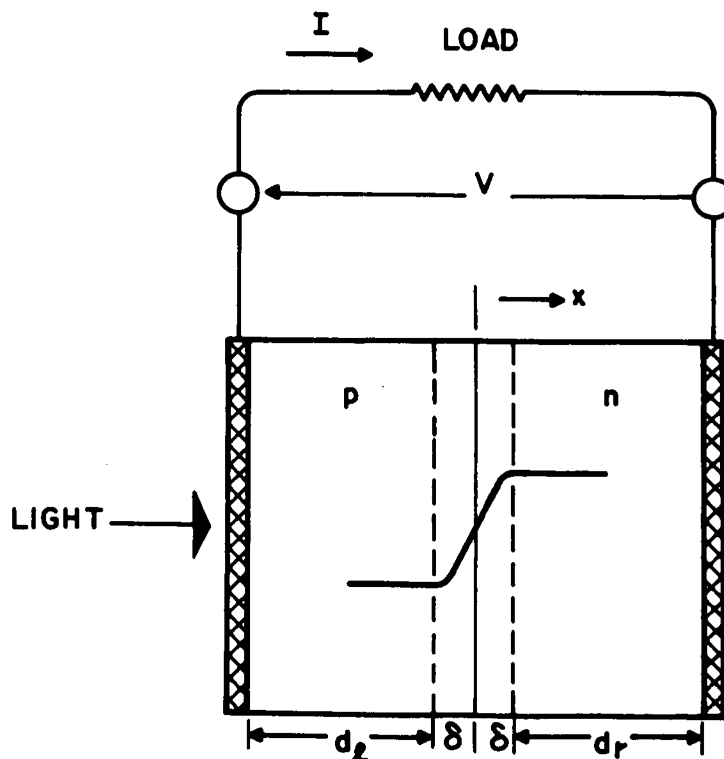

Figure 27. Photovoltaic junction geometry, after Cummerow

where

g_o = rate of generation at $x = 0$
α = optical absorption constant of semiconductor

If H_S photons $cm^{-2} \cdot sec^{-1}$ fall on the surface plane of the semiconductor, located at $x = -d_1$ after reflection by or absorption in the surface electrode, have occurred, then the generation rate at $x = 0$ is:

$$g_o = \alpha H_s \exp(-\alpha d_\ell) \quad (52)$$

Equations (51) and (52) were substituted into Eq. (50), which was then solved with boundary conditions suitable for a particular device geometry; e.g., for a device with either infinite thickness of the base and surface regions, or a device with finite thickness of both regions, but with zero surface recombination velocity at these surfaces*. The boundary conditions were:

$$p = p_n \exp\left(\frac{eV}{kT}\right) \quad \text{at } x = 0 \quad (53)$$

$$\frac{dp}{dx} = 0 \text{ at } x = d_r \text{ and } x = d_1 \quad (54)$$

or

$$\lim_{d_r \to \infty} p = p_n \quad (55)$$

where

p_n = equilibrium hole concentration in the n-region.

Cummerow then integrated Eq. (50) to provide p as a function of x and V, and obtained the hole current crossing the junction by applying

$$I_p(0) = -q D_p \left(\frac{dp}{dx}\right)_0 \quad (56)$$

---

*Cummerow quoted Hall as a source for this assumption, which appears to be based on the reflection of minority carriers by an n-n^+ junction. Although this reflection is possible in principle, it appears that in practice it is not sufficiently strong to prevent recombination at ohmic contacts, and an assumption of infinite recombination velocity at such contacts together with finite recombination velocity at the free front surface has been used by subsequent workers.

where

$I_p(0)$ = hole current at x = 0

A corresponding derivation provided $I_n(0)$, the sum of the electron and hole currents then constituting the total junction current as a function of V. Hence, it was found that

$$I = q\, gL' \left[\exp\left(\frac{qV}{kT}\right) - 1\right] - q g_o L \tag{57}$$

where L and L' are lengths related to the combined effects of the diffusion lengths for minority carriers on the two sides of the junction, g_o is the generation density rate for hole-electron pairs at the junction by photon absorption, and g is a term containing the sum of the thermal generation density rates for minority carriers on both sides of the junction. The first term on the right-hand side is consistent with Shockley's expression for the characteristic of diodes based on diffusion and recombination of injected carriers on both sides of the transition region, as discussed in Section III-D-2 above, while the second term gives the light-generated current for the case of not quite realistic boundary conditions.

Thus, Cummerow was the first to publish a comprehensive analysis of the photovoltaic effect in pn-junction devices in a valid approach, although it was more cumbersome than necessary because of the inclusion of the diode characteristic.

Cummerow then derived expressions for the maximum power delivered to an external load, by straightforward circuit analysis. He proceeded to calculate the theoretical efficiency by introducing measured material constant values appropriate for germanium. These included the minority-carrier diffusion lengths and lifetimes, the equilibrium majority-carrier densities, and one value of optical absorption constant, corresponding to monochromatic illumination. The results showed an efficiency increasing with increasing junction depth to a broad maximum for d_l = 0.002-0.004 cm, and increasing monotonically with increasing illumination level, with $\eta \approx 23\%$ at 0.002 $W \cdot cm^{-2}$ and η = 40% at 1 $W \cdot cm^{-2}$ for 0.01 ohm·cm material, under monochromatic 1.5-μm illumination. Cummerow also showed that increasing the device temperature decreases the conversion efficiency by dropping the working voltage, using the results for the junction characteristic.

Later in the same year, after the publication of the performance data for diffused-junction silicon cells by the Bell Laboratories group, Cummerow extended this original analysis to consider material constants appropriate to silicon (167), and to include an integration over the 5760°K blackbody spectrum in place of monochromatic illumination, using absorption coefficient data as a function of wavelength as published previously by Moss (168).

For material with

$$\mu_n = 1200 \text{ cm}^2 \cdot \text{V}^{-1} \cdot \text{sec}^{-1} \qquad \sigma_n = \sigma_p = 1.0 \text{ ohm}^{-1}$$

$$\mu_p = 400 \text{ cm}^2 \cdot \text{V}^{-1} \cdot \text{sec}^{-1} \qquad \tau_n = \tau_p = 10^{-5} \text{ sec}$$

the efficiency obtained was 17%, neglecting optical reflection from the front face.

Cummerow, in his first paper, also pointed out that increased efficiency could be obtained by using highly doped material (provided the carrier mobility was not seriously impaired), and he also felt that material with an energy gap close to the peak of the solar intensity distribution curve would give the highest theoretical efficiency. Thus, he recommended use of a semiconductor with an energy gap near 2.0 eV, larger than that of silicon.

This question of the optimum bandgap for solar energy conversion efficiency has since been of considerable theoretical interest. The point touched on by Cummerow was taken up in more detail by Rittner, also in 1954 (169). Rittner used an analysis similar to that of Cummerow, and plotted conversion efficiency as a function of forbidden bandgap for several carrier densities in the range $N_a = N_d = 10^{15}$ to 10^{19} cm^{-3}. For materials with E_g greater than that for silicon, mobility and lifetime values equal to those of silicon were assumed. The efficiencies shown were those obtained with a junction at the optimum depth. The results indicated that the optimum bandgap for solar energy conversion lay around 1.5 - 1.6 eV, and that this would give a maximum efficiency of about 25% for $N_d = 10^{19}$ cm^{-3}. Hence, Rittner proposed the use of AlSb as a promising material for solar energy conversion.

Pfann and van Roosbroeck, working from their photovoltaic effect analysis as described in Section III-B-3, provided an estimate of maximum theoretical efficiency for a silicon solar cell operating under earth-surface sunlight. The spectral distribution of sunlight as published by the Smithsonian Institute* was reduced to 89 mW $\cdot$ cm^{-2} to correspond to a solar elevation angle of 60° from the zenith for an average cloudless day at sea level, and used to calculate the maximum $I_L = 40$ mA $\cdot$ cm^{-2}. For this calculation, they neglected surface reflection loss and assumed each photon with energy $h\nu > E_g$ for silicon to create a hole-electron pair, as well as a collection efficiency of unity. Taking a value of $R_o = 10^8$ ohm $\cdot$ cm^2 (calculated from experimental junction measurement) an efficiency of 18% was calculated to be the maximum theoretically achievable for a cell of this type.

Thus, by the end of 1954, the fundamental analyses of both the junction characteristic and the photovoltaic effect at a p-n junction were well established. Work from 1955 to the present time has refined these basic results, and shown how various imperfections in the cells contribute to losses in conversion efficiency.

---

*Smithsonian Meteorological Tables, 6th Rev. Edition, Table 131, (The Smithsonian Inst., Washington 1951).

E. The Electron-Voltaic Effect and Radiation Damage

1. Semiconductor Damage and Annealing Studies

The first studies of the effects of high-energy particle bombardment on the electrical properties of germanium and silicon were performed by K. Lark-Horovitz et al. (170, 171). This work was performed at Purdue University and Oak Ridge National Laboratories. The Purdue work was initiated around 1947 under the support of a Signal Corps contract (172). Samples of p- and n-type semiconductor materials were bombarded with 10-MeV deuterons and 20-MeV alpha particles as well as neutrons. The results of the germanium studies indicated that the conductivity of p-type material tended to increase under irradiation, while that of n-type material decreased or converted to p-type. This was found to be true in germanium for all of the types of bombarding particles used. Deuteron-induced lattice defects were found to anneal out under prolonged heating at 400°C, while those caused by neutron bombardment were not so readily removed. Two years after the publication by Lark-Horovitz et al., W. H. Brattain and G. L. Pearson published an account of their studies on the effects of alpha particle bombardment on n-type and p-type germanium (173). They found essentially the same trend as the earlier workers, with conduction electrons being removed from n-type material at a rate of 78 electrons per alpha particle. After the material had been converted to p-type, holes (i.e., acceptors) were introduced at a rate of 8.6 per alpha particle. Some room-temperature annealing was observed. The results were found to agree fairly well with the theoretical predictions of Seitz. The first electron bombardment studies were performed by E. Klontz and K. Lark-Horovitz(174) using 0.7 to 2.0-MeV electrons to irradiate germanium, with results qualitatively similar to those found in the other studies. There were numerous other studies, both theoretical (175) and experimental (176), dealing with bombardment and annealing. The large majority of these were concerned with germanium, and only occasionally was silicon investigated, while Cleland and Crawford (177) published some data on indium arsenide which showed p-type InAs to be converted to n-type by neutron bombardment.

These studies were not intended to relate directly to the effects of radiation on photovoltaic or other devices although some of them were performed on semiconductor diodes. The discovery and investigation of the electron-voltaic effect, however, brought about a direct confrontation between the photovoltaic cell and radiation damage long before the discovery of the Van Allen radiation belts.

2. The Electron-Voltaic Effect

The electron-voltaic effect is the production of a current and voltage at a p-n junction as a result of bombarding the semiconductor containing the junction with beta particles (see Figure 28). It is the analog of the photovoltaic effect, with the difference that the electrons take the place of the photons. In this case each electron ionizes a number of atoms, giving rise to an electronic "gain". The observation of an electron-voltaic effect was first made by Ehrenberg, Lang, and West (178) in 1951, using selenium and

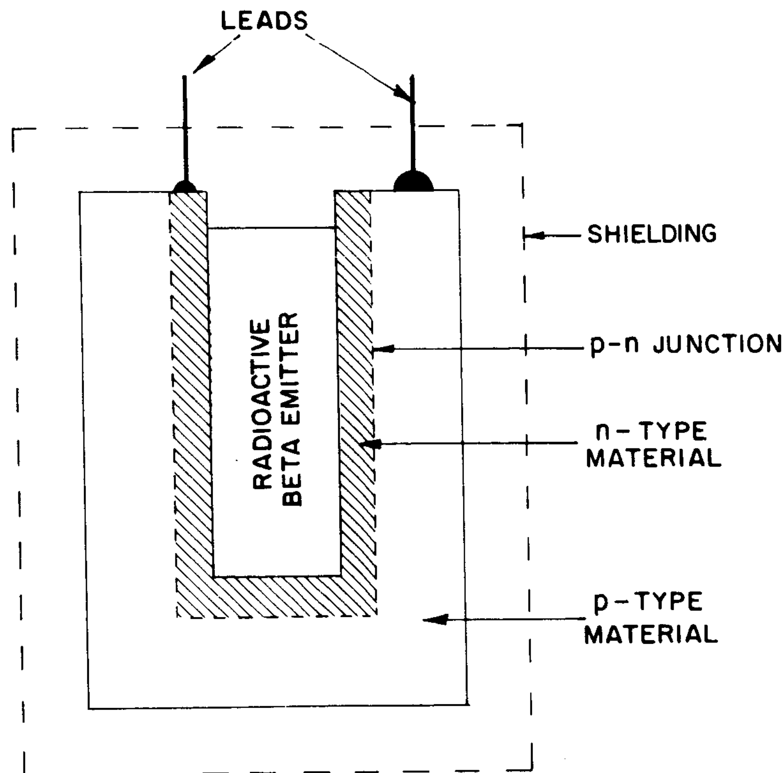

Figure 28. Schematic of electron-voltaic cell

copper oxide photovoltaic cells. The selenium cell was bombarded with a stream of electrons whose energy could be varied between zero and 80 keV. The maximum current gain was obtained with 50-keV electrons. Using a bombarding current density of approximately 10^{-8} A•cm^{-2} a gain (i.e., the ratio of electron-voltaic to bombardment current) of 500 was obtained for the electron-voltaic current at 50 keV and with a load of 700 ohms. The gain was found to be lower when higher bombardment currents were used. The energy dependence of the gain was thought to correlate with the penetration depth, and thus was dependent on device characteristics through the collection efficiency. To measure the effect on copper oxide cells, the authors found that it was necessary to remove some of the oxide layer. The threshold energy for observation of the electron-voltaic effect with the copper oxide cell was about 60 keV. From this point the gain increased with electron bombardment energy, reaching a value of 150 at 90 keV. These results were interpreted to indicate that the sensitive region of the copper oxide photocell was at the copper-copper oxide interface.

The first published account of the electron-voltaic effect in silicon and germanium was given by Rappaport early in 1954(179). Working under an Air Force contract, Rappaport used alloy junctions on germanium and silicon wafers with a 50 millicurie Sr^{90} -Y^{90} radioactive source (average beta particle energy 0.7 MeV) for bombardment. The silicon p-n junctions gave a maximum open-circuit voltage of 250 mV and a short-circuit

current of 10^{-5} A. This corresponded to a current gain of 1.5×10^5 (beta current was 3.2×10^{-10} A), giving a "cost" figure for carrier production of 4.7 eV per charge carrier. Used as an energy conversion unit in conjunction with a radioactive source with an available power of 200 μW, a single silicon junction gave an output of 0.8 μW into a matched 10,000-ohm load - an efficiency of 0.4%. Based on calculations for a wafer of optimum thickness, an efficiency of 2% was predicted.

Factors other than wafer thickness lowering the efficiency were high reverse saturation currents, bulk and surface recombination, backscattering, etc. Using the same source with germanium an open-circuit voltage of 30 mV and a short-circuit current of 2×10^{-5} A were obtained. The current gain was 1.9×10^5, with a "cost factor" of 3.7 eV per charge carrier. One of the junctions was used to power a transistorized audio oscillator. Such a power supply was expected to have a potentially long life; however, radiation damage effects were being noted which, it was felt, would tend to limit this lifetime. Later in the same year, Rappaport reported some results which confirmed, rather dramatically, this anticipation(180). He had found that the open-circuit voltage of the electron-voltaic cells could drop by as much as a factor of two during a 1-hour exposure to the 50 millicurie Sr^{90} -Y^{90} beta source. This exposure was determined to correspond to a change in the number of defects present by 10^{11} cm^{-3}. As a result of these observations and of changes observed in the rectifier characteristics, it was concluded that minority-carrier lifetime is extremely sensitive to radiation damage.

During the same year, Pfann and van Roosbroeck published the independent work dealing with both the photovoltaic and electron-voltaic energy conversion capabilities of p-n junctions (141), which was discussed in Section III-D-3. Silicon electron-voltaic cells were shown to be more efficient than germanium cells, both theoretically and experimentally. An estimate of the theoretical idealized efficiencies gave a figure of 2.4% for silicon and 0.034% for germanium. Germanium, however, has a higher threshold (0.63 MeV) for radiation damage than silicon (0.3 MeV). A silicon electron-voltaic cell showed a decrease of 45% in short-circuit current over a two-day period of operation. Some of this damage tended to anneal out, and after five weeks at room temperature the short-circuit current returned to 62% of its original value. The possible use of absorbers to provide partial or total protection was considered but the reduction in efficiency associated with this protection was considerable. For the case of the complete protection, the ideal overall efficiency was calculated to be reduced to 5.8×10^{-7} percent (germanium).

In 1959 Loferski and Rappaport published some preliminary work relating lifetime and short-circuit current changes to the properties of the defects (181). They developed an expression connecting short-circuit current with bombardment time. Using this expression in analyzing their experimental data, Loferski and Rappaport determined that the energy, $E_{L_{min}}$, necessary to displace an atom irreversibly from its normal position was, in the case of germanium $E_{L_{min}} \leq 23$ eV, and in the case of silicon $E_{L_{min}} \leq 27.6$ eV.

A comprehensive discussion of the results of this work on the electron-voltaic effect was given by Rappaport et al. in an additional publication (182). Although the electron-voltaic cell has not proven useful for present-day applications because of various factors such

as weight, lifetime, and efficiency, these early studies led to a fundamental understanding of the nature and effects of radiation damage in semiconductor devices and, in particular, in the electron-voltaic cell which is structurally very similar to the photovoltaic cell. This knowledge was to prove extremely valuable later when the advent of the space age brought large-scale application of photovoltaic cells in space, where they were exposed to radiation, predominantly from the then discovered radiation belts surrounding the earth.

IV. CONTEMPORARY DEVELOPMENTS (1955 - PRESENT)

(This Section is in preliminary form.)

A. Theory

1. Junction Characteristics

The diffusion theory developed by Shockley explained the experimental facts with good accuracy for germanium diodes at room temperature. For wider bandgap semiconductors, however, the experimental results were found to differ from the theory in important ways. For silicon diodes, the I-V characteristic is generally found to be of the form

$$I = I_{o(exp)} \left[\exp \left(\frac{qV}{AkT} \right) -1 \right] \tag{58}$$

where $A > 1$, and $I_{o(exp)} > I_{o(theor)}$, $I_{o(theor)}$ referring to the saturation current as determined from the diffusion theory. These two effects were later found to be generally related, diodes with large $I_{o(exp)}$ values having larger A values, and conversely. The analysis of Sah, Noyce, and Shockley (183) proved an important advance toward resolving the problem expressed by Eq. (58) for many practical diodes.

The basis of this analysis was the inclusion of recombination and generation phenomena through a trapping level in the p-n junction space-charge region, which had been excluded in the earlier diffusion theory. The effects of direct (band-to-band or radiative) recombination and Auger-type (three-body) recombination were assumed small compared with the intermediate-level process.

The kinetics of the recombination mechanism, which were investigated and described earlier by Shockley and Read (184), formed the backbone of this analysis. The following discussion will attempt to explain the aspects of the Sah-Noyce-Shockley theory (183) as far as they are relevant to solar cell theory, that is, primarily in their application to a p-n junction under small forward bias. A schematic of the band structure under consideration is shown in Figure 29.

Four processes can occur: (i) An electron drops from the conduction band into the trap, to recombine with a trapped hole. (ii) A trapped electron is emitted into the conduction band. (iii) A trapped electron drops into a hole in the valence band and recombines. (iv) An electron is emitted into the trap from the valence band (a process equivalent to a trapped hole being emitted into the valence band).

For process (i)

$$\text{Trapping rate} = n f_{tp} / \tau_{no} \tag{59}$$

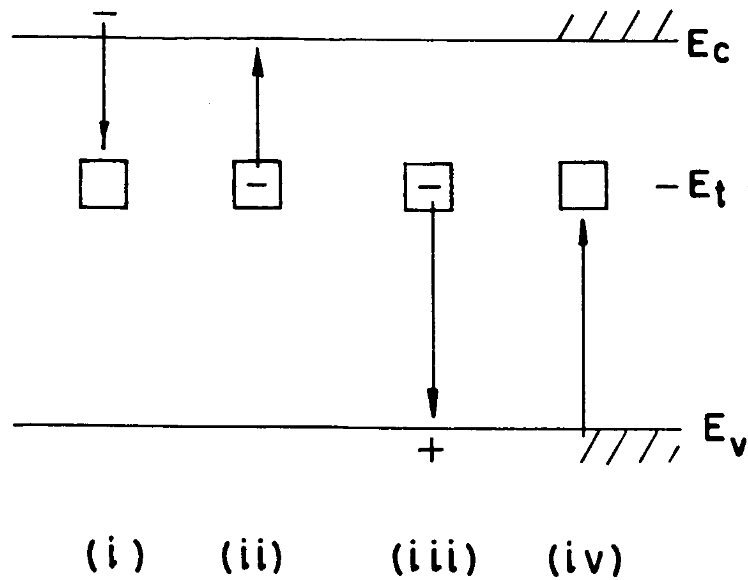

Figure 29. Energy band scheme for a semiconductor with trapping levels, after Sah et al.

where

n = density of electrons in the conduction band

f_{tp} = fraction of traps unoccupied by electrons

τ_{no} = lifetime of electrons injected into p-type material

Now:

$$n = n_i \exp\left(\frac{E_{fn} - E_{fi}}{kT}\right) \tag{60}$$

where

n_i = intrinsic electron density

E_{fn} = quasi-Fermi energy giving the distribution of electrons in the conduction band

E_{fi} = intrinsic Fermi energy

It is useful to define an electron density:

$$n_1 = n_i \exp\left(\frac{E_t - E_{fi}}{kT}\right) \tag{61}$$

where

n_1 = density of electrons in conduction band when $E_{fn} = E_t$

E_t = trap energy (see Figure 29)

Combining Eqs. (60) and (61):

$$n = n_1 \exp\left(\frac{E_{fn} - E_t}{kT}\right) \tag{62}$$

If

$$f_t = \text{fraction of traps occupied by electrons} = 1 - f_{tp} \tag{63}$$

then the rate of electron emission can be written as

$$\text{Emission rate} = a\, f_t \tag{64}$$

where a is a rate constant.

By Fermi-Dirac statistics

$$f_t = \frac{1}{1 + \exp\left(\frac{E_t - E_{ft}}{kT}\right)} \tag{65}$$

where E_{ft} = quasi-Fermi energy giving occupancy probability for trap level E_t.

In thermal equilibrium, $E_{ft} = E_{fn}$ and the trapping and emission rates must be equal. Under this condition, combining Eqs. (59) and (62-65):

$$a = \frac{n}{\tau_{no}} \cdot \frac{f_{tp}}{f_t} = \frac{n_1}{\tau_{no}} \tag{66}$$

Under nonequilibrium conditions (e.g., electrons injected into p-type material), the electron trapping rate will exceed the emission rate, and the net loss rate of electrons will be

$$U_{cn} = \frac{\left(n f_{tp} - n_1 f_t\right)}{\tau_{no}} \tag{67}$$

Similarly, for holes

$$U_{cp} = \frac{\left(p f_t - p_1 f_{tp}\right)}{\tau_{po}} \tag{68}$$

where

p = density of holes in valence band

p_1 = density of holes in valance band when the Fermi level is at E_t (thermal equilibrium conditions)

Under nonequilibrium but steady-state conditions,

$$U_{cn} = U_{cp} = U \text{ (say)}$$

Substituting $f_{tp} = 1 - f_t$ and solving Eqs. (67) and (68) simultaneously gives

$$f_t = \left(\frac{n}{\tau_{no}} + \frac{p_1}{\tau_{po}}\right) \Bigg/ \left[\frac{(n + n_1)}{\tau_{no}} + \frac{(p + p_1)}{\tau_{po}}\right] \tag{69}$$

and this can be substituted into Eq. (67) or (68) which gives, because of the thermal equilibrium condition $n_1 p_1 = n_i^2$

$$U = (pn - n_i^2) \Big/ [(n + n_1)\,\tau_{po} + (p + p_1)\,\tau_{no}] \tag{70}$$

This expression was then applied to a p-n junction with simplified parameters, to demonstrate qualitatively the effect of recombination-generation current on the I-V characteristic. The band structures of the three regions of the device under consideration are shown in Figure 30. To simplify the analysis, it is assumed that the trapping level is at the intrinsic Fermi level energy in all regions of the device, so that $n_1 = p_1 = n_i$.

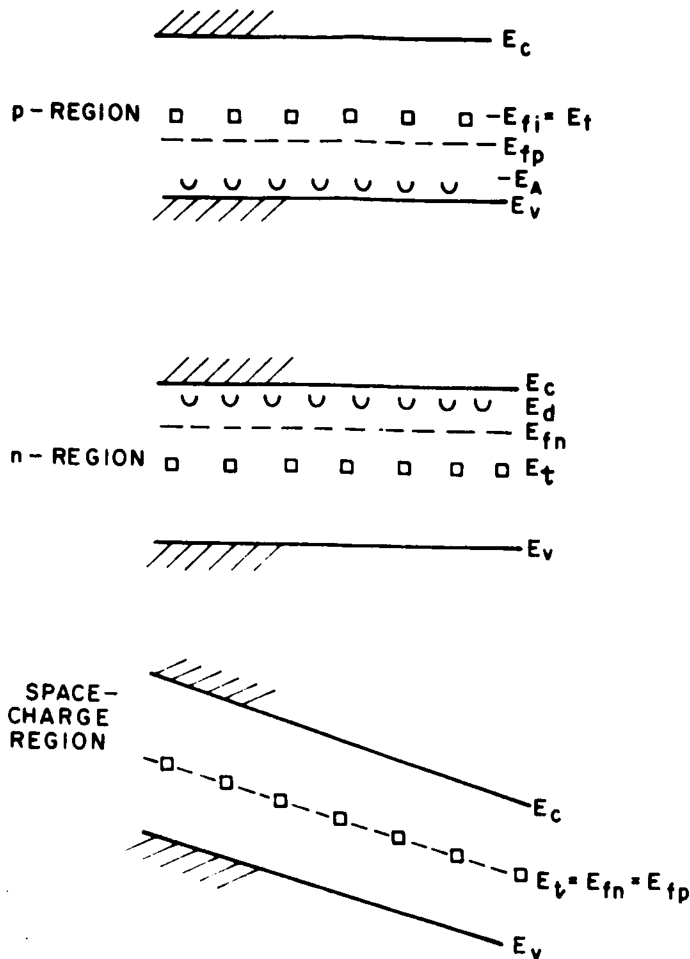

Figure 30. Band structures in the three regions of a p-n junction with trapping levels, after Sah et al.

It is also assumed for simplicity that the minority-carrier densities, lifetimes, and mobilities are the same in the p- and n-type regions. In a region which is appreciably p-type, the acceptor concentration must considerably exceed the trap concentration, and, hence, the equilibrium Fermi level must lie below E_t. Thus, in equilibrium most of the traps are vacant, ready to accept electrons which are injected. Writing

p_p = hole concentration in p-region at equilibrium

n_p = electron concentration in p-region at equilibrium

Then, if an excess concentration Δn of electrons arises by injection into the p-region

$$n = n_p + \Delta n \tag{71}$$

To maintain charge neutrality

$$p = p_p + \Delta n \tag{72}$$

The condition for "small injection" is that the hole concentration is not appreciably altered by the injection process.

Hence,

$$p_p >> \Delta n \tag{73}$$

and the following conditions apply

$$p = p_p >> p_1 = n_1 \tag{74}$$

Substituting into Eq. (70) and neglecting small quantities as indicated by the inequalities above,

$$U = \Delta n/\tau_{no} = (n-n_p)/\tau_{no} \tag{75}$$

Similarly, for the n-region

$$U = \Delta p = (p-p_n)/\tau_{po} \tag{76}$$

Now for n- and p-regions adjacent to the space-charge region in a reverse-biased junction, minority carriers generated in these regions will diffuse into the space-charge region, where they will slide rapidly down the potential gradient and be lost to the region of opposite conductivity type. Hence, in a p-type region adjacent to the space-charge region, n will be small, and Eq. (75) becomes

$$U = -n_p/\tau_{no} \tag{77}$$

Similarly, in an n-type region adjacent to the space-charge region

$$U = -p_n/\tau_{po} \tag{78}$$

The negative signs of the recombination rates indicate that a net generation process is occurring, as would be expected from the physics of the situation.

On the average, all minority carriers (both holes from the n-side and electrons from the p-side) generated within one diffusion length of the edge of the space-charge region will

cross the junction, thus giving rise to a total external current under reverse applied bias voltage of

$$I_d = -2q\, n_p L_o / \tau_o \tag{79}$$

per unit area of junction,

where

$n_p = p_n$

L_o = minority-carrier diffusion length on both sides of the junction

$\tau_o = \tau_{no} = \tau_{po}$

This diffusion current contribution is that contained in Shockley's earlier theory.

In the space-charge region of the device under reverse bias, as shown in Figure 30, carriers in both the conduction and valence bands are rapidly removed from the region by the field. Hence, recombination processes can be neglected in the space-charge region.

Therefore,

$$n_i >> n = p \tag{80}$$

and

$$U = -n_i / 2\tau_o \tag{81}$$

This gives rise to an external current

$$I_{rg} = -q\, W n_i / 2\tau_o \tag{82}$$

per unit area of junction, where W = space-charge region width.

The ratio of the current generated in the space-charge region to that generated by the diffusion processes is then

$$\frac{I_{rg}}{I_d} = \frac{W_{ni}}{4 n_p L_o} \tag{83}$$

Putting $n_p = p_n = n_i^2/n_n$

$$\frac{I_{rg}}{I_d} = \frac{Wn_n}{4n_iL_o} \tag{84}$$

For a material such as germanium where n_i is large at or above room temperature, this ratio is typically 0.1. For silicon, however, the ratio can be 10^3 or higher, which means that the current generated in the space-charge region dominates over that due to diffusion. Under reverse bias, where the space-charge region widens, the reverse saturation current will not saturate, but will increase with $V^{1/3}$ for linearly graded junctions, and $V^{1/2}$ for abrupt junctions.

This effect will be even more pronounced in semiconductors with short minority-carrier lifetimes (leading to small L_o) and with large bandgaps, resulting in still lower n_i values.

Sah et al. pointed out that if generation in the space-charge region dominates the reverse-bias characteristic, recombination in the same region can be expected to have a large effect on the forward-bias characteristic. Under conditions of small forward bias, the band structure of the device is as shown in Figure 31, as discussed in Shockley's original paper on p-n junction characteristics. At the center of the p-n junction [x = 0 in Figure 31], the carrier concentrations are determined by the deviation of the quasi-Fermi levels by V/2 from the Fermi level, which at this point is equal to E_{fi}

$$p = n = n_i \exp\left(\frac{qV}{2kT}\right) \tag{85}$$

The recombination rate at this point is then

$$U = \frac{n_i \exp(qV/2kT)}{2\tau_o} \tag{86}$$

Because the minority-carrier concentrations on each side of this center point fall off with distance, the excess carrier concentration falls off exponentially with a characteristic length of kT/qE where E is the electric field in the junction. Thus, the recombination current density is

$$I_{rg} = \frac{(kT/qE)qn_i}{\tau_o} \exp\left(\frac{qV}{2kT}\right) \tag{87}$$

If a linear potential gradient across the junction is assumed, then $E = (\psi_D - V)/W$, where ψ_D = built-in voltage of junction.

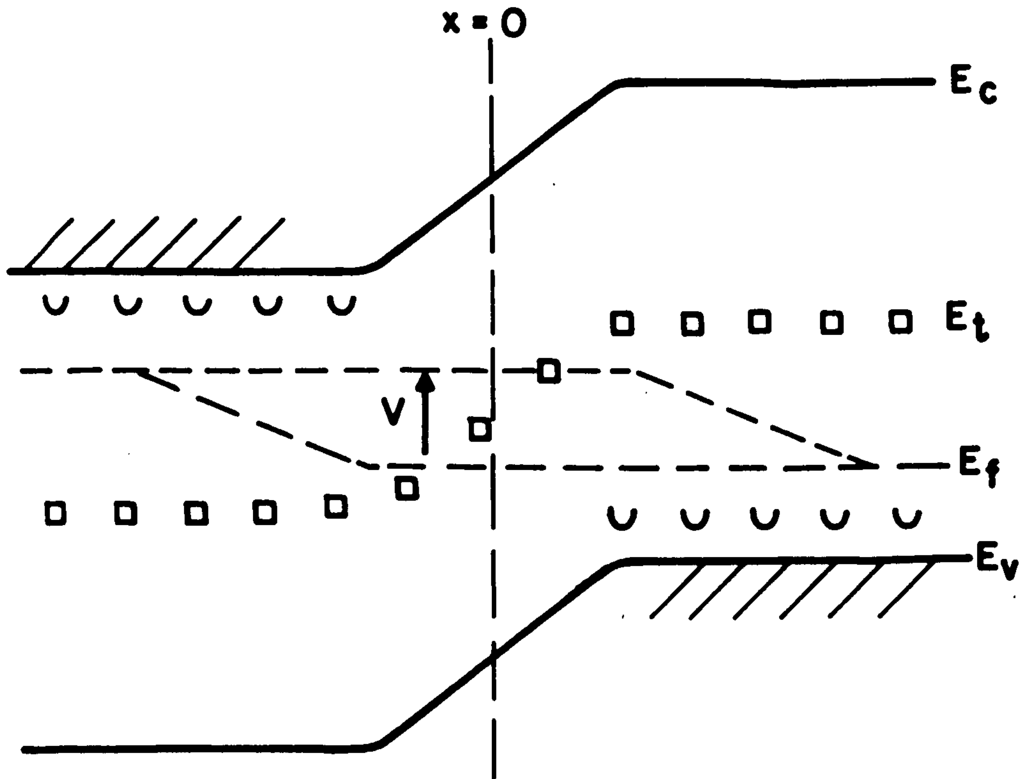

Figure 31. Band structure of a p-n junction under small forward bias

As shown by Shockley's original analysis, the diffusion current is given by

$$I_d = \frac{2qn_p L_o}{\tau_o} \exp\left(\frac{qV}{kT}\right) \tag{88}$$

The ratio of recombination current to diffusion current is

$$\frac{I_{rg}}{I_d} = \left(\frac{n_n}{n_i}\right) \left(\frac{W}{2L_o}\right) \left[\frac{kT}{q(\psi_D - V)}\right] \exp\left(\frac{-qV}{2kT}\right) \tag{89}$$

Again, for junctions in germanium this ratio is normally small, but for junctions in silicon it can be greater than 1, at low voltages. This theory predicts values of A in Eq. (58) as high as 2, for the cases where recombination inside the space-charge region dominates the forward current. Sah, Noyce and Shockley then proceeded to investigate a more general case, where the trapping level is located at an energy other than the intrinsic Fermi level. Using Fermi-Dirac statistics, the various carrier concentrations were determined from the energy levels present, and these were substituted into Eq. (86) to obtain the recombination rate. This rate was then integrated over the space-charge region to obtain the recombination-generation current arising in this region. To do this accurately, a linear variation of electrostatic potential could no longer be assumed (as

done in the previously discussed case), and the quasi-Fermi levels for holes and electrons had to be known as functions of distance in the junction region. Numerical methods had to be used to obtain a solution, and it would be inappropriate to devote the necessary space to present details here.

The major conclusions were:

In the region of large reverse bias, the current does not saturate as found in earlier p-n junction theories, but follows a $V^{1/3}$ law for linearly graded junctions and a $V^{1/2}$ law for abrupt junctions.

Under small forward bias, the recombination current density is given by

$$I_{rg} = \frac{qn_i}{(\tau_{po}\tau_{no})^{\frac{1}{2}}} W \frac{2\sinh(qV/2kT)}{[(\psi_D - V)q/kT]} \times f(b) \tag{90}$$

where

$$f(b) = \int_{\delta_1}^{\delta_2} \frac{d\delta}{\delta^2 + 2b\delta + 1} \tag{91}$$

with

$$b = \exp\left(\frac{-qV}{2kT}\right) \cosh\left[\frac{E_t - E_i}{kT} + \frac{1}{2}\ln\left(\frac{\tau_{po}}{\tau_{no}}\right)\right] \tag{92}$$

and

$$\delta_{1,2} = \left(\frac{\tau_{po}}{\tau_{no}}\right)^{1/2} \exp\left[\pm\frac{(\psi_D - V)_q}{2kT}\right] \tag{93}$$

Analysis of this expression for I_{rg} showed that the value of A in Eq. (58) will vary with the value of applied bias V and will have a maximum value of about 1.75.

The remainder of Sah, Noyce and Shockley's paper was devoted to analysis of transistor characteristics, and is of no application to photo-voltaic devices. This account of the theory has been given in detail because this represents the present status of rigorous analytical examination of diode characteristics theory. In practice, A values considerably larger than those which can be accounted for under this theory are observed. Various

explanations have been offered for this phenomenon, but as far as can be determined, none of these have been analyzed in sufficient detail to allow comparison between theory and experiment to unambiguously determine the validity or otherwise of the proposals. These matters are further discussed in the section of this report in which theoretical research is evaluated.

2. Ultimate Conversion Efficiencies

As described above, a calculation of maximum theoretical efficiency was first performed by Cummerow, whose results were extended by Rittner. These results were published on the eve of the announcement of the Bell solar battery, the first practical silicon cell. Following this event, Prince (145) published an account of the device, which included a calculation of the theoretical efficiency of silicon cells operated under earth-surface illumination. Prince's calculation followed these steps:

(i) The short-circuit current I_{sc} was calculated by assuming a unity collection efficiency and using that portion of the photon flux of earth-surface sunlight (from an early spectral distribution) for which the photon energies exceed the bandgap of the semiconductor used, since this determines the minimum energy required to create hole-electron pairs by photon absorption. He obtained a value for I_{sc} in silicon of 44 $mA \cdot cm^{-2}$, which he reduced to a "likely maximum" of 35 $mA \cdot cm^{-2}$ to allow for optical reflection losses.

(ii) I_o was calculated from Shockley's diffusion analysis of p-n junction behavior, for a junction formed between a heavily doped p-region and a moderately doped n-region, using measured values of material constants such as carrier mobility and lifetime.

(iii) From the I-V characteristic according to diffusion junction theory, including results of (i) and (ii) above, the maximum power available was calculated.

After performing these calculations for a variety of bandgaps, Prince was able to plot theoretical efficiency as a function of semiconductor energy gap. These calculations were, however, based on empirical semiconductor data obtained for silicon, which were assumed to apply also for materials with different bandgaps.

Loferski (185), working under a Signal Corps contract (186) aimed at investigating materials for photovoltaic power conversion devices, refined the previous analysis. This work used the solar spectral distributions for various atmospheric conditions and elevation angles, in their dependence on meteorological factors which alter the sunlight spectral content as well as that outside the atmosphere. For the ultimate-efficiency calculations, optical reflection and collection-efficiency effects were assumed not to contribute losses, and the saturation current I_o for the junction was calculated from the junction diffusion-theory analysis, using measured values for semiconductor conduction parameters. The analysis was thus, in principle, similar to those done before, but with more

accurate sunlight spectra used, providing families of curves showing conversion efficiency as a function of energy gap, for various air-mass, water-absorption, and cloud conditions. Further, Loferski considered the effect of the departures of I_0 from the values predicted by the diffusion theory, giving further families of efficiency/bandgap curves for values of I_0 increased by various constant factors, as well as for $I_0 \propto \exp(-E_g/2kT)$ instead of the normal $I_0 \propto \exp(-E_g/kT)$. These results showed that the effects of these departures from theory for I_0 was to shift the bandgap of the optimum material to higher values for the increased saturation currents, and to lower values for the $I_0 \propto \exp(-E_g/2kT)$ case.

Loferski also investigated the dependence of collection efficiency on junction depth, minority-carrier diffusion length, optical absorption constant, and surface recombination velocity, considering, however, collection from the diffused surface region only.

Vavilov's paper (187), in 1956, appears to be the first mention of efficiency analyses by Soviet workers. This analysis is a review of the work published by Pfann and van Roosbroeck and by Rittner, and adds nothing to their results. Similarly, the efficiency analysis work of Loferski and other Western authors is heavily drawn upon in a Soviet book containing sections on photovoltaic conversion (188) published in 1958; no new results (on such analyses) are quoted in this work.

The question of the effect of temperature on the optimum E_g value for solar energy conversion was taken up by Halsted of the GE Research Laboratory. Results of his analysis were reported briefly in 1957 (189), in which an analysis based on the methods of Prince (145) was used to plot solar conversion efficiency (theoretical maximum) as a function of E_g for temperatures between 300 and 600°K. The results showed that the optimum E_g shifts to higher values with increasing temperature, since the loss in I_{sc} with increasing E_g is more than compensated by the decrease in I_0 theoretically predicted. Although the predicted effects on I_0 are not those seen in practice, experimental work has shown that GaAs, with a larger bandgap than that of silicon can give higher efficiencies at temperatures above 150°C, even though the silicon cells are more efficient at room temperature.

The same question was taken up in great detail by Rappaport and Wysocki (190, 191), during work supported by the U.S. Army Signal Corps Research and Development Laboratory (192), a continuation of the contract which supported Loferski's analysis. The analytical approach was essentially that of Loferski, but three types of behavior governing I_0 were considered: (i) I_0 obeying the diffusion theory of Shockley, (ii) I_0 having contributions from both diffusion theory and recombination effects as discussed by Sah, Noyce, and Shockley (an account is given in IV-A-1), and (iii) I_0 due wholly to recombination current. The analysis for these three cases then proceeded according to Loferski's methods, but with measured (or estimated) values for semiconductor parameters such as mobility, lifetime, and effective masses, and intrinsic carrier densities for the materials Ge, Si, InP, GaAs, CdTe, AlSb, $GaAs_{0.7}$-$P_{0.3}$, $GaAs_{0.5}$-$P_{0.5}$, and CdS. This should be contrasted with the usual assumption of semiconduction parameters

being equal to those of silicon in the analyses of Prince and Wolf. Thus, the results obtained in this analysis reflect strongly the state of materials technology at the time the work was done. Even so, the results follow very much the form expected from Loferski's work, and the main conclusion is that GaAs should be superior to silicon for high-temperature use, a prediction borne out by practice, as mentioned above.

This paper was valuable in providing a large number of curves showing the effect of temperature and the various values of I_0 on the efficiency.

A logical extension of this type of analysis was given by Wolf and Prince (193, 194), with a more complete account having been given later by Wolf (195). Since this work is probably the most comprehensive of its type, a fairly full discussion will be given, to compare and contrast with the thermodynamic analysis given later. The cell considered is a planar p-on-n cell operating under direct sunlight, using the same spectral distribution as used previously by Prince. The analysis proceeded by the following steps:

(i) Reflection from the front surface of the cell need be only briefly considered, since it had been reduced to very low values (about 3%) by the mysterious black surface layer obtained from the boron trichloride diffusion process, or could otherwise be reduced to similar values by conventional optical coating techniques.

(ii) The effect of spectral dependence of optical absorption coefficient has two principal results. First only photons with energy greater than that required to create hole-electron pairs (i.e., $> E_g$) are absorbed in the cell (neglecting relatively minute free carrier absorption), and thus the portion of the sunlight spectrum which is usable for conversion in the cell is dependent on the bandgap of the semiconductor. Secondly, because the optical absorption coefficient in the hole-electron pair creation regime is finite, then in a cell of finite thickness, some photons potentially able to create hole-electron pairs will pass through the cell without being absorbed and will thus be lost. This effect is predominantly found at wavelengths close to the absorption edge, where the absorption coefficient is smaller. An expression showing the effects of these two processes was derived using Lambert's law of optical absorption, and involving the cell thickness and the variation of optical absorption coefficient with wavelength.

(iii) Photons having more energy than the minimum needed for hole-electron pair creation impart all of their energy to the free carriers on absorption, but very rapid processes cause the free carriers to lose energy by generating phonons (heat) until they are at the energy corresponding to the band edge [valence band edge (E_V) for holes, conduction band edge (E_C) for electrons]. Thereafter, the only energy available for useful work in the cell corresponds to the energy separation of the hole-electron pairs, $E_C - E_V = E_g$. Because

of (ii) and (iii), semiconductors with small E_g can absorb large numbers of photons, but each photon absorbed can potentially do only a small amount of useful work corresponding to E_g. Conversely, semiconductors with larger bandgaps (E_g) absorb a smaller number of photons, but each photon can potentially do a larger amount of work. Arising from the interaction of these two competing processes, a plot of usable energy as a function of E_g for illumination with the spectrum of sunlight shows that a maximum of 46% of the photon energy is potentially available to do useful work, and that this 46% occurs for $E_g = 0.9$ eV.

(iv) Hole-electron pairs are generated in the volume of the cell, but to contribute to power output, the minority carriers must diffuse to the junction plane of the cell. Because of the finite diffusion length for minority carriers, this collection process is not 100% efficient. Wolf and Prince set up and explicitly solved differential equations describing this process, including both the p- and n-regions of the cell, Lamberts optical absorption law being used to give the spatial dependence of carrier generation, and surface recombination in both regions being accounted for, through the boundary conditions. Thus, the carrier distributions as a function of distance from the front surface of the cell were derived. From these, expressions were derived for the output current contributions from the n- and p-regions as a function of wavelength of illumination. From these expressions the collection efficiencies as a function of wavelength, separately for the n- and p-regions, were plotted for a silicon cell with measured semiconductor parameters. These were added to give the total collection efficiency, from which the spectral response of the cell can be derived. A comparison between calculated and measured values for this function was given in (194).

(v) Although in principle the open-circuit voltage V_{oc} of a cell may reach E_g/q in the limiting case, $V_{oc} < E_g/q$ in practice, and the actual value of V_{oc} was calculated by Wolf and Prince using Shockley's diffusion theory for junction behavior, the calculation being essentially identical with that given by Loferski, as described above. As has already been pointed out, such a calculation relies on obtaining a value for the reverse saturation current (I_o) from empirical semiconductor parameters. Using Shockley's expressions, Wolf and Prince calculated a curve showing V_{oc}/E_g as a function of energy gap E_g, it being assumed that semiconductor parameters such as minority-carrier lifetime and mobility are the same as those measured in silicon; i.e., variations in I_o occur only by changes in E_g. This is a most important assumption, which has been made in all calculations of this type by other workers. On this assumption rest all calculations showing that increasing E_g increases V_{oc}; the validity of this result will be examined in the evaluation of cell theory later in this report.

(vi) Because of the exponential nature of the theoretical cell I-V characteristic, the actual cell voltage at the maximum power working point (V_m) is less than V_{oc}, and for similar reasons, the maximum power point current I_m is less than the short-circuit current I_{sc}, both by amounts which can be calculated from the cell characteristic. Wolf and Prince calculated a "curve factor" = $(V_m \times I_m)/(V_{oc} \times I_{sc})$ from the cell characteristic, again using Shockley's diffusion theory for the cell I-V curve.

(vii) Resistive elements in the cell equivalent circuit cause loss of power, but the effects of shunt resistance R_{sh} in parallel with the cell junction may be neglected in commercial silicon cells. However, series resistance R_s must be considered, especially since the analysis of (iv) showed that the diffused surface region should be as thin as possible to maximize collection efficiency, but also, that this tends to increase the contribution of the surface-layer resistance to the R_s of the cell.

Combining the effects (i) through (vii) an expression for overall conversion efficiency can be derived. In the "ideal cell", where surface reflection is zero, all photons with energy $\geq E_g$ are absorbed and produce one hole-electron pair each, where all such pairs contribute to cell output (i.e., unity collection efficiency), and where $R_s = 0$, a maximum efficiency may be calculated, which is a function of E_g because of the effects described in (ii), (iii), (v) and (vi). Wolf and Prince showed a curve for η_{max} as a function of E_g, indicating $\eta_{max} = 23.6\%$ for $E_g \approx 1.3$eV, the curve having a rather broad maximum and being in good agreement with the results of Loferski. Wolf (194) then goes on to discuss various schemes for improving the conversion efficiencies; these are discussed later together with proposals by others.

In this section we have seen how successively more comprehensive analyses of ultimate theoretical efficiency were derived for devices made with p-n junctions which were assumed to operate with characteristics described by Shockley's diffusion theory. Because these analyses all require values for semiconductor parameters such as lifetime, mobility, and surface recombination velocity, to give numerical results, they depend on empirical data.

This "practical" type of analysis is to be contrasted with other "theoretical" analyses which have been derived from thermodynamical arguments, and which are based on fundamental physical constants to provide numerical estimates of ultimate device conversion efficiency.

The first analysis of this type was performed by Müser, whose results were published in 1957* (196). Müser considered an energy conversion system operating as shown

*Müser's treatment is based on thermoelectric arguments which make the analysis of general application to several different devices, but which are somewhat cumbersome for use with specifically photovoltaic devices. Hence, the account given here differs in detail from that of Müser, but the basic arguments are identical.

schematically in Figure 32. The sun is considered to be a black-body at temperature T_1, which produces an energy flux N_{12} into the cell. This energy causes hole-electron pair creation in the semiconductor, and the resulting carrier densities can be characterized by a temperature T_2. Energy is lost from the carriers by three processes:

(i) Radiative hole-electron recombination, whereby photons are re-emitted from the semiconductor (N_{21} in Figure 32).

(ii) Nonradiative hole-electron recombination, which gives up heat to the semiconductor lattice (N_{23} in Figure 32).

(iii) Hole-electron recombinations which potentially are available to do useful work (N_{2M} in Figure 32).

Now the most efficient conversion of recombination energy into useful work will occur when M is a Carnot engine, and the useful energy output N is then given by

$$N = (N_{12} - N_{21} - N_{23}) \times \left(\frac{T_2 - T_3}{T_2} \right) \tag{94}$$

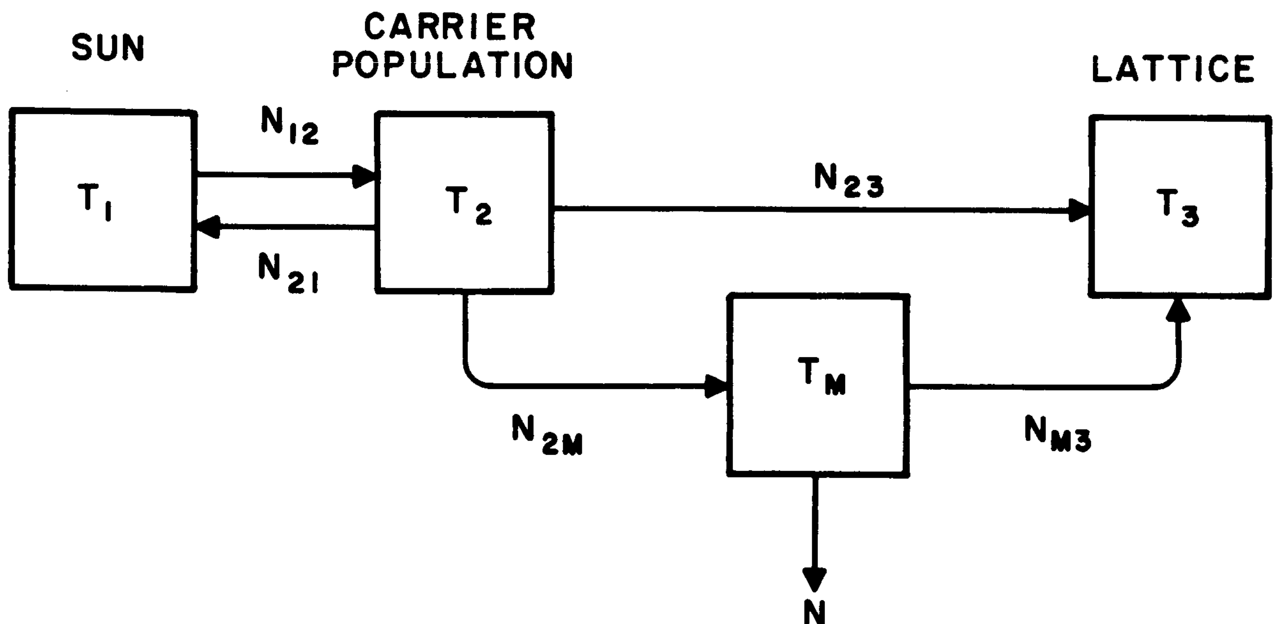

Figure 32. Energy conversion system, after Müser

Efficiency $\eta = N/N_{12}$; N_{12} is fixed, and hence η is maximized when N is maximized. Considering T_3 as fixed, N may be maximized by adjusting T_2, remembering that $(N_{21} + N_{23})$ is also a function of T_2.

Forming dN/dT_2 from Eq. (94) and equating to zero, it can be shown that

$$\frac{d\left(N_{21} + N_{23}\right)}{dT_2} = \left(N_{12} - N_{21} - N_{23}\right) \times \frac{T_3}{T_2\left(T_2 - T_3\right)} \qquad (95)$$

This specifies the temperature T_2 at which maximum conversion efficiency is obtained, and is derived from purely thermodynamic premises. To apply this to a photovoltaic converter, it is necessary to know how $(N_{21} + N_{23})$ varies with T_2. Müser then points out that in a semiconductor under illumination, the electron and hole densities (n and p) can be characterized by a temperature T_2 such that

$$pn = N_c N_v \exp\left[\frac{-E_g}{kT_2}\right] \qquad (96)$$

where N_c, N_v are the density of states in the conduction and valence bands, respectively

E_g is the forbidden bandgap

k is Boltzmann's constant

In the equilibrium case, for intrinsic material

$$p_o n_o = N_c N_v \exp\left(\frac{-E_g}{kT_3}\right) = n_i^2 \qquad (97)$$

where T_3 is the equilibrium temperature and $p_o = n_o = n_i$.

If the only recombination mechanism is a direct hole-electron annihilation, then recombination can be described by the expression

$$\frac{dn}{dt} = \alpha - \beta\, pn \qquad (98)$$

where

$\frac{dn}{dt}$ is the rate of change of electron density

α is the generation rate (which must include both thermal and photon-induced generation)

β is the recombination constant

In equilibrium, $dn/dt = 0$, and hence from Eq. (98)

$$p_o n_o = n_i^2 = \alpha/\beta \tag{99}$$

Also from Eq. (96) it can be shown that the recombination is exponential, with a rate for intrinsic material

$$\tau_i = \frac{1}{2\sqrt{\alpha\beta}} \tag{100}$$

Combining Eqs. (96), (97), (99) and (100) it can be shown that:

$$\beta \ (pn - p_o n_o) = \frac{n_i}{2\tau_i} \left\{ \exp\left[\frac{E_g}{k}\left(\frac{1}{T_3} - \frac{1}{T_2}\right)\right] - 1 \right\} \tag{101}$$

Since each electron-hole recombination causes energy E_g to be either radiated from the cell (for a radiative transition), or given up to the lattice (as thermal energy), then the rate of loss of energy from the excited electron distribution is (β pn E_g) per unit volume. However, thermal excitation processes continually supply energy to the electron distribution, at a rate ($\beta\ p_o\ n_o\ E_g$) per unit volume. Hence, the net rate of loss of energy per unit volume from an electron distribution is

$$\Delta = E_g \times \beta \ (pn - p_o n_o) = \frac{n_i E_g}{2\tau_i} \left\{ \exp\left[\frac{E_g}{k}\left(\frac{1}{T_3} - \frac{1}{T_2}\right)\right] - 1 \right\} \tag{102}$$

Thus $\Delta = N_{21} + N_{23}$ in Eq. (95), and by combining Eqs. (95) and (102), the (T_2) for maximum efficiency can be obtained. Then noting that in Figure 32

$$N_{2M} = N_{12} - (N_{21} + N_{23}) \tag{103}$$

N, and hence the efficiency, can be determined. These equations can only be solved by numerical methods, and aside from noting that he used $\tau_i = 10^{-4}$ sec, Müser gives none of the values of the parameters used in his solutions, so that it is difficult to check on his calculations for this stage of the analysis. It should be noted that N_{12} is the energy imparted to the carrier population by the incident illumination and does not include the energy in the photons which do not create hole-electron pairs, nor the excess energy ($>E_g$) imparted to hole-electrons pairs by photons of energy greater than E_g. The value of N_{12} is obtained by an integration similar to that of Wolf (described above), in which it is shown that a maximum of 46% of the black-body radiation is available to create the carrier population under illumination. Müser shows in a family of curves how (N/N_{12}) depends on illumination intensity and E_g, and he states that the maximum theoretical

efficiency for a silicon cell is 16%. This value is too low, for reasons which are not easy to ascertain since so little of the calculation is shown. However, a contributory factor is the τ_i value of 10^{-4} sec, which is much smaller than that implied by Shockley in a later analysis.

Rose (197) developed a thermodynamic analysis for the efficiency of the photovoltaic conversion process in 1960. Where Müser had ascribed a temperature to the carrier population in the devices, Rose developed an expression by which the effective temperature of the incoming photon stream was characterized. This was used to derive an expression for the maximum voltage which could be developed by a photovoltaic device, rather than deriving the conversion efficiency. Briefly, the derivation ran as follows.

If the device is illuminated uniformly from all directions by a light flux, then the flux can be described by a dimensionless number $L(\nu)$ which is the ratio of the incident flux of frequency ν, per unit area and unit ν, to the radiation which would be emitted by a black-body at the operating temperature of the device, at the same ν. Then

$$L(\nu) = \frac{f(T_2, \nu)}{f(T_1, \nu)} \tag{104}$$

where

$$f(T, \nu) = \frac{\text{const}}{\exp\left(\frac{h\nu}{kT}\right) - 1} \tag{105}$$

and const = $2\pi\nu^2/C^2$ which cancels in the ratio. Equation (104) defines a temperature T_1 which is characteristic of the incident radiation. For the case of nonuniform illumination, e.g., the sun in a 'cold' sky with no concentration, a geometrical factor will enter into the calculation of $L(\nu)$, but the analysis remains the same in principle. The best conversion efficiency will be achieved if a Carnot engine operates with a source temperature T_1 and a sink temperature T_2 for the conversion process, so that the maximum power output per unit area is given by

$$P = Q\,\frac{T_2 - T_1}{T_2} = \left[L(\nu) - 1\right] f(T_1)\, L\nu \left(\frac{T_2 - T_1}{T_2}\right) \delta\nu \tag{106}$$

where

Q = net heat flux per second

$\delta\nu$ = the frequency range of the incident illumination

and f(T) is a function relating the number of photons of frequency ν emitted per unit area and time by a black-body to its temperature T. Thus, the net photon flux onto the device, per unit area, is

$$N = (L(\nu) - 1) f(T_1) \delta\nu \tag{107}$$

For a device working at unity quantum efficiency, the output current I = N x q, and for P = I x V, Eqs. (106) and (107) can be combined to yield

$$qV = L\nu \left(\frac{T_2 - T_1}{T_2} \right) \tag{108}$$

Substituting for T_2 from Eqs. (104) and (105), one obtains

$$V = \frac{h\nu}{q} \left\{ 1 - \frac{kT_1}{h\nu} \left[\ln \left(\exp \left(\frac{h\nu}{kT_1} \right) - 1 + L(\nu) \right) - \ln L(\nu) \right] \right\} \tag{109}$$

[In general, Eq. (106) must be integrated over the frequency range, if this is wide enough to cause appreciable changes in L (ν).] Rose then goes on to show that for the high illumination level and low illumination level cases, the usual logarithmic and linear dependences of V on illumination level are obtained from Eq. (109). Also, a plot comparing theoretical and experimental dependence of (V) on (L) for a germanium photovoltaic cell is given, demonstrating the departure from ideal performance, particularly at low light levels. Clearly, integration of Eq. (106) over the sunlight spectrum, with insertion of a suitable geometrical factor into Eq. (104), would yield an expression for the theoretical conversion efficiency of a photovoltaic energy converter. Although this was not done by Rose, an account of the derivation above has been given here because the ideas developed in it form part of the basis for the analysis of Shockley below.

A theoretical analysis of the maximum conversion efficiency for a photovoltaic device was performed by Shockley and Queisser, under contract with the USAF Aeronautical Systems Command (198): the analysis was also published in (200) 1960 and (199) 1961. Believing that the analyses of the type described above were of limited use because of the need for empirical data on semiconductor properties to obtain conversion efficiency values, Shockley and Queisser derived an expression for cell efficiency from purely thermodynamic reasoning. The analysis proceeded by the following steps:

(i) The Sun is taken as a 6000 °K black-body, and it is assumed that each photon of energy $\geq E_g$ creates one hole-electron pair from which E_g of energy is available. The integration process of earlier analyses (e.g., Wolf or Müser) is repeated, Shockley's results showing that 44% of the energy is potentially available (cf. 47% for Wolf's data from the measured solar spectral distribution, 46% for Müser's data for a 6000 °K black-body).

(ii) The diode equation and its associated parameters are derived from purely thermodynamic reasoning: the derivation of a value for I_o by this method is the kernel of the treatment.

(iii) The maximum-power operating point, and the corresponding power, is derived by a curve-analysis method which is essentially conventional, as used by previous analyses (e.g., Loferski or Wolf).

Thus, the point at which Shockley departs from previous analyses is (ii) above, and only this portion of the analysis will be covered here.

Five generation and recombination processes were considered as occurring in a semiconductor to determine the rate of change of carrier concentration:

(i) Photon-induced generation, caused by the incident illumination.

(ii) The converse of (i), radiative hole-electron recombination.

(iii) Thermal (nonradiative) carrier-generation processes.

(iv) The converse of (iii), nonradiative recombination processes.

(v) Removal of carrier pairs to another region of the device, where they do useful work (crossing the p-n junction in the cell provides this removal process).

Expressions for these were derived in turn:

(i) If Q_s = carrier generation rate per unit area of cell exposed to the Sun, then Q_s is calculated from the Planck distribution integrated to provide the number of photons of energy $h\nu \geq E_g$; i.e.,

$$Q_s = \frac{2\pi}{c^2} \int_{E_g/h}^{\infty} \frac{\nu^2 \, d\nu}{\exp\left(\frac{h\nu}{kT_s}\right) - 1} \tag{110}$$

where

h = Planck's constant

ν = frequency

c = velocity of light

T_s = temperature of the Sun (6000 °K)

k = Boltzmann's constant

It is convenient to put

$$Q_s = Q(\nu_g, T_s) \tag{111}$$

Then if each photon with $h\nu \geq E_g$ creates one hole-electron pair, the rate of generation of carrier pairs per unit cell area is F_s where $F_s = Q_s$.

(ii) Consider a cell at a temperature T_c, completely surrounded by a black-body at the same temperature. Under this thermal-equilibrium condition, the rate at which photons with energy $h\nu \geq E_g$ are absorbed by the cell must equal the rate at which such photons are emitted by the cell by the radiative recombination process. For a cell under this equilibrium condition, Q_c photons with $h\nu \geq E_g$ are absorbed in unit time per unit area, where

$$Q_c = Q(\nu_g, T_c) \tag{112}$$

Under this condition,

$$F_{co} = 2\, Q_c \tag{113}$$

where F_{co} = recombination rate for radiative processes: the factor 2 appears because the cell has two sides for both absorption and emission of radiation.

Now this recombination rate is proportional to the product of hole and electron concentrations, i.e.,

$$F_{co} = \text{const. x } p_o n_o$$

where p_o, n_o, are the equilibrium hole and electron concentrations at equilibrium. Under illumination, these concentrations become p and n,

$$F_c = F_{co} \frac{np}{n_o p_o} = F_{co} \exp \frac{V}{V_c} \tag{114}$$

where V is the difference in energy between the quasi-Fermi levels for holes and electrons (see Section IV-A-1), and $V_c = kT_c/q$. V is the voltage appearing at the cell terminals.

(iii) and (iv) are accounted for by putting

R (O) = rate of generation of hole-electron pairs by thermal processes

R (V) = rate of recombination of hole-electron pairs by nonradiative processes

One notes that when $V = 0$, these processes are equal and thus balance, as required.

(v) If the current provided by the cell is I, then the rate at which carriers are removed from the active region is $-I/q$.

In the steady-state condition, the rate of change of carrier concentration is zero, so that the above processes can be combined

$$F_s - F_c(V) + R(O) - R(V) + I/q = 0 \tag{115}$$

(One notes that the sign of I in Eq. (115) is negative when the cell is delivering power.) It is useful to introduce the quantity f_c, which is defined as the ratio of the numbers of radiative to nonradiative recombination-generation currents

$$f_c = \frac{F_{co} - F_c(V)}{F_{co} - F_c(V) + R(O) - R(V)} \tag{116}$$

In the particularly simple case where the nonradiative processes fit the ideal rectifier equation (as in germanium, but not silicon), one can put:

$$R(V) - R(O) \exp \frac{V}{V_c} \tag{117}$$

Under conditions where the cell is surrounded by a black-body at temperature T_c, the unilluminated thermal-equilibrium characteristic for the device can be obtained from Eq. (115) by substituting Eqs. (114) and (117), and noting that in this condition $F_s = F_{co}$; the result is

$$I = I_o \left(\exp \frac{V}{V_c} - 1\right) \tag{118}$$

where

$$I_o = q\,[F_{co} + R(O)] \tag{119}$$

(The sign of I in this equation is the opposite of that in the original paper, to make it consistent with the remainder of this report.)

The value of I_o can thus be determined from Eq. (119) by noting that $Q_c = 1.7 \times 10^3$ $cm^{-2} \cdot sec^{-1}$ for $E_g = 1.09$ eV and $T_c = 300\,°K$. If nonradiative transitions are neglected ($f_c = 1$), this leads to an I_o value of 5.4×10^{-16} A for a 1-cm^2 cell (i.e., 1 cm x 1 cm cell, one surface of which is active, but both surfaces of which contribute to I_o).

Shockley then uses I_o values derived as above to calculate maximum efficiency as a function of E_g. Further, by insertion of various values of f_c between 1 and 10^{-12}, a family of efficiency vs. E_g values are generated. Shockley shows that according to the above analysis, the maximum theoretical efficiency for a silicon solar cell operating under direct sunlight (i.e., without concentrators) is 30%. This is considerably higher than the results calculated by the methods above, and the reasons for this are discussed by Shockley. Some of the calculations are summarized in Table I.

TABLE I. RESULTS OF ULTIMATE THEORETICAL EFFICIENCY CALCULATIONS

Author	Illumination Source	Illumination Intensity ($mW\,cm^{-2}$)	Optimum Eg (eV)	Efficiency Of Silicon Cell (%)
Cummerow	5760° K [(1)]	108	~2	17
Rittner	5760 °K [(1)]	100	1.50	22.5
Pfann + van Roosbroeck	Sunlight (see text)	86	not calculated	18
Prince	AM1 [(2)]	108	1.38	21.7
Loferski	AM1 [(2)]	106	1.43	20.5
Wolf	AM1 [(2)]	100	1.26	21.6
Müser	6000 °K [(1)]	∞	not calculated	16
Shockley	6000 °K [(1)]	100	1.35	30

[(1)] Black-body

[(2)] Air-Mass 1 sunlight (m = 1, w = 2)

The differences in the results of the various theoretical treatments outlined above have an important bearing on solar cell research, and the reasons for the differences, and their significance, have been discussed by many authors.

As was pointed out by Loferski (201), numerical differences arise between essentially similar analyses if the spectral distributions used in the calculations differ. For this

reason, type and intensity of illumination must be specified in comparing divergent results, and this is just as important in theoretical as in experimental work. From the theoretical viewpoint, however, there are more fundamental differences between various analyses, and these we shall discuss here.

The basic divergence of all theories of solar cells stems from the value to be assigned to the reverse saturation current I_o, and the factor A, in the diode equation

$$I = I_o \left(\exp \frac{qV}{AkT} - 1 \right) \tag{120}$$

Workers have taken four discernible positions on these; in the ideal cell:

(i) I_o should be determined by wholly thermodynamic considerations, in which the only required recombinations are radiative, and $A = 1$.

(ii) I_o should be given by the diffusion theory, and A should be 1.

(iii) I_o should be given by recombination theory, and A may have values $1 \leq A \leq 2$.

(iv) Experimentally determined values of I_o and A should be used, since none of the above theories comes near to describing results seen in practice.

Clearly, (i) and (iv) represent extreme opinions, and most workers take a position sitting on one of the fences dividing the possible dogmas.

Shockley and Queisser have defended the position that the only fundamentally required recombination processes are radiative, and that nonradiative recombinations may be regarded as "imperfection effects", an exception being made for Auger-process recombination.* The possibility of Auger-processes modifying the I-V curve to produce the experimentally observed diode characteristic was very fully examined by P.T. Landsberg, working with Shockley and Queisser, the results being reported in Reference (205).**

---

*In which energy and momentum are conserved in the recombination process by requiring that three carriers be involved. In the more usual nonradiative recombination processes, a large number of phonons must be produced to obtain this conservation.

**Note that in ASD-TDR-62-776, the text reference to Figure 19 on page 71 should be changed to Figure 18; also note that in the Figures, the graphs of 18 and 19 should be interchanged, but not the captions.

This work showed that although changes in the slope of the diode characteristic could be obtained if Auger processes were present, the changes are much too small to account for the experimental facts. Landsberg has also pointed out (202) that Auger effects probably become less significant as E_g increases. Since the major interest in solar cell theory is in materials with E_g greater than that for silicon, it appears that Auger effects probably do not play an important role in determining the efficiency of the cells.

As discussed in Section IV-A-1, Sah, Noyce, and Shockley showed that in the diode equation, A values between 1 and 2 could be accounted for by recombination-generation in the depletion region. Shockley and Henley (204) pointed out that if the recombination site density were position-dependent, and if the maximum-recombination plane in the depletion region moved to lower recombination-site densities under increasing forward bias, then values of $A > 2$ could result. This mechanism was analyzed in detail by Shockley and Queisser, under their USAF-funded study contract (205), and it was shown that if physically reasonable values were assumed for (i) the rate of change of recombination-site density with distance, and (ii) the ratio of hole-to-electron interaction cross sections for the recombination center, then this mechanism could not account for the experimentally observed values of A.

Wolf (195) has pointed out that the results seen in solar cell junctions are similar to those seen by Chynoweth and McKay (203) in very narrow junctions in silicon in which field emission occurs. Shockley and Queisser (205) discount the possibility of these effects being related, since the depletion regions in solar cells, although narrow, are not as small as those studied by Chynoweth and McKay. Since the field emission process is not as yet described by a quantitative theory, it is not possible to demonstrate that this process is not the cause of the anomalous effects observed, in the absence of a reasonably well-established alternative. Queisser and Shockley proposed that the mechanism leading to high A and I_0 values was caused by the presence of undesirable metal impurities in the silicon, introduced either by the use of low-grade silicon starting material, or during the cell processing steps. By examination of I-V curves of diodes cut from commercial cells, it was found that junction areas overlaid by contact regions exhibited characteristics nearer to the ideal. Further, it was shown that heat treatments which might cause precipitation of impurities (and hence their removal from the major active area of the junction), led in some cases to lower A and I_0 values. This precipitation effect was postulated as the cause of the soft reverse characteristics often seen in more efficient commercial cells, a point noted by other workers. However, a specific mechanism was not advanced to connect the postulated impurities and the experimental facts, so that a check on this hypothesis has not been made. In an effort to keep separate the historical account and the evaluation phases of the present research, further discussion on this subject (which inevitably involves some "editorializing"), will be given later.

The comparison of various estimates for maximum theoretical efficiency for solar cells was reviewed by Loferski (201). The conclusion reached was that none of the quantitative theories fitted the facts, and that the mechanisms giving rise to the experimentally

determined I_o and A values, and the connection between these, were unknown at the time the paper was written (1961). This appears to be the same as the present situation.

3. Power Loss Processes

The fundamental mechanism of operation of the photovoltaic cell has certain power loss processes associated with it which, even in an ideal cell, cannot be eliminated. These determine the ultimate theoretical conversion efficiency, and an account of these has been given in the preceding section. In a real cell, there are other power loss processes present, which, in principle, could be made as small as desired, but which in practice cannot, because of the limitations of technology. Considerable analytical work has been done to identify these processes, and to provide means for calculating their effects on cell performance. In this section, these loss mechanisms will be qualitatively described, and this description will be followed by a historical review of the analyses which have been performed.

Radiant energy impinging on a real solar cell undergoes a series of transformations before emerging as useful work output from the cell, and at each of these transformations, a proportion of the energy is lost. For the purpose of the present discussion, these processes are summarized in Figure 33; referring to the numbers on the chart:

(1) Optical reflection at the front surface of the cell is assumed zero in ultimate efficiency calculations and is, in fact, made small (3 to 5%) in the main sensitivity range of the cell by the application of antireflection coatings, whose action is described by well-known optical principles (206).

(2), (3), and (4) Electron-hole pair production by the absorption of photons occurs with a quantum efficiency of as close to unity as can be determined in a normal cell. However, under sunlight illumination, the majority of photons absorbed possess more energy than necessary to create hole-electron pairs, and this excess energy is lost by phonon creation. This is a fundamental loss mechanism, which enters into all ultimate efficiency calculations as described in the previous section of this report, and which in effect causes a loss of voltage.

(5) In ultimate efficiency calculations, the cell is assumed to be sufficiently thick to absorb all incoming photons by carrier pair creation. The actual thickness required in practice to effectively achieve this result varies with the optical absorption constant of the semiconductor used. For silicon cells, a thickness less than about 16 mils causes measurable losses in short-circuit current partly because an appreciable number of photons pass through the cell to be absorbed in the back contact. (If this is opaque, as is normally the case; if the contact covered only a portion of the cell back, some of these photons would be internally reflected at the silicon surface, the remainder would be lost by transmission out of the cell.) Some efforts have been made to reduce this loss by the provision of an optically reflecting back contact, but this

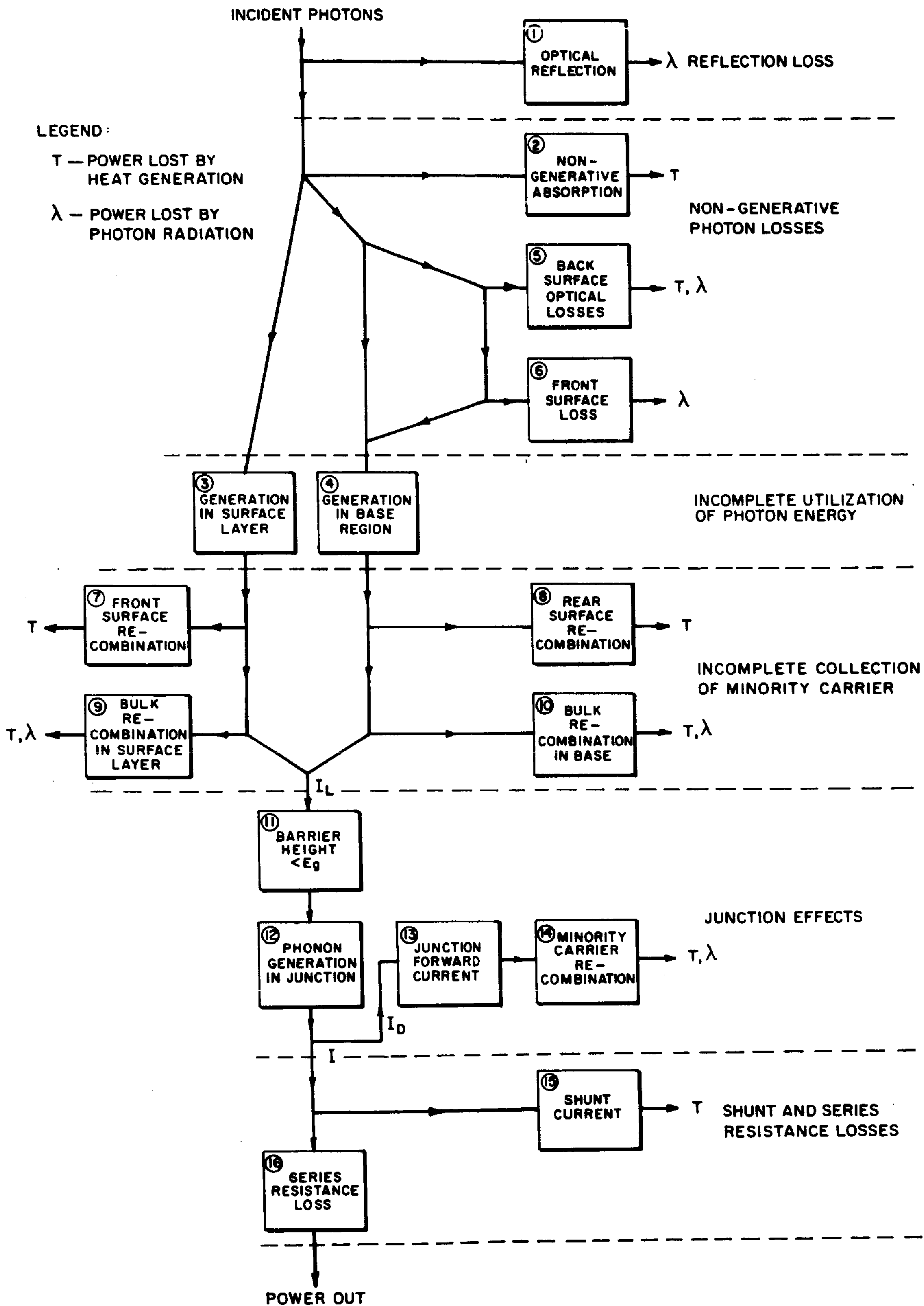

Figure 33. Energy flow chart for a p-n junction photovoltaic cell

appears to be incompatible with the requirement for a low-resistance ohmic contact. In the diagram, photoemission from the back contact has been assumed to be negligible, which is justifiable since in practical cells only low-energy photons reach this region, whereas photoemission normally requires rather large energies, and is also normally characterized by a low quantum efficiency.

(6) Any the photons reflected from the back surface make a second pass through the cell, some being absorbed to create carrier pairs, some being lost by passing through the whole cell thickness and out through the front surface.

(7) Recombination of minority carriers by way of surface-states is an appreciable loss mechanism which has been given considerable attention by many workers. Since the surface region is very thin, diffusion of minority carriers to the surface would be appreciable, if no fields existed in this region. However, in cells which have the surface region made by the diffusion process, an impurity concentration profile exists such that a field is present which aids in diffusion of the minority carriers away from the surface and toward the pn junction. This effect has also been thoroughly examined by theoretical analyses.

(8) Since the back of most cells is covered with an ohmic contact at which the minority-carrier lifetime is theoretically zero (and in practice very short indeed, 10^{-12} seconds or less), minority carriers which diffuse to this surface are rapidly lost by recombination, This process is the second factor contributing to loss of current when cell thickness is reduced: cf. (5) above. It has been given considerable analytical attention.

(9) and (10) Bulk recombination (which in the diagram also includes recombination in the depletion region) may occur by several mechanisms, some of which are fundamentally necessary, some of which are, in principle, avoidable. These processes have been fully discussed in the previous section of this report.

(11) In the ideal cell, the barrier height of the junction is equal to the energy gap of the semiconductor. In practice, it is less, by the amount $\Delta E = E_1 + E_2$ shown in Figure 34. This effect is minimized by providing large carrier concentrations in both n- and p-type regions by high donor and acceptor impurity concentrations (other cell parameters being equal). This effect is seen in real cells, being the reason why silicon cells made on 1-ohm·cm base material show better voltage values (for both V_m and V_{oc}) than cells made on 10-ohm·cm base material. This point has received analytical consideration since the original efficiency analysis of Cummerow.

(12) The separation of hole-electron pairs by the junction depends on the carriers moving to a region which minimizes their potential energy. This "sliding down a potential hill" process generates photons, and is a fundamental necessity in a cell (except for operation at absolute zero of temperature, where in theory it tends to zero). The actual amount of energy lost this way is determined by the I_o value of the junction, which has been discussed in the previous section.

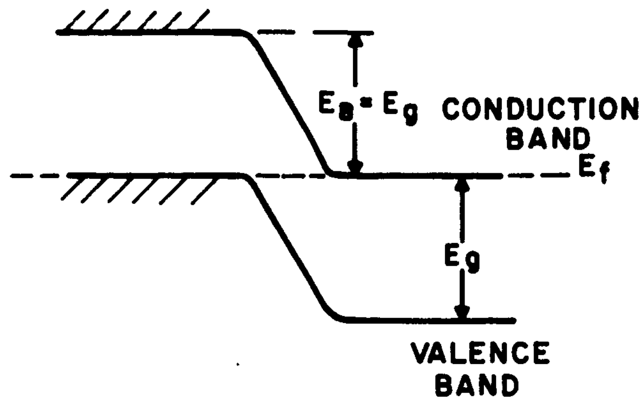

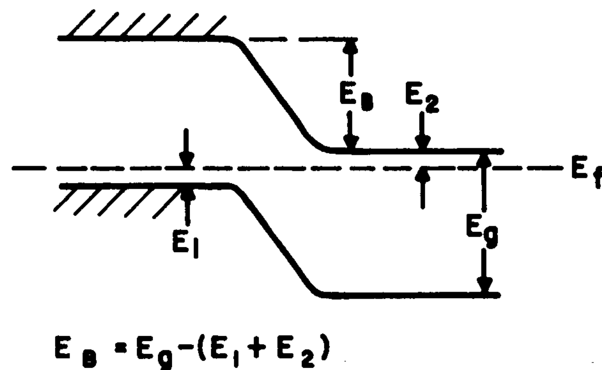

Figure 34. Band diagram showing the effect of low carrier concentration in reducing V_{oc}

(13) and (14) Some forward current in the junction is always present even in ideal cells. The actual amount of energy lost this way is determined by the value of I_0, which has been discussed in the previous section of this report.

(15) Leakage across the junction may be caused by imperfections in the junction, especially at the edges where ohmic conduction paths are easily formed. A related phenomenon with very different causes is the current caused by recombination in the depletion region, or by any of the other suggested additional-conduction mechanisms in the junction, such as field emission or tunneling. Some of these processes have been discussed in the previous section.

(16) Series resistance arises in a real cell by contributions from various cell regions. In silicon cells the largest contributor is usually the diffused surface region, which contributes a distributed resistance. Some analytical treatments have been

developed for this as a distributed element, but it has more usually been treated as a lumped circuit element. The development of gridded cells, as described in IV-B-1 has helped to reduce the magnitude of the losses from this contribution, and an analytical treatment of the effects of the grids has also been given. Other contributors to the total series resistance of a cell are the base-region resistivity, and the contact resistances. These can accurately be considered as lumped circuit elements, and have been always treated this way.

The way in which methods for the analysis of these effects have been developed during recent years will now be reviewed. The earliest theoretical efficiency calculations of Cummerow, Rittner, and Chapin (124) and others made note of the ways in which departures from the ideal cell would lead to lower efficiencies, but quantitative analyses for these effects were generally not given.

The calculation of the dependence of I_{SC} on wavelength of incident light (i.e., the spectral response) received the earliest complete treatment. The problem is conventionally approached by a one-dimensional analysis considering the spatial variation of minority-carrier generation with depth in the cell, using Lambert's law of absorption. The proportion of these carriers which reach the junction is calculated by applying the diffusion equation, with boundary conditions such that the minority-carrier density at the junction plane is zero, and with a recombination velocity at the front and back planes of the cell to account for the surface recombination. An integration is applied over the n- and p-regions of the device to obtain the I_{SC} value for a given wavelength. To obtain the I_{SC} value when a cell is operated under broad-band illumination, this calculation must be repeated to obtain a collection efficiency value for each wavelength used for the illumination (to allow for variations in optical absorption constant with wavelength), and a summation must then be performed to account for the dependence of illumination intensity on wavelength.

A complete analysis of this type was first published by Cummerow (166), although some assumptions on surface recombination effects made in this paper are not those described above. Cummerow assumed a reflecting surface for minority carriers at an ohmic contact, probably because an n-to-n^+ transition (or p-to-p^+) gives a field which will tend to prevent minority carriers from reaching the contact region. Thus, the minority carriers are prevented from reaching the zero minority-carrier lifetime region, which is contrary to the assumptions of other workers. In reality, it seems likely that although some field-assisted diffusion away from the contact occurs, the process provides only a small departure from the infinite-recombination-velocity condition usually assumed.

Harten and Schultz (208) used a similar analysis to that given above to show that the surface recombination velocity and minority-carrier diffusion length can be determined from spectral response measurements; the same point was made by Subashiev in 1960 (209) and by Loferski in 1961 (214).

The collection efficiency problem was analyzed by Rappaport, Loferski, and Linder with reference to the electron-voltaic effect (182), and the same analysis was then applied to photovoltaic cells by Loferski in 1956: the approach is that outlined above. Bir and Pikus (207) performed essentially the same analysis as Cummerow, and appear to have been the first to point out that the collection efficiency is maximized if a very shallow junction is used, when account is taken of surface recombination. This is one of the fundamental design philosophies for present-day cells. It should be noted that the work of Cummerow, Harten and Schultz, and Bir and Pikus, was all concerned with germanium cells. Prince and Wolf (109, 195) applied the above-outlined method in detail to silicon cells, and gave a complete derivation and solution for the relevant equations, in 1958 and 1960. The collection efficiency problem was analyzed using the above methods by Moss (219) and by Kleinman (220) in 1961, with special reference to comparing GaAs and silicon cells. The results from the two authors are divergent, Moss showing GaAs superior to silicon, Kleinman showing the converse. The difference arises from surface recombination effects, which particularly influence the performance of cells made with a material having a high optical absorption constant (as GaAs), since all carriers are generated close to the surface. As noted by Kleinman, however, the surface recombination effect does not affect GaAs cells as much, in practice, as one would expect from the analysis. This may be explained in part by field-assisted diffusion in such cells, as discussed below. Kleinman's approach to solution of the collection efficiency problem is interesting in that the functions for the spectral distribution of the incident light and the variation of the optical absorption constant with wavelength for the semiconductor, are both contained in a single expression which is integrated to obtain the overall collection efficiency, thus reducing the numerical integration steps.

The calculations up to 1960 had all assumed that minority carrier motion occurred by field-free diffusion. In 1960, Subashiev and Pedyash (210, 211), Moizhes (212), and Jordan and Milnes (213) independently published analyses showing the effect on minority carrier diffusion of the field produced by the non-uniform impurity concentration in diffused layer silicon cells. These calculations were based on the fact that an ionized impurity concentration change from n_1 to n_2 causes a potential difference of V volts where

$$V = \frac{kT}{q} \ln \left(\frac{n_2}{n_1} \right) \tag{121}$$

Although the actual potential change is small (~ 0.3 V), the field gradient is large because the potential change occurs across the thin surface region, causing fields of up to a few thousand volts per centimeter. A related analysis showing the effect of the diffusion impurity profile on the capacitance-voltage relationship for the junction was given by Lawrence and Warner (215) in 1960, but the analysis involved the use of numerical methods, so that the main value of the work lay in showing the regimes in which the graded and step junction approximations were reasonably accurate. Dale and Smith

(216) performed another analysis for spectral response including the surface-field effect, and also including a short minority-carrier lifetime in the surface region: the authors then applied the analysis to determine the surface recombination velocity and lifetime from spectral response measurements. This work therefore is a refinement of the measurement methods developed by Harten and Schultz (208), Subashiev (209), and Loferski (214), mentioned above.

In 1963, Wolf (217) showed that the effect of field-assisted diffusion in the surface region could be approximated with good accuracy by using a field-free analysis with the minority-carrier lifetime increased by a factor of ~ 4.4, thus enabling the simpler original analysis to be retained. This appears to be the present status concerning collection efficiency theory: one might add that extremely close agreement is now obtained between theory and practice for most cell types, the notable exception being CdS cells, where the fundamental operation of the device is not fully understood. The effect of reducing the cell thickness was analyzed by Wolf (194, 217), by insertion of appropriate boundary conditions into the solution of the differential equations for the collection efficiency. The correlation between this theory and practice was examined by Wolf and Ralph (224, 225), who found the current to fall with reduced cell thickness more rapidly in practice than would be expected theoretically. More recently, however, this correlation has been re-examined by Crabb and Treble (226), who found good agreement with the theory. Both groups of workers felt that the experimental results of Wolf and Ralph may have been caused by work damage extending into the base from the back contact of the cell, thus reducing the effective thickness of the device.

The second major loss factor which has received considerable theoretical evaluation is the effect of series resistance on the cell operation. Two areas of work are included here, one of which deals with the calculation of power losses caused by lumped-element effects, the second dealing with the effects arising from the distributed nature of the thin surface layer. It may be noted that both of these aspects received initial attention from Schottky during the 1930's (see II-2-b*).

The equivalent lumped-element circuit for the cell is as shown in Figure 35(a) for the ensuing account. Since R_s was a major cause of power loss in the initial cells made at Bell Laboratories, it is natural that it should be mentioned in the early reports of Chapin, Fuller, and Pearson (124), although their paper did not give a formal analysis. The point was taken up in detail by Prince (145), who by conventional analysis from the circuit of Figure 35(a) showed that the cell characteristic is given by:

$$\ln\left(\frac{I + I_L}{I_o} - \frac{V - IR_s}{I_o R_{sh}} + 1\right) = \frac{q}{kT}\,(V - IR_s) \qquad (122)$$

*Second Semiannual Report, NASW-1427, June 1967.

From this, a family of I-V curves was calculated, showing the effect of various values of R_s and R_{sh}, which demonstrated graphically the value of reducing R_s. Neglecting R_{sh} (which is reasonable for most silicon cells), analysis showed that the power generated by the device is given by

$$P = -IV = -I \left[\frac{kT}{q} \ln \left(\frac{I + I_L}{I_o} + 1 \right) + IR_s \right] \tag{123}$$

Thus, the power lost in the series resistance is a separable term in this treatment, which is an approximation valid for R_s small. Prince calculated a curve showing (power output) as a function of R_s. He also tackled the distributed sheet resistance problem by the method illustrated in Figure 35(b), where it is assumed that the "average" point of generation of current is one-quarter of the cell width from the edge. This simplification assumes that the potential variation over the surface of the cell is so small as to negligibly affect the forward current through the junction [I_D in Figure 35(a)], so that the net current contributions from all parts of the cell have the same density. Combining this with the first part of his analysis, and using a very simplified expression for I_L as a function of layer thickness t, Prince calculated a curve showing (power output) as a function of t for a cell 1 cm wide (W = 1 cm), with no grids. Hence, an $R_s = 0.5$ ohm and a conversion efficiency of 8% was calculated for the optimum t value ($\sim 2\,\mu$m). Similarly, Prince analyzed the dependence of the (power per unit area) and the (power per cell) on W, showing that there was a width giving optimum value for the former, which for a cell made with the semiconduction parameters measured in silicon, gave W = 1 cm for normal sunlight operation. This analysis is for an ungridded cell, but it is related to the grid optimization calculations which came later.

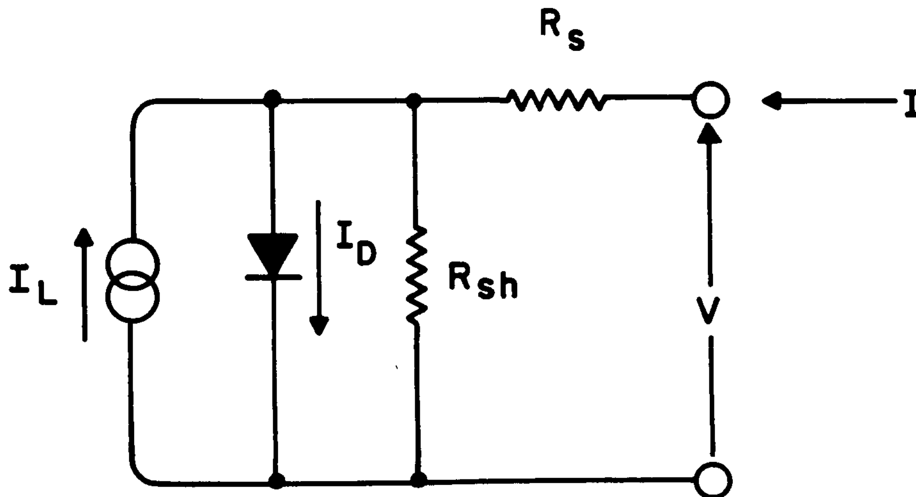

Figure 35(a). Equivalent circuit for a solar cell

Prince and Wolf (194) analyzed the effects of R_{sh}, using the methods of Prince described above, showing that in practice R_{sh} became significant only when cells were made to operate under low illumination levels. Hence, it was shown that a cell with a deeper diffused surface layer than usual would be better for low-level operation, since junction leakage effects could be minimized by increasing the surface layer thickness.

Wolf (195) provided a very complete analysis of the effects of various losses on cell performance, and followed the treatment of Prince for calculating the loss of power caused by a lumped R_s in the equivalent circuit Figure 35(a). However, gridded cells had now become the standard production type, and Wolf analyzed the effect of the grid geometry on the contribution of the distributed surface-layer and grid lines to R_s. The treatment followed the approximation of Prince in assuming an "average" current generation point one-quarter of the unit field width (S/4) from the grid line, as in Figure 35(b). However, Prince's cell now became, in effect, one "field unit" in the gridded cell, as shown in Figure 36. Using the same reasoning as was applied to the surface layer R_s contribution, the "effective length" of the grid line is taken to be W/2 for subsequent analysis. (Note that Prince's W has become Wolf's S.) Wolf then performed an analysis which resulted in expressions for the values of W, S, and T which would minimize R_s .

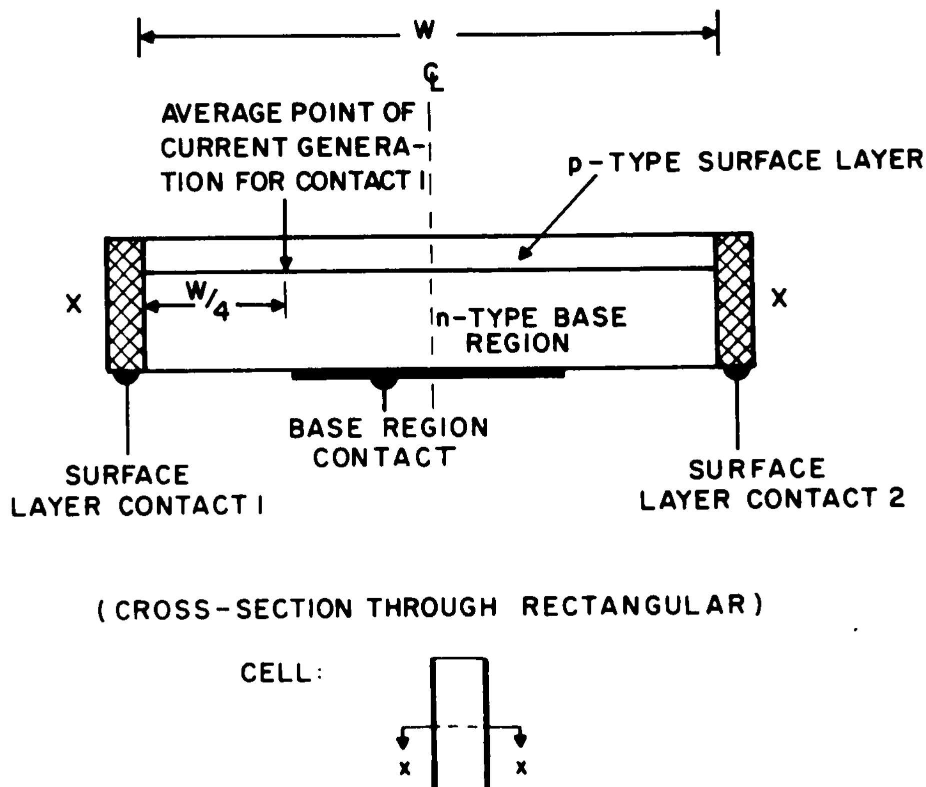

Figure 35(b). Cross section of a solar cell, showing dimensions as used by Prince for R_s calculation

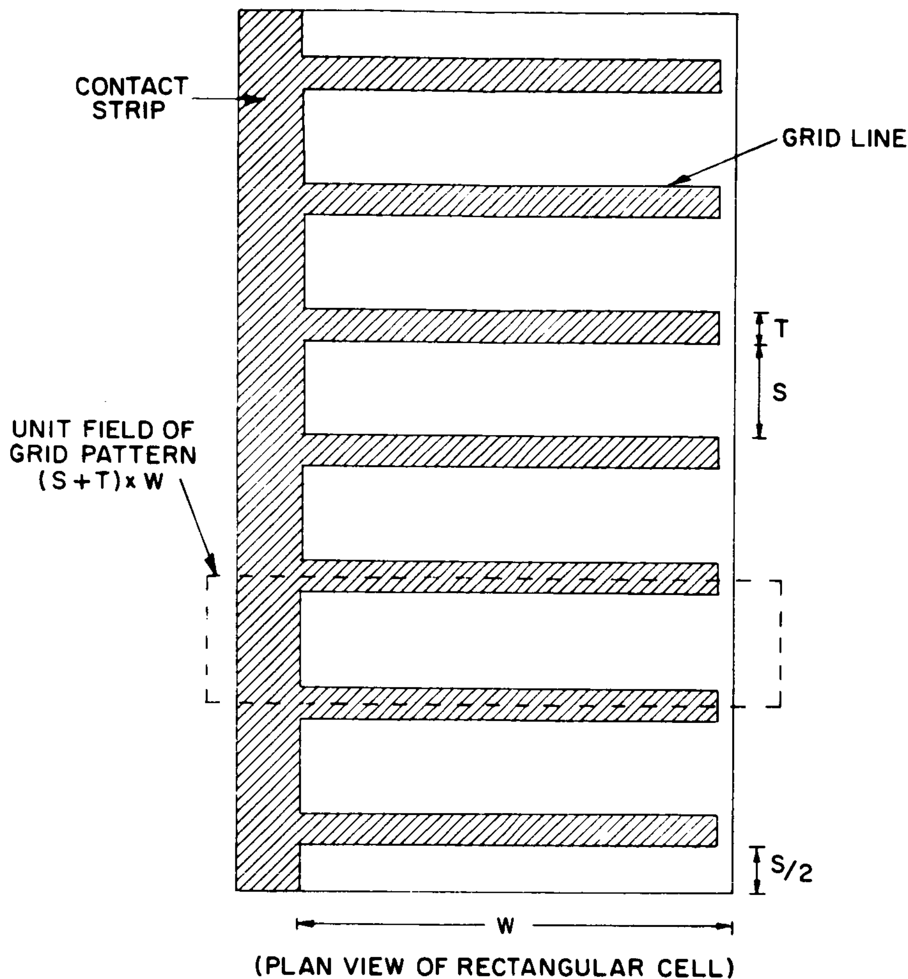

Figure 36. Cell geometry used by Wolf for R_s calculation

This analysis is in error in the assumption that minimizing R_s maximizes cell efficiency (since altering the cell dimensionally alters the output current flowing through R_s, and the power loss is determined by I^2R_s). This point was picked up by Lamorte (221), who provided an alternative analysis in which the power per unit area was maximized by allowing the grid spacing to vary, the grid line width remaining constant (i.e., S variable, T constant in the nomenclature of Figure 36). Lamorte assumed a linear variation of voltage over the cell surface, a questionable assumption justified by experimental measurements on GaAs cells, but a necessary one to provide a tractable analysis. Lamorte's analysis also neglects the resistance of the grid line, which may be justified for small solder-dipped Si and GaAs cells, but which invalidates the analysis for other cell types (e.g., evaporated-grid silicon cells without solder dip, or thin-film cells of the CdS type). Lamorte also makes no statement as to how the grid line width T should be chosen, a point which will be analyzed later in this work.

Lamorte's analysis proceeds by deriving an expression for power output from the cell in terms of the grid geometry and diode equation parameters and the light-generated current density and cell terminal voltage. This is then maximized by the usual methods, providing an expression giving the optimum S value for a given terminal voltage. However, to obtain solutions for the more general case where the cell operating voltage is also optimized, the calculation must be repeated over a range of terminal voltage values to provide simultaneously optimum values for both S and V. It should be pointed out, however, that the variation of S and V is probably slow in the range of most real cells, so that this lack of generality is not a serious objection to application of the analysis to real problems.

Theoretical calculations showing the effect of R_s on cell efficiency were performed at RCA Laboratories under a Signal Corps contract (192) during 1958-60 with special reference to GaAs cells; this aspect of the work under this contract was later published by Wysocki (218). In this analysis, the sheet resistance was analyzed truly as a distributed effect. It resulted in nonlinear differential equations for which numerical methods of solution were used. From such solutions, Wysocki plotted various curves showing how cell performance was influenced by the sheet resistance of the diffused layer. The same analysis was also reported by Moizhes (212) in 1960.

In 1967, Handy (222) reported the results of a theoretical analysis of the contributions to R_s of the various regions of a gridded solar cell, including an allowance for current paths from the surface layer direct to the contact strip without going through the grid line (see Figure 37), a point assumed negligible by Wolf and by Lamorte. Handy also provided an equivalent circuit for the R_s contributions, which was used in 1963 by Ralph and Berman (223) (with acknowledgment to Handy) as part of an experiment to correlate Wolf's theory for grid optimization with practice. This theory provided an optimum grid line thickness less than that technically feasible, so that this work was not as stringent a test of the theory as it might have been, especially as the experiments showed a scatter in results which was more than large enough to mask the effects being analyzed. This is the present situation with regard to the effects of R_s on cell efficiency.

The remaining practical consideration which has been examined theoretically concerns the impurity concentration in the n- and p-regions. In ultimate theoretical efficiency analyses, it is assumed that the carrier concentration is such as to bring the Fermi level E_f to the band edges in the two regions, so that the barrier height in the junction has a value E_g, as shown in Figure 38(a). In practice, the situation is usually as shown in Figure 38(b), and this has two effects:

(i) At a given voltage across the cell terminals, the junction current I_D in Figure 35(a) is greater. (ii) At a given current output from the cell, the voltage at the cell terminals is reduced, and Peltier heating occurs at the cell contacts, caused by phonon generation when the carriers traverse the bent hands at the contacts.

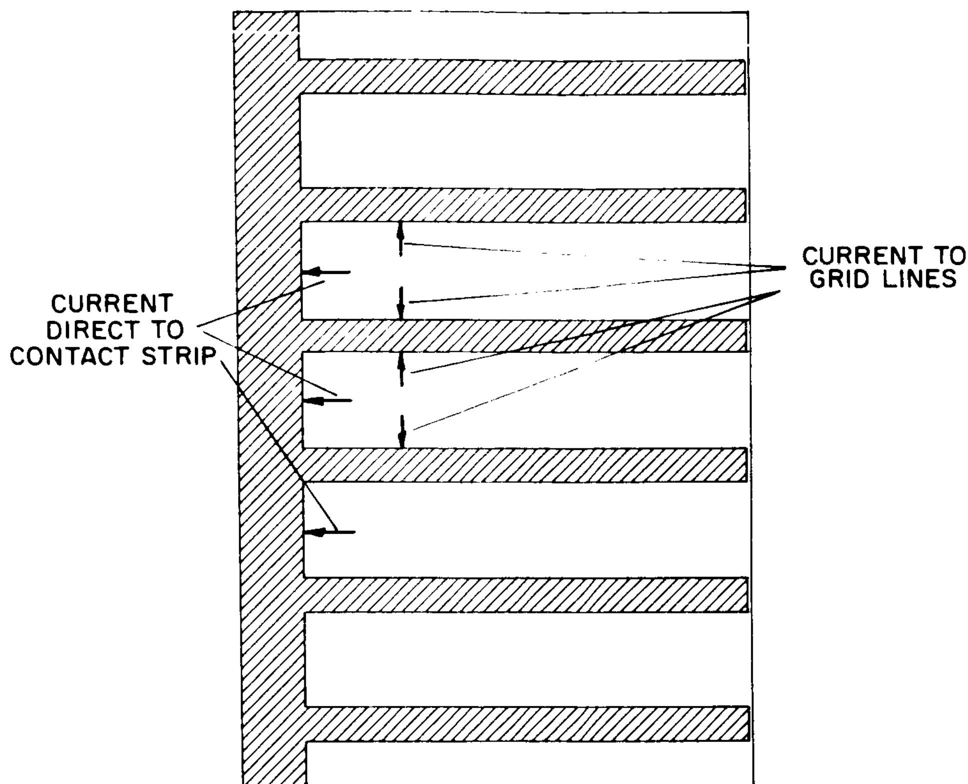

Figure 37. Current paths in a cell, as used by Handy for R_s calculation

At the maximum power point, both of these effects influence the cell operation. The value of heavy doping to produce large carrier concentrations and thus bring E_f to E_c and E_V was pointed out by Cummerow and other early workers, and the results were found in practice when cells made on 10-ohm·cm resistivity base silicon were made for radiation-resistance testing, such cells exhibiting a V_{oc} and conversion efficiency lower than those of the 1-ohm·cm cells previously used. The effect of the doping on cell performance received particular attention from Subashiev (210, 211), who pointed out the existence of the Peltier effect in this case. The theoretical and experimental results agree well on this point, so that further work has not been necessary.

In concluding this section, it is perhaps worth pointing out that the papers of Subashiev (211) and Wolf (195) provide comprehensive reviews of the ways in which real cells depart from the ideal.

4. Heterojunctions

Several types of energy-conversion cells based on heterojunctions have been investigated since 1955. These include metal-semiconductor (e.g., Pt-GaAs thin-film cells), degenerate semiconductor-semiconductor (e.g., CdS and CdTe cells), and semiconductor-semiconductor (e.g., GaP-GaAs cells). For these cells, the major research effort has been experimental, but the graded bandgap cell is a special case of a

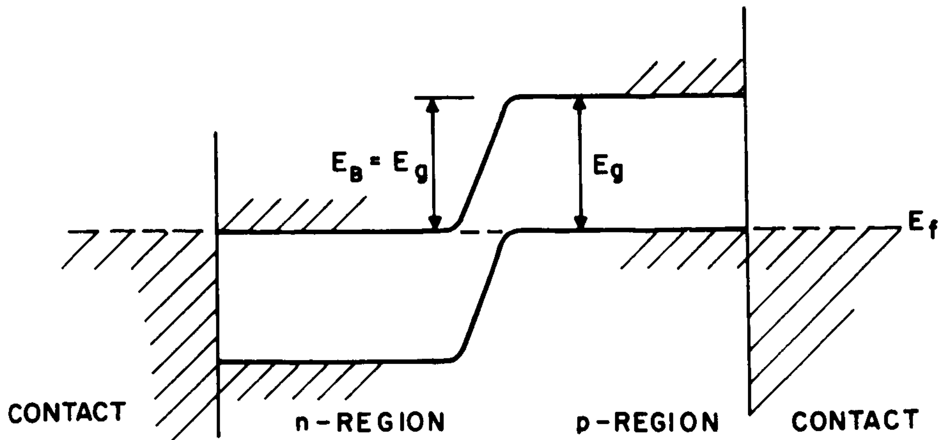

Figure 38(a). Band structure in a photovoltaic junction, barrier height = E_g

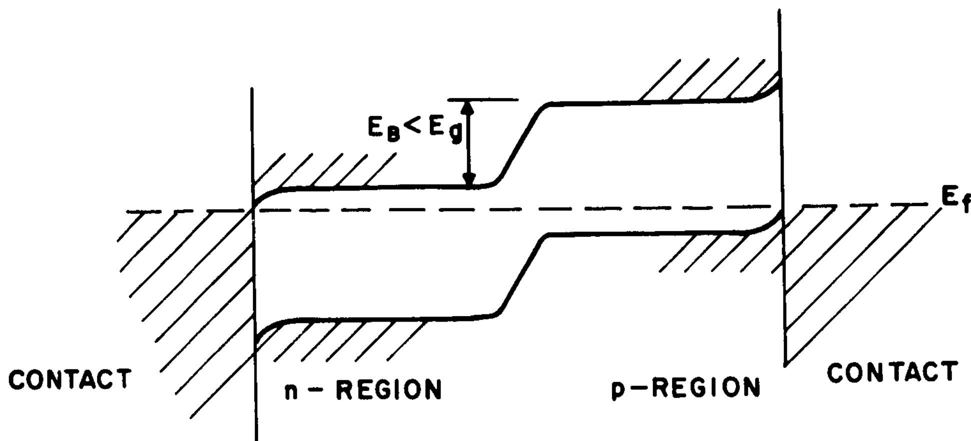

Figure 38(b). The same, barrier height < E_g

heterojunction cell, and this has received primarily theoretical attention. In this section, the theory underlying these cells types will be discussed.

An account of the development of the theory of metal-semiconductor contacts has already been given in Sections II-C-2 and III-D-2 above; it appears that this work of Schottky, Mott, and Bethe has received no further development in recent years, aside from the consideration of surface-state effects by Bardeen, as described in III-D-2. A comprehensive and unified account of the present understanding of metal-semiconductor contacts was given by Henisch (227) in 1957. The band structures of an ideal metal-semiconductor junction in equilibrium and under photovoltaic operation are shown in Figures 39(a) and 39(b), with pair creation by absorption of a photon of energy $h\nu$ shown schematically. In Figure 39(a) it is shown that the band-bending at the surface

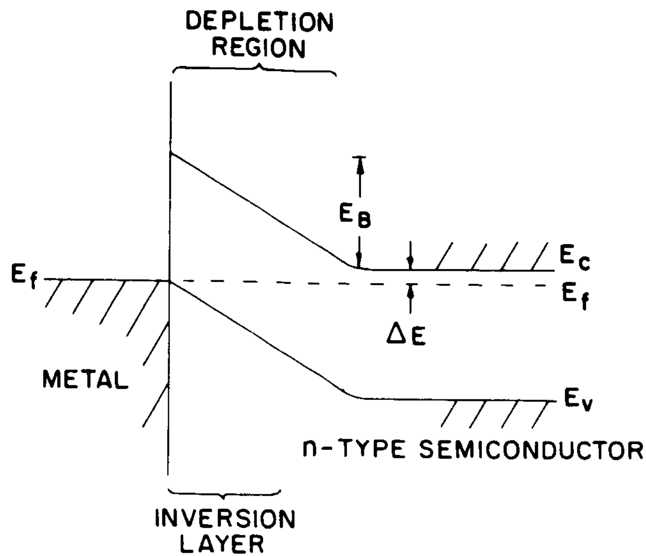

Figure 39(a). Band structure of a surface-barrier cell, equilibrium condition

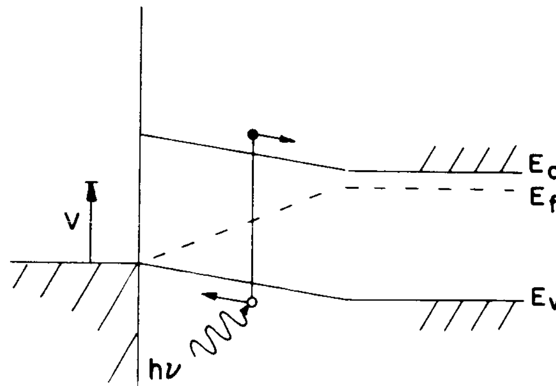

Figure 39(b). The same, under illumination

causes the Fermi level E_f to be closer to the valence band edge than the conduction band edge, thus forming a region of opposite conductivity type. This inversion layer is formed when a blocking metal contact is applied to either a p- or n-type semiconductor, and gives rise to a junction which behaves in many ways as a p-n junction. In particular, under illumination the junction exhibits all the characteristics of the p-n junction photovoltaic effect, and the cell theory can be analyzed the same way in both cases, the only change being to insert an appropriate value for I_o in the diode equation. For the p-n junction, I_o is as given in Section III-D-2:

$$I_o = \frac{b}{(1+b)^2} \cdot \frac{kT}{q} \cdot \sigma_i^2 \left(\frac{1}{\sigma_n L_p} + \frac{1}{\sigma_p L_n} \right) \quad (124)$$

$$= \frac{b}{(1+b)^2} kT \left(\mu_n + \mu_p \right) \left(\frac{1}{\sigma_n L_p} + \frac{1}{\sigma_p L_n} \right) \exp \frac{E_g}{kT} \quad (125)$$

For the metal-semiconductor junction, in the simplest case:

$$I_o = n_{pn} q \left(\frac{kT}{2 \pi m^*} \right)^{1/2} \exp \left(- \frac{E_B}{kT} \right) \quad (126)$$

where

n_{pn} = majority-carrier density in semiconductor

m^* = effective mass of majority carrier in semiconductor

E_B = barrier height as shown in Figure (39)

In practice, surface states are normally present, which have the effects described by Bardeen on E_B (see Section II-D-2), and which probably act also as recombination-generation levels localized at the junction, to cause the effects described by Sah, Noyce and Shockley, as described in IV-A-1. In addition, image forces act to lower E_B, and tunneling may be present, with the effects described by Henisch (227), leading to higher junction currents at small forward bias than would be expected from the simple diffusion theory underlying Eq. (126). Again, the same departures from the diffusion theory are seen in p-n junctions, as discussed in IV-A-1. This is the theory of the Pt-GaAs cells investigated at RCA Laboratories (228), and the surface-barrier Si cell investigated at Tyco Laboratories (229).

A great deal of experimental work has been done on cells made with a Cu_2S-CdS heterojunction, cells made with a Cu_2Te-CdS heterojunction, and cells made with a Cu_2Se-GaAs heterojunction, as described in Section IV-A-2. The cells on CdTe and GaAs behave in a way which indicates that the degenerate Cu_2Te and Cu_2Se layers behave essentially as metals, merely providing a contact to an inversion layer present at the semiconductor surface. Thus, the theory of these cells is assumed to be that developed for the metal-semiconductor cells described above. For the CdS cells, the behavior is such as to indicate that either the Cu_2S is playing an active role in the cell operation, or a group of trapping levels in the CdS is markedly influencing the photovoltaic behavior. This cell type is a special case, for which an accepted theory of operation has not been developed. An account of the proposed theories is given in the discussion of this cell in Section IV-A-2.

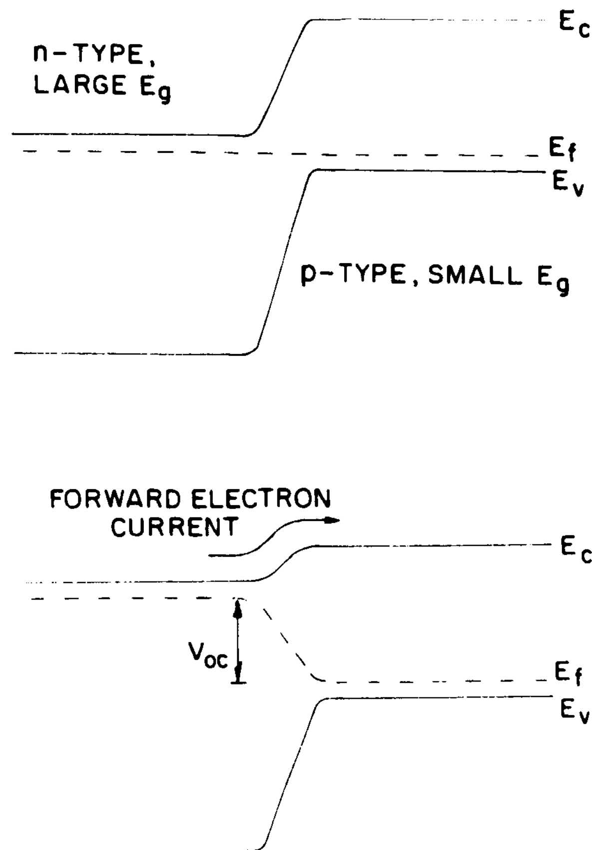

Figure 40. Band structure of a heterojunction cell

The heterojunction cell which has had the most analytical attention is the semiconductor, semiconductor cell. The band-structure of the simplest cell type is shown in Figures 40(a) and (b) in equilibrium and in photovoltaic operation. At first sight, it appears that such a cell may have a higher ultimate conversion efficiency than the single-energy gap cell, since the proportion of the photon energies of the solar spectrum which are converted into hole-electron pair energies is higher. However, as can be seen from Figure 40(b), the voltage developed by the cell is governed by the material with the smaller bandgap, since (in the case shown) V_{oc} is obtained when the electron current in the forward direction in the conduction band equals the light-generated current. (The case of p-type large E_g to n-type small E_g would result in the diode forward current consisting primarily of hole current, the principle remaining the same.) Thus, the device would have an efficiency no higher than that of a cell made with a p-n junction in the small E_g material, as was pointed out by Wolf (195).

A more elaborate type of cell was also considered by Wolf, and (in more detail) by Emtage (230). Emtage considered conduction and photovoltaic processes in a semiconductor with a band-structure as shown in Figure 41(a). Under illumination, a voltage is developed in such a material as was shown by Tauc (231), by a mechanism which

is illustrated in Figures 41(b) and (c). Emtage derived the equations governing current flow in such a device, by considering the transport of carriers in a material with position-dependent conduction parameters. The resulting relationships are complex, and a summary of the results for photovoltaic operation only will be given here; the reader is referred to the original paper for the complete analysis.

Consider the specimen under illumination sufficiently high to bring the electron and hole concentrations into approximate equality. If both carrier types have the same mobility, then the photovoltage developed is as shown in Figure 41(b) for the open-circuit condition, the hole and electron currents balancing, as shown, to give zero net current, and

$$V_{oc} \div \frac{E_{g1} - E_{g2}}{2} \tag{127}$$

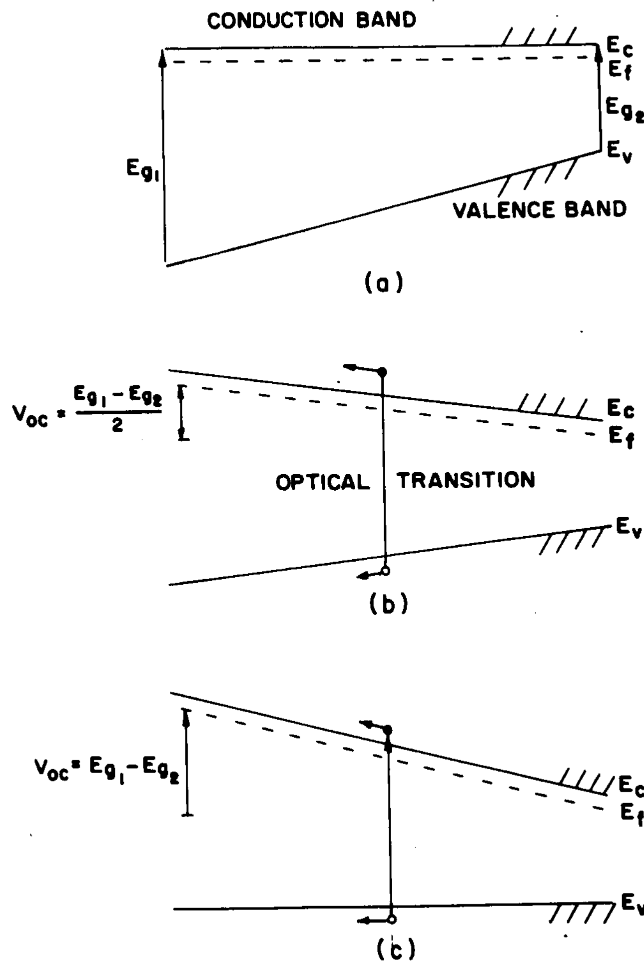

Figure 41. Band structures in a graded-bandgap semiconductor

Now if the hole mobility is much larger than the electron mobility, the open-circuit voltage case is as shown in Figure 41(c), and

$$V_{oc} \doteqdot E_{g1} - E_{g2} \tag{128}$$

The point made, then, is that at illumination intensities sufficiently high to bring the minority-carrier concentration into approximate equality with the majority carrier concentration, in the case of very different carrier mobilities, V_{oc} can tend to E_{g1} - E_{g2}. Now if a p-n junction is placed at the small bandgap end of the device, as shown in Figure 42(a), then a photovoltage tending toward E_{g1} will be obtained under the conditions described above, as shown in Figure 41(c). Emtage then considered a cell made by grading E_g using the GaAs-InAs alloy system, but concluded that the efficiency is only of the order of 20% when the device is operated under concentrated sunlight. If illumination tailored to the particular device were to be used, then the efficiency would improve, which is, of course, true for all cells. The efficiency is roughly the same for the graded bandgap cell and the p-n junction cell with energy gap E_{g2} because the I-V characteristic of the graded

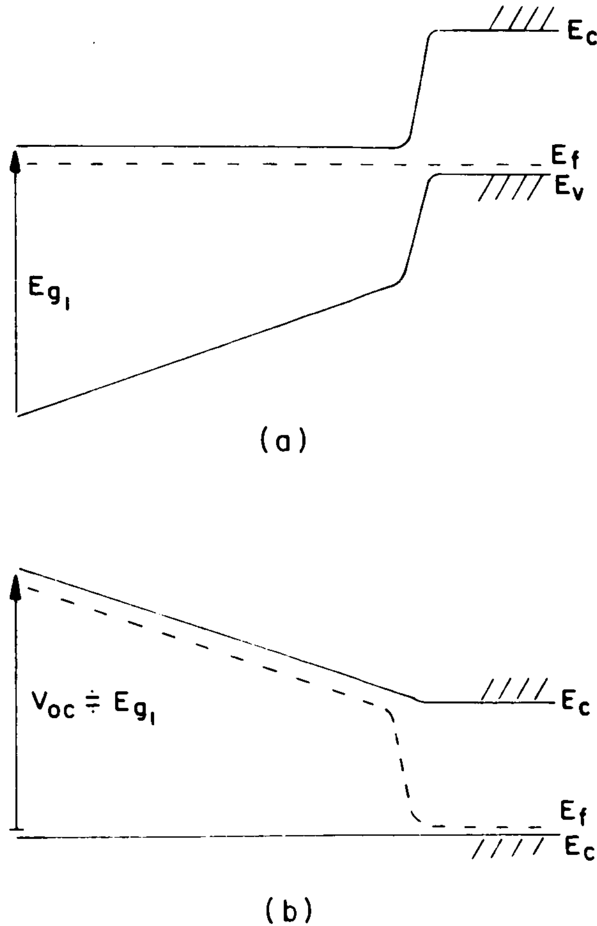

Figure 42. Band structure of a graded bandgap p-n junction cell, (a) in equilibrium, (b) under illumination

region is linear, leading to a total device characteristic as shown in Figure 43. The conclusion reached by Emtage for the conversion efficiency is the same as that arrived at by Wolf, though the analysis is different in the two cases.

The simple band structures used in the analyses of Emtage and Wolf for heterojunctions are not always valid. Oldham and Milnes (232, 233) have considered the I-V characteristics of abrupt heterojunctions with interface states present, and Van Ruyven (234) has used photovoltaic measurements to demonstrate the existence of such states in Ge-GaP heterojunctions.

It should also be pointed out that GaAs cells have been made with a GaP-GaAs heterojunction to allow the active junction to be well below the semiconductor surface, thus minimizing recombination losses via surface states. The theory of such cells has been discussed above; the cell behaves, in principle, as a regular p-n junction GaAs cell, with the same limitation on conversion efficiency, the wide-bandgap GaP merely acting as an optically transmitting conductive layer.

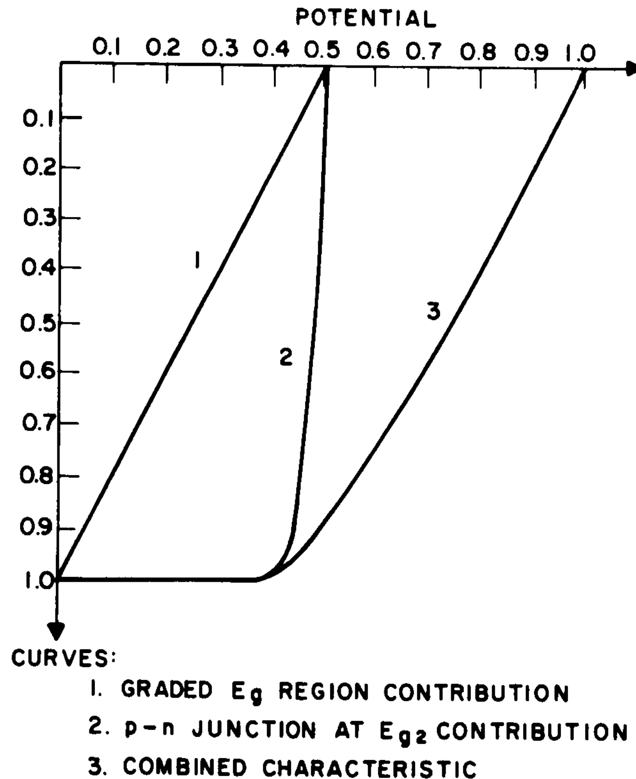

Figure 43. I-V characteristic of a graded-bandgap p-n junction cell

B. Silicon Solar Cells

1. Introduction

Before proceeding with the discussion of the development of the solar cell after 1955 it will be useful to introduce some background information. In considering the improvement of the solar cell one must first designate the characteristics or operational parameters of the cell which are both capable of and desirable of change. Taking the most abstract point of view we can consider energy conversion efficiency, weight, cost, and resistance to various environmental factors as the important parameters for improvement. These factors will play an important part in the following discussion of the development of silicon solar cells. A further breakdown and discussion of some of the very general categories listed above will be helpful before proceeding with the consideration of specific photovoltaic cells, such as the silicon cell.

A generalized breakdown of the relative values of the various cost factors involved in the fabrication of a solar cell is not easily obtained due both to some variation in technique and to the tendency of manufacturers to be somewhat secretive. It is generally agreed that materials are a significant portion of the cost, but little can be gleaned beyond this. It is possible, however, to discuss a number of studies that have been aimed at introducing innovations which would reduce the cost of specific areas of cell manufacture. This includes the use of cheaper materials (i.e., polycrystalline silicon), the production of large-area cells, and the development of new techniques for performing certain specific operations such as junction formation. It is in this relatively unstructured way that improvements in the cost factor of solar cells will be considered in the following discussions.

The weight of the cell itself (ignoring coverglasses and the like for the time being) is rather easily broken down. One has, first of all, the weight of the material (silicon, etc.), the weight of the contacts (grids, busbar, base contact), and the weight of any coatings or encapsulant (antireflection, etc.). In conventional single-crystal cells the vast majority of the weight is distributed between the weight of the material and the weight of the contacts. The majority of the programs designed to reduce the weight of the cell have concerned themselves with reducing the thickness of the material.

Under the heading "resistance to various environmental factors" one can lump a multitude of desired virtues; however, for most current cells and uses there is one single factor of overwhelming concern - radiation resistance. Other factors become important for particular missions (e.g., temperature) or particular types of cells (e.g., humidity for some thin-film cells) and will be discussed in context where appropriate. A specific section devoted to radiation resistance will be given elsewhere in this work and should be referred to for a more complete and coherent discussion of this subject. However, for the sake of completeness, and also coherence, brief discussions of developments in radiation resistance will be given, where appropriate, throughout the description of solar cell history and development.

A dominant requirement for solar cell research during the period these cells have been in use has been efficiency improvement. This has been analyzed in great detail by many workers, and an account of the various factors which determine the conversion efficiency of a solar cell has been given in the preceding Section IV-A-1. The improvement of efficiency has been the main motivation for many of the changes which have been made in practical cells, and an account of these follows.

The discussion covers the experimental development of the solar cell from the mid 1950's until the present. Investigations during this period were expanded to cover a wide variety of materials and techniques in the hope of finding new, more efficient types of solar cells. The most important material during this developmental phase has been silicon, and it is this material which will be discussed first. The discussion of silicon is broken into two parts. The first part covers the evolution of the solar cell as it exists today and discusses, for the most part, only those developments which were successful in improving the cell and bringing it to its present state. The second part discusses many of the experimental investigations which were not successful or were not or have not yet been completed. This break was made because it was felt that a more coherent account of the history of the solar cell would result if some of the extraneous material were presented separately.

2. Development of the Present Cell Types

The introduction of the Bell Laboratories solar battery and the work on the electron-voltaic effect marked the beginning of serious investigations into the development of large area p-n junction devices for energy conversion. At the time of disclosure the maximum efficiency of the Bell solar battery was 6%. Three types of losses were singled out as being major contributors to the discrepancy between the observed efficiency and the theoretically predicted maximum of 22%. These were surface reflection, bulk and surface recombination, and series resistance. Prince's analysis (145) indicated that the most important loss in these cells was due to series resistance. By optimizing the cell design Prince calculated that the series resistance of the cell as it then existed could be reduced to less than 1 ohm (his test samples had resistances of 2 to 6 ohms). This would give an increase of 30 to 40% in efficiency. In the same publication Prince also suggested the use of quarter-wavelength type antireflection coatings to improve the efficiency.

Advancements in cell efficiency were rapid during this early period. Within a year after the original announcement of the solar battery Chapin et al. (144) reported that the best efficiency had increased from 6% to 11% and that most of the units made were consistently around 8% in efficiency. With the exception of some improvements in contacting the cell, no clue is given about the developments leading to this increase.

An early experiment with the application of silicon solar cells to power a remote telephone repeater station, proved the severity of economical competition which photovoltaic solar energy conversion has to face in earth surface applications in well-developed

countries. After this, the interest in solar cells waned at Bell Telephone Laboratories for several years, and the development of silicon cells was carried forward during this interval predominantly by two smaller semiconductor device manufacturers.

Not long after the announcement of the Bell solar battery, development work on silicon solar cells was started in 1955 by National Semiconductor Products, a Division of National Fabricated Products, Inc., Evanston, Illinois, which later became the Semiconductor Division of Hoffman Electronics Corporation, El Monte, California. The first efforts were directed toward duplicating the processes and results achieved by the workers at Bell Telephone Laboratories.

Single crystals of silicon were pulled in rf-heated Czochralski crystal-growing furnaces, designed as improved versions of those in use at Bell Telephone Laboratories. DuPont high-purity silicon-crystal needles were used as raw material, resulting from the same basic process as described in Section III-B-2. Although the purity of this material had been improved through several steps of distillation of the silicon tetrachloride before its introduction into the reduction chamber, the ultimate purity of material resulting from this process was limited by the introduction of zinc from the reducing vapor and of boron and oxygen from the quartz lining of the reaction chamber.

The crystals were doped n-type by the addition of arsenic to the melt. The ingots, grown in the (100) direction, were of nearly circular cross section and therefore cut to wafers in the direction normal to the growth direction of the ingot, using diamond saw blades of approximately 0.020-in. thickness. In contrast to the cells prepared at Bell Telephone Laboratories at that time, which were of approximately 5/8 to 3/4 inch diameter, the cells prepared at National Semiconductor Products were of 1-1/8 inch diameter.

Diffusion was carried out near 1100°C, using boron tri-chloride in gaseous form as an impurity source. The structure of these early cells was similar to that of the Bell solar batteries, with both contacts on the back side of the cell, separated by a ring area, which was etched into the back of the wafer, and in which the p-n junction came to the surface of the wafer. The contacts were applied by an electroless nickel-plating process similar to that used at Bell Telephone Laboratories. The detailed specifications of this process were later found to be described in the Metal Plating Handbook.

Great difficulties were experienced in bringing the processes, particularly diffusion and contact application, under control. However, by the end of 1955, cells with efficiencies in the 6 to 8% range in earth surface sunlight were obtained. These efficiencies were comparable to those measured on cells fabricated at Bell Telephone Laboratories at that time.

The difficulties experienced with diffusion were partially associated with temperature control, control of the gas ambient, and with impurities contained in the diffusion source. While the first two problems were identified and, at least partially remedied reasonably soon, the third problem was not solved until several years later when the new source for boron tri-chloride of higher purity became available.

Early problems were also associated with achieving sufficiently high surface concentration of boron so that the series resistance of the diffused region was low enough so as not to contribute to large losses. Also, it was soon found necessary to achieve the mysterious velvet black surface appearance of the cells in order to achieve high efficiency. Achieving this surface was related to the temperature during diffusion and the gaseous ambient. Increasing the temperature for diffusion generally led to higher surface concentrations of boron, but also led to additional complications. These were found in the area of an alloy type surface layer formed in the diffusion process, which had to be removed by a subsequent chemical and mechanical process. This surface layer was always formed in the boron tri-chloride diffusion process, and would occasionally be found to be only loosely adhering to the surface of the wafers, in parts cracking and flaking off during removal of the wafers from the diffusion surface. In general, this layer would upon immersion in boiling concentrated nitric acid for a few minutes, change its appearance from a dark gray, consistent layer to a yellowish-light gray layer consisting of loose, powdery particles. After drying of the wafer, this layer could be removed by blowing or light brushing with a soft camelhair brush. Very frequently, however, it would be found that this transformation of the surface layer did not take place. Rather, a very tenaciously adhering greenish-medium gray layer would be found over part or all of the surface of the wafer. This layer was opaque to light and electrically insulating. Extensive, repeated boiling in nitric acid would occasionally help to soften this layer, and severe abrasion with stiff bristle brushes was some times partially successful. Otherwise, removal of this layer was in many instances found impossible. No chemical solution, including aqua regia was found which would dissolve this layer. Etching solutions which dissolve silicon would remove the silicon wafer (diffused layer) below this surface layer and let the surface layer float off without dissolving it. This problem of the inert surface layer has plagued silicon solar cell production for several years, and has contributed severely to low yields and high prices. In general, it was found that diffusion at lower temperatures and under careful exclusion of oxygen and humidity in the diffusion chamber would considerably reduce the problem, and some lots of boron tri-chloride would not cause this type of problem to occur, while others produced it consistently.

After diffusion, the process consisted generally in masking the entire front surface of the wafer and, on the back surface, a ring area with an internal diameter of 7/8 inch, which was an area somewhat larger than that to be covered by the ring contact (1 inch I. D.). The exposed area was then etched out to bare the base material. Subsequently, a larger part of the back surface was masked, exposing only the center 3/4 inch diameter circle for a sandblasting operation. The sandblasting abrasive was not to reach the region where the p-n junction was exposed on the backsurface of the wafer, since this would have caused shunting of the p-n junction. After the sandblasting operation, the masking was removed, the back surface of the wafer cleaned, and new masking material applied to a ring area (3/4 in I.D., 1 in. O.D.) over the region where the p-n junction reached the surface. Subsequently, the wafer was immersed in the nickel-plating solution, for deposition of the positive and negative contacts. After removal of the masking material and cleaning of the wafer surfaces, the wafer would be immersed in a liquid solder bath, in which solder would be deposited only on the metal coated surfaces of the wafer.

After experimentation with numerous waxes and cements, which were either found to be attacked by the strong, standard Si etching solutions, not to withstand the high temperatures of the plating baths, or not to be readily applicable or removable, considerable amount of experimentation was performed with specially cut sealing-gaskets of rubber, Kel-F elastomer and Teflon.

These gaskets were applied with clamp-like tools, to provide permanent and quick-change masking. Although this approach appeared attractive from the production-handling and economy viewpoint,too many difficulties were experienced with leakage of the etching solution, the sandblasting abrasive, or the plating solution underneath the masking material, causing high reject rates and destroying any potential economic advantages. The application of various die cut tape masks was experimented with next. This was found to be the most successful approach, after a Mylar base tape with a silicone adhesive was found, which would well withstand the highly acetic etching solution, the sandblasting, and highly basic, hot plating solution. A disadvantage was that the tape could not be removed by immersion in a chemical solution, but had to be peeled off manually, This would, however, leave the surface relatively clean since the adhesive would be stripped off together with the tape. This process, experimented with as early as 1955, has proven to be the most successful to the present date.

The next problem was associated with the control of the contacting method, using the electroless nickel-plating process. In order to obtain a low resistance ohmic contact to the base material, the surface of the latter had to be roughened by sandblasting. Then the wafer would be subjected to a cleaning process and immersed into the hot nickel-plating solution. With time it was found, that careful cleaning before plating and meticulous control of the composition of nickel-plating bath as well as of its temperature contributed significantly to the control of this process. The nickel-plating solution contains a large amount of ammonium hydroxide, which would rapidly evaporate from the baths which had to be maintained near 90° C. Enough ammonia had to be present in the nickel-plating bath to maintain the pH above 9.5. Ultimately it was learned that by adding an excess of ammonium hydroxide to the bath, which would cool off by this addition, and immersing the cells when the bath approached the process temperature of 90° C and the pH was still near 10.5 would lead to the most consistent production of well-adhering low-resistance contacts.

While several experiments were performed by using activators, like palladium chloride, to enhance the repeatability of the electroless nickel-plating process and the adhesion of the plated layer, it was found that, although the activators enhanced the deposition process, they by no means improved the adhesion of the plated layer. Rather, where it was found in plating without the activator, that improperly cleaned surface areas on the wafers would not be covered with nickel deposit, it was determined that such areas would be covered after plating with the use of activators, but that the deposit would not adhere to these areas on the wafer. These experiments were repeated several years, and every time the same results were observed. Therefore, as long as the nickel-plating process was used, it was generally carried out without the application of activators, but

rather with extreme care in the cleaning of the surfaces and strict control of the plating process. It may be noted with amusement, that in the early times of semiconductor process technology, difficulties were experienced based strictly on the inexperience of human operators with this technology, and on their non-realization of the critical importance of the control of these processes. Thus, it was found a few times that the contacting process led to bad results despite strict process controls. The reason was then traced to contamination of the abrasive in the sandblasting apparatus which, despite regulations to the contrary, had been used by someone to sandblast a greasy machine part or a sparkplug, and cleaning of the sandblaster and changing its abrasive eliminated the problem.

Difficulties were also experienced with the masking for the sandblasting, the etching and the plating processes. One problem experienced was that the sandblast masking would not be of sufficient adhesion to prevent the penetration of abrasive to areas which should not be sandblasted. This caused shunting across the p-n junction region where it met the surface of the wafer.

Difficulty of masking the ring areas, which frequently led to mis-alignment and contributed to low production yields and which prevented handling in an efficient production manner, led to a change in solar cell geometry. The positive contact was moved to the front surface forming a ring contact reaching to the perimeter of the cell, with the p-n junction exposed at the edge of the cell, and the negative contact covering the entire back surface. This method necessitated protection of the front surface during the sandblasting operation, and together with the back surface, during the etching operation, which now was performed after the fabrication of both contacts. For the latter it was now only necessary to protect a circular area on the face of the cell in a reasonably concentric manner with in the entire back of the cell exposed. This simplification led not only to considerably better production yields, but also an increase of the average efficiency of the cells. The reason for this increase was found in the reduction of the series resistance.

On the cells with both contacts on back surface, the negative contact occupied a circular area of 3/4 inch diameter. This means that only 44% of the exposed front surface had a negative contact area immediately behind it. The average of the charge carriers generated in the remaining 56% of the front area had to travel a distance of approximately 1/4 inch in the relatively high-resistivity base material, parallel to the wafer surface in a rather narrow channel, before reaching the contact. This contributed considerable series resistance and degraded the performance of the cells.

Immediately following the change of contact geometry on the circular cells, which was introduced at the beginning of 1956, a change in the cell geometry to a rectangular shape, with the positive contact strip extending along one long edge of the cell, was also introduced. Through these changes and improvements in the production processes, cells with average efficiencies of 6 to 8% were regularly made in 1956, with average

efficiencies of 12% being regularly obtained in the laboratory in 1958 on 1/2 x 2 cm cells and of 10% on 1 x 2 cm cells.

It may be noted, that the entire effort of development of silicon solar cells at that time was directed towards earth surface application. It was vaguely expected, that the introduction of this new energy conversion device would open up a wide range of possibilities for utilization of solar energy. The relatively low energy density of earth surface sunlight was not considered a significant hindrance, but it was realized from the outset, that the solar cell price would have to be low in order to attract large-scale applications. For this reason, emphasis was placed from the beginning on the introduction of efficient production processes and on the search for lower cost raw materials and procedures. The price of the raw silicon material at the time was in the 500 to 600 dollar range per pound in quantity procurement, and although DuPont projected potential price reductions of well over an order of magnitude for future mass production, prices in that low range have still to be realized.

The purity of the material that was available at that time, also contributed to high costs. The purity was marginal not only from the viewpoint of achieving the desirable resistivity range in the pulled crystals, but also because of frequent twinning occurring during the growth of the ingots because of excess impurities. Frequently, none or only small portions of an ingot could be used because of such twinning or of deviation from the desired resistivity range, which was already rather wide. Experiments performed as early as 1956 proved that cells prepared from wafers with one or two crystal boundaries could be as high in efficiency as single crystalline cells. However, cells containing many crystal boundaries, (crystallites under 1/4 inch in diameter) produced efficiencies of only a few percent or less. For this reason, solar cells containing one or two crystal boundaries were fabricated for some time, effecting a corresponding reduction in the ultimate cell cost, until specifications written for spacecraft application of solar cells eliminated this practice.

A multitude of potential earth surface applications were explored at that time. These included larger area solar power panels for providing electrical power for remote forestry observation stations, for providing power for remote buoys or lighthouses, for recharging flashlight batteries by mounting a strip of solar cells under a transparent cover on the outside of the flashlight housing (directed at army applications), and by incorporating a strip of solar cells under a clear plastic cover on the top of an Army helmet, to power a communications radio set contained on the inside of the helmet. Also explored were the application of solar cells to power transistorized radios and even record players, and quantities of cells were delivered rather early to be mounted on the outside the frames of spectacles which contained hearing aids.

With this activity towards finding earth surface applications for solar cells going on, it is not surprising that a small procurement by the U. S. Army Signal Corp. Research and Development Laboratory for a few hundred 1/2 x 2 cm solar cells, to provide power on the first Vanguard Space Satellite, went relatively unnoticed. Even when, in 1958, the

same group placed the first larger order, for several thousand 1 x 2 cm solar cells to provide the various interested government agencies with a small stockpile of solar cells, the huge potential for solar cells in space was hardly realized.

The early solar cells produced by Bell Laboratories and others were made by diffusing boron into n-type silicon wafers. In 1956 the first Russian publication on solar cells appeared (235). The Russian workers (Maslakovets et al.) used p-type silicon and diffused antimony into the surface to form a p-n junction. The reason for studying n-on-p cells, as stated by the authors, was twofold. The first was a matter of scientific interest as a contrast to the work which had been done by the Bell Laboratories people. The second was that the Russian manufacturing methods yielded silicon which was predominantly p-type, making this type material considerably cheaper and more readily obtainable than n-type silicon. Maslakovets et al. experimented with both single-crystal and polycrystalline cells. The polycrystalline cells were studied to evaluate the possibility of manufacturing cells with efficiencies of 1% to 2% out of relatively impure silicon ($\rho < 1$ ohm•cm). The efficiencies obtained on the polycrystalline cells were not encouraging, being less than 0.6%. The single-crystal cells were made from 5-ohm•cm material with a quoted minority carrier lifetime of 4 μsec. The maximum efficiency achieved (under a solar intensity of 91 mW•cm^{-2}) was 2.8%. This cell had an open-circuit voltage of 0.45 V and a short-circuit current density of 10 mA•cm^{-2}. This work indicated that the Russians, for economic reasons, were working with n-on-p cells long before the rest of the world realized the radiation-resistant virtues of this particular structure.

At the conference on photoelectric effects held in Kiev in 1957 two papers dealing with the Russian work on silicon solar cells were presented. The first, by Tuchkevich and Chebnokov (236), gave a few of the details concerning the construction of the n-on-p cells. The junctions were diffused to a depth of 15 to 20 μm and the cell was then etched to give a junction depth of 5 to 10 μm. Soldered contacts were used and the series resistance due to these contacts was approximately 2 ohms. Under a solar intensity of 80 mW•cm^{-2} one of the cells, whose I-V characteristic was shown, had an efficiency of 8%. This cell had a short-circuit current density of 22 mA•cm^{-2} and an open-circuit voltage of about 0.47 V. Another of the cells, measured under a 2700° color temperature tungsten lamp, had an efficiency of 9.5% at 100 mW•cm^{-2} intensity and 10% at an intensity of 120 mW•cm^{-2}. Measurements of minority-carrier lifetimes in the n- and p-regions gave lifetimes of 1 to 100 μsec for electrons in the p-type material and less than 1 μsec for holes in the n-type material. Better efficiencies were anticipated if recombination losses and the series resistance could be reduced. The temperature dependence of the open-circuit voltage was found to be linear, with a slope of 2.57 x 10^{-3} V•°C^{-1}. Extrapolation of the temperature dependence data gave a value of 1.1 eV for the gap energy. Measurements of the open-circuit voltage as a function of short-circuit current (light intensity) indicated that the ideal diode equation was not obeyed and a constant term had to be introduced in the exponential to account for this. The plots of open-circuit voltage versus the logarithm of short-circuit current showed three distinct linear segments. The first and third segments of the room-temperature plot, corresponding to low and high intensity

respectively, required a constant in the exponential (A) lying between 1.0 and 1.1. The second segment had A between 2.1 and 2.2. Several other cells had A values of 6 to 7 for the second segment, while the A values of the other two segments did not exceed 2. At liquid-nitrogen temperature the values of A increased drastically. For the first and third segments of the curve, A values ranged from 8 to 15, while the third segment had values of A between 17 and 33. Vavilov et al., in the other paper on silicon cells given at the conference (237), determined the value of A from dark I-V measurements. They obtained a value of A = 1.0 for zero bias and $1.35 < A < 1.4$ and constant for a finite bias. This paper also showed spectral response data on cells with junction depths of 2, 9, and 15 μm. This was apparently part of an attempt to optimize the junction depth. It was noted that the cells were made with an antireflection coating which was a natural result of the diffusion process rather than a separately deposited film. Removal of the film caused a decrease of about 21% in short-circuit current. The presence or absence of the antireflecting film had no appreciable effect on the surface recombination velocity according to the authors. The idea that the junction should be extremely close to the surface appears not to have been fully appreciated, since no cells were made with junctions less than 2 μm deep. Some data on solar cell performance under high illumination intensity were shown. The cell tested had an efficiency of 4.8% under normal earth solar intensity. This dropped to 2.1% at an intensity seven times the normal solar intensity. The temperature of the cells was maintained at 25°C for these measurements.

By 1958 the maximum observed efficiency of the silicon solar cell had increased to 14%. Unfortunately, the details of the work resulting in this increase do not appear in the literature of the time. A sales pamphlet written by N. J. Reigner of the Semiconductor Division of the Hoffman Electronics Corp. in April 1958 attributed the high efficiency to improved production techniques. The pamphlet gave information and specifications on a 5-W solar cell module produced by Hoffman for terrestrial use. Any number of the units could be connected together to provide the required amount of power for a given application. Hoffman began manufacturing silicon solar cells in 1955 shortly after the announcement of the development of the solar battery by Bell Laboratories. The module consisted of 144 circular cells (approximately 1 in. diameter) mounted on an aluminum tray with a glass cover and was designed to deliver 5 W of power under an illumination of one Langley. Prince and Wolf (194) also of Hoffman then, gave a figure of 14% for the maximum observed efficiency in a publication discussing silicon photovoltaic devices. Three types of photovoltaic devices were discussed: the photodiode, the solar cell, and the low-level solar cell. The general device characteristics were developed through the use of equivalent-circuit models. Some of the theoretical and experimental work necessary in designing the devices was also described. Three design considerations for the solar cell were discussed. These were reflection losses at the surface, generation of electron-hole pairs, and the diffusion and collection of the minority carriers. Measurements indicated that the reflection losses of the cells (apparently without antireflection coatings) did not exceed 6% for most of the wavelength range of interest, and it was concluded that no significant improvement could be expected in this direction. Likewise, the fact that unity quantum efficiency existed for electron-

phonon interactions in silicon precluded any gains in this direction. The investigation of minority-carrier diffusion and collection led to several interesting results. First, it was concluded that most of the contribution of minority carriers came from the base or n-region in the long wavelength response. This confirmed the experimental finding that long minority-carrier lifetimes in the base were necessary for good collection efficiencies. Secondly, the need to make the p-layer as thin as possible was confirmed. Finally, the surface recombination velocity was found to have very little effect on the collection efficiency. Figure 44 is a silicon solar cell as shown by Prince and Wolf.

The low-level solar cell was designed specifically to operate at low light intensities (less than 1 foot-candle). The only important design change was a widening of the junction region. This was necessary to reduce the internal field emission, associated with narrow junctions, which lowered the impedance of the junction at small biases (low level illumination) and hence reduced the efficiency.

Some possible applications for the solar cell were also discussed in this paper. The applications fell into three categories. The first was as energy conversion devices like the 5-W module discussed above. The next application was that of a control device operating a relay or acting as the input for a transistor amplifier. The other suggested application was as a light meter, either linear or logarithmic depending on the loading condition.

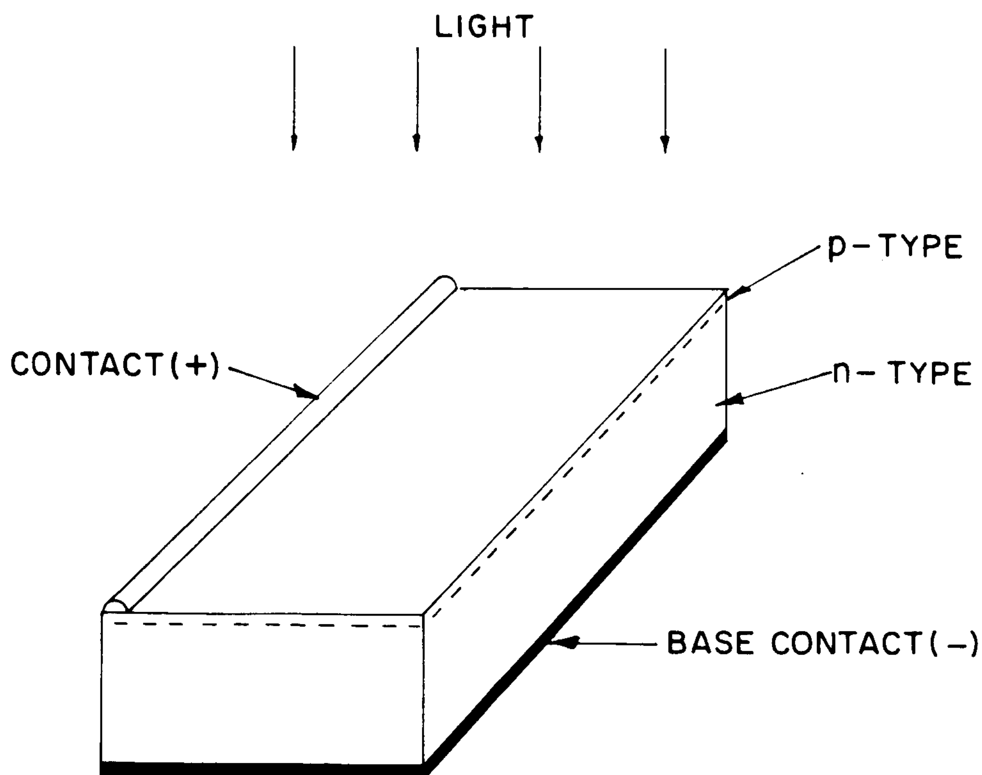

Figure 44. Silicon solar cell circa 1958, after Prince and Wolf

The first space use of solar cells occurred in 1958 with the launching of Vanguard I on March 17. Vanguard used an array of 108 2-cm x 1/2-cm cells as a secondary power source. The results of some tests which were designed to evaluate silicon solar cells for possible space use were given in a Lockheed Missile System Division report written by Brown et al. in June 1958 (238). Factors evaluated included spectral response, thermal effects, thermal shock, aging, and the effects of meteorite puncture. The spectral response apparatus used was unique in that the light source used was the sun. A solar tracking system, mounted on the roof of the laboratory building, reflected a column of sunlight down a vertical shaft into the laboratory where it was focused onto the input of a monochromator. The cells tested (obtained from Hoffman) had an area of 2 cm^2 and an average efficiency of about 10%. The temperature dependence of the cell characteristics was as expected; however, 75% of the cells suffered severe permanent damage under the thermal shock test which consisted of immersion in liquid nitrogen. The meteorite puncture was simulated by drilling with a 0.12-in.-diameter diamond drill and by electric arc discharge. In general, a single puncture reduced the power output by 10 to 40%. Apparently the punctures resulted in shorting of the junction.

In the same year Loferski and Rappaport published an experimental study of the effect of radiation damage on silicon solar cells (239). The study was intended to give an estimate of the lifetime of a solar power source on the International Geophysical Year earth satellite. The cells were irradiated with electrons, protons, alpha particles, x-rays, and ultraviolet radiation, the last two having no measurable effect. As a result of the tests, a drop of 25% in power output was estimated to require an exposure time under the assumed conditions of 10^5 years.

Rappaport (240) quoted a figure of 7 to 10% for the average efficiency of production silicon cells around 1958. He estimated the cost for a 1-kW solar cell power supply at $200,000, the major cost being that of producing the single-crystal silicon wafers. The estimated weight of the power supply was 20 pounds. Much of Rappaport's discussion dealt with materials alternative to silicon.

No dramatic increase in efficiency was reported in 1959, although some improvements were made. Improvements in the growth techniques result in reduced frequency of dislocations and other imperfections, in the silicon crystals as reported by H. J. Yearian of the Purdue Research Foundation (241). Working under a Signal Corps contract Yearian was able to reduce the dislocation density of grown silicon single crystals to less than 10 cm^{-2}. This was accomplished primarily by reducing the contamination of the gas flowing over the crucible in which the silicon was grown by isolating the gas from the heater. This also resulted in a reduced occurrence of twinning.

The most important improvement occurring in 1959 was the introduction of an alloyed aluminum contact for the p-layer. By slow heating and cooling of the aluminum a silicon-aluminum alloy was formed which gave a rectifying contact with n-type silicon and an intimate ohmic contact with the boron-diffused p-layer. The contact had a very low series resistance, resulting in an improved conversion efficiency (242). The same

alloy, when formed by a fast heating and cooling cycle, formed a contact that was ohmic with respect to n-type material, with a contact resistance (0.1 to 0.2 ohm for a 2-cm^2 area) comparable to that of the plated contacts of the time (194). The alloyed contact for the p-layer was developed by the International Rectifier Corporation under a Signal Corps contract. A considerable portion of the support for solar cell work during the middle and late 1950's was supplied by the Signal Corps.

The two major commercial suppliers of silicon solar cells in 1959 were Hoffman Electronics Corp. and International Rectifier Corp. J. Kalman of Hoffman published a summary of the characteristics of the commercially available silicon cells (244). This summary is reproduced in Table II.

A variety of cell sizes was available, ranging from 1/8 cm^2 to 4-1/2 cm^2. The highest short-circuit current density was 30 $mA \cdot cm^{-2}$, while the open-circuit voltages ranged from 0.48 to 0.55 V, with all of the Hoffman cells around 0.55. The efficiencies ranged from 4% to greater than 9%. The high short-circuit current densities might seem somewhat surprising since no attempt was made to put antireflection coatings on the cells; however, during the cell fabrication process a thin coating of silicon oxide was suspected to form naturally and probably cause some reduction in reflection losses. One would suspect that these cells were somewhat series-resistance limited because no grid lines were used.

The use of grid lines to reduce series resistance appears to have become widespread around 1960, and various grid geometries are illustrated in Figure 45, with results in Figure 46. All of the major manufacturers reported improved cell efficiency due to this innovation (245, 246). Dale and Rudenberg of Transitron Electronic Corp. reported (246) improving the average efficiency of laboratory-produced cells from 8 - 10% to 12 - 15%. This was accomplished through the use of a silicon monoxide antireflection coating to reduce reflection losses and the introduction of an aluminum alloy grid structure to reduce the series resistance. These changes resulted in an increase of the maximum power voltage by 0.05 V, and reduced reflection losses to 2%. Investigators at Hoffman Electronics reported average efficiencies between 12% and 13% for experimental runs of gridded cells (247). International Rectifier Corp. apparently introduced a peripheral electroded cell as well as the grid line structure used by most other manufacturers (248, 249). The average efficiency of these production line cells was quoted as 10 to 12% with a maximum of 14%. Apparently as an advertising gimmick, International Rectifier produced a panel ("The Solar King") consisting of 10,640 cells having efficiencies of 4 to 5% and mounted it on the roof of an electric car (1912 Electromobile). The array was said to be capable of charging the car's batteries under "optimum conditions."

The use of optical coatings, both to reduce relfection losses and to control cell temperature, became a matter of increasing concern in 1960. As was mentioned earlier a surface coating of silicon monoxide (or dioxide) formed naturally during the diffusion of the junction of the p-on-n cells. This layer reduced reflection losses considerably. Dale and Rudenberg (246) pointed out the advantages of being able to control the diffusion process

TABLE II. CHARACTERISTICS OF COMMERCIAL SILICON CELLS (1959) AFTER J. KALMAN

Manufacturer	Dimensions (cm)	Active Area (cm^2)	Output with Matched Load at 10,000 foot-candles			Avg. Conversion Efficiency (%)	Short-Circuit Current (mA)	Open-Circuit Voltage (mV)
			(mV)	(mA)	(mW)			
Hoffman Electronics								
2A	2.86 dia.	4.75	400	85	34	5-8.5[a]	130	550
200A	1/4 of 2A	1.20	400	21	8.4	5-8.5[a]	32	550
220C	2 x 2	3.8	400	65	26	5-8.5[a]	100	550
120C	1 x 2	1.8	400	34	13.6	> 9	40	550
110C	1 x 1	0.9	400	17	6.8	5-8.5[a]	20	550
52C	0.5 x 2	0.8	400	15	6.0	5-8.5[a]	20	550
51C	0.5 x 1	0.4	400	7.5	3.0	5-8.5[a]	10	550
55C	0.5 x 0.5	0.2	400	3.8	1.5	5-8.5[a]	5	550
58C	0.5 x 0.25	0.1	400	1.8	0.72	5-8.5[a]	3	550
Intern'l Rectifier			Output with Incident Energy of 100 mW/cm^9 (1 sun)[b]					
S1020	1 x 2	1.75	350-400	17.5	7	4	35	480
S1020A	1 x 2	1.75	400	26	10.5	6	40	500
S1020B	1 x 2	1.75	400	35	14	8	48	550
S0520	0.5 x 2	0.75	350-400	7.5	3	4	16	480
S0520A	0.5 x 2	0.75	400	11.2	4.5	6	18	500
S0520B	0.5 x 2	0.75	400	15	6	8	22	550
S510	0.5 x 1	0.37	350-400	3.8	1.5	4	8	480
S510A	0.5 x 1	0.37	400	5.6	2.25	6	9	500
S510B	0.5 x 1	0.37	400	7.5	3	8	11	550

(a) Average range. (b) 10,000 foot-candles ≡ 1 $kW \cdot m^{-2}$.

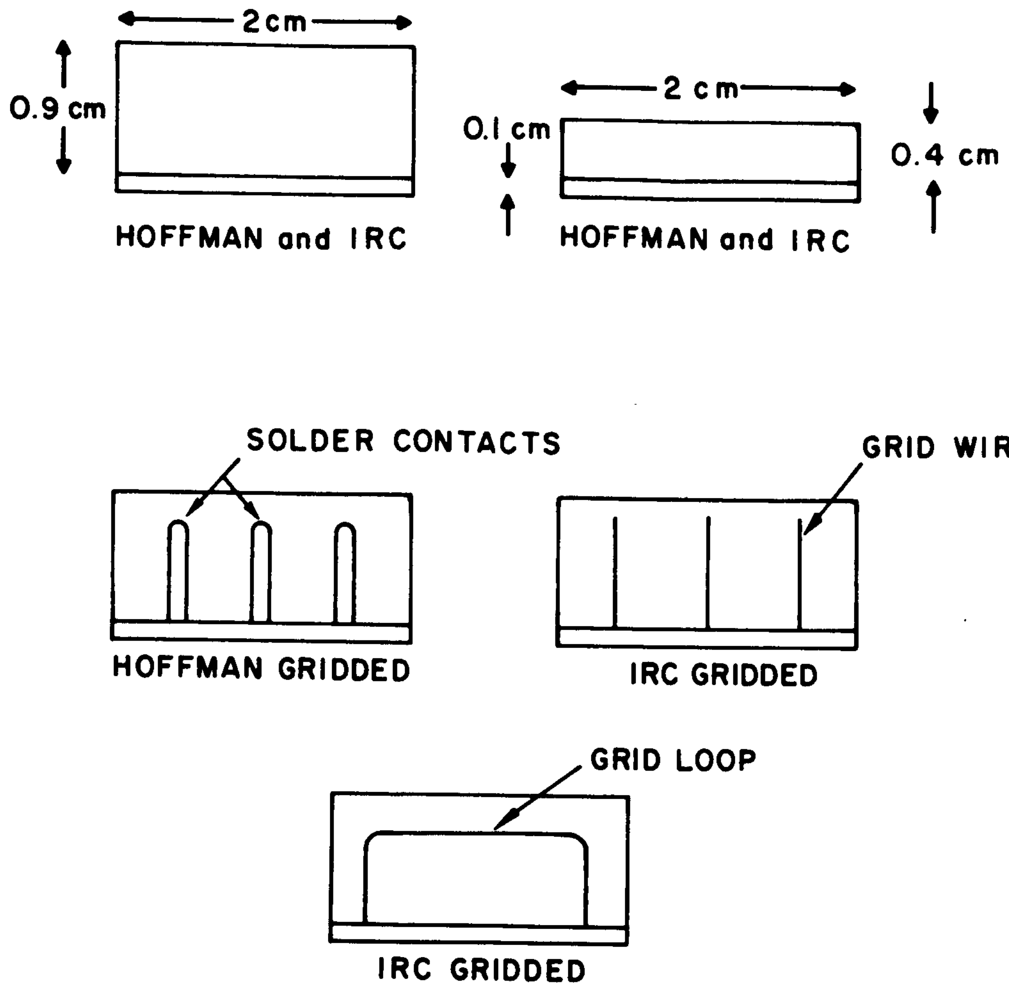

Figure 45. Popular cell types circa 1960

and the optical properties of the surface separately. They were able to accomplish this by the evaporation of a thin film of silicon monoxide. The Russians had also realized the value of antireflection coatings (250) for their n-on-p cells, although they did not use evaporated films. They settled on silicon dioxide as a coating because of its stability. After attempting a chemical deposition technique they decided on a straightforward oxidation of the silicon. The chemical technique left undesirable impurities on the surface of the silicon wafer. Improvements of 20 to 25% in short-circuit current through the use of the silicon dioxide coating were reported. The details of the oxidation process were not given; however, the process was apparently thermal and, hence, not amenable to separate control of the optical properties and the diffusion process. No efficiencies were given for the cells used in these experiments.

The use of coated glasses and directly applied coatings to control cell temperature were discussed by Escoffery and Luft (251), but this had little bearing on the evaluation of the silicon solar cell per se and will not be discussed in this section. The interest in cell temperature control had been stimulated by the use of solar cells in satellites, an

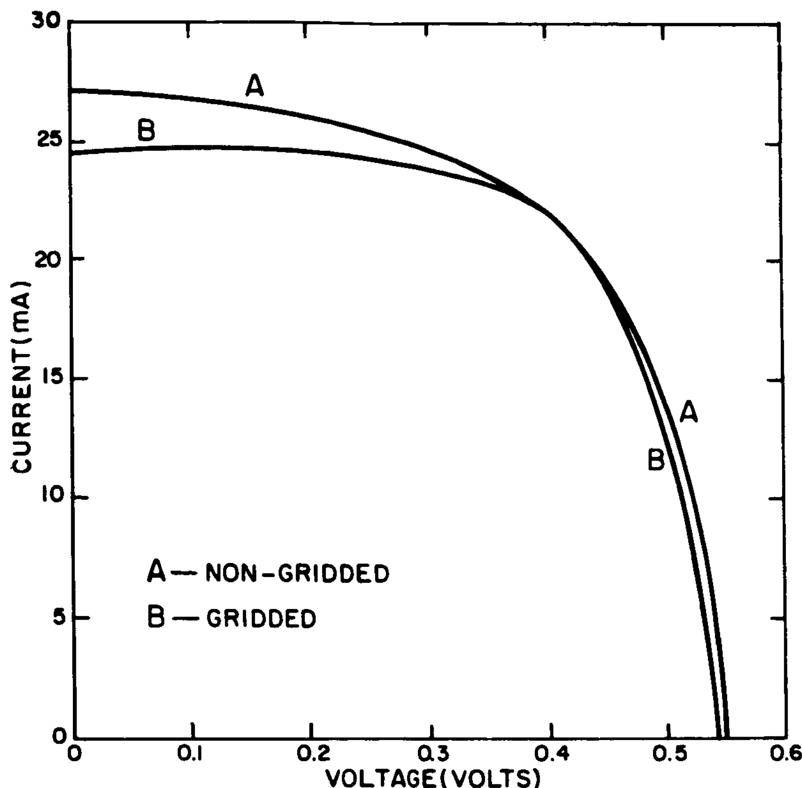

Figure 46. Characteristics of typical gridded and nongridded silicon cells of equal efficiency; after Evans and Menetrey

application which also aroused interest in radiation damage. A few authors showed data on radiation damage in 1960. Dale and Rudenberg(246) reported that an integrated flux of 5 x 10^{13} 2-MeV electrons cm^{-2} reduced the efficiency of an 8.4% efficient silicon cell to an efficiency of 5.5%. The reduction resulted primarily from a reduction of the base (n-type) minority-carrier lifetime from 3 μ sec to 0.02 μsec. A more comprehensive set of data was given in Reference (196) which provided a summary of the findings of several investigators (Lockheed, G. E., S. T. L., and RCA). Table III summarizes the high-energy particle densities in the various Van Allen belts as recorded by various satellites (252) at the time. Table IV summarizes the results of the investigations of several of the above companies.

An important conclusion of Table III was that the lower-energy protons might possibly cause more damage to the solar cell than the high-energy protons.

Reference (245) also provides a good survey of the general characteristics of the commercially available cells in 1960. Both Hoffman and I. R. C. are quoted as producing 13% efficient cells in quantity.

The introduction of grid stripes removed the requirement that the diffused layer must be made thick to reduce series resistance losses. The allowed the separate optimization

TABLE III. TYPE, ENERGIES, AND FLUX OF CHARGED PARTICLES

	Location	Energy	Flux
Electrons	Inner belt	> 20 keV	10^9 $cm^2 \cdot sec^{-1}$ $steradian^{-1}$
	Inner belt	> 600 keV	10^7 $cm^2 \cdot sec^{-1}$ $steradian^{-1}$
	Outer belt	> 20 keV	10^{11} $cm^{-2} \cdot sec^{-1}$ "
	Outer belt	> 200 keV	10^8 $cm^{-2} \cdot sec^{-1}$ "
	Outer belt	> 2.5 MeV	10^6 $cm^{-2} \cdot sec^{-1}$ "
Protons	Inner belt	> 40 MeV	10^4 $cm^{-2} \cdot sec^{-1}$ "
	Outer belt	> 60 MeV	10^2 $cm^{-2} \cdot sec^{-1}$ "

TABLE IV. EXPERIMENTAL DATA REDUCTION OF SOLAR CELL EFFICIENCY DUE TO PARTICLE BOMBARDMENT

Source	Particle	Energy (MeV)	Flux (particles cm^{-2})	Power Reduction (%)
Lockheed	Proton	3	5×10^9	25
		12	2×10^{11}	25
		12	10	50
STL	Electron	0.5	$2\text{-}8 \times 10^{13}$	25
RCA	Proton	17.6	10^{15}	50
	Electron	1.7	5×10^{14}	50

of junction depth to provide a better match to the solar spectrum. Several experimental and theoretical studies of the variation of the spectral response of the cells with junction depth were published during the period 1960-1961 (253, 254). These studies showed that moving the junction closer to the surface improved the spectral response of the cell in the blue region and hence gave higher efficiencies. Cells with grid stripes and an optimized junction depth were expected to give a short-circuit current 10% higher than that of the ungridded cells under outer space sunlight conditions (254).

Another advance, originating around 1959, was an increase in the minority-carrier lifetime in the base region resulting in an increase in the long wavelength response (255). The increase in minority-carrier lifetime was a result of the availability of purer materials and improved crystal growing and diffusion techniques. The changes in lifetime in the base region initially caused some confusion in the measurement of cell efficiencies. The cells appeared to be more efficient than was actually the case when tested under tungsten light source due to the infrared content of the tungsten light. The combination of the grid contacts, improved base region lifetime, and optimized junction depth resulted in the considerable improvement in average cell efficiencies experienced in the period 1959-1961.

The improvements in cell efficiency resulted in a cost reduction on a dollars per watt basis. An additional improvement in cell cost during the period 1960-1961 resulted from a factor of two drop in the cost of silicon as reported by Prince (256) who gave a cost figure of 100 to 300 dollars per watt for cells in 1961.

The radiation damage suffered by cells exposed to Van Allen Belt radiation continued to be a matter of serious concern. Several government-sponsored projects at that time had as part of their mission the investigation of radiation effects and possible ways of reducing losses caused by them. An important development in this area occurred in mid-1960 with the discovery that n-on-c cells were considerably more radiation-resistant than p on n cells, by workers at the RCA Laboratories (257, 258). The initial experiments showed that the n-on-p cells required 7.6 times as many particles (1.5-MeV protons) to produce a 25% decrease in efficiency as did a p-on-n cell of the same efficiency. Later investigations (259,260) revealed a similar resistance to electron irradiaton. There was some concern at the time that the n-on-p cells might be inherently less efficient than the p-on-n cells; however, this fear has proven groundless. Several French publications on silicon solar cells appeared in 1961 (261-266). Most of these described laboratory studies intended to produce high-efficiency cells. Most of the French investigators had settled on phosphorus-diffused n-on-p cells as holding the greatest potential for achieving high efficiencies (263-265). Two reasons were given for this. First, it was felt that the phosphorus-diffusion process (using P_2O_5) was much easier and gave much more reproducible results than the boron trichloride process. Second, it was possible to get the high impurity concentrations necessary for reducing series resistance losses at much lower temperatures with the phosphorus-diffusion process. This would aid in reducing the drop in minority-carrier lifetime observed after heating. The phosphorus diffusion resulted in a film being formed on the surface of the cell, the film being a mixture of silicon dioxide and phosphorus anhydride. This layer was etched and oxidized several times until the short-circuit current was optimized. Efficiencies of 14% were reported. Salles (264) discussed some of the problems of carrying cell fabrication from a laboratory to a production process. Problems of matching and interconnecting cells for arrays were also discussed by Salles.

The status of solar cell development at the end of 1961 was summarized by Iles (267). Most cells were made from Czochralski-grown silicon with a resistivity of around 1 ohm·cm. Grade IV (solar grade) silicon was used since the small gain obtained by

using better grade material was much less than the variation introduced by changes in the quality of the crystal-growing procedure. Different crystallographic orientations were found to have little effect on cell output. (100) grown crystals were normally used because their shape gave less waste in cutting. The junctions were formed by the boron-diffusion process and were, in general, less than 2 μm deep. The heating and cooling during diffusion degraded the bulk minority-carrier lifetime by a factor of 2 to 3 which was felt to be tolerable. Cells with junction depths greater than 1 μm used only a judiciously placed single top contact while those with junction depths less than 1 μm used any of a variety of grid line configurations. These included 3-line and 5-line patterns running parallel to either the short or the long dimension of the cell. Some of these had both main contacts on the bottom of the cell with the grid wrapping around the edge. Most cells had junction depths of 0.4 to 1.0 μm with a diffused layer depletion region width of 0.03 μm. Average resistivity of the diffused layer was 0.014 ohm·cm (15 to 25 ohm·square^{-1}) with a maximum surface impurity concentration of 5 x 10^{20} cm^{-3}. Bulk minority-carrier lifetime for the cells was in the 3 to 10-μsec range while diffused layer lifetime was of the order of 10^{-9} to 10^{-10} sec. At low values of current density the cells did not obey Shockley's diffusion theory or the space charge recombination theory of Sah et al. (see Section IV-A-1). The gettering effect experiments of Hooper and Queisser (268) in which glassy oxide layers were used to getter metallic impurities in silicon solar cells indicated that these materials were at least partially responsible for the anomalous behavior of the junctions. They suggested that the use of cleaner material might result in higher efficiency cells. However, it was suspected by other investigators that, for cells operating under normal sunlight, the junction does behave according to diffusion theory. A good percentage of the experimental work during 1960-61 was aimed at improving cost, reducing weight, and increasing cell area. Projects along these lines included work on dendritic cells, epitaxial silicon, and arrays of silicon spheres imbedded in plastic. These are discussed in detail later in this section. Work on efficiency improvement included studies of stacked cell assemblies and beam-splitting arrangements to break up the solar spectrum and direct the appropriate portions to cells with differing bandgaps. These are also discussed elsewhere. The efficiencies of the best cells were around 15%. Clear-cut ideas for improving individual cell performance appear to be lacking although the work of Shockley and Queisser aroused some interest in the elimination of unwanted (i.e., nonradiative) recombinations.

New developments in the field of radiation damage in 1961 included the discovery by Vavilov et al. (269) that lithium atoms interact with radiation defects in silicon so as to neutralize the damage site as a trapping level. Tests were made on lithium-doped silicon samples which had been irradiated with 0.9-MeV electrons. The samples contained considerable amounts of oxygen. Electrical measurements on the samples indicated that some of the deep levels introduced by the electron bombardment disappeared when they were heated to 330 to 350°K. The disappearance was accompanied by a sharp decrease in carrier density. Vavilov and his co-workers concluded that the lithium ions diffused rapidly through the lattice at the higher temperature until they encountered a lattice defect where they tended to become localized. A localized ion would then capture an electron from the conduction band, thus neutralizing the site and causing a decrease in the carrier density. The idea that this type of interaction might provide a means of increasing the effective radiation resistance of less oxygen-rich material does not appear, although the

effects of oxygen were apparently understood. A more detailed account of these and related experiments appear the following year (1962) (270). At about this time some investigators at RCA, working under government contract, began to look into the possibility of producing radiation-resistant devices, including solar cells, through the use of lithum doping (271).

An interesting publication in 1963 by Smith et al. (272) described the design and fabrication of the power supply for the Telstar satellite. The Bell group decided to design and produce their own cells (through the Western Electric Co.) rather than buy them from some of the other commercial suppliers. The primary reason for this was a concern for the effects of Van Allen Belt radiation on the power supply. The superior radiation resistant qualities of n-on-p cells over p-on-n cells had been firmly established; however, the n-on-p cells were not in production in commercial quantities at the time that developmental work for Telstar was begun. Preliminary studies indicated that a suitable n-on-p cell could be nearly as economical in quantity fabrication as p-on-n cells of comparable initial performance in space and a developmental program was initiated late in 1960. The work was described in considerable detail by Smith et al. The final cell had the following characteristics:

Base material—p-type, 1 ohm·cm, 15-mil-thick wafer, area 1 x 2 cm.

Contacts—5 grid lines + busbar, evaporated titanium silver with solder dip finish, width of grid 0.006 in.

Antireflection Coating—evaporated SiO, thickness - 800Å.

Efficiencies for a group of 10,000 cells ranged from 9.25% to 12.0% with an average of approximately 10.75%. The cells were designed to be sensitive in the blue-green region. No effort was made to obtain good wavelength response (such as requiring high lifetime in the starting material) because the response in this region is severely degraded by radiation. The paper gave a complete description of the assembly and testing of the power supply.

Developments in 1964 included work on wrap-around contact cells (273). A number of wrap-around contact cells were fabricated by workers at RCA and assembled into 10-cell modules similar to those used on Nimbus satellites. The cells give a 5% increase in active area over normal cells. The modules showed a 4% increase in power output over that of the Nimbus modules.

The status of solar cell manufacture in the United States as of early 1964 was summarized by V. Magee of the British firm of Ferranti Ltd. in a report covering his tour of American industry (274). The standard cell was a phosphorus-diffused n-on-p cell using either 10 ohm·cm (for radiation resistance) or 1 ohm·cm (higher voltage, and better load characteristic) base material depending on the power supply specification. Optimum junction depth was felt to be 0.3 to 0.5 μm by most manufacturers. All but one of the manufacturers checked used an evaporated layer of silicon monoxide or

dioxide (thickness approx. 900 Å) for an antireflection coating. The other manufacturer used the technique of building in the oxide layer as part of the diffusion process, a technique used by Ferranti also. There were two common approaches to the contacting problem. The first was based on the evaporation of two metals followed by sintering. In this process a thin layer of either chromium or titanium was evaporated onto the silicon active surface. This was followed by a much thicker layer of silver. The surface was then sintered at low temperature to improve contact strength and provide low resistance. The other approach was to deposit first a layer of gold by evaporation or chemical deposition and then deposit nickel over it by an electroless technique. This second approach was considerably cheaper, but there was some difficulty in ensuring a sufficiently low contact resistance. Samples of production cells were obtained from both Hoffman and Heliotek. These cells were believed to be representative of the best performance levels obtained by the American manufacturers at the time. The efficiencies of Hoffman's 1 ohm•cm cells ranged from 10.7% to 10.9% while those of the 10-ohm•cm cells were between 10.4% and 11.6%. Heliotek supplied only 10-ohm•cm cells, which had efficiencies of 11.2% to 11.4%.

Another report by Ferranti (278), published in 1965, indicated the status of British solar cell manufacture. The manufacturing procedures were essentially identical with those of most American manufacturers as outlined above with the exception of the application of the grid contact and the formation of the antireflection coating. The antireflection coating was formed simultaneously with the junction diffusion by oxidation of the surface as above. The grids were applied by a combination of chemical plating and photolithographic techniques. A layer of electroless nickel was first deposited on the surface of the silicon. This was built up with a layer of copper and finally a layer of gold to prevent tarnishing. No solder dipping techniques were used. The cells were comparable to those of American manufacturers and averaged around 10.5% efficiency for air mass zero (space) conditions. Cost figures for the British cells were given by Butcher et al (278), also of Ferranti. The costs ranged from \$300,000 kW^{-1} to \$110,000 kW^{-1} for cell thicknesses between 10^{-2} cm and 4 x 10^{-2} cm, respectively. These figures correspond to weight-to-power ratios of 2.07 $kg \cdot kW^{-1}$ and 7.4 $kg \cdot kW^{-1}$. The cost of American cells around the same period was given by Rappaport as \$100,000 kW^{-1} (277).

No major improvements in silicon solar cell efficiency have been reported after 1961 or so. Yields and, consequently, average efficiencies, have improved somewhat but still remain well below the maximum. Considerable effort has been expended on radiation resistance and the reduction of cell cost and weight during the 1960's. Thinner cells (225,275), drift field cells (230), "blue shifted" cells (280), and dendritic cells (277) were studied both theoretically and experimentally by various investigators along with numerous other innovations. This work was paralleled by the increasing developmental work on thin-film cells and compound semiconductor cells which had potential cost, weight, and radiation-resistance advantages.

The most important recent development in solar cells has been the development of the lithium-diffused radiation-resistant cell. Work on this originated in 1962 and has been

supported by a number of NASA contracts (279-81). The cells have been shown to have a definite ability to recover from radiation damage (282). There is, however, a considerable lack of understanding regarding the nature of the radiation-induced defects in lithium-doped silicon and the annealing process. Figure 47 shows a comparison between changes in diffusion length for a lithium-doped cell, and a control cell made from the same silicon material as the lithium-doped cell under 1-MeV electron bombardment. Irradiation was stopped periodically and the cells were allowed to anneal at room temperature for the times indicated. The generally held view is that the damage site involves a pairing between a defect and a lithium ion. The recovery mechanism then involves the diffusion of another lithium ion to the damage site and its pairing with the lithium-defect complex. It has been established that the speed and extent of recovery are strongly dependent on the amount of free or unpaired lithium. There is some evidence that a cell structure which incorporates a diffused phosphorus layer next to the junction (i.e., between lithium-diffused region and p-region) to give a three-layered p/n/n structure gives a device with improved radiation resistance without sacrificing the ability to recover. While high-efficiency (13 to 14%) lithium doped cells have been produced, the lithium-doped cells, on the average, appear to have lower efficiencies than comparable cells without lithium doping. The properties and possibilities of the lithium cells are receiving considerable attention at this time.

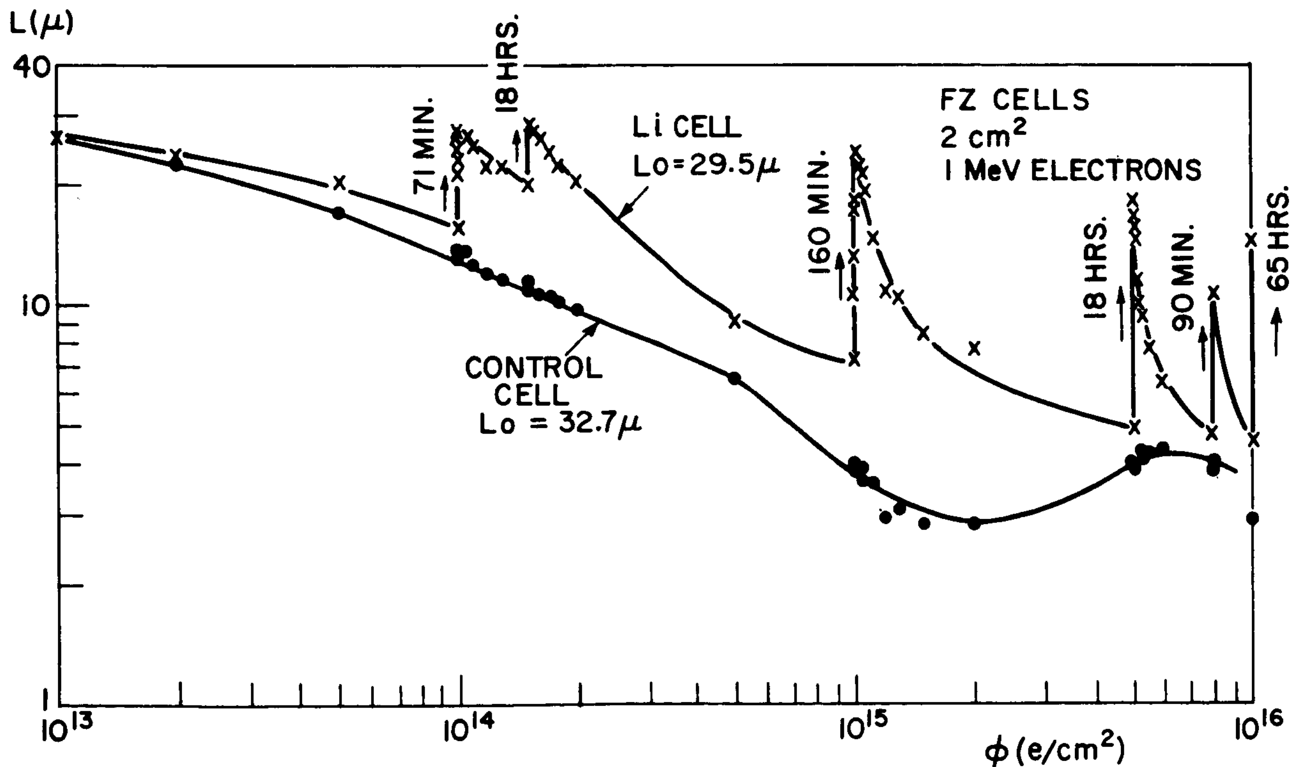

Figure 47. Comparison of the performance of n/p and Li-doped silicon cells under irradiation

3. A Brief History of Various Unsuccessful or Incomplete Attempts at Cell Improvement

a. Cost Reduction: The earliest attempts at effecting a large cost saving in the production of silicon solar cells were the attempts to introduce polycrystalline material. Russian investigators appear to have pursued this approach as an alternative during the earliest phases of their work (235). The earliest polycrystalline cells had efficiencies which were an order of magnitude or more below those of the single-crystal cells of the time and therefore were felt to be not promising. Several years after the initial work the Russians reported much better efficiencies for the polycrystalline cells (283). Efficiencies of 4 to 8% (on an active area basis) were reported for cells measured under a solar intensity of 75 $mW \cdot cm^{-2}$. The cells which had these efficiencies made use of a mesh-type grid contact to eliminate the resistance due to the grain boundaries. Approximately 30% of the total surface area of the cells was occupied by contacts. Gliberman et al. estimated that the use of polycrystalline material would reduce the cost of a solar cell power supply by a factor of 2 to 3.

A more recent evaluation of the possibilities of polycrystalline silicon for solar cells was given by Berman and Ralph (284). The cells produced in these experiments also made use of a mesh-type grid initially; however, tests indicated that the standard 5-line grid pattern used on single-crystal cells was also near the optimum for the polycrystalline cells. Both p-on-n and n-on-p polycrystalline cells were investigated. The spectral response of the p-on-n polycrystalline cells peaked at about 0.73 μm compared with about 0.85 μm for single-crystal cells. The shift to shorter wavelengths was attributed to a reduced minority-carrier lifetime in the base region due to recombination centers associated with the grain boundaries. In general, the p/n polycrystalline cells were more efficient than the n/p polycrystalline cells. The best n/p cell efficiency as measured under sunlight (~ 100 mW at Table Mountain, Calif.) was approximately 8%, while several p/n cells measured under the same conditions had efficiencies exceeding 11%.

The cost analysis of polycrystalline cell production indicated that further developmental work was necessary to improve the yields to the point where the cells would be competitive with single-crystal cells before any cost saving could be realized. The cost of single-crystal material (1964) was about \$0.40 per gram, while the cost of polycrystalline material was about \$0.11 per gram. The slightly higher breakage rate experienced with the polycrystalline material necessitated an adjustment in the average number of grams of material needed to produce a cell. This adjustment resulted in an average material cost per cell of \$0.80 for single crystal and \$0.28 for polycrystal. The manufacturing cost for both types of cell was estimated to be approximately \$2.30 per cell. When it was assumed that the yields for both types of cells were 100% (i.e., the efficiencies are high enough for all finished cells to be usable) a simple calculation showed that a 17% decrease in cost could be realized by using the polycrystalline material. This figure would apply in any case where the yield distributions of the two types of cells were identical. In reality, one had to assume some minimum acceptable efficiency for the cells and then make the comparison. When a minimum efficiency of 10% was assumed, calculations showed that for the p/n configuration 80% of the polycrystalline

cells would have to equal or exceed the 10% figure in order for the cell cost to just equal that of the single-crystal cells (99% of single-crystal p/n cells were > 10%). For the n/p cells the breakeven point was a yield of 77% with efficiencies greater than or equal to 10%. The p/n polycrystalline cells averaged around 8 to 10% in efficiency and the n/p cells somewhat lower. No significant cost advantage could be expected until these efficiencies could be raised to the 10 to 11% range. This analysis was concerned only with reducing the materials cost and did not consider any possible modifications of the cell manufacturing process which might provide further cost savings in the production of polycrystalline cells.

One technique with potential for reducing production costs which has received considerable attention is the use of larger area cells. The philosophy behind this approach is simply the reduction of handling costs per square cm. of cell. A number of interesting ideas for the production of large-area cells have been explored. The most straightforward approach is simply to grow larger (wider) silicon crystals. Cherry (285) reported the growth of crystals with diameters of 6 to 8 inches. A wafer cut from such a crystal would have an area of 48 square inches. Not surprisingly, the breakage during handling of these wafers was extremely high. It was anticipated that special tooling might alleviate this; however, no further reports on single-crystal cells made from wafers of this area appear in the literature. The same approach, with more reasonable dimensions, was explored by Prince (286). He reported that techniques for the growth of large crystals and for the fabrication of solar cells with areas of 3 in. from them had been developed to the point of manufacturing feasibility. Efficiencies greater than 12% were measured on some of the cells. When weighing the desirability of fabricating large-area cells in this fashion it must be remembered that the cutting losses as well as the breakage may increase on a percentage basis. Also, there will be a power loss due to series resistance even for an optimized grid pattern, although this can be minimized by increasing the thickness of the grids (at additional cost). Losses at interconnections are also more significant for larger area cells.

Some of the more novel ideas for producing large-area cells (including the 48-in.^{2} cells above) were studied under government sponsorship. These included growth of epitaxial silicon films, recrystallization of evaporated silicon films, various techniques for producing sheets of silicon single crystal (285), and arrays of silicon spheres imbedded in plastic (286). The epitaxial growth process made use of the thermal decomposition of a silicon compound such as $SiCl_4$ to deposit a thin film of silicon onto an oriented single-crystal substrate. The substrate was intended to be of a material which could be peeled or dissolved away without damaging the silicon film. The original studies were performed using silicon substrates. It was also hoped that it might be possible to add the proper dopants during the growth of the film to produce a p-n junction, thereby eliminating another costly process. Epitaxial silicon techniques have been developed to the state where controllable and reproducible films can be grown on silicon and sapphire substrates today. However, it is doubtful that these techniques are the most economical for producing films of the proper thickness for acceptable efficiencies and of a realistic area (considering the fragility of large-area films). A proposed variation of the epitaxial process consisted of evaporating a suitable thickness of silicon onto a polycrystalline

substrate, the substrate material being such that it would not be wetted by the silicon. The film was then to be recrystallized by passing a hot molten zone along it, and it could then be removed. The degree of success achieved with this approach is not known.

The Signal Corps (287) sponsored work on a large-area silicon solar cell composed of silicon spheres (286). The silicon spheres were obtained by cutting single-crystal silicon into cubes and tumbling them to make then spherical with a nominal diameter of 3 mm. After lapping and etching a p-layer (~3 μm deep) was formed on the surfaces of the spheres by boron diffusion. The spheres were then arranged in a hexagonal closely packed array on a plastic sheet and partially immersed in a semipolymerized plastic. The plastic was cured and a multilayered metallic film was deposited over the spheres and the plastic to provide contact to the p-layer. More plastic was used to cover the metal film, and the sheet was then lapped to expose a portion of the spheres. The exposed portions of the spheres were etched to remove the p-layer from this portion. More plastic was again added until the spheres were completely submerged. The surface of the unit was lapped, exposing only the n-type material. A metallic film was evaporated over the lapped surface, contacting the n-type material and providing a means for external contacting. A final insulating film of plastic completed the cell. Efficiencies near 10% were measured on these cells; however, a cheap technique for producing the spheres was needed. In addition, one would expect that this type of cell would be particularly vulnerable to radiation of several types. An alternative approach using crushed silicon powder or chips yielded efficiencies of the order of 1%, non-uniformity of the individual components being a major difficulty. This last method has been used recently by some Philip's workers to produce cadmium sulfide solar cells.

Attempts have been made to produce silicon sheet by squeezing bars of silicon while subjecting them to high temperatures as in the rolling mill technique. Materials produced by this technique contained, not unexpectedly, a large number of strains and distortions. It was suggested that annealing might reduce these to the point where the material could be used in the fabrication of solar cells. This is questionable, especially considering the general effects of prolonged annealing or minority-carrier lifetime.

The most successful technique for producing silicon sheet has been the application of dendritic growth (288-290). This technique begins by seeding two coplanar dendrites from a single seed. A silicon web freezes between the coplanar dendrites as they are pulled from the melt. The thickness of the web is controlled by the pull rate. Typical pulling speeds are 1/4 to 1-1/2 inches per minute. The thickness varies with pulling speed at a rate of about 30 mil/(inch per minute). The width of the web tends to increase as the growth proceeds. When the web is first seeded the edge dendrites are about 1/4 inch apart. They then separate, thus widening the silicon sheet, at a rate which is generally not constant but averages around 0.1 inch per foot of web pulled. The widening of the web can be quite erratic and sometimes reverses. This obviously reflects the difficulties of controlling the growth process. The steady-state width of the web is a critical function of the temperature and temperature gradients around the dendrite tips under the melt surface. The temperature here must be controlled to within 0.02°C.

Most grown web is 1 to 2 cm wide and 10 to 15 mils thick. Continuous lengths exceeding 8 feet have been grown. After growth the web is scribed to remove the dendrites and to provide a sheet of constant width. The sheets are then processed into cells using essentially the same techniques that are used in fabricating normal solar cells. Both p-n and n-p cells have been made with areas ranging from 1 x 15 cm^2 to 1 x 30 cm^2. Efficiencies as high as 13% have been reported for p-n cells (288) (1 x 15 cm^{-2}). Most of the recent work has been on n-p cells. A pilot line run of this type of dendritic cell reported late in 1965 had the following yield characteristics (1 x 30-cm^2 area cells) (290):

Efficiency	Yield
$\geq$ 9%	100%
$\geq$ 10%	68%
$\geq$ 11%	18%

Average efficiency for this run was 10.85% with a maximum of about 11.5%. The major difficulties with the dendritic cells are the requirement of maintaining uniformity over the length of the sheet and the handling problems associated with thin materials (291). The feasibility of the technique has certainly been established. It is difficult to make a cost comparison with conventional silicon cells on the basis of the information published up to this time.

In summary, the use of large-area cells offers potential savings in handling costs both for the cell manufacturer and the panel manufacturer. Historically, the traditional solar cell size has been 1 cm x 2 cm, although the 2 cm x 2 cm cell has been used during the past few years and has achieved acceptance due to savings realized from its use. The dendritic technique has realized considerable success in producing silicon sheet. A number of the drawbacks of large-areas cells including breakage, etc., have been outlined. Additional factors to be evaluated when considering large-area cells for array fabrication are reliability, which may decrease when large-area cells are used, and the number of cells necessary to provide the desired voltage, which, for a fixed array size, may preclude the use of large-area cells.

Another approach which has been explored for possibly reducing production costs is the use of ion implantation techniques for junction formation (292). The junction is formed by bombarding the surface of the silicon with phosphorus ions with energies of 80 to 200 keV. An annealing step is necessary after bombardment. The annealing is intended to allow the implanted impurity atoms to take up substitutional positions and thus become electrically active. Typical annealing temperatures are 700 to 750°C with annealing times up to 16 hours. The junction depth is a function of the resistivity of the silicon material and the energy of the bombarding ions. Extremely low energies (below about 70 keV) cause sputtering of the cell surface, increasing the surface recombination velocity. An energy of 80 keV gives a junction depth of about 0.4 μm in 10-ohm.cm material. Single-crystal cells with efficiencies greater than 10% have been made by this

technique with the major limitation being the resistance of the doped layer. This was expected to be overcome through use of ion implantation equipment with higher current capabilities. Recent trends (291) have been to combine the ion implantation process with the use of dendritic materials in an attempt to develop an automated process for producing low-cost solar cells with high power-to-weight ratios. Ion implanted dendritic cells with efficiencies of 9.4% (AMO) have been fabricated; however, serious handling and materials problems have prevented the setting up of a competitive production process.

b. Weight Reduction: Weight has always been a matter of concern in the space application of solar cells. Initially, the concern was generated by the low thrust capabilities of the rockets available at the time. Despite the current availability of high-thrust boosters the demand for considerably higher energy power supplies has caused a continuation of interest in reducing cell weight. One technique, and virtually the only one of significant interest, for reducing cell weight is simply to reduce the thickness of the base material. Various techniques for producing thin silicon sheets have been discussed in the preceding section and will not be discussed here. What must be considered is the effect on cell efficiency of reducing cell thickness. Since long wavelength photons are absorbed at a considerable depth in the silicon base region an appreciable loss in energy absorption can occur if the thickness is reduced below 200 μm. In addition to this loss the closer proximity of the back contact, which is a surface of high recombination velocity, to the p-n junction reduces the average minority-carrier density in the base region, thus reducing the collection rate at the junction. Wolf and Ralph (224) performed a theoretical analysis of the effect of varying cell thickness on collection efficiencies and short-circuit currents and produced curves relating these factors to the thickness. Experimental data, however, showed a more rapid loss of short-circuit current with thickness than was predicted by the theory. Recent experiments by Crabb and Treble (226) in which considerable care was taken to eliminate work damage at the back surfaces of thin silicon cells indicate that conditions at the back contacts were the source of the disparity. Crabb and Treble found that the behavior of their cells agreed quite well with the theory. An interesting side effect of the reduced red response, as was pointed out by Wolf and Ralph, is that the thinner cells are more radiation-resistant. Recent measurements have confirmed that the thinner cells do, in fact, deliver constant power over larger values of integrated radiation fluxes than their thicker counterparts. Ralph (293) has recently published engineering and design data for thin cells which includes the variation of cell power-to-weight ratio with cell thickness. Calculations on 2-ohm·cm base cells show an increase in power-to-weight ratio from approximately 100 watts per pound for 12-mil-thick cells to 250 watts per pound for a 4-mil-thick-cell and to about 450 watts per pound for a 2-mil-thick cell. Similar calculations for 10-ohm·cm material show that these cells go from slightly less than 100 watts per pound at the 12-mil thickness to about 230 watts per pound at a thickness of 4 mils. The thin cells offer considerable potential for weight reduction if the restrictions on area are not too great or the power requirements not too high.

c. *Efficiency:* The theoretical maximum efficiency of the silicon solar cell is 22%. The maximum efficiency observed on current cells is about 15%. No significant change in the maximum efficiency of experimental and production cells has occurred over the past seven years. There has been a gradual improvement in the average efficiency because of better materials, improved processing techniques, etc., but the maximum has remained essentially constant. Several ideas for obtaining radical increases in efficiency have been proposed since the introduction of the "Solar Battery". Many of these have dealt with materials other than silicon or combinations of two or more materials. These will be discussed in the later sections of this work. Others have not yet gone beyond the idea stage and are discussed in the theory section. There have also been some experimental attempts at improving silicon cell efficiencies (other than those which achieved success and have been discussed previously). Some of the experimental investigations along this line are described.

The first power loss which occurs is that due to reflection. Antireflection coatings have successfully reduced this loss to a minimum in contemporary cells; however, as a matter of historical interest one other approach to solving this problem will be mentioned. In 1960, Dale and Rudenberg proposed an alternative approach to reducing reflection losses which consisted of cutting a pattern of inverted tetrahedral pits into the surface of the cell (246). Each pit acted as a corner reflector so that incident light under went three reflections before emerging. The structure was said to have a reflectivity of only 4% and had the advantage of being independent of wavelength. It did, however, give a high series resistance. The technique would seem to be rather expensive and presents some serious contacting problems.

Efforts to improve absorption include the use of reflective back contacts (294) and the use of fluorescent materials to convert a single high-energy photon to two or more photons of lower energy (295). As was mentioned in the introduction, photons which are transmitted through the cell are usually absorbed in the back contact giving rise to heat which degrades cell performance. If contacts with suitable interface reflection properties for the longer wavelengths could be devised some of these photons could be caused to pass through the cell a second time, increasing the probability of absorption as well as reducing heating. This technique would be especially applicable to the thin silicon cells. Attempts to provide such a contact with aluminum (the conventional contact is titanium-silver) deposited by several techniques were at first unsuccessful (294), primarily because of problems with processing technology. Recent reports (291) indicate that alloyed aluminum contacts have been used to successfully increase reflection at the back surface (and consequently increase efficiency) of thin silicon cells. In addition, the aluminum contact is reported to reduce the surface recombination velocity and increase infrared rejection. The characteristic of the back surface of the silicon is a critical factor in controlling the reflecting properties of the back contact. Aluminum contacts on a rough surface have characteristics superior to those on a polished surface. Under air mass zero conditions the cells with reflecting contacts had short-circuit currents averaging 61.3 mA while those without reflecting contacts averaged 59.5 mA (8-mil-thick cells were used). The potential for improvement by using this approach in thicker cells is not as great. No experimental data are available on the conversion of high-energy photons to multiple low-energy photons.

Proposals for increasing collection efficiencies include the use of drift fields and the transformation of photon energies in such a way as to increase the probability of collection of the carriers generated. Drift fields in solar cells were analyzed by M. Wolf in 1963 (217). The details of this analysis are discussed in the section on theory. There has been some experimental work on drift field cells (296); however, these have shown no promise of efficiency increases. Efforts to shift photon energies to give better collection efficiencies through the use of dyes and fluorescent materials on the surface of silicon solar cells were reported by the Hoffman Electronics Corp. around 1960 (295). In every case the efficiency of the solar cells was either degraded by the presence of the additional layer or was not affected. The attenuation of useful low-energy photons by such layers would probably offset any gains due to photon transformation and, hence this approach is not very promising.

Another approach to reducing series resistance losses (other than the use of grid lines) was to coat the cells with a transparent conductive coating (294). This coating was used in conjunction with the conventional grid stripes. Two coatings were tested, tin oxide and gold-impregnated silicon monoxide. Neither coating improved cell efficiency, and investigations in this direction were quickly abandoned.

C. Compound Semiconductor Cells

As noted in Section III-C, the success of the early silicon cells was closely followed by work on compound semiconductor cells by Gremmelmaier (GaAs), Talley and Enright (InAs), Reynolds (CdS), and Avery et al. (InSb). In this section, the progress in this field of research will be followed from 1955 to the present day. However, work on thin-film cells (which have been based almost exclusively on compound semiconductors) will be described later. In an effort to provide maximum continuity, an account will be given of the development of cells based on each compound for the entire period 1955 to the present. Thus, the following account is not in overall chronological order. Where connections exist in the development of cells of different materials, suitable indications have been given in the text.

In general, the choice of semiconductors for investigations aimed at making solar cells has been governed by two factors: (i) the theoretical considerations of optimum E_g, as described in Section IV-A-1 above, and (ii) the state of materials technology for the candidate compounds. Generally, of course, the theoretical considerations have been dominant, and the research effort has frequently been aimed at making good the deficiencies of the materials technology. It is a remarkable fact that in no case has this effort been sufficiently successful to provide a serious competitor for the silicon solar cells in use today, for conversion efficiency and cost.

1. Gallium Arsenide

With both of the above considerations in mind, an early subject for investigation and one which has provided the most promising cells, has been GaAs. As mentioned in III-C-3, the first report on a cell made of this material was by Gremmelmaier, who obtained a cell on a polycrystalline wafer showing a sunlight conversion efficiency of 4%.

The next group to enter the field was that working under Rappaport at RCA Laboratories, and work in these laboratories and at others in RCA, has provided almost the entire Western effort in this field. The work was initially funded by the Signals Corps (186) during the period April 1955 to August 1957. Several materials were investigated (CdTe, InP, experimentally and others theoretically), aside from GaAs. Difficulty was experienced in obtaining GaAs wafers of sufficiently low impurity concentration and with adequately large single crystals, so the results were variable. However, 1-mm^2 cells formed by Zn, Cd, and Hg diffusion into wafers cut from ingots showed efficiencies up to 6.5%, and later cells of about 20-mm^2 formed by Cd diffusion showed efficiencies of up to 3.4%. Initial difficulties with contacting were eliminated, leading to cells with reasonably low R_s losses. However, measurements showed I_o to be 10^5 times larger than that predicted by diffusion theory, and to vary with temperature as exp $(E_g/2kt)$ rather than exp (E_g/kt). This reduced the working voltages below those theoretically predicted, though not disastrously so, V_{oc} values up to 0.9 V being seen. However, the I_{sc} values were nearly a factor of ten lower than those predicted. This was found to be due not to surface recombination, but to low minority-carrier lifetimes. At the time these were ascribed to non-stoichiometry and crystal defects in the GaAs, whereas they are now known to arise from direct recombinations between free holes and electrons. In addition to these diffused-junction cells, small-area junctions were also made by alloying of Zn or In dots, followed by chemical removal of the bulk of the alloying material to expose the p-n junction. Naturally, such a technique would not, in general be applicable to large-area cell manufacture. Jenny, Loferski, and Rappaport reported briefly on the results obtained, in 1956 (153), also giving a spectral response curve for the Cd-diffused cells. This curve showed the expected onset of photo-current at a wavelength corresponding to E_g=1.35 eV, as would be expected.

Soviet workers were quick to take an interest in the possibilities of GaAs photocells, as witnessed by a report by Nasledov and Tsarenkov (297) in 1957. GaAs cells were prepared in n-type polycrystalline wafers by diffusion of Cd, reference being made to the RCA work. Diffusion was performed in a sealed ampoule in which two temperature zones existed, the GaAs wafer being at 1050°C, and the second zone being at 850°C to maintain the vapor pressure of Cd at a value sufficiently low to prevent attack of the GaAs surface. Results comparable to those of the RCA group were obtained, the spectral response being shown, and an efficiency of 2.8% for a device 1.8 mm^2 being obtained. However, I_{sc} values

of up to 8.3 $mA \cdot cm^{-2}$ were obtained (rather higher than the RCA work), whereas the poor contacts used (a pressed tin contact to the diffused layer) resulted in a larger R_s, with a corresponding power loss. The polycrystalline wafer used for this study indicated that here also difficulty was being encountered in obtaining starting material of adequate quality.

In 1957, Gremmelmaier (298) reported further work involving GaAs cells, in which γ-irradiation was used to excite a p-n junction, and from these measurements a diffusion length was calculated. This was found to be 8 μm for a diffused junction in GaAs, with a maximum lifetime of 9 nanosec.

Meanwhile, the work at RCA continued, under further funding by the US Army Signals Corps(192). The objective of this work was to make cells capable of operating at higher temperatures than silicon cells. The main research done was on cell fabrication techniques, to evolve manufacturing methods capable of yielding cells with an area comparable to silicon cells, and with sunlight conversion efficiencies of 8%. Work on GaP-GaAs, CdTe, and CdSe cells was also done under this contract, and will be described later.

The work on GaAs covered three main areas during the period July 1958 to October 1960:

(i) Diffusion process parameters such as diffusion time, temperature, and dopant material and its concentration were varied in a systematic way to maximize cell efficiency. It was found necessary to maintain a low surface concentration of dopant during diffusion to prevent attack and alloying of the GaAs surface. When the sealed ampoule technique was being used for diffusion, a limited amount of dopant was weighed into the ampoule to provide the desired vapor pressure at the diffusion temperature (cf. the two-zone diffusion ampoule technique used by Nasledov). Zn and Cd were used for this work, and the best results were obtained with low diffusion temperatures (~ 700° C), and junction depths of ~ 1 μm. It also proved necessary to control carefully the cooling rate at termination of the diffusion, too rapid cooling leading to blistering of the GaAs surface by rapid out-diffusion, too slow cooling leading to alloying of the GaAs surface. Later in the work, the open-tube diffusion technique was used, in which the dopant (Zn) was passed over the wafers in a stream of carrier gas, thus allowing greater control of the diffusion ambient during processing. Problems were encountered in obtaining a sufficiently high surface concentration in this case, but again control of the rate of temperature drop at the end of diffusion was found to be necessary, and this could be controlled to provide the required surface concentration while still avoiding alloying. The best results from ampoule and open-tube processes were comparable, the cells having sunlight efficiencies of 7% with areas of 0.7 cm^2 and junction depths of 1 μm or less.

(ii) Measurements of spectral response were combined with theoretical analysis as described in Section IV-A-1 to provide estimates of minority-carrier lifetime and diffusion lengths. Although this work was hampered by lack of accurate optical absorption data for GaAs, it was estimated that a minority-carrier lifetime of 10^{-10} sec was being obtained in the finished cells, and this was causing a serious reduction in collection efficiency. To deal with this problem, post-diffusion treatments to improve minority-carrier lifetime were investigated. These involved low-temperature diffusion of Cu or Ni into the cell at about 300° C, but the results were largely negative. The most effective way of improving the collection efficiency was found to be reduction of the junction depth by a combination of shallow diffusion and post-diffusion surface etching.

(iii) Measurements were made of cell efficiencies at high temperatures and after 8.3- MeV proton irradiation, and the results were compared with those obtained on silicon cells. With the discovery of the natural radiation belts surrounding the Earth, radiation resistance had become an important parameter in solar cell studies. Radiation was found to lower cell efficiency by introducing defects which lowered minority-carrier lifetime and mobility, thus reducing minority-carrier diffusion length. Since silicon cells required a large diffusion length to overcome the low optical absorption coefficient of the material, it was clear that such cells were easily damaged by radiation. It was hoped that GaAs, with its intrinsically high optical absorption coefficient, and thus a less stringent requirement for large minority-carrier diffusion lengths, would prove more radiation-resistant. The rate of loss of efficiency with increasing temperature for the GaAs cells was not found to behave as theoretically predicted, but a performance superior to that of silicon cells was seen. Thus, a GaAs cell of 7% efficiency at room temperature provided better efficiency above 150° C that a silicon cell with 10% efficiency at room temperature. The radiation-resistance measurements indicated that the GaAs cells were more resistant to radiation damage than silicon cells, but since the starting efficiencies of the GaAs cells were low (~ 3%), the results were not considered to be of great significance. The early results of this work were also reported at the 13th Annual Power Sources Coference in 1959(299). The behavior of I_0 with increasing temperature was described as being the cause for the cell efficiency variation with temperature not following the theory, as was initially reported during the earlier work(186).

Further progress was reported a year later at the 14th Annual Power Sources Conference (300), the results already described being presented, but in addition some performance data were given for the cells now being made by Lamorte's group working at RCA's Somerville plant, under the sponsorship of the USAF (301). This contract commenced in April 1959 and was concluded in May 1962. Building on the exploratory work done at RCA Laboratories, production techniques were developed for cell manufacture,

and the area capability and conversion efficiency were greatly improved. This work was reported in detail and has been the only major industrial program applied to GaAs cell development.

A major effort was applied to growing suitable starting material in the form of single-crystal GaAs ingots from which 1cm x 2 wafers could be cut with a minimum of waste. This involved refinement of the Bridgman technique, using a seed to avoid polycrystallinity and supercooling. A progressive freeze was obtained by moving the furnace relative to the ampoule to provide orderly and slow growth, a point found necessary to improve the crystal quality by minimizing defects. Treatment of the quartz ampoule inner surface to minimize wetting and resulting mechanical stress in the crystals was also found to be necessary.

Most of the crystals used were germanium-doped, a few being tin-doped, both providing n-type base material. The ingots were grown with the (111) axis along the ingot, so that slicing across the ingot was used to provide wafers with (111) planes exposed. The slices were polished before diffusion, and chemical polishes were found to yield consistently better cells than mechanical polishes, probably by giving less work damage. Initially, the sealed-ampoule diffusion system was used but an open-tube process was quickly adopted because of the improved control possible with this system. Various furnace geometries were used in an effort to optimize the diffusion process. The majority of the best cells were made in two types of furnaces, one a resistance-heated tube furnace, the other using a radiant-heating system. Results showed the latter to give the best results by a small margin. The resistance-heated tube furnace thermal mass set a limit on the heating and cooling rates which could be achieved, whereas the radiant-heating system, in which the wafer was heated directly by radiation from a hot body, was found to provide much more rapid heating and cooling cycles. This made possible the diffusion of much shallower junctions, using a short high-temperature cycle with high surface concentration of diffusant. (This may be contrasted with the original work done at RCA Laboratories, in which shallow junctions could only be formed by low-temperature diffusion). The radiant-heating technique was also felt to minimize cell contamination, by having the GaAs at a higher temperature than the furnace walls. However, slice temperature control in this type of furnace was found to be more difficult than in tube-type furnaces, leading to a greater spread in cell characteristics.

The etching process originally used by RCA Laboratories to reduce the surface region thickness was also further developed. The principal difficulty encountered here was the provision of controls to stop the etching once the optimum surface region thickness had been reached. (The optimum represents the best trade-off between surface region sheet resistance and collection efficiency, as described in Section IV-A-1). Initially this was done by etching briefly, checking the cell characteristic, etching again, checking, etc., until the efficiency maximum was

reached. Clearly, such a technique could be applied to production only with difficulty, but a fixed-time etch process was found not to give adequate reproducibility. Eventually, a system was devised whereby the cell current (I_{SC}) was monitored continuously during etching, the process being terminated on reaching the I_{SC} maximum. Interestingly, it was found that this etching caused changes in the diode characteristic, since the junction was within a diffusion length of the surface, so that surface recombination influenced the conduction.

Contacts and grids were applied to the cells by vacuum deposition of silver followed by solder coating using preformed solder strips to avoid the dipping process, which had been found to severely degrade cell performance. Finally, an antireflection layer of a 1/4-λ SiO coat was applied by vacuum evaporation.

Over the three-year duration of this work, the cell efficiency steadily improved, moving from the feasibility-study cell types developed by RCA Laboratories (0.7 cm^2, 7% efficiency), to a 2-cm^2 cell with a yield curve peak at 5.5% (1959-60), 7.5% (1960-61), and 8.5% (1961-62). The maximum cell efficiency seen was in the 13 to 14% interval. Detailed measurements of the variation in conversion efficiency with temperature confirmed the initial RCA Laboratories' results, the cell performance falling by 0.02 to 0.03% per C° for GaAs, compared with 0.035 to 0.045% per C° for silicon cells. The behavior of cell performance under proton irradiation was also measured. The critical flux (required to cause a degradation of 25% in cell efficiency) was found to be in the interval 1.5 to 6 x 10^{12} 17-MeV protons cm^{-2} for the GaAs cells, compared with 1.5 to 2.0 x 10^{11} cm^{-2} for n/p silicon cells with similar initial efficiencies. Another point of comparison between GaAs and silicon cells was brought out by the radiation work. This showed that the matched load for the GaAs cells changed by only 5% under an irradiation does of 10^{12} 17-MeV protons cm^{-2}, whereas for n/p silicon cells under the same dose the matched load resistance had changed by more than 50%. Thus, operating under fixed load impedance conditions (as would be normal on a spacecraft), the GaAs cells would provide a considerably more stable power supply under irradiation.

Research on various alternative cell formation processes was also pursued under this work. A small number of n-on-p cells were made, and although these had a lower efficiency than the p-on-n cells (2.3%), it was felt that this type of cell would be worthy of further study, since the electron mobility of GaAs is much higher than the hole mobility, and thus the surface layer resistance in an n/p cell should be correspondingly lower than in a p/n cell with the same junction depth. (It would appear that the minority-carrier diffusion length should be greater in the p-type base also, for the same reason. This should act to increase the collection efficiency, a point not mentioned in the reports. However, the potential efficiency increase available here would be small because of the already high collection efficiency, and might well be outweighed by the increase in cell resistance from the increased base region resistivity.) Another cell process which received rather

more attention was the epitaxial growth of GaAs on GaAs, to form the surface layer. Two deposition systems were used, both based on the halide transport process:

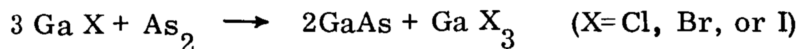

$$3\,GaX + As_2 \longrightarrow 2GaAs + GaX_3 \quad (X = Cl,\ Br,\ or\ I)$$

In the first, and reactants were formed by passing HCl over heated GaAs. In the second, GaCl was formed by passing $GaCl_3$ over heated Ga, with the arsenic being sublimed from the solid. Although the cells made by this technique exhibited low efficiencies, this was felt to be a reflection of the processing technology rather than a fundamental limitation. The control of the carrier concentration which is possible in the GaAs grown this way is particularly interesting, a point which has been exploited more recently by groups working on other types of GaAs devices. Gobat, Lamorte, and McIver (305) and Lamorte (306) published summaries of the results obtained, during 1962. However, the maximum cell efficiencies seen were not as high as those quoted in the Final Report (301).

Meanwhile, the Soviet work under Nasledov continued (302), and at the end of 1959 had apparently reached a status comparable with that of the RCA work, though it is not possible to make an exact comparison, since the Russians do not give cell areas or conversion efficiencies. However, the cells were being made on polycrystalline GaAs (indicating that single-crystal GaAs was less readily available in the USSR than in the U.S. at this time.)

Further, the junction depths quoted ($\sim 10\ \mu m$) miliate against a good cell efficiency, which is borne out by the poor blue response of the cells in the spectral response curves shown. The cells were apparently made by the same technique as those reported earlier (diffusion of Zn or Cd into n-type base material of 10^{17} carriers cm^{-3}). However, the cell contacting techniques had improved, evaporated Ag contacts to the p-layer being used (cf. the work of RCA Somerville, above).

In 1960, the results were published of research at TI laboratories (Dallas), apparently internally funded (303). The cells were of structure similar to those made at RCA Somerville, having a 1 x 2 cm n-type base with a shallow Zn-diffused junction, and an antireflection $1/4$-λ coating of vacuum-deposited SiO. However, contacts were made by the electroless nickel process, and this probably was a major contribution to the rather large R_S value which can be deduced from the I-V characteristic shown. The current density for the cells was about 13 $mA \cdot cm^{-2}$, comparable to that of the RCA work in 1962. An efficiency of 7% was quoted for the TI cells, which is almost exactly the same as that for the RCA cells of this period (1960).

The original research at RCA Laboratories continued during the period November 1960 to October 1961, again under Signals Corps funding (304). Only a portion of this contract effort was devoted to GaAs cells, radiation studies on silicon cells also being performed. A solution-regrowth process was investigated for making

p-n junctions in GaAs cells. This involved immersion of the base wafer in a solution of GaAs and dopant in gallium at a high temperature (~700°C); the temperature of the solution was then raised slightly to dissolve a little GaAs from the wafer surface to perform a cleaning operation, followed by a slight lowering in solution temperature to cause precipitation of GaAs onto the wafer surface, the regrown material containing dopant to provide a conductivity type opposite to that of the base wafer. In this way both p/n (Cd or Zn in solution) and n/p (Sn in solution) cells were made. This provided a surface layer with a very high carrier concentration (5×10^{18} to 2×10^{19} cm^{-3}), but the resulting poor operating characteristics of the diodes gave low efficiencies. Also, difficulty was encountered in obtaining uniform regrowth, so that large-area cells were not obtained.

GaAs cells from the RCA Somerville production line were used in radiation damage studies. Under bombardment with 800-keV electrons, the degradation was found to be the same as that for n/p silicon cells, the critical flux (to produce a drop of 25% in efficiency) being about 2×10^{16} cm^{-2}. The main efficiency loss occurred by a drop in I_{SC}. Under bombardment with 19 MeV protons, however, the cells were considerably more resistant than n/p silicon cells, with results similar to those obtained by the RCA Somerville group (see above). The reasons for the difference in behavior under electron and proton bombardment was not clear.

In 1962, the Astro-Electronics Division of RCA, under contract to the USAF, provided information pertinent to array manufacture using GaAs cells (307). The results were pertinent to systems fabrication only and were therefore beyond the scope of the present work. The status of GaAs cells was compared with that of silicon and other cells by Loferski in 1963 (308), and the reasons for the efficiencies seen were discussed. In particular, the significance of the low minority-carrier lifetimes was now understood, the work of Hall (309) and Mayburg (310) being quoted, concerning the likelihood of direct recombination processes occurring in GaAs. The fact that GaAs is a direct bandgap material was now appreciated, so that lifetimes greater than about 10^{-8} sec could not be expected in material with a carrier concentration of 10^{17} cm^{-3}. However, Loferski calculated that the short diffusion length value resulting from this would be offset by the optical absorption coefficient, so that in principle (i.e., with no surface recombination), collection efficiencies close to unity should still be achievable. In practice, the best GaAs cells had an I_{SC} density of 17 $mA \cdot cm^{-2}$ (the calculated theoretical maximum being 32 $mA \cdot cm^{-2}$) under 100 $mW \cdot cm^{-2}$ sunlight illumination. Loferski quotes the maximum conversion efficiency seen as being 13%, corresponding to the data given by Lamorte (301).

By now, the greatest amount of money being spent on solar cell research was concerned with radiation testing, and comparisons between silicon and GaAs cells under various radiation conditions could be made more accurately. Wysocki (311) published results on GaAs cells irradiated under both protons and electrons with various energies, obtained with the support of the USAF (307) and NASA (312). These

showed that under high-energy electron (5.6 MeV) and proton (1.8 to 9.5 MeV) bombardment, the critical flux for GaAs cells was a factor of ten higher than n/p silicon cells. For 0.8-MeV electrons, the performance of the two cell types were comparable, as mentioned above. For low-energy protons (0.1, 0.4 MeV), however, the GaAs cells were more susceptible to damage than n/p silicon cells. Wysocki attributed this behavior pattern to the fact that the GaAs cells operated by collection from the region of the cells very close to the illuminated surface, so that particles absorbed primarily in this region (i.e., low-energy particles) would have a large influence on cell operation, whereas more penetrating radiation would have little effect. In silicon, on the other hand, the major response came from the base region of the cell, so that the converse would be true. The results fitted with this picture, which was also supported by spectral response measurements. These showed that the silicon cells lost mainly red response under irradiation since the longer wavelengths were absorbed less strongly and thus generated carriers deep in the base region. For the GaAs cells, however, the blue response was mainly lost under irradiation, since the longer wavelength photons could penetrate sufficiently far into the cell to be absorbed near the junction. Thus, a coherent picture of radiation damage in GaAs cells was established.

Progress in the Soviet work was reported by Gutkin et al. in 1962 (313). The original junction formation methods (Zn or Cd diffusion in quartz ampoules with two regions at different temperatures) were still in use, but the starting material was now Czochralski-pulled single crystal with 10^{17} electrons$\cdot$cm^{-3}. (This should be contrasted with the Bridgman technique being used at RCA Somerville; unfortunately, no process details are given by the Russians but the solution to the problem of maintaining an adequate As_2 pressure in the growth chamber in equipment which requires rotating and sliding motions of the pulling head is a difficult one.) The cells were 5.5-mm-diameter discs, with indium contacts: the discontinuance of the use of silver electrodes (reported earlier) was not explained. Although performance measurements were not reported, it appears that the cells were of low efficiency since the junction depths were still ~ 10 μm, and the spectral response curves show a correspondingly poor blue response. Measurements of spectral response were made over the temperature range 78 to 417°K, the operating temperature presumably being limited to below 429°K (156°C) by melting of the In contacts. The junction I-V characteristics were measured and found not to obey the Shockley or Sah, Noyce, Shockley theories, it being postulated that the effects seen were due to furface recombination effects, as had been suggested by Lamorte's work. In addition to the photovoltaic work, photodiode characteristics were also described, suggesting that the devices were intended for detectors as much as energy converters. Only in 1963 (314) was any mention made of Russian devices in which the shallow junction (~1 μm) characteristic of efficient cells was used. This later work was entirely devoted to the use of the devices as photodiodes, however.

In 1962, further support for the RCA Somerville GaAs cell production facility was obtained from the USAF (315), and work aimed at optimizing production processes using a pilot line was pursued during the period June 1962 to February 1964. During this period, the GaAs crystal-growing process was modified, to replace the Bridgman technique (in which progressive freezing was obtained by relative motion between the ampoule and the furnace), with a gradient-freeze technique in which furnace and ampoule were fixed. Multizone temperature control in the furnace was used with programmed power supplies to move a temperature profile along the ampoule, thus inducing progressive freezing of material from the seed onwards. This produced more reproducible material, and enabled production volume to be increased. Small changes were also made in the arsenic overpressure (governed by the cold zone temperature in the ampoule), to reduce boat wetting, and in the selection methods for seed crystals, to improve GaAs quality.

The radiant-heating diffusion process investigated earlier did not prove to be capable of being adequately controlled, so the original open-tube technique was used. This involved a 13-minute diffusion at 720° C in a nitrogen atmosphere, using Zn as diffusant. The junction depth thus produced was 1.5 μm on the average. After etching to expose the base material at the back of the slice, the cells were cut to size with an ultrasonic tool. Both grids and back contacts were deposited by vacuum evaporation of nickel and silver, followed by a sintering operation at 600° C under a hydrogen atmosphere. Most of the cells were equipped with nickel tabs to facilitate array construction, the tabs being attached with a Ag-Pb eutectic solder. The surface thickness was then reduced to ~ 0.5 μm by etching in $KOH:H_2O_2$ solution using the etch-and-test process developed earlier (see above). Finally, an antireflection coating of SiO was vacuum-evaporated onto the cells. A large effort was made under this work to develop trays, jigs, etc., to maximize the efficiency of the manufacturing processes. Many details of these together with statistical information on the pilot line operation were given in the Final Report. Fundamentally, the cells were the same as those manufactured under the previous contract. However, the yield curve on the pilot line peaked at 9.5% conversion efficiency at the end of the program (cf. 8.5%, 1961-62), with a noticeably smaller spread in cell characteristics than earlier. Testing of the cells under various operating conditions generally yielded no surprises, the cells being stable. However, for operating temperatures above 200° C, degradation in V_{oc} was noted during the first few hundred hours of operation, typically from a starting value of 0.86 V down to 0.60 V, and with a small decrease in I_{sc}. This was found to occur only in cells with tabs, and to be caused by degradation of the p-n junction under the contact area. It was felt that this indicated that the tab attachment method needed modification, but it was concluded that the cell was intrinsically stable. Operation of the cells at high temperatures and at high light levels (up to 700 to 800 $mW \cdot cm^{-2}$) showed the cells to be much superior to n/p silicon cells under these conditions, as was expected. In addition, radiation-resistance measurements on the cells were quoted, the results being those reported by Wysocki (311). Finally, it should be noted that although the pilot cells were all 1 cm x 2 cm units, a small number of experimental 2 cm x 2 cm cells were also made, which showed efficiencies up to 10.2%.

In spite of the great advances made in GaAs cell technology and performance during this program, the cells could not compete with conventional silicon cells for normal space mission requirements, so that further development has largely ceased in the period 1964 to the present. But a few notes on the research are in order. The Russian work under Butkin continued with comparisons between theoretical and experimental spectral response curves for cells with surface layer thicknesses down to 1 μm (316). Work aimed at investigating the influence of crystal orientation on the quality of p-n junctions (317) showed that the orientation did not affect the diffusion within the limits of experimental error. However, the report was notable in that Bridgman crystals were now being used in place of the Czochralski material used earlier, as mentioned above. Further work by Gutkin (318) showed that the spectral response of GaAs p-n junctions at photon energies considerably higher than the band edge (measurements were made up to 5.4 eV) indicated a fundamental change in the quantum efficiency of the absorption process. The band structure was examined to consider the various transitions which could occur in the absorption. It was concluded that the most likely process was impact ionization, in which an electron excited into the conduction band had enough energy to cause a valence-to-conduction band transition in a second electron, thus creating another hole-electron pair. Further measurements on low-energy proton irradiation of GaAs cells were reported by Wysocki et al. (319). As before, the GaAs cell behavior showed a rapid loss of I_{sc} under irradiation, and the measurements allowed a model to be developed for predicting the effects of irradiation on performance for the range of proton energies below 6 MeV.

This is then the present situation for GaAs single-crystal cells. The most efficient cells made had a structure closely analogous to that of conventional silicon cells, in that they consisted of a shallow p-n junction formed by diffusion into homogenous base material, with gridded surface contacts, and SiO antireflection coatings. Although the cells have proven advantages over silicon for use in high-temperature and/or radiation environments, the cell costs remained more than an order of magnitude higher than for silicon cells, partly because of the high cost of starting material and partly because GaAs is inherently a more difficult material to work with than silicon. Hence, there is no production of GaAs cells at the present time, and research on such cells has all but ceased, except for radiation damage investigations.

2. <u>GaP and GaP-GaAs Cells.</u>

It was realized early in the research on GaAs cells that a potential difficulty would be a loss in collection efficiency by surface recombination, because the high optical absorption constant caused most carrier pair production within 1 μm or so of the surface. Since it had been established that GaAs-GaP alloys had good semiconducting properties, there appeared to exist the possibility of making a cell consisting of a p-n junction in GaAs, with the front surface of the cell consisting of layer of GaP grading through GaP-GaAs alloy to the base GaAs. The band diagram of

such a cell would be as shown in Figure 48. Thus, the GaP layer would act virtually as a passive part of the cell, providing an optical "window" allowing all photons with energies less than 2.2 eV to be absorbed in the junction region of the cell, where the field gradients existing because of the graded bandgap in the alloy should aid the collection process. Photons of energy >2.2 eV would be absorbed in the surface layer, and although some of these might diffuse to the junction, it was assumed that most would be lost by surface recombination. However, because of the solar spectral distribution, this would not cause any great loss of power in the device.

Experimental attempts to make a device operating along these lines were first made by the RCA Laboratories group, under the auspices of the GaAs cell work (186, 192). In addition, a group at the Eagle-Picher Laboratories obtained ARPA support to specifically investigate this type of cell (320). Both groups approached cell fabrication in the same way, making the GaP layer by diffusing P into GaAs, the As outdiffusing from the surface region of the GaAs and being replaced by P. X-ray diffraction studies by the RCA group established that a surface layer of GaP could indeed be formed this way, and both groups obtained working cells. However, the efficiencies were low (~ 4%), and although these were comparable or better than the regular GaAs cell efficiencies at the beginning of the work, the GaAs cells soon improved beyond what could be achieved with the GaP-GaAs cells, so that the alloy approach lost its initial momentum. However, the RCA group continued to investigate the possibilities for several years, and similar work was done at RCA Somerville (301).

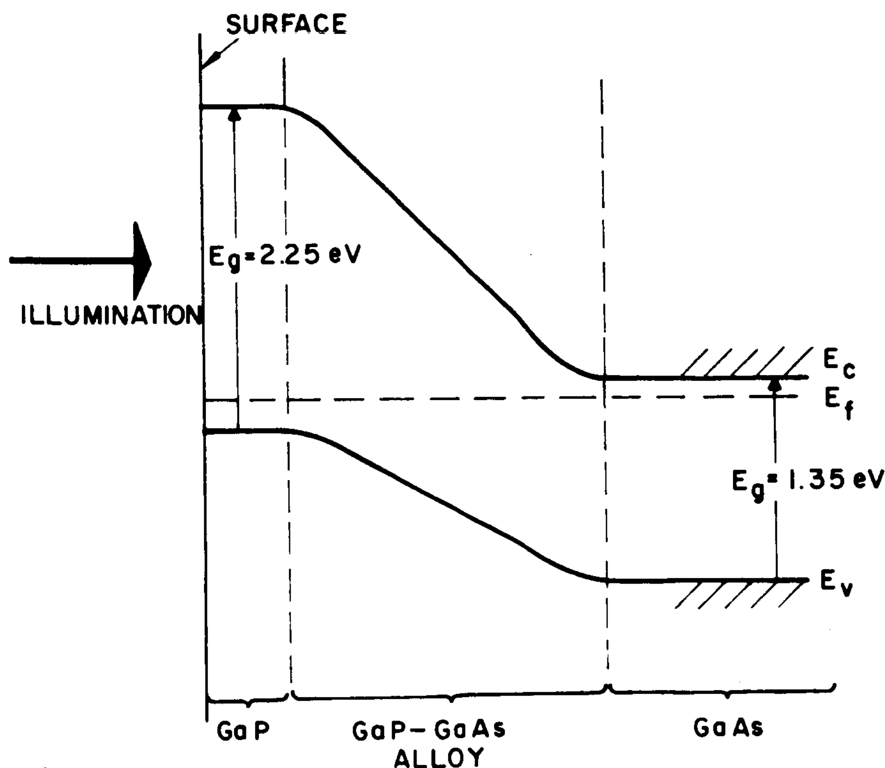

Figure 48. Band structure of a GaP-GaAs heterojunction solar cell

In addition, the RCA Laboratories group experimented with GaP cells made on pure GaP base material (192, 300). Although the theoretical maximum efficiency of this material is only 10%, as was shown by the theoretical analysis done under this work (185), the anomalous response of the CdS cell had demonstrated that such an analysis might not be applicable to all semiconductors. However, the GaP cells which were made showed only the theoretically expected response (to photon energies exceeding $E_g = 2.25$ eV), so that the device would only have application at very high temperatures (~ 500° C) where other semiconductors could not be used. The GaP cells made at RCA Laboratories exhibited V_{OC} values up to 1.2 V, but showed low I_{SC} values, due partly to poor GaP and partly to contact resistance problems, it being difficult to make good ohmic contacts to large-bandgap semiconductors.

Extensive work on GaP, including observations of the photovoltaic effect, were made by Grimmeis of Philips Laboratories, Aachen, in 1960 (321). Although this work was done with point-contact junctions rather than large-area p-n junctions, the spectral response results are relevant to solar cells. These measurements showed that although the major peak in the photovoltaic response occurred at 4200 Å, as would be expected from the E_g value, a second response occurred in the wavelength region 5000 to 7000 Å, with a peak at ~ 5600 Å. This extrinsic response was believed to occur by the absorption of photons by two-step processes, via intermediate levels existing inside the forbidden bandgap, as shown in Figure 49. The intermediate levels were thought to arise from Ga and P vacancies. Because a photovoltage was seen even when the point-contact was shielded from the light, it was concluded that the photovoltages were being developed at p-n junctions between randomly occurring p- and -n-type regions in the crystals. Such as extrinsic response implied that the analysis of Loferski for efficiency vs. E_g may indeed not apply to GaP, as had been postulated by the RCA group. The largest program to develop GaP solar cells was a contract between Monsanto Research Corporation and NASA, during June 1963 to August 1964 (322, 323). Because of the difficulty in obtaining GaP in single-crystal wafer form with adequate purity, this work was done with layers of GaP grown on GaAs substrates. The deposition process used was the same in principle

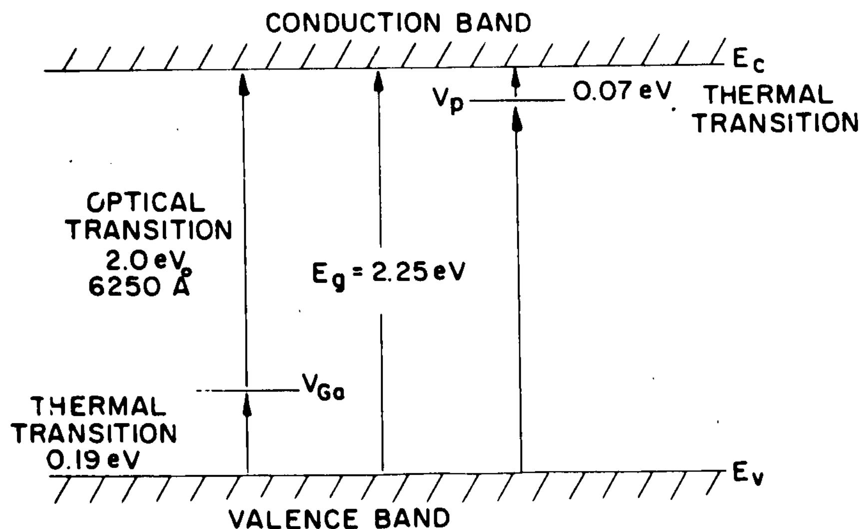

Figure 49. Transitions occurring in a GaP cell to cause extrinsic spectral response, after Grimmeis

as that used by the RCA Somerville group for the epitaxial growth of GaAs, described above, using the halide transport reaction. However, the Monsanto group aimed at producing thick GaP layers which could be self-supporting; the maximum GaP layer thickness achieved was 460 μm, though most cells were made with GaP thickness of less than 100 μm, and in some cases as low as 10 μm or less. Doping of the epitaxial material with Te, Zn, and Sn was investigated, but the major effort was spent on lowering the impurity concentration, and nominally undoped material was n-type in the range 10^{16} cm^{-3} or lower. Cells were made in this nominally undoped material by diffusion of Zn or Cd in a sealed quartz ampoule at temperatures generally around 800 to 850° C, to produce shallow junctions (typically 1 μm). Difficulty was encountered in controlling the results of the diffusion process, and this was ascribed to compensation in the starting material.

Contacts to the GaAs base were made with vacuum-evaporated Au-Sn alloy, and to the surface of the GaP by vacuum-evaporated Ag. Most cells were then etched in aqua regia (with the contacts masked) to improve I_{sc}, presumably by reducing surface recombination and layer thickness. Antireflection coatings were not used. The cells generally had areas of 0.1 to 0.5 cm^2, and measurements were made of electrical properties over a temperature range of 25 to 500° C, and of spectral response. Two distinct families of cells were made by apparently identical processing. One cell type exhibited only the intrinsic spectral response, with a peak at 4700 Å, corresponding to the expected E_g, while the second showed principally an extrinsic response, with a broad peak at 7000 Å. The intrinsic cells had V_{oc} values 1.0 to 1.35 V and I_{sc} values of 2 mA · cm^{-2}, whereas the extrinsic cells had V_{oc} values around 0.7 V, and I_{sc} values up to 5.0 mA · cm^{-2} in 94 mW · cm^{-2} sunlight. The best cell was of the extrinsic type, with an efficiency of 2.5%, and the best intrinsic cells had efficiencies of 1.1%. The intrinsic cells were found to have V_{oc} values less than theoretically predicted, but the rate of fall in V_{oc} in both cell types was found to be close to the theoretical value of 3×10^{-3} V · °C^{-1}. Thus it was verified that the intrinsic cells were capable of operation up to 350°C, at which temperature the best V_{oc} value seen was 0.4 V.

This work therefore confirmed that GaP cells could indeed exhibit extrinsic response, but could also be made to behave in a wholly intrinsic fashion. This should be contrasted with the behavior of CdS cells, which have E_g=2.4 eV, but which always exhibit extrinsic behavior with an effective E_g=1.2 eV. The Monsanto work did not make clear the nature of the mechanism of the extrinsic response, though there is no reason to doubt that this would be a two-step excitation, either involving one thermal and one optical transition (after Grimmeis) or two optical transitions. The nature of the impurity causing the intermediate level was not known, but it was provisionally identified as due to oxygen. It is notable that a photovoltaic response from the GaAs-GaP interface was sought and not found; its absence is surprising. However, experimental results with cells from which part of the base GaAs had been removed appear to rule out the possibility that the extrinsic response arose at this heterojunction.

In the follow-on contract (324,325) further work was done along the same lines, a major effort being made to form high-purity GaP. The cell efficiencies were improved slightly, the best intrinsic cell having an efficiency of 1.3% under sunlight at room temperature, and a V_{oc} = 0.44 V at 350° C, with an area of 0.14 cm^2. The good high-temperature behavior of these cells suggested their use under concentrated sunlight, and the efficiency was found to increase markedly under high-intensity illumination, a value of over 5% being found at 400 $mW \cdot cm^{-2}$, compared with 1.3% for the same cell at 80 $mW \cdot cm^{-2}$. The efficiency improvement was due to a rapid rise in I_{sc} above 300 $mW \cdot cm^{-2}$. This cell was made on alloy material with composition $GaAs_{0.43}P_{0.57}$. The cause for the superlinear dependence of I_{sc} on illumination intensity was not known. For normal use, however, the cell efficiencies remained low, so that the work was discontinued, and there has been no work on GaP solar cells done in the West for the past two years.

However, recent reports have been made indicating that Gutkin's group at the Joffe Physicotechnical Institute at Leningrad, who worked for some years on GaAs cells (see above), have now taken an interest in GaP-GaAs cells. In 1965, Kagan et al. (326) reported experiments similar to those done by the RCA and Eagle-Picher groups some years earlier. However, the junction diffusion followed the GaP layer formation in the Russian work, the converse sequence being used in the US work. The GaP layer was formed by replacing As with P by diffusion into GaAs base material, a layer 5 to 7 μm thick being formed which was graded from pure GaP at the surface to pure GaAs in the base. The junction-formation diffusion was done with Zn in a sealed quartz ampoule, and a range of junction depths were produced. On measuring the spectral response of these cells, it was found that the response curve peak shifted progressively from 4700 Å (corresponding to the E_g for GaP) to 8500 Å (corresponding to the E_g for GaAs) as the junction depth increased. This correlated well with the results one would expect for this series of experiments. The temperature dependence of the cell behavior was measured from 40 to 180° C, and the I_{sc} was found to increase linearly over this range, as would be expected. The V_{oc}, however, showed a broad maximum of 0.65 V around 100 to 120° C for some cells, and this indicated that two competing processes were probably occurring, one the normal degradation in V_{oc} with increasing I_o on increase of temperature, the other a mechanism depending on the presence of traps and associated with thermal transitions in the bandgap of the GaP. Cell areas and conversion efficiencies were not quoted.

Cells similar to those made by the Monsanto group were reported by Alferov et al. in 1965 (327). In this case, the GaP was grown as an epitaxial layer on a GaAs wafer, by the halide-transport process used by the Monsanto group, but instead of the usual open-tube system, a sealed quartz ampoule was used. This contained the source wafer in a zone maintained at 700° C, with the source (polycrystalline GaP) in a zone maintained at 900° C, and $CdCl_2$ to provide dopant (Cd) and transport agent (Cl); the process details were given in (328). The spectral response curves, however, showed that in contrast to the Monsanto cells, the Russian devices had the

p-n junction formed between the p-type GaP and the n-type GaAs, so that the spectral response was remarkably constant over the range 1.3eV (band-edge for the GaAs) to 2.2eV (band-edge for the GaP; photons with energy >2.2 would be absorbed in the surface of the GaP and would thus not reach the active junction). The devices had $V_{OC}=0.5$ V, and showed a linear dependence of I_{SC} on illumination intensity.* Device areas were not quoted, and the given efficiency of 8% (for operation under "white light") is not consistent with the other data ($V_{OC}=0.5$ V, illumination of 1.5×10^{-5} W, matched load resistance 400 kilohms).

Further Soviet work on GaP-GaAs devices was reported by Gutkin et al. in 1966 (329). This work was done on devices made by diffusing P into GaAs wafers, however, and thus implies a reversion to earlier techniques. Spectral response curves with two peaks (one at the GaAs band edge, one at the GaP band edge) were in general obtained, and the measurements were taken out to photon energies of 5.4 eV. In contrast to the measurements on GaAs cells (318), these measurements showed no evidence for quantum efficiencies >1 for the absorption of high-energy photons, and this was correlated with the differences between the band structures for GaP and GaAs.

This then is the present status of GaP and GaP-GaAs cells. The GaP cells show extrinsic response in some cases; this implies that the material may be worthy of further investigation, a point which will be taken up later in this work. Intrinsic GaP cells appear to have no applications at the present time, and their efficiencies cannot be expected to ever be greater than 10%. GaP-GaAs cells have generally shown low conversion efficiencies, but it appears that this is due mainly to poor materials technology, and that further development of the epitaxial growth processes which have proved so successful for GaAs, may offer further possibilities for improvement in this type of cell.

3. Other III-V Compounds

Little work has been done on the other III-V semiconductor materials compared with that done on GaAs and GaP. Of these other materials, aluminum antimonide (AlSb) has received attention principally because the theoretical efficiency calculations of Rittner, Loferski, and others indicated that the bandgap of AlSb should be close to the optimum for sunlight conversion efficiency (see IV-A-1). The earliest report of photovoltaic phenomena appears to be that of the Czechoslovak worker Abraham (330). Spectral response measurements for photoconductivity and the photovoltaic effect were obtained from polycrystalline specimens, over the wavelength range 0.5 to 1.35 μm and for temperatures from 126 to 295°K. The specimens used were

*Note that in Figure 2 of the original paper, curves 1 and 2 are the inverse of their appelations in the figure captions.

freshly cleaved from polycrystalline ingots, the conductivity type and contacting methods not being indicated. It appears probable therefore that the photovoltages observed were generated either at randomly occurring p-n junctions between crystallites of opposite conductivity type or at metal-semiconductor blocking contacts. The photovoltaic response showed an almost monotonic increase (presumably in I_{SC}) as the wavelength was shortened from 1.3 to 0.5 μm. The photoconductive spectral response was quire different, showing a maximum at around 0.8 μm; the reason for this difference was not clear. Abraham also noted that photosensitivity was lost within a few days after cleaving and could not be restored by etching.

This phenomenon is the greatest drawback to the practical application of AlSb in devices. The material is attacked by oxygen or water vapor to form Al_2O_3 or $Al(OH)_3$. The oxide forms a tenacious surface layer on single crystals, and the hydrate causes polycrystalline material to decompose, although single crystals are attacked only slowly. This phenomenon occurs even if the AlSb is stored under normal high vacuum ($\sim 10^{-6}$ Torr), so that it is extremely difficult to prepare material even for experimental use. It is not surprising, therefore, that there was little work done on AlSb for some years, while the other III-V compounds were worked on widely.

However, during the period June 1960 to June 1962, much progress was made in advancing the state of the materials technology art for AlSb, under a USAF-sponsored program at Electro-Optical Systems, Inc., Laboratories in Pasadena (331). The greater part of this work was done in developing crystal growth methods and slicing, etching, and diffusion techniques for AlSb. Only an outline of this side of the work is given here; the Final Report on this work contains a great deal of detail on the technology involved, and the reader is referred to this if such detail is required.

Commercially available aluminum was not of sufficient purity for semiconductor use, so that purification methods were evolved to provide suitable starting material. These involved a zone-refining step, which removed all impurities but oxygen and magnesium. These were removed by heat-treating the aluminum for 20 to 40 hours at 1000° C under high vacuum; the Mg evaporates, and most of the surface covering of oxide is also lost.

Special Czochralski crystal-pulling equipment was developed to allow Sb to be added to the molten aluminum at the end of the heat-treatment cycle, the seed to be immersed in the melt, and crystal growth to be completed, before the material was exposed to oxygen. At the start of the work, single-crystal AlSb was not available as seed material, and single-crystal growth was eventually obtained by selection of larger and larger crystals from polycrystalline boules from successive growths. Difficulty was also encountered in containing the molten AlSb, and only pure alumina

crucibles were found to be capable of withstanding attack by the melt. Nominally undoped AlSb was always p-type, and n-type crystals were made by doping the melt with Se. It was found that if slicing could be performed fairly rapidly (a few minutes) normal wafer-cutting techniques using water could be employed, the attack on the AlSb being fairly slow. Various etches for dislocation detection, crystallographic identification, and polishing were developed.

Measurement of conduction parameters showed a maximum resistivity of 3 ohm • cm in the purest p-type material, which was believed to contain residual copper. The n-type material was, of course, compensated, and resistivities up to 4.5 ohm · cm were obtained. The highest Hall mobility for holes was 440 $cm^2 \cdot V^{-1} \cdot sec^{-1}$, whereas electron mobility in n-type material was found to be only 50 $cm^2 \cdot V^{-1} sec^{-1}$, reflecting the compensated nature of this material. Carrier lifetimes were found to be short, 1 nanosec or less. Optical measurements showed results supporting the belief that AlSb is an indirect energy-gap material.

A large number of diffusion experiments were performed, using Se, Te, and Sn as n-type diffusants, and Zn and Cd as p-type diffusants. All diffusion was performed in sealed quartz ampoules. Various difficulties with separate-phase formation were encountered with Se and Te as diffusants. Only certain of these materials were found to make satisfactory photovoltaic junctions, however.

Ohmic contacts also proved to be difficult to achieve, presumably because of Al_2O_3 surface films. The best results were obtained with pure In or Cd to p-type material, and In-Se alloy to n-type applied by a soldering iron. All vacuum-evaporated contacts proved to be rectifying, and plated contacts were also unsatisfactory.

Device fabrication proved to be a formidable problem. Diffused junction diode characteristics were obtained which showed A values >2, as for most other materials, so the device characteristics were not unusual to any great degree. From the forward and reverse characteristics, the presence of a deep-lying level in the energy gap was deduced, but this is also not necessarily of great significance. However, although photovoltages above 0.6 V were obtained with point contacts, the application of large-area contacts to the back of the cells, and small ohmic contacts to the diffused surface, in every case caused a major reduction of photovoltage value. Although some I-V curves were obtained under illumination, the I_{sc} values were very small, and cell efficiencies never exceeded 0.5%.

The EOS work may be contrasted with a program of development for AlSb run at RCA Mountaintop during 1964-66, under NASA funding (332, 281). The RCA group worked with AlSb purchased from a commercial supplier (Bell and Howell), and hence the emphasis of the work was on cell fabrication rather than materials preparation. The problems of diffusion encountered in the EOS work were also met, diffusants being found to form separate-phase compounds by reaction with Sb, leaving a surface deposit which interfered with diffusion and degraded cell

performance. Both n-and p-type base material were used during the earlier work, but later work concentrated on n-type. Sealed-ampoule diffusion was used, with Zn as a diffusant for the most satisfactory cells. It was found that for the short diffusion times used, the diffusion depth was much less than that calculated from published diffusion-constant data, and the actual junctions were about 2 μm below the surface. The early work (332) produced cells with V_{OC} values up to about 0.7 V, and I_{SC} values up to 3.5 mA $\cdot$ cm^{-2}, but low I_{SC} values for most of the cells, and the I-V curve shapes, showed that blocking rather than ohmic contacts were being obtained. Various contacting techniques were investigated, including silver-epoxy, evaporated Ti-Ag followed by sintering, and evaporated Al followed by sintering, for both n-and p-contacts. Because of this problem cell efficiencies were less than 1%. Further work on the contact problem eliminated the double-junction effect by using Pb applied by ultrasonic soldering to the n-type base. The diode characteristics were also improved by post-diffusion etching to remove surface layers. Although efficiencies of somewhat less than 3% were achieved, these cells were found to be highly unstable, degrading in V_{OC} after only a few hours either in air or in a dessicator. Further, the junction characteristics were found to be very sensitive to edge treatments on the cells (i.e., treatments of the regions where the junction comes to the cell surface), indicating that leakage effects were a major problem; the same observations were also made in the EOS work. Spectral response measurements were made on these cells, and the results were as would be expected from the known optical absorption curve for the material. The cell efficiencies obtained were thus rather low, and the materials technology problems highly intractable, so that further work on AlSb cells has not been done. This is the present status of work on AlSb cells; bearing in mind the nature of the material, it is remarkable that even this modest success should have been achieved.

The remaining III-V compound with an energy gap in the range in which good solar conversion efficiency should be obtained is InP. The first work aimed at developing solar cells of this material was done at RCA Laboratories under a Signals Corps contract, starting in 1955 (186). Since starting material was not available commercially, ingots were grown in-house by melting the elements in a quartz tube with two temperature zones, the lower temperature controlling the P pressure. Polycrystalline p- and n-type material was obtained, with a high carrier concentration. Diffusion was used to prepare p-n junctions, Cd, Zn and Hg being used as p-type dopants, and the best results were obtained with the latter. The best cell obtained showed V_{OC}=0.74 V (cell area 0.2 cm^2), and a conversion efficiency of about 1%.

The cell performance was severely limited by high series resistance arising in the contacts. Some photosensitive diodes were also made by alloying Zn onto the crystal surface, but such devices were for experimental purposes only. At the time, experimental effort and results were limited by the lack of good single-crystal InP. The situation remained thus for some years, as reported by Rappaport in various papers up to 1961 (240, 190, 333, 334).

Nothing further appears to have been done on InP cells until the recent report of experimental results by Galavanov et al. at the Joffe Institute in Leningrad (335). With the general advances in compound semiconductor technology which had been made since the early RCA Laboratories' work, a big advance in cell performance was to be expected. Even so, the reported cell areas were only of 0.1 cm^2, prepared by Zn or Cd diffusion into n-type single-crystal base material in a sealed quartz ampoule. Under solar irradiation of 70 $mW \cdot cm^{-2}$ the device showed $V_{oc} = 0.74$ V $I_{sc} = 10$ $mA \cdot cm^{-2}$, and efficiency of 6.7%. The spectral response was also measured, and showed the expected from, with a sharp rise in response for photons with energy slightly greater than that corresponding to the band edge. However, a rapid loss of collection efficiency on going to higher photon energies (i. e., loss of blue response) indicated a deep junction, implying that the cells would be capable of considerable development to provide better efficiencies. The tone of this Russian report indicates that further work can be expected in this area, and this group appears to be alone in this field of research at the present time.

The remaining III-V compounds for which photovoltaic effects have been reported are InSb and InAs. These materials both have small energy gaps (InSb, E_g=0.167 eV; InAs, E_g= 0.35 eV) so that good solar conversion efficiencies cannot be expected, and both materials are of interest primarily as infrared detectors. However, for such use the device temperature for InSb must be reduced to suppress the intrinsic conduction which is appreciable in this material at room temperature.

Results with alloyed junctions produced with Cd and In dots on n-type InSb were reported by Galavanov in 1959 (336). The diode characteristics and photovoltaic response were measured over a temperature range from 300 to 77°K, and the results showed that the photovoltage reached values of between 10 and 20 mV at 77°K and decreased rapidly at temperatures above 167°K.

Results with InAs were reported by Gutkin in 1967 (337). This work was aimed at spectral response measurements in the range of photon energies $h\nu >> E_g$, to provide information on impact-ionization studies. The cells were made by diffusing Cd into n-type single-crystal InAs with a carrier density 0.5 to 1.0 x 10^{17} cm^{-3}. The spectral response data were taken at temperatures of 100 and 295°K, and the response near the band edge was as expected, a sharp rise being seen in photocurrent for photon energies increasing beyond 0.4 eV. For photon energies > 0.8 eV, a further rise in quantum efficiency was seen, which continued to the limit of the measurement spectral range at 4.8 eV. This rise in quantum efficiency was attributed to impact ionization by electrons which have large energies imparted to them by photons with energies $h\nu > 2 \times E_g$. The results therefore correlate with the observations of this effect in GaAs, by Gutkin (318) and CdTe (341, 342) by Dubrovskii.

4. Cadmium Sulfide

The second major group of compound semiconductors from which photovoltaic cells have been successfully made is comprised of the II-D compounds. In several cases the materials technology of members of this group is particularly well suited to the achievement of reasonable semiconducting properties in polycrystalline thin films. Hence, a good deal of the research on these materials has been done on thin-film cells, notably CdS and CdTe, and an account of this work will be found in a later section of this work. However, the initial work on CdS and CdTe, and a proportion of the subsequent work on these materials, was done on single-crystal or polycrystalline wafers of the semiconductors, and an account of this work will now be given.

The earliest of the II-VI materials to be worked on was CdS. An account of Reynold's discovery of the photovoltaic effect in CdS in 1954 has been given in Section III-C-3. Following this discovery, a program of research and development aimed at producing CdS cells for energy conversion, for use on the Vanguard satellite, was initiated at the Aerospace Research Laboratory where Reynolds' work was done, and with outside laboratories under USAF funding. Exploratory work was done at the Harshaw Chemical Company Research Laboratories in 1954, cells with efficiencies up to 1% being made (349)*, and this work revealed the need for better starting material. Work aimed at providing this was done at Clevite Laboratories, Eagle-Picher Laboratories, and at Harshaw. By 1957, three growth methods had been developed.

(i) The reaction of Cd vapor with H_2S at 950° C to produce needles and small platelets.

(ii) The growth of large crystals by sublimation from a powder starting material, in a sealed tube at about 1000° C, the crystals forming slowly on the cooler parts of the tube: this method had been developed initially by Reynolds.

(iii) The growth of crystals from the melt, a process made difficult by the high temperature required (1750° C), and the high pressure needed to prevent sublimation from the melt (100 atmospheres): this process was worked on by the Eagle-Picher group.

*This reference contains a brief historical account of the early work on CdS, and Shirland notes that most of this work was never published. Hence, this reference has been the only available source for some of the early work, except for Reynolds' publications referenced above.

Method (ii) proved to be the most applicable to solar cells, and by 1960 the process had been refined to produce fairly reproducible results and large crystals. The process used by the Harshaw group in 1960 consisted of:

(i) A sintering step in which the purest available starting material (usually 'luminescent grade' CdS) in powder form was heated to ~ 600° C under vacuum until outgassing stopped: this process removed water vapor, free Cd, and other impurities.

(ii) A crystal growth step in which a charge of sintered material was heated in a sealed tube filled with inert gas (e.g., N_2) at a temperature of ~ 1275° C, and CdS crystals were formed on the cooler parts of the tube (~ 1260°), the growth taking place over a period of some days. The details of this process were reported by the Harshaw group (350). Various dopants were used to give the required conductivity, the most successful impurities being $InCl_3$ and B. It may be noted that p-type conductivity in CdS has never been observed conclusively; most work has been done with In-doped n-type base material, mainly because this appears to give the most reproducible results in the desired range, and to introduce the minimum number of extraneous effects.

The Harshaw work developed various methods for making the photosensitive barrier contact to the CdS. All of these involved depositing either metallic copper or a copper compound (e.g., Cu_2O or Cu_2S) either by vacuum evaporation or electroplating. The best results up to 1960 were obtained by electroplating Cu onto the cell surface using a strongly acidic plating bath, to produce a layer of finely divided copper particles which were then oxidized, followed by a final processing step at 300 to 350° C for 10 to 20 seconds. These cells were of the rear-wall type; i.e., the illumination passed through the CdS crystals to the junction, the active region being on the unilluminated side of the cell, the converse of the normal silicon-cell practice. For this reason, ohmic contact to the base CdS was made by means of a 'picture-frame' electrode, to allow the maximum transmission of light into the cell. The exact nature of the barrier was not known at the time, though it was postulated that a very thin surface layer of p-type CdS containing cuprous ions was present. The cell performance measured at this time showed efficiencies of 5%, with V_{oc}=0.5 V and I_{sc}=13.5 mA · cm^{-2} under 122-mW · cm^{-2} illumination. Spectral response measurements on rear-wall cells showed an onset of photovoltaic response at wavelengths between 7500 Å and 8500 Å, and a sharp cut-off at 5200 Å, caused by absorption in the base CdS. Some front-wall cells were also made, in which sufficient Cu_2O was etched away from the barrier layer to allow illumination on this side of the cell to penetrate to the junction. In these cells, the spectral response showed the anomalous extrinsic response described above, and added to this was the expected intrinsic response of the CdS absorption, which extended the response to wavelengths less than 3000 Å, with a peak around 4000 Å. The efficiency figures given in (350) are those for typical cells, it should be noted. As early as 1958, the Harshaw group had obtained efficiencies up to 7.6% under 100 mW · cm^{-2} sunlight in cells 1 x 1 cm, with V_{oc} = 0.5 V.

Early interest in the extrinsic response of CdS cells was shown by several workers. Reynolds (351) proposed that the response arose from the presence of an intermediate energy level in the forbidden band of the CdS, electron-hole pairs being created by excitation of electrons from this intermediate level into the conduction band. However, to account for both the photovoltaic and photoconductive phenomena seen in CdS, Reynolds proposed that it would be necessary for this intermediate energy level to form a band rather than a set of spatially separated levels. Reynolds' experimental work had showed that the prior illumination history of the cell partially determined the photocurrents seen, and this observation correlated with photoconductivity results reported by Lashkarev et al. (352-354) in which conductivity quenching by IR, and photoconductivity enhancement with prior illumination with green light, was seen. Further work on the spectral response of the photovoltaic effect was reported by Woods and Champion of GE Laboratories, England (356). Correlating measurements on the photoconductivity and photovoltage in copper-doped CdS these workers also concluded that impurity band conduction was occurring. They also reported the first published results on bias light measurements, in which the crystal was illuminated simultaneously by two separate monochromatic sources at different wavelengths (7000 and 9000 Å), and the photogenerated current induced by 7000 Å illumination was found to be remarkably increased by a comparatively small amount of illumination at 9000 Å, to the degree that one photon of 9000-Å light was found to increase the photocurrent as much as four photons of 7000-Å light. (The peak of the spectral response curve lay at 7000 Å.) This enhancement effect was ascribed to an increase in the lifetime of free holes, the minority carriers in the n-type base material.

An alternative theory to account for the extrinsic photovoltaic response of the CdS cells with supporting experimental results, was first advanced by Williams and Bube (357). The experimental results were obtained with barrier contacts formed by electroplating copper and other metals, onto n-type CdS crystals. No heat treatment was used in the processing of these contacts, and, hence, it was felt that the diffusion of copper into the CdS was wholly absent, and the junction was purely a metal-semiconductor barrier. Spectral response measurements showed that the extrinsic photovoltaic response was present in these cells, though to a smaller degree (compared with the intrinsic response) than in the copper-diffused junctions being made by the CdS solar-cell groups. However, it was shown that the response in the extrinsic wavelength region increased as the copper thickness was increased (the thinnest copper layers were optically transmitting), indicating that the carriers photoexcited across the barrier were electrons photoemitted from the copper into the CdS. However, photoemission can be checked by the use of the "Fowler Plot" showing photocurrent as a function of photon energy at the threshold of photoemission (358). The form of the experimental curve obtained by Williams and Bube was of the shape expected for photoemission, but indicated a threshold wavelength of the onset of photoemission corresponding to 1.1 eV, whereas the same threshold calculated from the photoconductivity data was 0.4 eV, and the discrepancy could not immediately be explained. Further, Williams and Bube found that the extrinsic response of the cells was much reduced on heat-treating the cells in a manner similar to that used to enhance the response

in solar-cell manufacture. Thus, there existed some doubt whether the positive identification of photoemission in the specimens of Williams and Bube proved that this was also the basis of operation for the CdS solar cells.

Experimental results on photovoltages seen when metal contacts to CdS were unequally illuminated were reported by Kallman in 1960 (359). Voltages up to 0.2 V were obtained, but the response was seen only for illumination with photons of energy near to or higher than the fundamental absorption edge of CdS. Hence, this effect was not of great significance for the development of CdS solar cells.

Results of Russian work on CdS photovoltaic cells were reported by Paritskii et al. in 1961 (360). Those were concerned with the response time of the cells under pulsed illumination, and the authors supported the photoemission mechanism of Bube and Williams.

Bockemuehl et al. studied photovoltaic, photorectification, and field-effect modulation properties of junctions formed by diffusing Cu into photoconductive, dark-insulating CdS crystals (361). The results indicated that in these junctions two barriers existed, one at the metal-semiconductor surface, the other in the semiconductor bulk. Under reverse bias, the space charges associated with these barriers altered to give a single dipole space-charge region, a condition which could be produced by application of a bias of less than 1 V.

It was found that under monochromatic illumination by light of a wavelength which created hole-electron pairs and thus caused a photovoltage, V_{OC} values of 0.2 to 0.4 V were seen. When a second monochromatic beam of IR was added, the V_{OC} rose to 0.5 to 0.6 V and I_{SC} also increased. However, under reverse bias sufficient to redistribute the space-charge, the IR was found to quench the photoconductivity arising from the main illumination. These effects were ascribed to the IR increasing the drift mobility of the holes by causing detrapping, which would aid the collection of the minority carriers (holes) in the photovoltaic effect, but cause a loss of space-charge in the space-charge region, leading to a reduction in photoconductive gain. [For an account of the mechanism giving photoconductive gain by minority-carrier trapping, see Bube (363).] Thus, the results of Bockemuehl et al. in providing evidence for photoexcitation from intermediate levels in the forbidden bandgap, tended to support Reynolds' proposal for the origin of the extrinsic response in CdS photocells, rather than the photoemission mechanism of Williams and Bube.

By measuring photovoltages produced when a fine light spot was moved across Cu and blocking Au contacts deposited on an n-type CdS crystal, Fabricius (370) obtained evidence that the generation of the photovoltage was localized in the depletion region of the Au-CdS contact, thus indicating that the mechanism of Williams and Bube was not responsible for the photovoltaic effect in these specimens. Since the

Au-CdS and Cu-CdS contacts were produced by vacuum evaporation followed by heat-treatment to cause diffusion, whereas Williams and Bube had avoided any diffusion in preparing specimens, it was to be expected that the results of the two sets of experiments should be different.

The operation of CdS cells was also analyzed by Grimmeis and Memming in 1962 (371). Experiments were performed using diodes made by diffusing Cu, Ni, or Ag from evaporated films deposited on n-type crystals of about 1-ohm · cm resistivity, followed by removal of the remaining metal layer by etching. Thus, it was felt that the specimens could contain only p- and n-type semiconducting regions, and no metal-semiconductor barriers. It was concluded that the photovoltaic effects measured in these specimens occurred at p-n junctions, and the device I-V characteristics were shown to be consistent with this. However, the question remained whether this was a junction between p- and n-type CdS, or between n-type CdS and some other semiconductor material (i. e., a heterojunction). The correlation between the spectral responses for the photoconductive and photovoltaic effects in CdS was felt to eliminate the need for any other type of material being active in the photovoltaic effect, since the photoconductivity was a bulk effect in the CdS, and there was no suggestion that this was in any way associated with the presence of another semiconductor material. It was concluded that the extrinsic response must arise from transitions from an impurity band in the CdS bandgap, as suggested by Reynolds. The model proposed consisted of a junction between normal n-type CdS base material, and a region of p-type CdS having an impurity band in the forbidden energy gap, the band arising from the presence of a high density of levels in the middle of the CdS bandgap, introduced by the Cu dopant.

In 1963, Spitzer and Mead (372, 373) reported work tending to support Williams and Bube's conclusion that the extrinsic response in CdS cells arose from photoemission of electrons from a metal into the CdS. Spitzer and Mead used specimens prepared by cleaving n-type CdS crystals in an evaporant stream of metal, under high vacuum. Thus, it was felt that the contacts produced in this way should be free of contaminant effects introduced by interaction between the CdS and the atmosphere, whereas in earlier work such interactions could reasonably be expected to arise, and lead to surface states which would modify the energy band structure at the junction. Diode I-V characteristics, spectral response, and capacitance-voltage measurements, were made on the specimens. Determinations of the barrier height at the junction from these measurements were consistent and showed that the value of the barrier height was related to the work function of the metal used to form the barrier. The experiments covered a range of metals from Pt (which produced a barrier height of 0.85 eV) to Al (which produced an ohmic contact, barrier height < 0.10 eV). Some measurements were also made on specimens produced by depositing the same metals on CdS cleaved in air, and for these, much less correlation between work function and barrier height was found. This indicated the presence of surface states, which would affect the barrier height by the mechanism discussed by Bardeen, as described in Section III-D-2. The consistency of the

barrier-height values measured in the vacuum-cleaved specimens suggested that the junctions produced in this way were of the metal-semiconductor type, with no intermediate region of opposite conductivity type, or of a different material. Thus, the extrinsic response must arise from photoemission, as proposed by Williams and Bube.

Further experimental evidence relevant to the debate on the mechanism of the CdS cell was presented by Palz and Ruppel in 1964 (362). Photoconductivity and photovoltage responses were both measured in the same samples, which consisted of CdS vapor-grown platelets with one ohmic In contact and one evaporated blocking contact of Te, Au, or Ag. The electrodes were 0.75 mm apart, on the same side of the crystal, and the specimen was illuminated on this same side. The crystals were high-resistivity photoconductive CdS, with a dark resistivity of 10^{14} ohm · cm. The photocurrent was measured with a 6-V applied bias, and the open-circuit photovoltage was measured without external bias. The illumination system used two light sources, one with a fixed wavelength, obtained with an optical filter, the other varied by use of a monochromator. The results showed that the photoconductivity induced by the fixed-wavelength light was quenched by the light of variable wavelength, photoconductivity minima being found for quenching light of wavelengths 9500 and 14,600 Å regardless of the fixed-wavelength used. The converse results were found for the photovoltage measurements, the photovoltage reaching maxima for variable-wavelength light which produced photoconductivity minima, and again the wavelengths of these maxima and minima were independent of the fixed-wavelength used, though the absolute values changed for different fixed-wavelengths. These results were explained by proposing that the photoconductivity quenching and photovoltage enhancement were both caused by the freeing of holes by the variable-wavelength light. This would occur because photoconductive gain is dependent on the minority carriers being trapped (363), whereas photovoltages are generated by mobile minority carriers.

The conclusions follow the experimental results seemingly inescapably, and thus the work of Bockemuehl et al., and Palz and Ruppel, supported Reynolds proposition that photoexcitation from intermediate energy levels existing in the forbidden bandgap formed the basic extrinsic response mechanism for CdS cells. However, the experiments were performed on crystals of a type very far removed from those used for cell manufacture, so that a strict correspondence between the two situations cannot be assumed.

The theory of photovoltaic effects which could be seen in photoconductive materials was considered by Keating (364), working from the assumption that the photo-induced minority- and majority-carrier densities were high compared with the dark concentrations. (The normal semiconductor photovoltaic theory assumes that the photo-induced majority-carrier density is small compared with the dark majority-carrier density.) The theory was first established in general terms, and then applied to heterojunctions and homojunctions in photoconductors, and to junctions

between photoconductors and semiconductors. Keating then discussed the relationship between the theory and reported measurements and postulated mechanisms in CdS cells, and concluded that the most likely explanation of CdS cell operation would be based on the existence of a CdS-Cu_2S heterojunction. However, it was felt that the physical situation in the real cells was so far from the idealized junction structures analyzed in the theory that such an identification was tentative only.

With the demonstration of the success of the thin-film CdS cell by groups working at Harshaw Laboratories and Clevite Laboratories, research and development of cells intended for power generation has been concentrated on these, rather than on the single-crystal cells. Further work on the theory of CdS cells has also been done with special relevance to the thin-film CdS cells; this is dealt with in the next section of this report. However, as shown by the above account, considerable work has been done on single-crystal cells, aimed at elucidating their mechanism of operation. It will be appreciated from this account that considerable controversy exists on this subject, and no doubt research and analysis will continue for some time before a conclusion is reached.

5. Cadmium Telluride

The earliest work directed toward the use of CdTe in solar cells was that done under Signals Corps funding at RCA Laboratories, starting in 1955 (186). Since the theoretical efficiency calculations showed that the energy gap of CdTe lay close to the optimum for solar energy conversion, a major interest was taken in this material. As for most of the semiconductors investigated under this contract, suitable material was not available commercially, and consequently a good proportion of the experimental effort was put into growing crystals from which photovoltaic cells could be made. CdTe polycrystalline ingots were prepared by reacting the constituent elements in a graphite boat sealed in an evacuated quartz ampoule. The graphite boat was found necessary to avoid attack of the quartz by the melt. Gradient freezing was used to form the ingots, which were made in both conductivity types, the type being determined by the stoichiometry of the material (loss of Cd giving p-type conductivity), as well as by the presence of impurities. (This stoichiometry dependence of conductivity type is unusual, since the solid solubility of the constituent elements in a compound semiconductor is usually very low indeed, so that departures from stoichiometry result in the formation of a separate solid phase. This effect is especially pronounced in GaAs.) The CdTe initially produced was of high resistivity (~ 1000 ohm· cm), but improvements in the purity of the starting materials, and the provision of the graphite boat, enabled the resistivity to be brought down to ~ 30 ohm· cm. Diffusion of Au, Ag, and Cu into the CdTe was performed from layers of these metals deposited on the crystal surface, in a sealed quartz ampoule. The results were complicated by the loss of Cd from the CdTe, causing conductivity type inversion, for diffusion temperatures above 700° C. However, by adding excess Cd to the diffusion ampoule, and by limiting the process

temperatures, some photosensitive p-n junctions were prepared. These showed V_{oc} values up to 0.55 V, but the I_{sc} values were extremely small (microampere range) because of high series resistance in the devices, arising from the low conductivity of the base material.

Another early report of the photovoltaic effect in CdTe was given by Van Doorn of Philips Laboratories, Eindhoven, in 1956 (338). From the specimen preparation procedure given, it appears that the junction may have been a metal-semiconductor barrier rather than the p-n junction claimed by Van Doorn, since the contact was apparently formed by allowing $AuCl_3$ solution on the surface to react with the CdTe, followed by removal of the $AuCl_3$ by KCN. However, the spectral response results shown by Van Doorn show a good photovoltaic response with a sharp rise in V_{oc} at photon energies slightly less than 1.5 eV, corresponding to the band edge of the CdTe. These measurements were made over a range of temperatures, and were used to calculate the change in E_g with temperature.

An early Russian interest in the work was reported by Lomakina et al. (339). Cells were made on n-type polycrystalline wafers to 1 to 2 cm^2, by diffusion of elements from Group I of the periodic table. (Specific elements used were not indicated.) Spectral response measurements indicated an energy gap value of 1.34 eV, rather less than that reported by Van Doorn. Apparently quite reasonable diode characteristics were seen ($I_o = 7.25 \times 10^{-9}$ A $\cdot$ cm^{-2}, A = 1.65), and the cells showed V_{oc} values of >0.5 V, I_{sc} values of 2 mA $\cdot$ cm^{-2}, and conversion efficiencies around 2% under 30 mW $\cdot$ cm^{-2} sunlight. Such a low illumination intensity would minimize the effects of losses due to series resistance. Further reports of this Russian work appeared in 1960 (340-342) showing a distinct improvement in the cell quality. These devices were made on both p- and n-type single-crystal wafers, by coating the crystal surface with suitable metallic dopants [quoted as Au in Ref. (342)], followed by heating; the remaining metal film was used as an electrical contact to the diffused region, and this film had an optical transmission of $\sim$ 50%. The I-V characteristics shown indicate good diode characteristics, with V_{oc} = 0.65 V, I_{sc} = 8 mA $\cdot$ cm^{-2}, and conversion efficiencies of 4% for operation under 89 mW $\cdot$ cm^{-2} sunlight. The energy conversion performance was measured over the temperature range 110 to 380°K, the efficiency falling to about half of its room-temperature value at $\sim$ 100° C (380°K). Spectral response measurements showed the expected rise at the band edge, but a good response was maintained throughout the range 4000 to 8000 Å, indicating a shallow junction. In Reference (341), a most interesting analysis of the diode characteristic was performed, in which the departures from the diffusion theory of Shockley were discussed. The diode characteristics for deep-diffused junctions were found to fit quantitatively the Sah, Noyce, Shockley theory with recombination-generation in the space-charge region. Shallow junctions, however, were found to show a larger current than theoretically predicted at lower voltages, and this was thought to be due to tunnel current in the narrow junctions produced under these conditions. This explanation of the observed diode characteristics thus closely parallels the account given by Wolf for silicon solar cells (344).

Spectral response measurements into the high-photon-energy region were made by Dubrovskii on these cells (342), and these showed that the quantum efficiency of the devices fell from the band-edge with increasing photon energy up to ~ 4.0 eV, but then increased again at higher photon energies up to the limit of the measurements at ~ 5.4 eV. This was ascribed to impact ionization by the carriers produced on absorption of photons with energies $h\nu > 2 \times E_g$. This work was therefore a forerunner for the results reported by Gutkin in 1965 (318), in which this same pheonmenon was observed in GaAs. Further observations on the optical properties of CdTe were reported by Dubrovskii in 1961 (343), in which impurity response on the low-energy side of the band edge was seen; the results are not of importance for photovoltaic energy conversion purposes. The last report of this Russian work on CdTe solar cells appeared in 1961 (345). The cells were apparently of the same type as before, and the efficiency had been improved to 6%, with V_{oc}=0.75 V, and I_{sc} = 9.8 mA · cm^{-2}, under solar illumination of 77 mW· cm^{-2}; the cell area was ~ 1 cm^2.

Work in the U.S. directed toward the development of single-crystal CdTe cells was performed at the Armour Research Foundation, funded by the Signals Corps, starting in 1959 (346). This work was almost entirely concerned with developing crystal growth, purification, cutting, polishing, and etching techniques, and with investigating diffusion. Diodes were made for experimental purposes, but successful solar cells were not made.

With the demonstration of the feasibility of thin-film CdTe cells, and the start of the GE project to develop these in 1961 (described in the next section), interest in CdTe cells in the US shifted away from single-crystal work.

However, Rodot's group at CNRS, France, reported work on cells made on single-crystal CdTe (347), using the methods developed for use with thin-film cells by Cusano at Ge. Cells were made on n-type single-crystal base material, In doped, by deposition of a thin layer (~ 1 μm) of high-resistivity intrinsic CdTe by vapor deposition onto a CdTe base wafer at 300° C. This was followed by flash evaporation of a thin film of Cu_2Te, which formed a blocking contact to the semiconductor. The diode characteristics and capacitance-voltage measurements made on the cells indicated that the cells contained p-n junctions formed between the n-type base material and a surface p-region formed by copper entering the high-resistivity CdTe film, and providing an acceptor level. The band-structure proposed for the junction was closely similar to the "Mott barrier" discussed in II-C-2,* as shown in Figure 50: d = 1.6 μm, V_o = 1.0 to 1.3 eV, with the degenerate Cu_2Te acting as a metal. The best single-crystal cell obtained had V_{oc} = 0.5 V, I_{sc} = 14 mA· cm^{-2}, and an efficiency of 5%, under 62-mW · cm^{-2} tungsten light (2800°K). The nature of the junction band structure in these calls was further discussed by Rodot (348);

*Second Semiannual Report, NASW-1427.

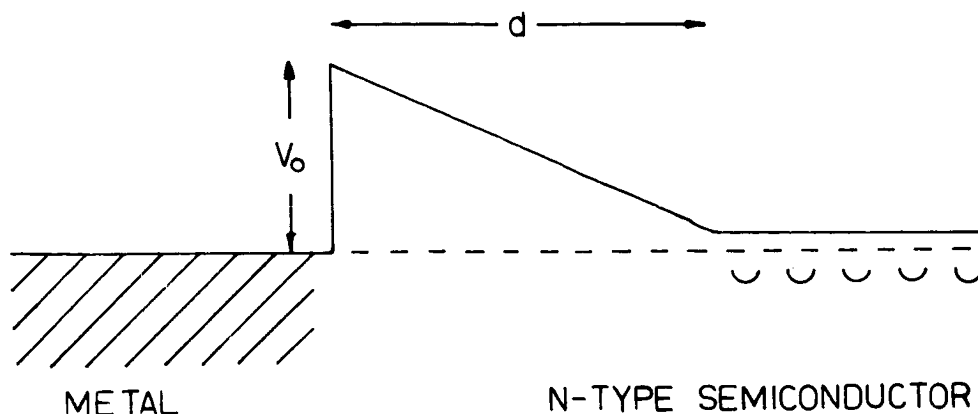

Figure 50. Band diagram of a 'Mott Barrier'

it was concluded that this could behave either as a graded p-n junction or as a metal-semiconductor barrier, depending on the conditions of preparation.

This, then, is the current status of single-crystal CdTe cells. Efficiencies up to 5% have been seen, but these are no better than the thin-film cells made with this material. Since it is considerably easier to prepare polycrystalline thin films of CdTe suitable for photovoltaic device use than to grow single-crystal material with comparable properties, the current state of the technology discourages work on single-crystal cells.

6. Other II - VI Semiconductors

Photovoltaic effects have been reported in other II-VI semiconductors, but without major effort to develop energy-conversion devices. Metal-semiconductor barriers were used to obtain photovoltages in CdSe in a series of exploratory experiments done at RCA Laboratories in 1960 (192). The CdSe crystals were grown by vapor deposition from powdered starting materials, in a sealed tube at about 1000 °C; the method was closely similar to that developed by Reynolds and others for use with CdS, as described above. Very small photocurrents were obtained, and a maximum V_{oc} = 0.04 V was seen. The spectral responses of the devices were measured, showing a long "tail" extending into the infrared. Because of the small photovoltaic responses seen, this work was not pursued further. Recently, however, work in the Ukraine by Komashchenko and Fedorus (365) has indicated an interest in cells made by depositing Cu_2Se barrier layers on n-type CdSe single-crystals. Under 150-mW · cm^{-2} illumination, V_{oc} = 300 to 350 mV, I_{sc} = 30 mA · cm^{-2}, and an efficiency of 3% were obtained. In addition, cells with various metallic blocking contacts were made (Ag, Au, Cu, and Pt). Analysis of spectral response measurements showed that the cells with Cu_2Se barriers, and those with metallic barriers, all behaved as normal metal-semiconductor junctions, and the difficulties associated with explaining CdS-cells did not exist in this case.

Russian work on ZnS single-crystal cells has also recently been reported (366). The samples were prepared on wafers cut from n-type single-crystal ZnS formed by vapor deposition (presumably a development of Reynolds' method for growing CdS crystals). The junctions were formed by vacuum-evaporating a thin layer of Cu onto the crystal surface, followed by a heat treatment at 650°C for a few minutes to cause diffusion of Cu into the ZnS. Measurements of diode characteristics and the spectral response of the photovoltaic effect showed normal results, ZnS having a wide bandgap, and thus responding only to light of wavelength less than 5000 Å. The I-V characteristics showed departures from diffusion theory, with $A \approx 2$ in the diode equation. Because of the wide bandgap ($E_g = 3.9$ eV) ZnS cannot be expected to be applicable to solar energy conversion, from theoretical efficiency considerations.

The remaining compound semiconductor in which photovoltaic effects have been observed is SiC. This material also has a large bandgap ($E_g = 2.86$ eV), and would thus not be expected to be applicable to energy conversion. The measurement of the photovoltaic effect in SiC was first reported in 1957 by Choyke and Patrick (367), who used the spectral response of p-n junctions to determine the optical bandgap of the material. Specimen preparation methods were not given. Russian work on alloyed-junction devices was reported by Kholuyanov in 1960 (368). The spectral dependence of photo-emf was measured over the temperature range 200 to 493°K, and the results were consistent with an energy gap of about 3 eV. The device sensitivity was low, and it was suggested that this was due to surface recombination. Kholuyanov pointed out that such devices might find application as UV detectors for use at high temperatures.

In 1962, Thiessen and Jungk reported observations of the photovoltaic effect in SiC illuminated with light of energy less than that corresponding to the bandgap (369). The cells were made by alloying silicon and aluminum into n-type single-crystal wafers, or silicon and antimony into p-type wafers. The spectral response measurements showed a photovoltage peak at 1.5-eV photon energy, although this was found to vary in some cells, depending on the particular crystal used. It was proposed that photoexcitation of electrons from valence to conduction band was occurring via an intermediate energy level in the forbidden band. The best response obtained showed $V_{OC} = 0.6$ V and $I_{SC} = 0.1$ mA under illumination of $7.5\ mW \cdot cm^{-2}$. The I-V curve shape was good, indicating a good fill-factor, but series resistance effects would be minimized by the low illumination intensity used for the measurement.

As mentioned initially, there is no possibility that the intrinsic photovoltaic response in SiC can be used for efficient energy conversion. However, the extrinsic response described by Thiessen and Jungk implies that this effect could be used for power generation, although there have as yet been no reports of such work. The materials difficulties with SiC are such that almost all the work has been done with alloyed junctions. These are not usually conducive to the manufacture of large-area

devices, but it is not impossible to conceive solar cells made from SiC by this method, and the stability of the material may have relevance to some special applications.

7. Summary

In this section, then, a historical account has been given of the development of photovoltaic cells made from single-crystal (and in some cases polycrystalline) wafers of compound semiconductors. The present status of work with each of the cell types has been described, and it is seen that although none of the cells has exhibited a conversion efficiency or a cost-effectiveness as good as the present commercially available silicon cells, the special properties of most of the cell types offer opportunities which have not yet been fully exploited. For this reason, this field has potential which can only be realized through research. It is for this reason that the US Government agencies have actively supported and contributed to this effort in the past, and the recent increase in Soviet work in this area testifies to similar thinking elsewhere.

D. High Voltage Photovoltaic Effect

The first recognition of the high-voltage photovoltaic effect, and systematic analysis of the effect, was made by the group working under a U.S. Army Signals Corps contract (186) at RCA Laboratories, in the period November 1956 to February 1957. The effects were seen in CdTe thin films deposited on glass substrates, with the evaporant stream during deposition striking the substrate obliquely rather than at the usual normal incidence. Voltages of up to 320 V were developed under illumination, between conducting contacts on the substrate ('TIC coating') ~2 in. apart. The conclusions reached on this effect were:

(i) The oblique deposition of CdTe, ZnS and CdSe produced films showing the effect.

(ii) The photovoltages varied as the logarithm of the illumination intensity.

(iii) The photovoltage changed rapidly with temperature, decreasing with increasing temperature.

(iv) The specimen resistance was high (10^9 ohms/□ or higher), and the characteristic appeared ohmic.

(v) The entire specimen contributed to the effect, the voltage not being developed at isolated regions.

Bearing in mind these observations, it was proposed that the specimen structure was as shown in Figure 51 (a), with the band structure as shown in Figure 51 (b). The voltage was developed by serial addition of small photovoltages arising at the grain boundaries.

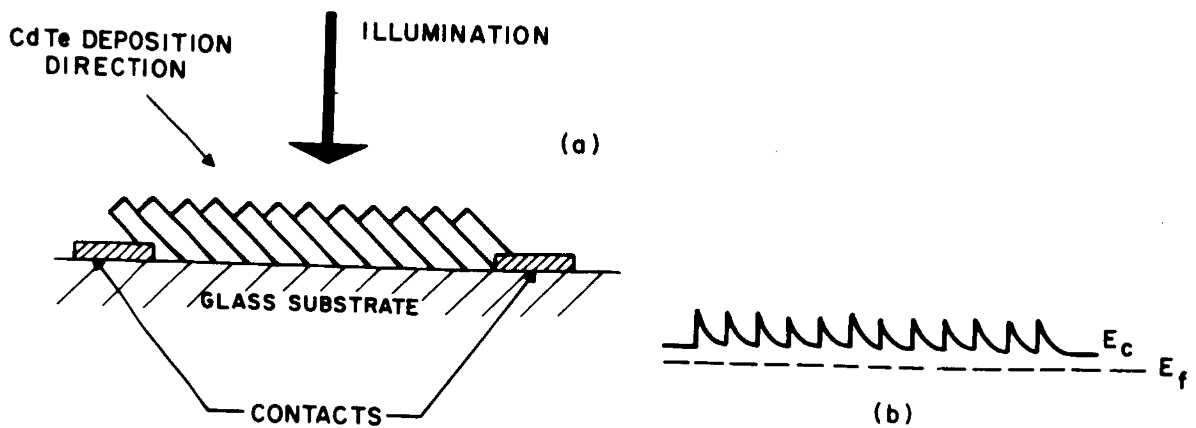

Figure 51. (a) Disposition of crystallites in a CdTe film showing the high-voltage photoeffect, after Pensak. (b) Band structure of a CdTe film showing the high-voltage photoeffect, after Pensak

The results reported exhibited another characteristic seen by all subsequent workers in this field: the voltages measured were highly variable, and could even be reversed in direction by heat treatment of the specimen. Although they did not observe photovoltages in PbS, it was recognized by this group that the observation of photovoltages up to 2 or 3 V in PbS films by Starkiewicz, Sosnowski, and Simpson (374) implied that these workers had seen the effect without realizing fully the significance of a photovoltage greater than bandgap. The RCA group proposed the use of the effect for photovoltaic power generation, although the high resistance of the cells was noted as being a possible problem area. It appears that the work which has been done in succeeding years has added to the range of materials known to exhibit the effect, has elucidated the underlying mechanism to some degree, but has done virtually nothing to bring the application of the effect any closer.

Apparently independently of the RCA Laboratories work, a Russian group reported the observation of larger-than-bandgap photovoltages in PbS films deposited under vacuum at an oblique angle (375). This report showed a photomicrograph of a cross section of one of the specimens used, demonstrating a markedly dendritic surface texture. These workers also found a strong dependence of photo-emf on illumination angle, results showing that the photovoltage could be made to change sign by illuminating the specimen through the glass substrate rather than on the exposed surface. Again, heat treatment was found to strongly influence the behavior of the specimen.

Following the initial work done at RCA Laboratories, continuing interest and progress was shown by those associated with this group, resulting in a series of publications during 1958. Pensak (376) published the results noted above for CdTe as did Goldstein (377), and these workers reported more fully on their results in 1959 (380) while Merz (378) and Ellis et al. (379) reported on effects seen in single-crystal wafers of ZnS. The latter reports take particular concern of the mechanism underlying the effect. Crystallographic studies of the vapor-grown ZnS platelets used as specimens showed that the (111) crystallographic direction always lay parallel to the plane of the platelet, and that the surface exhibited a set of microscopic parallel striae. It appeared that these striae were demarcation lines between regions of cubic and hexagonal material,

and Merz pointed out that this growth pattern could be obtained by a rotation of the crystalline axes by 60° in the same direction about the (111) or (0001) axis at each interface. Because the direction of rotation was the same at each boundary, a net polarization or directionality could be introduced into the structure by this growth habit, leading to the additive effects seen for the photovoltages. By counting striae and measuring the volts-per-centimeter developed by these specimens, these workers concluded that each junction contributed about 0.15 V to the output. Merz showed that this would be consistent with the band picture for the structure, which was essentially the same as that shown in Figure 51 (b).

In 1958 and 1959, work on ZnS single-crystal specimens in which photovoltages up to 20 were seen, was reported by Cheroff, Keller, and Erick (381, 382) working at IBM Laboratories. The results were similar to those of the RCA group, but in addition spectral response measurements were performed which showed that the sign of the photovoltage was dependent on wavelength of illumination. This result had been reported earlier in 1959 by Lempicki (383, 384), who also confirmed that the larger-than-bandgap photovoltages appeared only along the (111) direction, and also appeared only in crystals containing stacking faults, in agreement with the work of Merz and Ellis et al. The wavelength dependence of photovoltage was found to show a sharp positive maximum near 3400 Å, with smaller negative values for both longer and shorter illumination wavelengths.

An explanation of the observed effects was offered by Tauc in 1959, which accounted satisfactorily for the phenomena (385). Tauc proposed the existence of two junction types, which could arise from a combination of the difference in E_g values for cubic and hexagonal material, together with systematic changes in impurity concentration. The resulting band diagram is shown in Figure 52. Under high intensity illumination with photon energy $E_{g\,cub.}$, a photovoltage ΔE per structural unit is produced. On increasing the photon energy, a photovoltage caused by the barriers in the stacking faults appears, which has a value

$$V = \frac{\Delta E_2}{q} = \frac{(E_{g\,hex} - E_{g\,cub})}{q} > \frac{-\Delta E_1}{q} \tag{129}$$

Since ΔE_1 and ΔE_2 are in opposite directions, the overall photovoltage changes sign. On further increase of photon energy to $E_{g\,hex}$, the gradient in the hexagonal material produces a photovoltage ΔE_3, and the overall photovoltage decreases to zero:

$$-\Delta E_1 + \Delta E_2 - \Delta E_3 = 0 \tag{130}$$

With further increase of photon energy, the ΔE_2 contribution decreases so that the overall photovoltage becomes negative, and the experimentally observed dependence of photovoltage on wavelength is obtained.

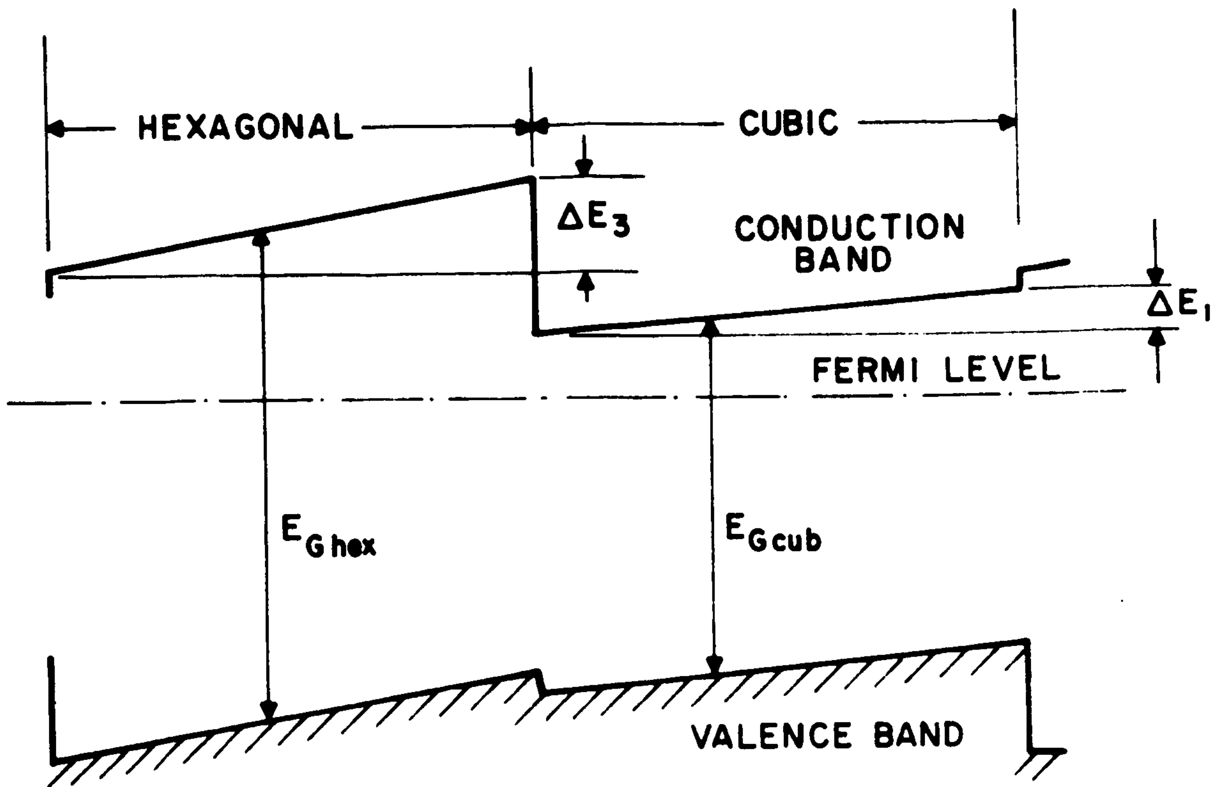

Figure 52. Band structure leading to the high-voltage photoeffect, after Tauc

An alternative hypothesis was advanced by Hutson (386) in 1961, who was associated with Cheroff in the IBM Laboratories group which investigated the high-photovoltage effect. Hutson pointed out that the nature of the barriers assumed to exist in the specimens showing the effect by Pensak, Merz, and others was not clear. Hutson proposed that the barriers arose by the piezoelectric effect caused by strain gradients occurring at stacking faults and grain boundaries. The gradients were assumed to arise because of the difference in thermal expansion coefficient between cubic and hexagonal ZnS, the strain arising from differential expansion between ZnS and substrate. Clearly, this hypothesis did not cover the case when free platelets of ZnS were used for specimens, as in the work of Merz.

Further measurements on the dependence of the photovoltage on illumination wavelength for ZnS, over the temperature range 77 to 580°K, were reported by Cheroff (387) in 1961. Where as the photocurrent increased uniformly with increase of temperature, the photovoltage was found to reach a minimum at 430°K, and to increase with increasing temperature above this point. Hence, Cheroff felt that a simple p-n junction theory could not fit the observed facts, and an explanation of the type proposed by Hutson was presumably felt to be more likely.

The range of materials known to exhibit the high-voltage photovoltaic effect was considerably extended by the work of Lyubin and Fedorova in 1960 (393) and 1962 (394). Work with CdTe layers was reported, the spectral dependence of photovoltage being measured, and a photovoltage sign reversal at about 5,500 Å being seen. In addition, high photo-emf's were seen in Sb_2Se_3, Sb_2S_3, Sb_2S_3-Sb_2Se_3, Sb_2S_3-Bi_2S_3, and $2Sb_2S_3$-Bi_2S_3, and photo-emf sign reversals were reported as occurring in some of these samples with change of illumination wavelength and direction, as for CdTe. Lyubin and Fedorova found no consistent correlation between deposition angle and photovoltage direction, observing photo-emf's up to 80 $V \cdot cm^{-1}$ for films deposited at normal incidence. They thus rejected the hypothesis of Pensak, Goldstein et al., proposing initially that the underlying anisotropy arose from photocurrents existing during film formation, although it is not clear how such photocurrents could arise before the anisotropy was present. The later report (394) favors the mechanism of Semiletov for the photo-emf formation.

From 1962 onwards, the bulk of both the experimental and theoretical work has been done by Soviet workers from several laboratories, interest in the U.S. apparently having waned because the high specimen resistance, and lack of uniformity of results indicated that the application of the effect to power generation would not be possible.

Semiletov (388) reported the results of electron-diffraction measurements on CdTe vacuum-deposited thin films, which established that although crystalline CdTe normally exists with the cubic zincblende structure, in thin films a hexagonal wurtzite structure can also be stable. Semiletov's earlier work had also shown that in CdTe films containing both phases, the transitions between the two stacking patterns were not random, but occurred with a certain regularity. This was analogous to the system proposed by Merz to explain the high-voltage effect in ZnS. Semiletov established that in CdTe films showing high photovoltages:

(i) The crystalline orientation was strongly influenced by the deposition direction, the (111) or (0001) axes being parallel to the direction of the impinging evaporant.

(ii) Two phases were present (cubic and hexagonal).

(iii) A large number of stacking faults existed in the hexagonal phase.

Observation (i), coupled with the hypothesis that the photovoltage was always developed along the polar (111) or (0001) axis (as had been established by Merz for ZnS), showed why oblique deposition is necessary for CdTe high-photovoltage specimens, since depposition normal to the substrate would result in crystallites having the (111) or (0001) direction perpendicular to the substrate. Semiletov's results therefore tend to support Merz's explanation for the effect. Novik and coworkers in a series of publications during 1962 and 1963 described experiments performed on CdTe layers formed by vacuum deposition onto cleaved surfaces of NaCl, KCl, and KBr (389-391). The substrate was found to have an orienting effect on the grown film, but the CdTe was found to form the alternating cubic-hexagonal growth pattern characterized by Semiletov, and this result thus supported Merz's work.

The later publication by Novik (391) reported that the application of an electric field of 10-12 $kV \cdot cm^{-1}$ normal to the substrate surface during deposition caused a marked drop and in some cases a reversal in the photo-emf direction for one field polarity, but a negligible effect on photo-emf for the opposite field polarity. Novik's report of a photo-voltage of 1 $kV \cdot cm^{-1}$ for CdTe films grown on KBr appears to be the largest field strength seen to date.

Neumark, working at Philips Laboratories (New York), proposed a theory of high photo-voltage production (392) based on the work of Tauc and Hutson but differing from these theories in important respects. Feeling that the fields due to nonuniform donor concentrations in the hexagonal and cubic regions, as proposed by Tauc, were unlikely, Neumark proposed that the necessary fields arose from spontaneous polarization of hexagonal ZnS. The resultant band structure is as shown in Figure 53, and the mechanism of photo-voltage production and its dependence on illumination wavelength follow the analysis of Tauc, described above.

In 1963, Karpovich and Shilova (406) described work amplifying the results of Lyubin and Fedorova on thin films of Sb_2S_3. It was found that residual oxygen was necessary during deposition to obtain photovoltaic films, and the usual oblique deposition process was used. The results were given for experiments in which photovoltage was measured as a function of deposition angle, illumination angle, light intensity, and wavelength, over the temperature range 90 to 350°K. A photovoltage sign reversal with illumination

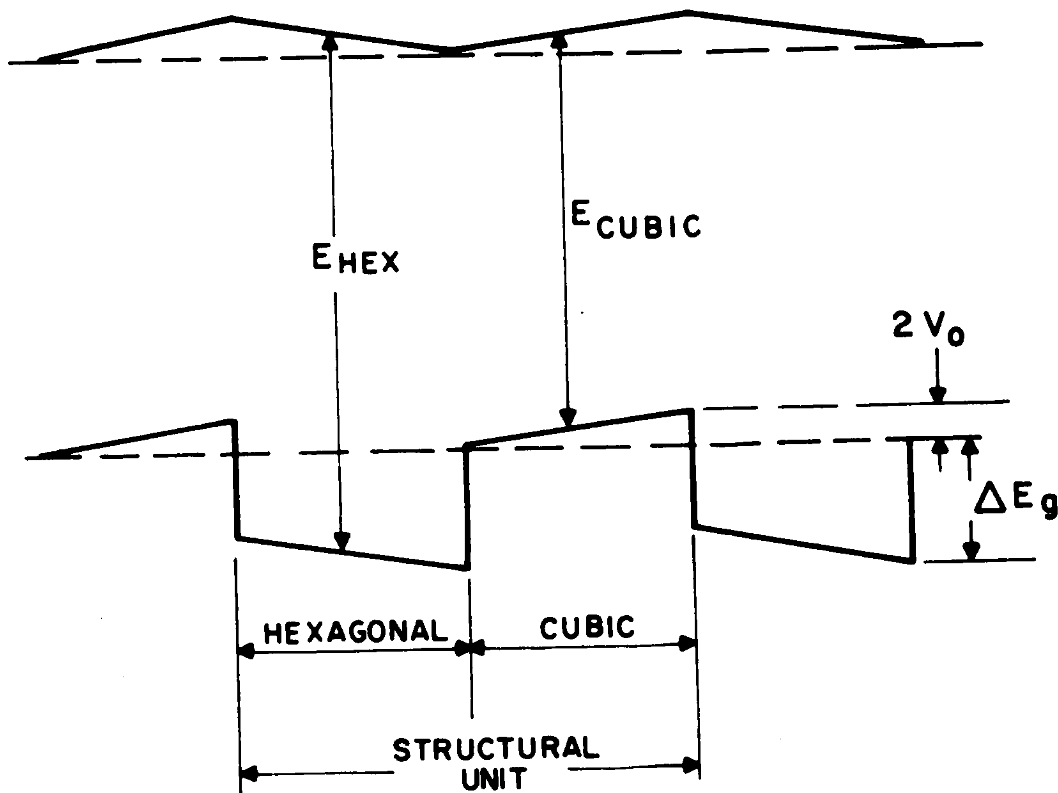

Figure 53. Band structure leading to the high-voltage photoeffect, after Neumark

angle and wavelength was seen for some specimens. An explanation in terms of competing p-n junctions of different "qualities" at the grain boundaries was offered.

In 1964, Brandhorst and Potter (394) reported the observation of photovoltages larger than the bandgap in silicon and SiC films grown under vacuum on MgO and SiO_2 substrates. The specimen resistances were in the 10^{10}-ohm·cm range, and voltages of up to 5.2 V were observed. On removal of the illumination, the photovoltages were observed to decay at a rate corresponding to a time constant of some tens of seconds. This suggested that trapping effects were the cause of the photovoltage, and Brandhorst and Potter proposed an explanation for the effect based on space charge produced by a nonuniform distribution of trapping centers.

In 1964 appeared the first of a continuing series of publications by Adirovich and his co-workers. These reported specimen preparation methods and experimental results obtained with silicon films (395, 396) and GaAs films (397) prepared by vacuum evaporation. Spectral response and photovoltage dependence on illumination angle were investigated, with results not significantly different from those reported for CdTe, described above. In (398) and (399), possible mechanisms for the high-voltage photoeffect were discussed. The conclusion was reached that the Dember effect was the cause of the photovoltage in Ge, Si, and GaAs films, but that in CdTe the multiple p-n junction effect was present. This was mainly based on the evidence that in Ge, Si, and GaAs films, a photovoltage sign reversal was observed on rotating the direction of illumination relative to the specimen plane by 180°, whereas for the CdTe films this effect was not seen. This observation runs contrary to the results of Lyubin and Fedorova (393), but these results appear to be at variance with those of most other workers, so that this is perhaps caused by experimental difficulties rather than having a more fundamental significance. More recently, Adirovich has considered transient effects in CdTe photovoltages (400), obtaining results consistent with the cells operating with a series array of p-n junctions. Adirovich's conclusion that the high photovoltages seen in silicon films were due to the Dember effect runs contrary to the hypothesis of Brandhorst and Potter, described above, and Adirovich points out that there is reason to doubt the validity of the analysis of these authors.

In 1966, Perrot, David, and Martinuzzi (402) also reported the observation of high photovoltages in GaAs films prepared by a method superior to that employed by Adirovich, eliminating any suspicion that the sample preparation technique used by the latter may have led to specimen inhomogeneities which would invalidate the results.

Korsunskii and Fridman (403) reported capacitance measurements on CdTe films exhibiting the high-voltage photoeffect, which support the multiple p-n junction hypothesis of operation. Palatnik and Sorokin (404) have reported an investigation of the effect of the substrate material on the photovoltages seen in CdTe films, showing that films on single-crystal sapphire produced markedly higher photo-emf's than those formed on glass. The effect of substrate temperature during film growth on the magnitude of the photo-emf was found to lead to lower voltage values with increasing crystallite size, again supporting the multiple-p-n-junction hypothesis.

Recently, Ignatyuk and Novik (405) have reported the observation of high photovoltages (up to $800 V \cdot cm^{-1}$) in films of ZnTe vacuum-deposited onto cleaved NaCl, KCl, and KBr crystals, thus adding another material to those known to exhibit the photovoltages larger than bandgap.

This, then, is the present situation regarding the high-voltage photoeffect. It is seen that the initial results, so promising for application to power-generation systems, have been amplified by the subsequent work, but no solution to the problem of high device impedance has been found. The explanations offered for the phenomena fit the facts better now than during the early work, but there seems to be little doubt that the last word has not been spoken on this topic, since the wide range of experimental results defy simple explanations. In any case, the present situation indicates that there is no possibility of employing high-photovoltage devices as energy converters in the near future.

E. Photoeffects in Organic Materials

Organic compounds exhibit three types of photoelectric behavior:

(i) photoconductivity

(ii) sensitization of photoeffects in other materials

(iii) photovoltaic action

Of these effects, the first is of no direct significance for the purposes of the present work, whereas the other two may have applications in the future. Although photoelectric effects in organic compounds were first studied during the 19th century, it is only recently that an appreciable research effort has been applied to the field. For this reason, the whole topic of electrical activity in organic materials is not as familiar as the analogous activity in inorganic materials. The first part of this section attempts to provide some background information on electrical conduction in organic materials, and the two later parts will describe sensitization and photovoltaic effects.

1. Electrical Conduction in Organic Solids

The material presented here has largely been drawn from Gutmann and Lyons' recent book on organic semiconductors (407), to which the reader is referred if more detail is needed. This is a relatively young field of research (the above reference is the first book devoted entirely to the subject), and there still exists considerable controversy over some of the basic issues; where two theories are extant, both have been mentioned.

In elemental inorganic semiconductors, the bonds which hold the atoms in the crystalline lattice are of the same strength as those which bind neighboring atoms together; this remains very nearly true in the inorganic compound semiconductors. Hence, there is a

strong interaction between the allowed energy levels for electrons of the component atoms, and a well-developed band structure is present as a consequence. However, in organic solids, the bonds between atoms which make up each molecule of the compound are, in general, much stronger than the bonds between molecules which form the crystal lattice. There is strong coupling between the electron energy levels within the molecule, but a weak coupling between electron energy levels in adjacent molecules. A continuous band structure throughout the solid does not arise, and the resulting discontinuities in band structure between adjacent molecules can provide a major barrier to electrical conduction. Thus, electrical conduction occurs by the production of a free electron or hole by a transition between energy levels inside the molecule, followed by the motion of the free carrier past the intermolecular barrier. It is the effect of this second process which sets organic conduction processes apart from their inorganic analogs.

Two mechanisms have been proposed for the motion of the free carriers past the intermolecular barriers. One postulates that the barriers are sufficiently narrow to allow electrons to tunnel through them, the second says that the barriers are of such dimensions that electrons must pass over the top and "hop" from molecule to molecule.

When an organic photoconductor is illuminated, it is believed that (in most cases) an electron is excited from a lower to a higher energy state within the molecule. Conduction will now be governed by the rate at which electrons can pass through the intermolecular barriers. If tunnelling processes occur, therefore, the photocurrent should be relatively insensitive to temperature, whereas if hopping processes occur, an exponential dependence of photoconductivity on temperature should be seen, with the exponential constant a measure of the barrier height. In practice, both types of behavior have been seen, and it seems reasonable to suppose that both processes can, in fact, occur.

Now the processes discussed above reasonably lead to electrical conductivity values of 10^{-4} $(\text{ohm}\cdot\text{cm})^{-1}$ or smaller. Some organic materials exhibit conductivities of 1.0 $(\text{ohm}\cdot\text{cm})^{-1}$ or higher, however, and this observation reaches its limit with graphite, which has a conductivity of 10^4 $(\text{ohm}\cdot\text{cm})^{-1}$, approaching the metallic. It is necessary to consider how this may occur.

It is believed that the conduction electrons in an organic solid come from the π orbital in aromatic compounds. This π orbital is a unique feature of the benzene ring; a representation of the orbital is shown in Figure 54. It appears as a pair of donut-shaped regions above and below the plane of the benzene ring, and in these regions the 18 electrons forming the ring bonds are most likely to be found. From the point of view of electron energy, the orbital is a single entity, and no barrier to electron motion between the two regions of the orbital exists. In solids with a crystal structure such that π orbitals from adjacent molecules can overlap appreciably, easy electron transfer between molecules can occur. Normally, this mainly happens when the planes of benzene rings are linked to form sheets, as in the extreme case in graphite. This mechanism also implies that electrical conduction parallel to the plane of the rings will be easier than conduction

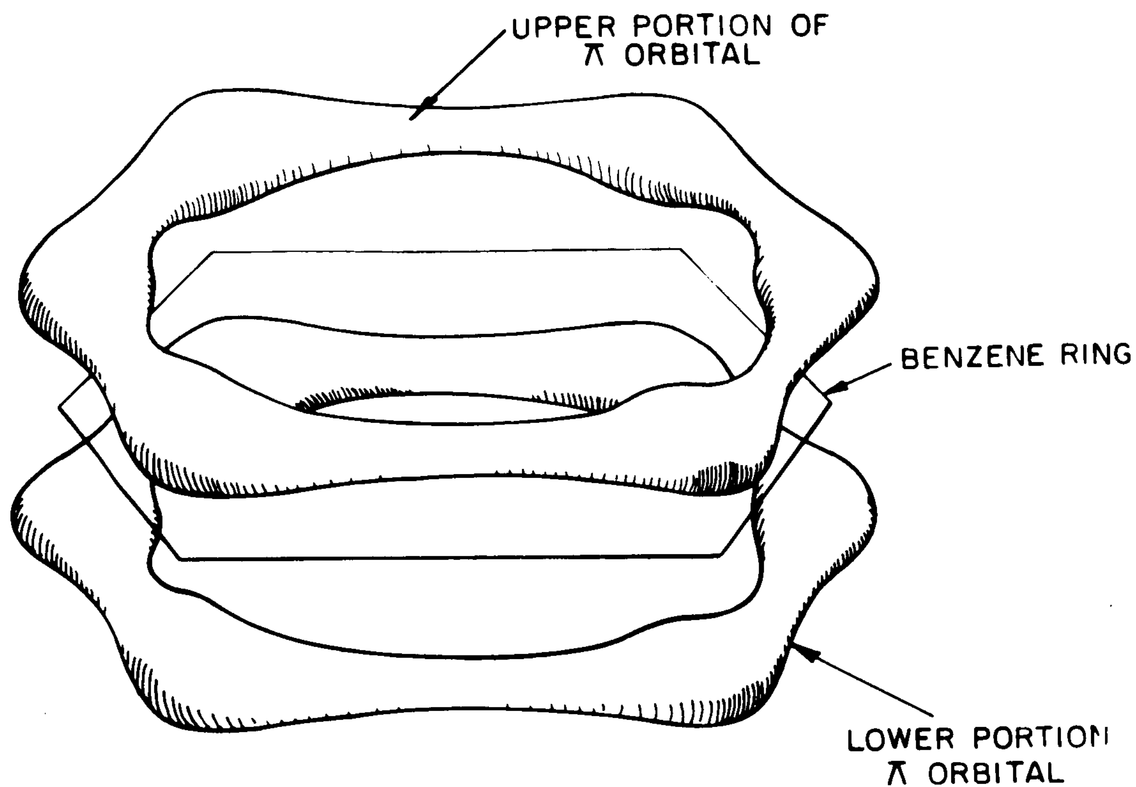

Figure 54. Representation of the π orbital for a benzene ring

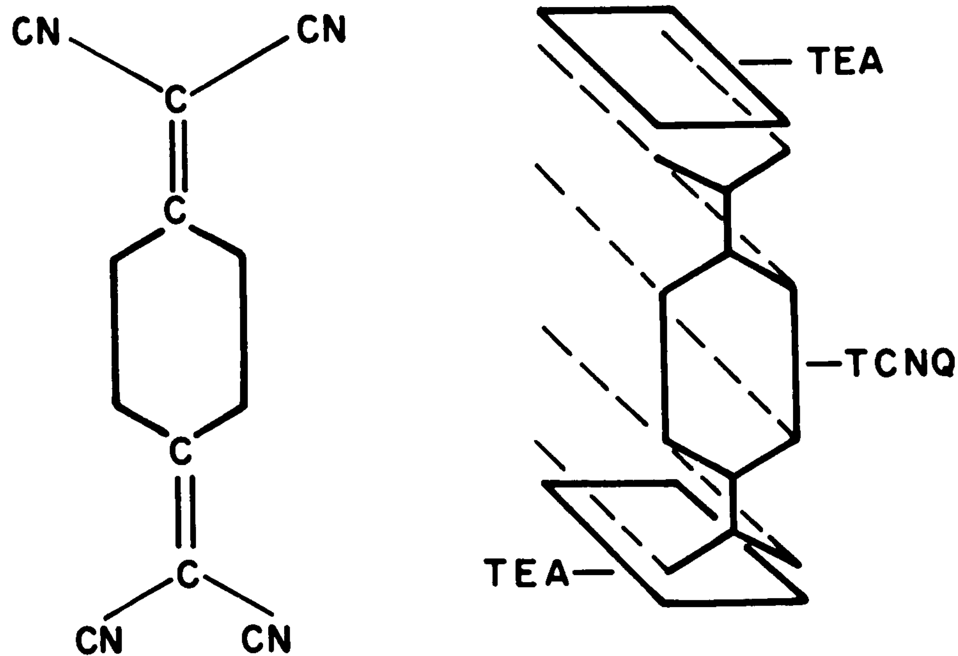

Figure 55. The structure of TEA salt of TCNQ

perpendicular to the plane of the rings, as is observed. This same phenomenon appears to occur in the TEA* salt of TCNQ,* where stacked columns of benzene rings parallel to each other occur (see Figure 55). The conductivity of this salt is about 1.0 $(\text{ohm}\cdot\text{cm})^{-1}$ and is a maximum parallel to the stacking direction.

Another group of organic compounds with large conductivities are the "free-radical" solids, in which an unbonded valence electron occurs. An example is DPPH**, with the structure shown in Figure 56. The unpaired electron is free to move in the molecule without any transition to a higher energy state, and this may explain the high conductivity of this and similar free-radical solids.

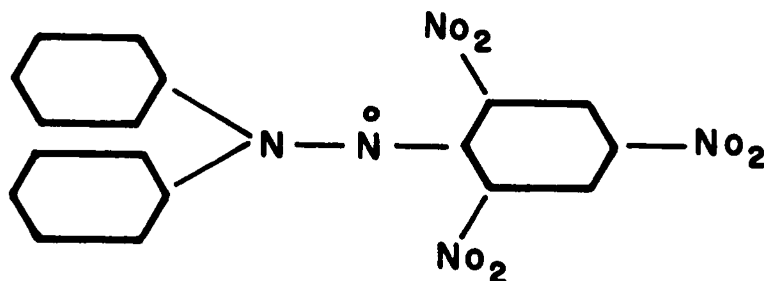

α, α'– DIPHENYL – β – PICRYLHYDRAZYLE (DPPH)

Figure 56. The structure of DPPH

A third group of high-conductivity solids is comprised of the charge-transfer complexes. In these, two molecular species are present, one an electron donor type and the other an electron acceptor type, although in some compounds, different regions of one molecule may exhibit the necessary donor and acceptor characteristics. Because of the partially ionic character of the intermolecular bonding in these solids, the interaction can be strong enough to cause appreciable band formation, thus raising the conductivity.

Another class of compounds also has high conductivity for a related reason. These are the polymers, in which bonding between constituent molecules occurs by the polymerization process, leading to strong intermolecular bonding and interaction. This process could, in principle, proceed to the point where a crystal lattice formed of strong covalent bonds would be produced, as in the inorganic semiconductors. In fact, few polymers show high conductivities, but the above explanation may account for the results with poly-copper-phthalocyanine, which after heat treatment can have a conductivity of 0.25 $(\text{ohm}\cdot\text{cm})^{-1}$. Similarly, the TCNE† polymeric chelates have high conductivities [20 $(\text{ohm}\cdot\text{cm})^{-1}$], but these are also charge-transfer complexes. Graphite would also, in principle, fall into the category of polymers, and this would account for the fairly high conductivity parallel to the ring planes ($\sim 10^3$ $(\text{ohm}\cdot\text{cm})^{-1}$).

*TEA = triethyl amine
TCNQ = tetracyanoquinodimethane
**DPPH = diphenyl-β-picrylhydrazyle
† TCNE = tetracyanoethylene

This account has stressed the mechanisms underlying those compounds which exhibit high conductivity because the major difficulty with organic photovoltaic devices fabricated up to the present has been their high internal impedance.

However, use as photovoltaic semiconductors is only one of two possible uses for organics. Dyes may also prove useful as sensitizing materials, used in conjunction with inorganic semiconductors. Dyes, in general, exhibit photoconductivity, but have resistivities much too high to make them interesting as semiconductors. It should be noted that although the photoconductive and photovoltaic spectral response of many organic materials follows the optical absorption curve, this is not always true, since organic molecules are sufficiently complex to allow a large number of photon absorption mechanisms other than straightforward electron transitions. This is in contrast to inorganic semiconductors, where optical absorption normally takes place by breaking bonds in the crystal lattice to form electron-hole pairs.

2. Sensitization

The fact that certain organic materials can act as sensitizers in silver halide photography was first observed during the 19th century (408,409). The sensitizing material is applied as a thin film to the emulsion side of the plate or film, and increases the long-wavelength (red) response. The mechanism of the effect is now understood (410); the fundamental photographic process relies on photoconductivity in silver iodide, and the sensitizer acts by absorbing low-energy photons and transferring the energy to the AgI_2 either as a free electron or as an exciton which reacts with the AgI_2 to create a free electron. This effect, although understood only recently, was the first application of the photoelectric sensitivity of organic materials.

The sensitization of photoconductivity in silver halides, CdS, and other semiconductors has been much studied recently, and a wide variety of organic compounds have been found to be capable of displaying the phenomenon. There has been, and still is, considerable debate over the mechanism of energy transfer between the sensitizer and the base material. This is partly due to direct contradictions in the experimental evidence obtained by different groups, probably resulting from differences in the sample preparation techniques. The situation in this respect appears to resemble that existing during the early work on semiconduction, before the means for growing single crystals of semiconductor grade purity were available. As Gutmann and Lyons point out, it is not at present possible to prepare organic compounds free of other organic contaminants with the degree of purity possible with inorganic compounds or elements. For this reason, the whole subject of organic semiconduction is in a state of flux, since only a few of the experimental results are firmly established, and the interpretations of the effects seen vary widely.

Nelson has reported an extended series of experiments aimed at investigating photoconductivity sensitization (412-417). The semiconductor used was CdS, and the photoconductive response to light in the wavelength range 6000 to 9000 Å was found to be

increased by pinacyanole, kryptocyanine, and neocyanine (412). It was also observed that with some experimental cells, photovoltages were generated, as discussed in the next section of this report. Similar sensization effects for chlorophyll a and methyl chlorophyllide a were also seen by Nelson (413).

Later work by Nelson was aimed at elucidating the processes occurring during sensitization. When a dye molecule on a CdS surface is excited by the absorption of a photon, four possible events may follow:

(i) The energy is transferred directly from the dye to the CdS without the formation of a free charge carrier (exciton transfer, or resonance transfer).

(ii) A free carrier is formed, which passes into the CdS.

(iii) A photon is re-emitted from the dye, or

(iv) the energy is degraded by phonon production in the dye molecule.

In the sensitization process, (i) or (ii) is apparently dominant over (iii) or (iv), and hence the mechanism debate centers on whether (i) or (ii) is the process giving rise to sensitization. Nelson proposes that the photovoltaic effects seen between dye and CdS demonstrate that electron transfer between dye and substrate occurs, and hence that this is the mechanism of sensitization. As Nelson points out, the evidence is not conclusive, but this model fits the observed facts better than the alternatives.

A great deal of work has been done by the Russian group working under Terenin, on sensitization effects. Experiments by Putseiko (418) were performed using ZnO, and the measurements made were of photoconductivity (measured directly), and the production of a photo-emf at the surface of the ZnO, (using the "Bergmann condenser" method.) The results indicated that many dyes acted as sensitizing agents, and that the conductivity type of these dyes could be either p- or n-type. This was taken to indicate that the fundamental process occurring during sensitization involved the transfer of energy directly from dye to semiconductor, the energy then creating free carriers in the inorganic semiconductor. In this way, the sense of the photovoltage would depend only on the nature of the inorganic semiconductor, as was observed. Putseiko also found that the spectral sensitivity of the sensitization effect followed that of optical absorption in the dye, and that the thinnest dye layers (down to one monolayer of molecules) produced the largest effects. However, some sensitization could be obtained by pressing a disc of dye against the semiconductor surface, without the necessity for producing the more usual intimate dye-substrate contact by deposition of dye from a solvent.

Thus, there appears to exist the possibility that the long-wavelength sensitivity of inorganic semiconductors photovoltaic cells may be increased by the application of the sensitization effects described above. The compound semiconductor cells, and probably the CdS cells particularly, are the most likely to make use of the phenomenon. It appears

that a comprehensive experimental program is the only way of approaching this question, and such a program has not yet been run. It is also clear that the practical application of this effect in cells for space use would require that the sensitizing material be stable under UV and particle irradiation. This is a problem area for organic materials, and will be more fully discussed in the evaluation sections of this work.

3. Photovoltaic Effects

Photovoltages have been seen at electrolyte-organic, metal-organic, and organic-organic interfaces, though the latter is unusual.

Electrolyte-organic photovoltages were reported by Kallman and Pope (420) in 1959, using NaCl solutions and anthracene crystals. The maximum photovoltage observed was 0.2 V, under unstated illumination conditions, with a low power conversion efficiency because of the high internal impedance of the cell. For obvious reasons, such Becquerel cells are of no practical interest for power conversion systems for space use, and the significance of such work is for research purposes only.

Photovoltages ranging from millivolts to some hundreds of volts have been reported for metal-organic contacts; Gutmann and Lyons (407) provide a useful summary of the data from many authors. In most cases, uncertainty exists concerning the origin of these voltages, some authors concluding they are due to Dember effects, others to contact effects. In some instances, particularly for the 230 V observed when polyethylene was irradiated with UV (419), the effects may be due to charge release, as noted by Gutmann and Lyons. The photovoltaic work can best be summarized as follows:

The majority of the specimens have been made in the "sandwich-cell" configuration of Figure 57(a), though some use has been made of the "surface-cell" geometry of Figure 57(b). In the sandwich cell, the electrodes are usually metallic, or one may be a conducting coating ('TIC') on the glass substrate; the two electrode materials may or may not be the same. The cell may be illuminated from either side, one electrode usually being made either thin, or given a grid pattern, to provide optical transmission. The surface cell may have both electrodes of the same or of different materials, and either or both electrodes may be illuminated. Many different electrode and organic materials, deposited by various techniques, have been investigated using these cells, and the results are tabulated by Gutmann and Lyons, as noted above. The main conclusions to be drawn from this work are that organic materials exhibit photovoltages analogous to those seen with inorganic semiconductors, but that none of the cells made to date has exhibited a power conversion efficiency comparable to those using inorganic materials.

However, such results as have been obtained have prompted an interest in investigating photovoltages in organic materials for power conversion by the group working under Golubovic at the USAF Cambridge Research Laboratories, and this group has also sponsored a program of research by university and industrial laboratories (421) over the

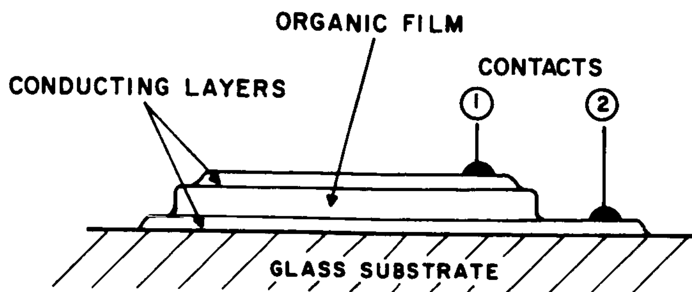

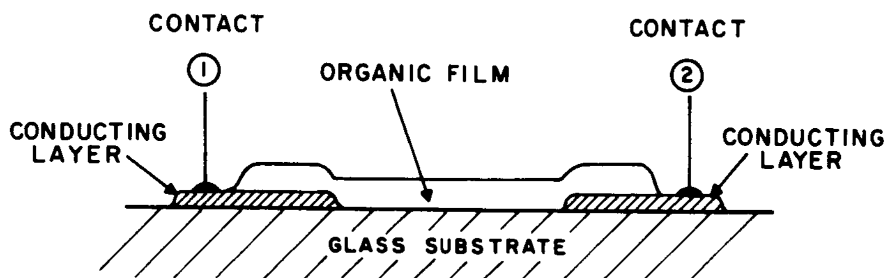

Figure 57. Cells for the investigation of conductivity in organic films

years 1960 to the present. The results of this work have not been widely reported, but recent publications by Golubovic (422)* and Mukherjee (423) summarize the present status. Golubovic's results have been obtained with sandwich cells with Al and Au electrodes, using either single or double organic layers. Organic materials studied have been tetracene, pentacene, and aceanthraquinoxaline. It was found that the addition of a second layer of organic material, particularly of the charge-transfer complexes such as TCNQ, TEA-TCNQ, and chloranil, increased both the photovoltage and photocurrent in these cells. Clearly, internal resistance in the cell is the factor limiting the present efficiency. Photovoltages up to 760 mV were seen, with current densities in the $\mu A \cdot cm^{-2}$ range for illumination densities of low tens of $mW \cdot cm^{-2}$. The spectral response of the cells in general followed that of the optical absorption in the organic material.

Photovoltages possibly arising from p-n junctions between two organic materials have been reported by Meier and Haus (424), and Needler (425). This type of behavior appears to be unusual in organic materials, and metal-organic contacts appear to be more likely to yield useful photovoltaic cells.

---

*The authors of this report are grateful to Dr. Golubovic for supplying a prepublication copy of this paper.

Photovoltages have also been reported by Nelson, Putseiko, and others as occurring at organic-semiconductor interfaces. Nelson's work (413) was done using a modification of the surface cell, in which one of the electrodes was CdS, with a metal contact to the CdS, while Putseiko's work was done with a sandwich-type cell with one of the electrodes of ZnO. Since most semiconductors (and particularly the compound semiconductors such as ZnO and CdS) exhibit photovoltages caused by an inversion layer at the surface, so that any type of conductor applied to the illuminated surface can be used to form a photovoltaic cell, it appears that the claims that the photovoltage arose in the organic material should be carefully examined, and that the effects seen are possibly due to the usual surface-barrier effects in the inorganic material, modified by the sensitization effects discussed above. Because CdS is always n-type, surface inversion-layer effects will always give rise to a photovoltage of the same sign, which is contrary to the experimental evidence, so that this simple explanation clearly is not always applicable. However, Nelson's band-diagram for the semiconductor-organic contact also suffers from the same difficulty, so that it appears that band-diagram explanations for organic semiconductor effects may be misleading.

This then is the present state of work on organic semiconductors as it pertains to energy conversion. Further evaluation of this work, and a discussion of the future possibilities, will be given later in this work.

REFERENCES

87. Ohl, R.S., U.S. Pat. 2,402,661; 2,402,662; 2,402,663 and 2,407,678. Scaff, J.H., U.S. Pat. 2,402,582.

88. Scaff, J.H., Theuerer, H.C., and Schumacher, E.E., Trans. AIME 185, 383 (1949).

89. Kingsbury, E.F., and Ohl., R.S., Bell Syst. Tech. J. 31, 802 (1952).

90. Torrey, H.C., and Whitmer, C.A., Crystal Rectifiers (McGraw Hill Book Co., Inc., New York 1948).

91. Pfann, W.G., J. Metals 4, 747 (1952).

92. Keck, P.H., and Golay, M.J.E., Phys. Rev. 89, 1297 (1953).

93. Bridgman, P.W., Proc. Am. Acad. Arts Sci. 60, 303 (1925).

94. Czochralski, J., Z. Physik. Chem. 92, 219 (1918).

95. Benzer, S., Phys. Rev. 70, 105 (1946).

96. Benzer, S., Phys. Rev. 72, 1267 (1947).

97. Teal, G.K., Phys. Rev. 78, 647 (1950); Phys. Rev. 81, 637 (1951).

98. Scaff, J.H., and Ohl, R.S., Bell Syst. Tech. J. 26, 1 (1947).

99. Pearson, G.L., and Bardeen, J., Phys. Rev. 75, 865 (1949).

100. Burton, J.A., Physica 20, 845 (1954).

101. Burton, J.A., et al., J. Chem. Phys. 21, 1987 and 1991 (1953).

102. Prince, M.B., Phys. Rev. 92, 681 (1953).

103. Prince, M.B., Phys. Rev. 93, 1204 (1954).

104. Burton, J.A., et al., J. Phys. Chem 57, 853 (1953).

105. Dash, W.C., and Newman, R., Phys. Rev. 99, 1151, (1953).

106. Welker, H., Z. Naturforsch. 7a, 744 (1952); 8a, 248 (1953).

107. Welker, H., Physica 20, 893 (1954).

108. Welker, H., Scientia Electrica 1, 152 (1954).

109. Madelung, O., (Translated by Meyerhofer, D.) Physics of III-V Compounds (John Wiley and Sons, Inc., New York, 1964).

110. Jenny, D.A., and Bube, R.H., Phys. Rev. 96, 1190 (1954).

111. Smith, R.W., RCA Review 12, 350 (1951).

112. Reynolds, D.C., et al., Phys. Rev. 96, 533 (1954).

113. Hall, R.N., and Dunlap, W.C., Phys. Rev. 80, 467 (1950).

114. Pearson, G.L., and Sawyer, B., Proc. IRE 40, 1348 (1952).

115. Armstrong, L.D., Proc. IRE 40, 1341 (1952).

116. Hall, R.N., Proc. IRE 40, 1512 (1952).

117. Teal, G.K., Sparks, M., and Buehler, E., Phys. Rev. 81, 637 (1951).

118. Goucher, F.S., et al., Phys. Rev. 81, 637 (1951).

119. McAfee, K.B., and Pearson, G.L., Phys. Rev. 82, 190 (1952).

120. Saby, J.S., and Dunlap, W.C., Jr. Phys. Rev. 90, 630 (1953).

121. Dunlap, W.C. Jr., Phys. Rev. 94, 1531 (1954).

122. Fuller, C.S., and Ditzenberger, J.A., J. Appl. Phys. 25, 1439 (1954).

123. Pearson, G.L., and Fuller, C.S., Proc. IRE 42, 760 (1954).

124. Chapin, D.M., Fuller, C.S., and Pearson, G.L., J. Appl. Phys. 25, 676 (1954).

125. Dunlap, W.C., Jr, Bohm, H.V., and Mahon, H.P., Jr., Phys. Rev. 96, 833 (1954).

126. Smits, F.M., Proc IRE 46, 1049 (1958).

127. Houstoun, R.A., Phil. Mag. 39, 902 (1948).

128. Billig, E., and Plessner, K.W., Phil. Mag. 40, 568 (1948).

129. Lehovec, K., Physical Rev. 74, 463 (1948).

130. Benzer, S., Phys. Rev. 69, 683 (1946).

131. Benzer, S., Phys. Rev. 70, 105 (1946).

132. Sosnowski, L., Phys. Rev. 72, 641 (1947).

133. Benzer, S., Phys. Rev. 72, 1267 (1947).

134. Becker, M., and Fan, H.Y., Phys. Rev. 78, 301 (1950).

135. Fan, H.Y., Phys. Rev. 75, 1631 (1949).

136. Pietenpol, W.J., Phys. Rev. 82, 120 (1951).

137. Rothlein, B.J., Sylvania Technologist 4, 86, Oct. 1951.

138. Rothlein, B.J., and Fowler, A.B., IRE Trans. on Electron Devices ED-1, 67 (1954).

139. Shive, J.N., Proc. IRE 40, 1410 (1952).

140. Ruth, R.P., and Moyer, J.W., Phys. Rev. 95, 562 (1954).

141. Pfann, W.G., and van Roosbroeck, W., J. Appl. Phys. 25, 1422 (1954).

142. Brattain, W.H., and Shockley, W., Phys. Rev. 72, 345 (1947).

143. Pearson, G.L., Bell Labs Record 32, 232 (1954).

144. Chapin, D.M., Fuller, C.S., and Pearson, G.L., Bell Labs Record 37, 241 (1955).

145. Prince, M.B., J. Appl. Phys. 26, 534 (1955).

146. Sosnowski, L., Starkiewicz, J., and Simpson, O., Nature 159, 818 (1947).

147. Starkiewicz, J., Sosnowski, L., and Simpson, O., Nature 158, 28 (1946).

148. Talley, R.M., and Enright, D.P., Phys. Rev. 95, 1092 (1954).

149. Avery, D.G., et al., Proc. Phys. Soc. 67B, 761 (1954).

150. Mitchell, G.R., Goldber, A.E., and Kurnick, S.W., Phys. Rev. 97, 239 (1955).

151. Gremmelmaier, R., Z. Naturforsch. 10a, 501 (1955).

152. 1st Interim Report, Contract No. DA-36-039-SC-64643.

153. Jenny, D.A., Loferski, J.J., and Rappaport, P., Phys. Rev. 101, 1208 (1956).

154. Reynolds, D.C., and Leies, G.M., Electrical Engineering 73, 734 (1954).

155. Reynolds, D.C., et al., Phys. Rev. 96, 533 (1954).

156. Reynolds, D.C., and Czyzak, S.J., Phys. Rev. 96, 1705 (1954).

157. Seitz, F., The Modern Theory of Solids (McGraw-Hill Book Co., New York, 1940).

158. Bethe, H.A., Rad. Lab. Report # 43-12-(1942).

159. Meyerhoff, W.E., Phys. Rev. 71, 727 (1947).

160. Bardeen, J., Phys. Rev. 71, 717 (1947).

161. Shockley, W., Bell Syst. Tech. J. 28, 435 (1949).

162. Starkiewicz, J., Sosnowski, L., and Simpson, O., Nature 158, 28 (1946).

163. Sosnowski, L., Starkiewicz, J., and Simpson, O., Nature 159, 818 (1947).

164. Sosnowski, L., Soole, B.W., Starkiewicz, J., Nature 160, 471 (1947).

165. Fan, H.Y., Phys. Rev. 75, 1631 (1949).

166. Cummerow, R.L., Phys. Rev. 95, 16 (1954).

167. Cummerow, R.L., Phys. Rev. 95, 561 (1954).

168. Moss, T.S., Optical Properties of Semiconductors, (Academic Press, Inc., New York, 1959).

169. Rittner, R.S., Phys. Rev. 96, 1708 (1954).

170. Lark-Horovitz, E., Bleuler, E., Davis, and Tendam, D., Phys. Rev. 73, 1256 (1948).

171. Cleland, J.W., et al., Phys. Rev. 83, 312 (1951).

172. Davis, R.E., et al., Phys. Rev. 74, 1255 (1948).

173. Brattain, W.H., and Pearson, G.L., Phys. Rev. 80, 846 (1950).

174. Klontz, E., and Lark-Horovitz, Phys. Rev. 82, 763 (1951).

175. Fletcher, R.C., and Brown, W.L., Phys. Rev. 92, 585 (1953).

176. Brown, W.L., et al., Phys. Rev. 92, 591 (1953).

177. Cleland, J.W., et al., Phys. Rev. 83, 312 (1951).

178. Ehrenberg, W., Lange, C., and West, R., Proc. Phys. Soc. 64A , 424 (1951).

179. Rappaport, P., Phys. Rev. 93, 246 (1954).

180. Rappaport, P., Phys. Rev. 94, 1409 (1954).

181. Loferski, J.J., and Rappaport, P., Phys. Rev. 98, 1861 (1955).

182. Rappaport, P., Loferski, J.J., and Linder, E.G., RCA Rev. 17, 100 (1956).

183. Sah, C.T., Noyce, R.N., Shockley, W., Proc. IRE 45, 1228 (1957).

184. Shockley, W., and Read, W.T., Phys. Rev. 87, 835 (1952).

185. Loferski, J.J., J. Appl. Phys. 27, 777 (1956).

186. Contract # DA-36-039-SC-64643, Investigations of Materials for Photovoltaic Solar Energy Converters, 5 Interim Reports and Final Report covering the Period April 15, 1955 to August 31, 1957.

187. Vavilov, V.S., Atomic Energy (USSR) 1, 121 (1956).

188. Semiconductors in Science and Technology, Vol. II, ed. A.F. Joffe, Chapter 16 "Semiconducting Photoelements" by V.K. Subashiev and M.S. Sominskii. Akad. Nauk. SSSR (1958).

189. Halsted, R.E., J. Appl. Phys. 28, 1131 (1957).

190. Rappaport, P., RCA Review 20, 373 (1959).

191. Wysocki, J.J., and Rappaport, P., J. Appl. Phys. 31, 571 (1960).

192. Contract #DA36-039-SC-78184, Investigation of High-Temperature, Improved Efficiency Photovoltaic Solar Energy Converter (July 15, 1958 to Oct. 31, 1960), and Contract #DA36-039-SC87417, Semiconductor Photovoltaic Conversion (Nov. 1, 1960 to Oct. 31, 1961).

193. Wolf, M., and Prince, M.B., Proceedings of Congress for Solid State Physics and its Applications in Electronics and Communications, Brussels, (Academic Press, Inc., New York, 1958).

194. Prince, M.B., and Wolf, M., J. Brit. IRE. 18, 583 (1958).

195. Wolf, M., Proc. IRE 48, 1246 (1960).

196. Muser, H.A., Z. Phys. 148, 380 (1957).

197. Rose, A., J. Appl. Phys. 34, 1640 (1960).

198. Contract # AF33(616)-6707, Research Study of Photovoltaic Solar Cell Parameters, Final Report, # ASD-TR-61-423, also Contract # AF33(616)-7786 A Study of Photovoltaic Cell Parameters, Final Report # ASD-TDR-62-776.

199. Shockley, W., and Queisser, H.J., J. Appl. Phys. 32, 510 (1961).

200. Queisser, H.J., and Shockley, W., Bull. Am. Phys. Soc. II 5, 160 (1960).

201. Loferski, J.J., Acta Electronica 5, 350 (1961).

202. Landsberg, P.T., and Beattie, A.R., J. Phys. Chem. Solids 8, 73 (1959).

203. Chynoweth, A.G., and McKay, K.G., Phys. Rev. 106, 418 (1957).

204. Shockley, W., and Henley, R., Bull. Am. Phys. Soc. II 6, 106 (1961).

205 Contract# AF33(616)-7786, A Study of Photovoltaic Solar Cell Parameters, Technical Documentary Report # ASD-TDR-62-776.

206. Heavens, O.S., Optical Properties of Thin Solid Films (Dover Publications, Inc., New York, 1965) pp. 208-215.

207. Bir, G.L., and Pikus, G.E., Sov. Phys. Tech. Phys. 2. 419 (1957).

208. Harten, H.U., and Schultz, A., Z. Physik. 141, 319 (1955).

209. Subashiev, V.K., Sov. Phys. Solid State 2, 187 (1960).

210. Subashiev, V.K., and Pedyash, E.M., Sov. Phys. Solid State 2, 194 (1960).

211. Subashiev, V.K., Sov. Phys. Solid State 2, 181 (1960).

212. Moizhes, B. Ya., Sov. Phys. Solid State 2, 202 (1960).

213. Jordan, A.G., and Milnes, A.G., IRE Trans. on Electron Devices ED7, 242 (1960).

214. Loferski, J.J., and Wysocki, J.J., RCA Review 22, 38 (1961).

215. Lawrence, H., and Warner, R.M., Bell Syst. Tech. J. 39, 389 (1960).

216. Dale, B., and Smith, F.P., J. Appl. Phys. 32, 1377 (1961).

217. Wolf, M., Proc. IEEE 51, 674 (1963).

218. Wysocki, J.J., RCA Review 22, 57 (1961).

219. Moss, T.S., Solid State Electronics 2, 222 (1961).

220. Kleinman, D.A., Bell Syst. Tech. J. 40, 84 (1961).

221. Lamorte, M.F., Adv. Energy Conversion 3, 551 (1963).

222. Handy, R.M. , Solid State Electronics 10, 765 (1967).

223. Ralph, E.L., and Berman, P., Proc. 17th Ann. Power Sources Conf. (1963).

224. Wolf, M. and Ralph, E.L., Proc. 4th Photovoltaic Specialists' Conf. (1964).

225. Wolf, M., and Ralph, E.L., IEEE Trans. on Electron Devices ED-12, 470 (1965).

226. Crabb, R.L., and Treble, F.C., Nature 213, 1223 (1967).

227. Henisch, H.K., Rectifying Semiconductor Contacts, (Oxford, 1957).

228. Contract #AF33(615)-2259, Improved Thin Film Solar Cells, 3 quarterly reports plus Final Report AFAPL-TR-65-123 (Jan. 1966); Contract #AF33(615)-3486, Advanced Thin-Film Solar Cells, 3 quarterly reports plus Final Report AFAPL-TR-67-4 (Jan. 1967).

229. Contract #AF19(628)-2845, "Solar and Thermal Energy Storage and Conversion Systems, Tyco Laboratories.

230. Emtage, P.R., J. Appl. Phys. 33, 1950 (1962).

231. Tauc, J., Rev. Mod. Phys. 29, 308 (1957).

232. Oldham, W.G., and Milnes, A.G., Solid State Electronics 6, 121 (1963).

233. Oldham, W.G., and Milnes, A.G., Solid State Electronics 7, 153 (1964).

234. Van Ruyven, L.H., Phys. Stat. Solidi 5, K109 (1964).

235. Maslakovets, Yu. P., et al., Sov. Phys.-Tech. Phys. 1, 2316 (1956).

236. Tuchkevich, V.M., and Chebnokov, V.E., Proc. of the Conference in Kiev, page 339 (1957).

237. Vavilov, V.S., Galkin, G.N., and Malovestskaya, V.M., Proceedings of the Conference in Kiev, page 345 (1957).

238. Browne, M.E., Francies, A.B., and Enslow, G.M. LMSD Report No. 5021, June 1958.

239. Loferski, J.J., and Rappaport, P., RCA Review 19, 536 (1958).

240. Rappaport, P. Talk presented at Advanced Energy Sources Conference, Nov. 1958, Pasadena, Calif.

241. Yearian, H.J., Third Quarterly Report, Contract # DA-36-039-SC-77991, Feb. 1959.

242. Nash, H., and Luft, W., Electronic Industries 18, 91 (1959).

243. Matlow, S.L., and Ralph, E.L., J. Appl. Phys. 30, 541 (1959).

244. Kalman, J., Electronics 32, 59 (1959).

245. Evans, E., and Menetrey, W. R., Wright Air Dev. Div. Report No. 60-699, Vol. 5, (Contract # AF33(616)-6791), Sept. 1960.

246. Dale, B., and Rudenberg, H.G., Proc. 14th Annual Power Sources Conf., page 22 (1960).

247. Ralph, E.L., and Biekofsky, H.F., Report #2, Contract # AF33(600)-40497 (Hoffman Elec. Corp.), June 1960.

248. Escoffery, C.A., and Luft, W., Automation Progress 5, 332 (1960).

249. Escoffery, C.A., Semiconductor Products 3, 35, (1960).

250. Malovetskaya, V.M., Vavilov, V.S., and Galkin, G.N., Soviet Physics-Solid State 1, 1099 (1960).

251. Escoffery, C.A., and Luft, W., Solar Energy 4, 1 (1960).

252. Van Allen, J.A., Geophys. Res. 64, 1683 (1959).

253. Terman, L.M., Solid State Electronics 2, 1 (1961).

254. Wolf, M., Solar Energy 5, 83 (1961).

255. Prince, M.B., United Nations Conf. on New Sources of Energy, 1961.

256. Prince, M.B., Acta Electronica 5, 330 (1961).

257. First Quarterly Report, Contract # NAS5-457, July 15 to Oct. 15, 1960, RCA Laboratories.

258. Final Report, Contract # DA36-039-SC78184, RCA Laboratories.

259. Lamond, P., and Berman, P., Proc. 15th Annual Power Sources Conf., p. 106 (1961).

260. Baicker, J.A., and Faughnan, B.W., J. Appl. Phys. 33, 3271 (1962).

261. Desvignes, F., Communication du Colloque International sur les Dispositifs à Semiconductors 1, 571 (1961).

262. Desvignes, F., Acta Electronica 5, 275 (1961).

263. Beauzée, C., Acta Electronica 5, 305 (1961).

264. Salles, Y., Acta Electronica 5, 341 (1961).

265. Valdman, H., Compt. Rend. 252, 246 (1961).

266. Valdman, H., Rodot, M., and Rodot, H., Comm. du colloque International sur les Dispositifs à Semiconductoures 1, 1 (1961).

267. Iles, P.A., IRE Trans. on Military Electronics MIL-6, 5 (1962).

268. Hooper, W.W., and Queisser, H.J., Proc. IRE 50, 486 (1962).

269. Vavilov, V.S., Smirnova, I.V., and Chapnin, V.A., Sov. Phys.-Solid State 4, 830 (1962).

270. Smirnova, I. V., Chapnin, V. A., and Vavilov, V. S., Sov. Phys.-Solid State 4, 2469 (1963).

271. Contract #NAS-10239, RCA Laboratories.

272. Smith, K.D., et al., Bell Syst. Tech. J. 42, 1779 (1963).

273. Final Report, Contract # NAS5-3812, May to Nov. 1964, RCA, Mountaintop, Pa.

274. Magee, V., Report on American Industry Tour, March 1964, Ferranti Ltd., Semiconductor Dept.

275. Wolf, W., Paper # 5.5 at A.I.Ch. E.-I. Chem. E. Joint Meeting, London, June 1965.

276. Mandelkorn, J., Proc. 19th Annual Power Sources Conf., May 1965.

277. Rappaport, P., Paper # 5.6 at A.I. Ch. E.-I. Chem. E. Joint Meeting, London, June 1965.

278. Butcher, O.C., Barnett, D., and Webb, H.G., Ferranti report-undated.

279. Radiation Damage in Silicon, Contract # NAS5-3788, RCA Laboratories.

280. Contract # NAS5-9131, July 1965, RCA Laboratories.

281. Material Development for Solar Cell Applications, Contract # NAS5-9576 RCA, Mountaintop, Pa.

282. Wysocki, J., Conf. Record 6th Photovoltaic Specialists Conf. 3, 96 (1967).

283. Gliberman, A. Ya., Zaitsera, A.K., and Landsman, A.P., Soviet Physics - Solid State 2, 1583 (1961).

284. Final Report, Contract # DA36-039-SC-9077, June 1962 to July 1964, Heliotek Corp.

285. Cherry, W.R., Proc. 13th Annual Power Sources Conf., pp. 62-66, April 1959.

286. Prince, M.B., Proc 14th Annual Power Sources Conf. pp. 26-27, May 1960.

287. Contract #DA36-039-SC-85243.

288. Final Report, Contract #AF33(657)-7649, Oct. 1961 to Oct. 1962, Westinghouse Electric Corporation.

289. Riel, R.K., and Tarneja, K.S., Proc. 17th Annual Power Sources Conference (1963).

290. Final Report, Contract #AF33(657)-11274, May 1963 to July 1965, Westinghouse Electric Corporation.

291. Burrill, J.T., et al., Conference Record 6th Photovoltaic Specialists Conf. 3, 81 (1967).

292. Reports under Contract #AF33(615)-2292, (1965), Ion Physics Corporation.

293. Martin, J.H., and Ralph, E.L., 1967 IECEC Photovoltaic Workshop, August 1967, Miami Beach, Fla.

294. Third Quarterly Report, Contract #NAS5-3686, August 1964 to Nov. 1964. RCA, Mountaintop, Pa.

295. Hoffman Electronics Corp., Proposal to Air Force Cambridge Research Laboratories (1960).

296. Reports under Contract #NAS5-9609, (1965-1966), Texas Instrument, Inc.

297. Nasledov, D.N., and Tsarenkov, B.V., Proc. of the Conference in Kiev (1957).

298. Gremmelmaier, R., Proc. IRE 46, 1045 (1958).

299. Loferski, J.J., Rappaport, P., and Wysocki, J.J., Proc. 13th Annual Power Sources Conf., p. 59 (1959).

300. Wysocki, J.J., Loferski, J.J., and Rappaport, P., Proc. 14th Annual Power Sources Conf., p. 32 (1960).

301. Gallium Arsenide Solar Cell, Contract #AF33(616)-6615.

302. Nasledov, D.N., and Tsarenkov, B.V., Fiz. Tver. Tela 1, 1467 (1959); translation Sov. Phys.-Solid State 1, 1346 (1960).

303. Bylander, E.G., Hodge, A.J., and Roberts, J.A., J. Opt. Soc. Am. 50, 983 (1960).

304. Semiconductor Photovoltaic Conversion, Contract #DA36-039-SC-87417, Triannual Reports and Final Report, Nov. 1, 1960 to Oct. 31, 1961.

305. Gobat, A.R., Lamorte, M.F., and McIver, G.W., IRE Trans. Mil. Elect. ME-6, 20 (1962).

306. Lamorte, M.F., Proc. 16th Annual Power Sources Conf., p. 71 (1962).

307. Applied Research Program on High-Temperature Radiation-Resistant Solar-Cell Array, Contract #AF33(657)-8490, Technical Documentary Report ASD-TDR-63-516, vols. I and II.

308. Loferski, J.J., Proc. IEEE 51, 667 (1963).

309. Hall, R.N., Proc. IEE 19B, 923 (1960).

310. Mayburg, S., Solid State Electronics 2, 195 (1961).

311. Wysocki, J.J., J. Appl. Phys. 34, 2915 (1963).

312. Radiation Damage to Silicon Solar Cells, Contract #NAS5-457, 3 quarterly reports and Summary Report, July 1, 1960 to July 1, 1961.

313. Gutkin, A.A., Nasledov, D.N., Sedov, V.E., and Tsarenkov, B.V., Fiz. Tver. Tela 4, 2338 (1962); translation Sov. Phys.-Solid State 4, 1712 (1963).

314. Gutkin, A.A., Nasledov, D.N., and Sedov, V.E., Fiz. Tver. Tela 5, 1138 (1963); translation Sov. Phys.-Solid State 5, 831 (1963).

315. Manufacturing Methods Program for GaAs Solar Cells, Contract #AF33(657)-8921, Applications Report #ML-TDR-64-164 and Final Report #ML-TDR-64-165, 15 June 1962 to 28 February 1964.

316. Gutkin, A.A., Nasledov, D.N., and Sedov, V.E., Fiz. Tver. Tela 7, 81 (1965); translation Sov. Phys.-Solid State 7, 58 (1965).

317. Gutkin, A.A. Kagan, M.B., Sedov, V.E., and Shernov, Ya. I., Fiz. Tver. Tela 7, 2538 (1965); translation Sov. Phys.-Solid State 7, 2046 (1966).

318. Gutkin, A.A., Magerramov, E.M., Nasledov, D. N., and Sedov, V. E., Fiz. Tver. Tela 8, 712 (1966); translation Sov. Phys. Solid State 8, 570 (1966).

319. Wysocki, J.J., Rappaport, P., Davison, E., and Loferski, J.J., IEEE Trans. on Electron Devices ED-13, 420 (1966).

320. Investigation of Integrally Composed Variable Energy Gap Photovoltaic Solar Energy Converter, Contract DA-36-039-SC-85246.

321. Grimmeis, H.G., and Koelmans, H., Philip's Rs. Rpts. 15, 290 (1960).

322. Development of Improved Single-Crystal GaP Solar Cells, Contract #NAS3-2776, Final Report, NASA CR-54273, June 12, 1963 to Aug. 12, 1964.

323. Epstein, A.S., and Groves, W.O., Advanced Energy Conversion 5, 161 (1965).

324. Improved Single-Crystal CaP Cells, Contract NAS3-6014, August 12, 1964 to August 11, 1965.

325. Epstein, A.S., and DeBaets, M.C., Solid-State Electronics 9, 1019 (1966).

326. Kagan, M.B., Landsman, A.P., and Chernov, Ya. I., Fiz. Tver. Tela 6, 2700 (1964); translation Sov. Phys.-Solid State 6, 2149 (1965).

327. Alferov, Zh. I., Zimogorova, N.S., Turkan, M.K., and Tuchkevich, V.M., Fiz. Tver. Tela 7, 1235 (1965); translation Sov. Phys.-Solid State 7, 990 (1965).

328. Alferov, Zh. I., Korol'kov, V.I., Mikhailova-Mikheeva, I.P., Romanenko, V.N., and Tuchkevich, V.M., Fiz. Tver. Tela 6, 2353 (1964); translation Sov. Phys.-Solid State 6, 1865 (1965).

329. Gutkin, A.A., Kagan, M.B., Magerramov, E.M., and Chernov, Ya. I., Fiz. Tver. Tela 8, 3097 (1966); translation Sov. Phys.-Solid State 8, 2474 (1967).

330. Abraham, A., Czech. J. Phys. 6, 624 (1956).

331. Research on Materials Exhibiting Photovoltaic Phenomena, Contract # AF33(616)-7482, Final Report, #ASD-TDR-62-841, 15 June 1960 to 15 June 1962.

332. Research and Development Study on Improved Radiation Resistance and Conversion Efficiency of Silicon Solar Cells, Contract #NAS5-3686, 20 Feb. 1964 to 19 Feb. 1965.

333. Rappaport, P., and Wysocki, J.J., Acta Electronica 5, 364 (1961).

334. Rappaport, P., Adv. Energy. Conv. 1, 3 (1961).

335. Galavanov, V.V., Kundukhov, R.M., and Nasledov, D.N., Fiz. Tver. Tela 8, 3402 (1966); translation Sov. Phys.-Solid State 8, 2723 (1967).

336. Galavanov, V. V., and Erokhina, N. A., Sov. Phys.-Solid State 1, 1096 (1960).

337. Gutkin, A. A., Magerramov, E. M., Mikhalova, M. P., and Nasledov, D. N., Fiz. Tver. Tela 8, 2044 (1966); translation Sov. Phys.-Solid State 8, 1624 (1967).

338. Van Doorn, C. Z., and DeNobel, D., Physica 22, 338 (1956).

339. Lomakina, G. A., Vodakov, Yu. A., Naumov, G. P., and Maslakovets, Yu, P., "A Tube Photelectric Element of Cadmium Telluride". (Publication information on this paper is not available.)

340. Vodakov, Yu. A., Lomakina, G. A., Naumov, G. P., and Maslakovets, Yu. P., Fiz. Tver. Tela 2, 3 (1960); translation Sov. Phys.-Solid State 2, 1 (1960).

341. Vodakov, Yu. A., Lomakina, G. A., Naumov, and Maslakovets, Yu. P., Fiz. Tver. Tela 2, 15 (1960); translation Sov. Phys.-Solid State 2, 11 (1960).

342. Dubrovskii, G. B., Fiz, Tver. Tela 2, 569, (1960); translation Sov. Phys.-Solid State 2, 536 (1960).

343. Dubrovskii, G. B., Fiz. Tver. Tela 3, 1305 (1961); translation Sov. Phys.-Solid State 3, 943 (1961).

344. Wolf, M., Proc. IRE 48, 1246 (1960).

345. Naumov, G. P., and Nikolaeva, O. V., Fiz. Tver. Tela 3, 3748 (1961); translation Sov. Phys.-Solid State 3, 2718 (1962).

346. Investigation of Single Energy Gap Photovoltaic Solar Cell Materials, Contract # DA-36-039-SC-87381, Final Report, Nov. 1961.

347. Bernard, J., Lancon, R., Paparoditis, C., and Rodot, M., Rev. Phys. Appl. 1, 211 (1966).

348. Rodot, M., paper presented at 29th Meeting of the Propulsion and Energetics Panel, AGARD, Liège Belgium (June 1967).

349. Shirland, F. A., Adv. Energy Conv. 6, 201 (1966).

350. Photovoltaic Cadmium Sulfide, Contract # AF33(616)-3466, ARL Technical Report #60-293.

351. Reynolds, D.C., Encyclopedia of Chemical Technology, First Supplement Vol. pp. 667-680, (Interscience Publ., New York, 1957).

352. Lashkarev, V.E., Fedorus, G.A., and Sheinkman, M.K., "Concerning the Diffusion of Photo-Carriers in CdS Single Crystals", Proc. of the Conference in Kiev (1957).

353. Lashkarev, V.E., "An Investigation of Certain Photo-Electric Properties of CdS-type Semiconductors," Proc. of the Conference in Kiev (1957).

354. Lashkarev, V.E., Laxarev, D.P., and Sheinkman, M.K., "Concerning the Mechanisms for the Passage of a Current Through a Metal-Semiconductor Contact, " Proc. of the Conference in Kiev (1957).

355. Antes, L.L., Trans. IRE on Component Parts CP-4, 129 (1957).

356. Woods, J., and Champion, J.A., J. Electronics and Control 7, 243 (1959).

357. Williams, R., and Bube, R.B., J. Appl. Phys. 31, 968 (1960).

358. Hughes, A. L., and DuBridge, L.A., Photoelectric Phenomena (McGraw-Hill Book Co., New York, 1932).

359. Kallmann, H., Phys. Rev. 117, 1482 (1960).

360. Paritskii, L.G., Rogachev, A.A., and Ryvkin, S.M., Fiz. Tver. Tela 3, 1613 (1961); translation Sov. Phys.-Solid State 3, 1170 (1961).

361. Bockemuehl, R.R., Kauppila, J.E., and Eddy, D.S., J. Appl. Phys. 32, 1324 (1961).

362. Palz, W., and Ruppel, W., Phys. Stat. Solidi 6, K161 (1964).

363. Bube, R.H., Photoconductivity of Solids (John Wiley and Sons, Inc., New York, 1960) pp. 75-77.

364. Keating, P.N., J. Appl. Phys. 36, 564 (1965).

365. Komashchenko, V.N., and Fedorus, G.A., Fiz. Tekh. Poluprovodnidov 1, 495 (1967); translation Sov. Phys.-Semiconductors 1, 411 (1967).

366. Georgobiani, A.N., and Steblin, V.I., Fiz. Tekh. Poluprovodnikov 1, 329 (1967); translation Sov. Phys.-Semiconductors 1, 270 (1967).

367. Choyke, W.J., and Patrick, L., Phys. Rev. 105, 1721 (1957).

368. Kholuyanov, C.G., Fiz. Tver. Tela 2, 1909 (1960); translation Sov. Phys.- Solid State 2, 1722 (1961).

369. Thiessen, K., and Jungk, G., Phys. Stat Solidi 2, 473 (1962).

370. Fabricius, E.D., J Appl. Phys. 33, 1597 (1962).

371. Grimmeiss, H.G., and Memming, R., J. Appl. Phys. 33, 2217 (1962).

372. Mead, C.A., and Spitzer, W.G., Appl. Phys. Letters 2, 74 (1963).

373. Spitzer, W.G., and Mead, C.A., J. Appl. Phys. 34, 3061 (1963.)

374. Starkiewicz, J., Sosnowski, L, and Simpson, O., Nature 158, 28 (1946).

375. Berlaga, P.Ya., Rumsh, M.A., and Strakmov, L. P., Rad. i Elektron 2, 41 (1957).

376. Pensak, L., Phys. Rev. 109, 601 (1958).

377. Goldstein, B., Phys. Rev. 109, 601 (1958).

378. Merz, W.J., Helv. Phys. Acta 31, 625 (1958).

379. Ellis, S.G., Herman, F., Loebner, E.E., Merz, W.J., Struck, C.W., and White, J. G., Phys. Rev. 109, 1860 (1958).

380. Goldstein, B., and Pensak, L., J. Appl. Phys. 30, 155 (1959).

381. Cheroff, G., and Keller, S.P., Phys. Rev. 111, 98 (1958).

382. Cheroff, G., Erick, R.C., and Keller, S.P., Phys. Rev. 116, 1091 (1959).

383. Lempicki, A., Phys. Rev. 113, 1204 (1959).

384. Lempicki, A., Am. Phys. Soc. Bull. 4, 36 (1959).

385. Tauc, J., J. Phys. Chem. Solids 11, 345 (1959).

386. Hutson, A.R., Bull. Am. Phys. Soc. II. 6, 110 (1961).

387. Cheroff, G., Bull. Am. Phys. Soc. II. 6, 110 (1961).

388. Semiletov, S.A., Fiz. Tver. Tela 4, 1241 (1962); translation Sov. Phys.- Solid State 4, 909 (1962).

389. Novick, F. T., Fiz. Tver. Tela 4, 3334 (1962); translation Sov. Phys.-Solid State 4, 2440 (1962).

390. Novik, F. T., Rumsh, M. A., and Zimkina, T. M., Kristallografiya 8, 378 (1963); translation Sov. Phys.-Cryst. 8, 295 (1963).

391. Novik, F. T., Fiz. Tver. Tela 5, 3142 (1963); translation Sov. Phys.-Solid State 5, 2300 (1964).

392. Neumark, G. F., Phys. Rev. 125, 838 (1962).

393. Lyubin, V. M. and Fedorova, G. A., Dokl. Akad. Nauk SSR 135, 833 (1960); translation Sov. Phys.-Doklady 135, 1343 (1966).

394. Lyubin, V. M., and Fedorova, G. A., Fiz. Tver. Tela 4, 2026 (1963); translation Sov. Phys.-Solid State 4, 1486 (1963).

395. Adirovich, E. I., and Yuabov, Yu. M., Dokl. Akad. Nauk SSR 155, 1286 (1964); translation Sov. Phys.-Doklady 9, 296 (1964).

396. Adirovich, E. I., Rubinov, V. M., and Yuabov, Yu. M., Dokl. Akad. Nauk SSR 157, 76 (1964); translation Sov. Phys.-Doklady 9, 549 (1965).

397. Adirovich, E. I., and Gol'dshtein, Dokl. Akad. Nauk SSR 158, 313 (1964); translation Sov. Phys.-Solid State 9, 795 (1965).

398. Adirovich, E. I., Rubinov, V. M., and Yuabov, Yu. M., Fiz. Tver. Tela 6, 3180 (1964); translation Sov. Phys.-Solid State 6, 2540 (1965).

399. Adirovich, E. I., Rubinov, V. M., and Yuabov, Yu. M., Dokl. Akad. Nauk SSR 164, 529 (1965); translation Sov. Phys.-Doklady 10, 844 (1966).

400. Adirovich, E. I., Rubinov, V. M., and Yuabov, Yu. M., Dokl. Akad. Nauk SSR 168, 1037 (1966); translation Sov. Phys.-Doklady 11, 512 (1966).

401. Adirovich, E. I., and Shakirov, N., Dokl. Akad. Nauk SSR 173, 298 (1967); translation Sov. Phys.-Doklady 12, 226 (1967).

402. Perrot, M., David, J. P., and Martinuzzi, S., Rev. Phys. Appliquée (suppl. J. Phys. Appliquee 1,), 165 (1966).

403. Korsunskii, M.I., and Fridman, V. M., Fiz. Tver. Tela 8, 263 (1966); translation Sov. Phys.-Solid State 8, 213 (1966).

404. Palatnik, L.S., and Sorokin, V.R., Fiz. Tver. Tela 8, 2795 (1966); translation Sov. Phys.-Solid State 8, 2233 (1967).

405. Ignatyuk, V.A., and Novik, F.T., Fiz. Tver. Tela 8, 3661 (1966); translation Sov. Phys.-Solid State 8, 2929 (1967).

406. Karpovich, I.A., and Shilova, M.V., Fiz. Tver. Tela 5, 3560 (1963); translation Sov. Phys.-Solid State 5, 2612 (1964).

407. Gutmann, F., and Lyons, L.E., Organic Semiconductors, (John Wiley and Sons, Inc., New York, 1967).

408. Moses, J., Monatsh. Chem. 8, 373 (1887).

409. Rigollot, H., Compt. Rend. 116, 873 (1893).

410. Mees, C.E.K., The Theory of the Photographic Process, (The Macmillan Co., New York, 1954).

411. Terenin, A., Proc. Chem. Soc. London, 321 (1961).

412. Nelson, R.C., J. Opt. Soc. Am. 46, 13 (1956).

413. Nelson, R.C., J. Chem. Phys. 27, 864 (1957).

414. Nelson, R.C. J. Opt. Soc. Am. 48, 1 (1958).

415. Nelson, R.C., J. Opt. Soc. Am. 48, 948 (1958).

416. Nelson, R.C., J. Opt. Soc. Am. 51, 1183 (1961).

417. Nelson, R.C., J. Opt. Soc. Am. 51, 1186 (1961).

418. Putseiko, E.K., Sov. Phys. Dokl. 129, 1268 (1960).

419. Wintle, H.J., and Charlesby, A., Photochem. Photobiol. 1, 231 (1962) (quoted by (407)).

420. Kallman, H., and Pope, M., J. Chem. Phys. 30, 585 (1959).

421. Contract #AF18(604)-5995, Crystal Structure of Potential Solar Conversion Materials (Boston Univ.); Contract #AF19(628)-414, Photoconductivity of Organic Solids (Univ. of Arizona); Contract #AF19(628)-1660 Electron Injection and Conduction in Organic Solids (Franklin Inst.); Contract #AF19(628)-2446, Photoconductive and Photovoltaic Effects in Organic Solids (NY Univ.); Contract #AF61(052)-769, Solid-State Properties of Organic Donor-Acceptor Complexes (Univ. of Groningen); Contract #AF19(628)-4363, Determining Nature of Charged Carriers in Organic Semiconductors (General Dynamics).

422. Golubovic, A., Thin-Film Organic Photovoltaic Cells (to be published).

423. Mukherjee, T.K., Record 6th Photovoltaic Specialists Conf. 1, 7 (1967).

424. Meier, H., and Haus, A., Z. Elektrochem. 64, 1105 (1960).

425. Needler, W.C., J. Chem. Phys. 42, 2972 (1965).